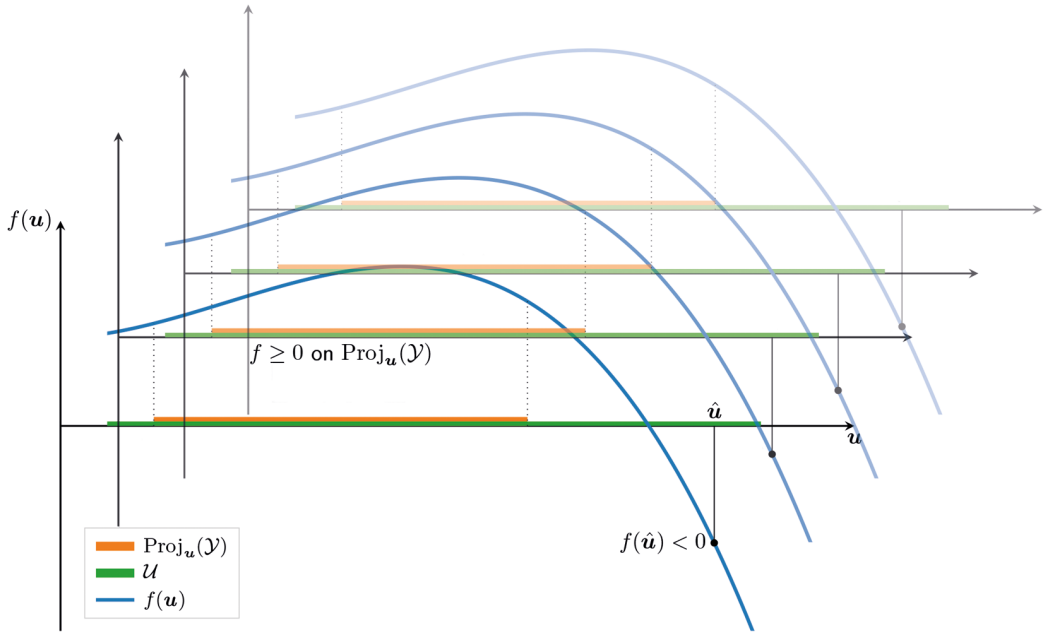

FAU Studies Mathematics & Physics 16

Denis Aßmann

Exact Methods for Two-Stage Robust Optimization with Applications in Gas Networks

FAU UNIVERSITY PRESS

Denis Aßmann

Exact Methods for Two-Stage Robust Optimization with Applications in Gas Networks

FAU Studies Mathematics & Physics

Band 16

Herausgeber der Reihe:
Prof. Dr. Karl-Hermann Neeb und Prof. Dr. Klaus Mecke

Denis Aßmann

Exact Methods for Two-Stage Robust Optimization with Applications in Gas Networks

Erlangen
FAU University Press
2019

Bibliografische Information der Deutschen Nationalbibliothek:
Die Deutsche Nationalbibliothek verzeichnet diese Publikation in der Deutschen Nationalbibliografie; detaillierte bibliografische Daten sind im Internet über http://dnb.d-nb.de abrufbar.

Der vollständige Inhalt des Buchs ist als PDF über den OPUS Server der Friedrich-Alexander-Universität Erlangen-Nürnberg abrufbar:
https://opus4.kobv.de/opus4-fau/home

Bitte zitieren als
Aßmann, Denis. 2019. *Exact Methods for Two-Stage Robust Optimization with Applications in Gas Networks.* FAU Studies Mathematics & Physics Band 16. Erlangen: FAU University Press, DOI: 10.25593/978-3-96147-234-5

Verlag und Auslieferung:

FAU University Press, Universitätsstraße 4, 91054 Erlangen

Druck: docupoint GmbH

ISBN: 978-3-96147-233-8 (Druckausgabe)
eISBN: 978-3-96147-234-5 (Online-Ausgabe)
ISSN: 2196-7482
DOI: 10.25593/978-3-96147-234-5

Exact Methods for Two-Stage Robust Optimization with Applications in Gas Networks

Exakte Verfahren für zweistufige robuste Optimierung mit Anwendungen in Gasnetzwerken

Der Naturwissenschaftlichen Fakultät
der Friedrich-Alexander-Universität
Erlangen-Nürnberg

zur

Erlangung des Doktorgrades Dr. rer. nat.

vorgelegt von

Denis Aßmann
aus Schwabach

Als Dissertation genehmigt
von der Naturwissenschaftlichen Fakultät
der Friedrich-Alexander-Universität Erlangen-Nürnberg

Tag der mündlichen Prüfung:	4. Juli 2019
Vorsitzende/r des Promotionsorgans:	Prof. Dr. Georg Kreimer
Gutachter/in:	Prof. Dr. Frauke Liers
	Priv.-Doz. Dr. René Henrion

Acknowledgments

First of all, I am extremely grateful to my supervisor, Prof. Dr. Frauke Liers, for giving me the opportunity to pursue my Ph.D. Her personal dedication to always be available for discussions as well as her unwavering support and guidance over the years have greatly contributed to the success of this work.

I would also like to extend my deepest gratitude to Prof. Dr. Michael Stingl. Our numerous constructive discussions, his valuable feedback as well as his enthusiasm were both inspiring and motivating.

I also wish to thank Prof. Dr. Alexander Martin for creating such a familiar and pleasant working environment—not only in our working group but also in the entire CRC154.

I am particularly grateful for the assistance and helpful advice given by Dr. Lars Schewe and Prof. Dr. Martin Schmidt. Whatever the question was—mathematically, technically, or other—both always did their very best to help.

It also was a great pleasure to work with Prof. Dr. Juan Vera[1]. I am grateful for many fruitful discussions on polynomial optimization and for giving us a new perspective on our robust problems.

It has always been a pleasure to work on my CRC154[2] project. In this regard, my special thanks go to my fellow Ph.D. students for the many joyful hours together, my mentor Dr. René Henrion, and the DFG for their financial support.

My sincere thanks go to all former and current colleagues in our group, as well as some of the Matlab enthusiasts a few doors down the floor. I really enjoyed our time together at the university. In particular, a big thank you to everyone who has proofread this work.

Finally, I want to express my heartfelt gratitude towards my friends, my partner, and my family. Thank you very much for the many years of support and your faith in me.

[1] Tilburg University, NL

[2] CRC/Transregio 154—Mathematical modelling, simulation and optimization using the example of gas networks (trr154.fau.de)

Zusammenfassung

Erdgas ist heutzutage einer der wichtigsten Energieträger und gilt als Schlüsseltechnologie zum Erreichen der politisch gesteckten Klimaziele. Hierbei gelten Gaskraftwerke als flexible Puffer, um Schwankungen der Stromerzeugung aus regenerativen Energiequellen kurzfristig auszugleichen. Darüber hinaus stehen die Gasnetzbetreiber in Folge der Liberalisierung des europäischen Gasmarktes vor zusätzlichen Herausforderungen. Im neuen Entry-Exit-Modell ist es Aufgabe der Gasnetzbetreiber, die Transportierbarkeit aller möglichen Marktergebnisse über das Netz zu gewährleisten. Der Betrieb von Gasnetzen unter unsicheren Bedingungen erfordert daher zunehmend neue Entscheidungshilfen.

Zu diesem Zweck wird in dieser Arbeit eine Klasse allgemeiner zweistufiger robuster Optimierungsprobleme untersucht, deren Variablen der zweiten Stufe eindeutig durch nicht-konvexe Nebenbedingungen bestimmt werden. Diese Struktur findet sich beispielsweise im Gasnetzbetrieb unter Unsicherheit.

Drei allgemeine Lösungsmethoden werden für diese Problemklasse entwickelt. Die ersten beiden Ansätze nutzen Ideen aus der polynomiellen Optimierung, um Zulässigkeit oder Unzulässigkeit einer Problemvariante mit leerer erster Stufe zu entscheiden. Beide Ansätze verwenden polynomielle Formulierungen, die mittels der Lasserre Relaxierungshierarchie durch semidefinite Programme approximiert werden. Die Effektivität der Methoden wird an zyklischen Gasnetzen untersucht. Es zeigt sich, dass robuste Zulässigkeit oder Unzulässigkeit oft bereits auf einem niedrigen Niveau der Lasserre Hierarchie entschieden werden kann.

Der dritte Ansatz basiert auf einer Transformation des zweistufigen Problems in ein normales, einstufiges Optimierungsproblem. Dazu werden mehrere Subprobleme gelöst, deren Optimalwerte die rechte Seite des transformierten Problems bilden. Die Anzahl der zu lösenden Subprobleme kann dabei durch einen zusätzlichen Aggregationsschritt signifikant verringert werden. Für eine Anwendung auf Gasnetzprobleme werden gemischt-ganzzahlige Relaxierungen der Subprobleme entwickelt. Abschließend wird die Leistungsfähigkeit des Ansatzes durch Benchmarks an mehreren Gasnetzinstanzen verdeutlicht, darunter ein realistisches Modell des griechischen Erdgasnetzes. Insgesamt können somit robuste Lösungen für große Netze unter Unsicherheit innerhalb kurzer Zeit gefunden werden.

Abstract

Today, natural gas is one of the most important sources of energy and is regarded as a key instrument for achieving the politically set climate goals. Gas-fired power plants are valued as flexible buffers to compensate for fluctuations in electricity generation from renewable energy sources at short notice. Additionally, gas network operators face new challenges as a result of the liberalization of the European gas market. In the new entry-exit model, the gas network operators have to ensure that all possible market outcomes can be transported over the network. Hence, the operation of gas networks under uncertain conditions increasingly requires new aids for decision-making.

To this end, this thesis investigates a class of general two-stage robust optimization problems whose second-stage variables are uniquely determined by non-convex constraints. This structure occurs, e.g., in gas network operations under uncertainty.

Three general solution methods are developed for this problem class. The first two approaches use ideas from polynomial optimization to decide feasibility or infeasibility of a problem variant with an empty first stage. Both procedures use polynomial formulations that are approximated by semidefinite programs using the Lasserre relaxation hierarchy. The effectiveness of the methods is investigated on cyclic gas networks. It can be observed that often a low level of the Lasserre hierarchy is sufficient to decide robust feasibility or infeasibility.

The third approach is based on a transformation of the two-stage problem into a normal, single-stage optimization problem. To this end, several subproblems have to be solved whose optimal values form the right-hand side of the transformed problem. An additional aggregation step can significantly reduce the number of subproblems that have to be considered. For a practical application to real-world gas network instances, mixed-integer linear relaxations of the subproblems are developed. Finally, the performance of the approach is demonstrated by benchmarks on several gas network instances, including a realistic model of the Greek natural gas network. Overall, robust feasible solutions for large networks under uncertainty can be found within a short time.

Contents

Notation

Number spaces and special sets Let $\mathbb{N} = \{1, 2, \ldots\}$ and $\mathbb{N}_0 = \{0, 1, \ldots\}$ be the set of natural numbers excluding and including zero, respectively. Let $\mathbb{R}$ ($\mathbb{C}$) be the set of real (complex) numbers. We write $\mathbb{R}_{\geq 0}$, $\mathbb{R}_{\leq 0}$, $\mathbb{R}_{>0}$ for the sets of nonnegative, nonpositive, and (strictly) positive real numbers, respectively. Sets are generally written in a calligraphic font, e.g., $\mathcal{S} \subseteq \mathbb{R}$. We denote with $\mathcal{S}_1 \setminus \mathcal{S}_2 \coloneqq \{x \in \mathcal{S}_1 \mid x \notin \mathcal{S}_2\}$ the set difference of two sets $\mathcal{S}_1, \mathcal{S}_2$.

Vectors and matrices We typeset scalars in a normal font, e.g., $x \in \mathbb{R}$. A bold font is used for multi-dimensional objects such as vectors, matrices, and vector-valued functions. For example, an n-dimensional real vector is written as $\boldsymbol{x} = (x_i)_{i=1,\ldots,n} \in \mathbb{R}^n$ with individual elements x_i in normal font. Let $\mathcal{B} \subset \{1, \ldots, n\}$ be a subset of indices. We write $\boldsymbol{x}_\mathcal{B} = (x_i)_{i \in \mathcal{B}} \in \mathbb{R}^{|\mathcal{B}|}$ for the subvector that arises from restricting $\boldsymbol{x}$ to the indices in $\mathcal{B}$.

Matrices are treated similarly. Let $\boldsymbol{A} \in \mathbb{R}^{m \times n}$ be a real $m \times n$ matrix. We write $\boldsymbol{A}_{\cdot 1}, \ldots, \boldsymbol{A}_{\cdot n} \in \mathbb{R}^m$ for the columns and $\boldsymbol{A}_{1\cdot}, \ldots, \boldsymbol{A}_{m\cdot} \in \mathbb{R}^n$ for the rows of $\boldsymbol{A}$. Individual entries are given by $\boldsymbol{A} = (A_{ij})_{i=1,\ldots,m,\, j=1,\ldots,n}$. We write $\boldsymbol{A}_\mathcal{B} = (\boldsymbol{A}_{\cdot j})_{j \in \mathcal{B}}$ for the submatrix that contains all columns indexed by $\mathcal{B}$.

Graphs Let $\mathcal{G} = (\mathcal{V}, \mathcal{A})$ be a digraph with nodes $\mathcal{V} = \{v_1, \ldots, v_n\}$ and arcs $\mathcal{A} = \{a_1, \ldots, a_m\} \subseteq \mathcal{V} \times \mathcal{V}$. A *path* of length $k \in \mathbb{N}_0$ in $\mathcal{G}$ is an alternating sequence of nodes and arcs, i.e., $v_{i_1}, a_{i_1}, v_{i_2}, \ldots, a_{i_{k-1}}, v_{i_k}$, where either $a_{i_j} = (v_{i_j}, v_{i_{j+1}})$ or $a_{i_j} = (v_{i_{j+1}}, v_{i_j})$ for $j = 1, \ldots, k-1$. Furthermore, all nodes in the path are pairwise distinct. A *cycle* is a path where we allow the first and the last node to be identical, i.e., $v_{i_1} = v_{i_k}$.

Paths (and cycles) are represented as vectors in $\mathbb{R}^{|\mathcal{A}|}$ that are indexed by the set of arcs $\mathcal{A}$. The entries of a path's incidence vector $\boldsymbol{P} = (P_a)_{a \in \mathcal{A}} \in \mathbb{R}^{|\mathcal{A}|}$ are $P_a = 0$ if a is not part of the path and $P_a = +1$ (resp. -1), if a appears in the path and its direction agrees (resp. disagrees) with the path's direction.

We call $\mathcal{G}$ *connected* if a path exists between all pair of nodes $v, w \in \mathcal{V}$. A graph that is connected and contains no cycles is called a *tree*. A *subgraph* of $\mathcal{G} = (\mathcal{V}, \mathcal{A})$ is a graph $\mathcal{G}' = (\mathcal{V}', \mathcal{A}')$ where $\mathcal{V}' \subseteq \mathcal{V}$ and $\mathcal{A}' \subseteq \mathcal{A}$. Any subgraph of $\mathcal{G}$ that is a tree and whose vertex set is equal to $\mathcal{V}$ is called a *spanning tree*.

We would like to point out that in the end, we treat graphs as if they were undirected; the direction of the arcs is only needed for the direction of the flow.

1 Introduction

In the modern world, more and more data is being collected in all areas of life and used as a basis for decision-making. However, this data is often incomplete or represents reality only inaccurately. It is therefore all the more challenging to make good decisions for the real situation while taking these uncertain data into account. There are numerous mathematical approaches such as robust optimization that can be used for decision-making under uncertainty. In this thesis, we develop solutions for a class of two-stage robust optimization problems and exemplarily apply them to the operation of gas networks under uncertainty.

The energy transition is one of the major political and societal challenges of the 21st century. It is characterized by a structural change of energy supply away from fossil or nuclear fuels towards more environmental-friendly renewable energy sources. Energy production from renewable energy sources has increased sixfold in the period from 2000 to 2017 and now amounts to about $30\,\%$ of total generation; see AG Energiebilanzen e.V. (2019a). In the same period, coal and nuclear power generation decreased while energy production using natural gas increased steadily. Germany is committed to phasing out nuclear power generation until the end of 2022 (Bundesgesetzblatt 2011), and recently proposals have been made to phase out coal by 2038 (Kommission WSB 2019). Due to the decline of coal and nuclear power generation, the importance of natural gas, which is a comparatively clean fossil fuel, will continue to increase during this transition towards renewable energies.

Renewable energies such as wind or solar power are characterized by strong seasonal fluctuations. Gas-fired power plants can be operational at very short notice and hence can compensate these fluctuations. Once a high proportion of renewable energy sources is reached ($60\,\%$ to $70\,\%$), large amounts of surplus electricity will be generated on a regular basis. In order for the surplus energy to be used at a later point in time, efficient energy storage systems are required, e.g., by using power-to-gas technologies (Varone and Ferrari 2015). These technologies produce methane or hydrogen from electrical energy and store them in existing pipeline networks or regular storage facilities. Gases stored in this way can then be extracted again and used to generate electricity.

Closely linked to all these new challenges is the transport and trading of natural gas on the German and European level. As Germany can only produce about $7\,\%$ of its natural gas demand, it depends on imports from abroad; see AG Energiebilanzen e.V. (2019b) and BAFA (2019). Being located in the

heart of Europe, Germany also serves as an important transit country for natural gas. Recently, the liberalization of the natural gas market in Europe has led to a separation between transport infrastructure and gas traders; see Hewicker and Kesting (2009) and Gotzes et al. (2015) for a summary. In the past, trading was almost exclusively carried out directly between the pipeline operators and their customers. In the new entry-exit system, market participants trade gas without taking the physics of gas transport into account. The role of gas network operators is to ensure that any possible market outcome can be transported through the network. On the whole, the lower market entry barrier and the higher flexibility favor a dynamic market situation with more frequent trades between a growing number of consumers and producers; see WEC (2016) and ACER (2015).

Hence, gas network operators are facing novel challenges such as more dynamic network usage and a greater influence of uncertain factors due to the transition to renewable energies. We consider a setting where a gas network has to be operated without full knowledge of all parameters. Situations like this arise, e.g., when the fluctuation of future demand is uncertain, when the precise gas composition is not known due to power-to-gas usage, or when intangible aging effects of the pipelines affect the gas flow. Hence, the following question is the focus of this work:

> *Is there a configuration of the gas network such that feasible operation can be guaranteed for all parameters from a set of likely values?*

Mathematical challenges and research goals This question, even without uncertain parameters, leads to a rich set of mathematical problems and models; see Koch et al. (2015) and Ríos-Mercado and Borraz-Sánchez (2015). The behavior of gas in a pipeline network is described by the Euler equations, a set of partial differential equations (PDEs). Solutions of these equations are usually nonlinear and non-convex, even under simplified conditions. Additionally, there are other network elements besides pipes such as compressors and control valves, which are often expressed as a mixture of continuous and discrete variables. All these aspects lead to mathematical formulations that can be very difficult to solve, even in the nominal setting, i.e., in the absence of uncertainties.

Integrating uncertainties into these already established models leads to a variety of new mathematical challenges. Here, we study uncertain problems in the sense of robust optimization; see Ben-Tal, El Ghaoui, and Nemirovski (2009). That is, we want to give strong guarantees that a solution is in a certain sense immunized against all possible realizations from a previously specified set of parameters.

A mathematical model of the considered gas network problem under uncertainty leads to a class of two-stage robust optimization problems with a non-convex second stage and a uniqueness property of the second-stage variables. We investigate this problem family in a general and abstract setting.

Problems of this kind are challenging for two reasons: First, there is no general theory for robust treatment of non-convex models. Second, the two-stage structure leads to additional complexities that are NP-hard even for linear programs (LPs); see Ben-Tal et al. (2004).

Our goal is to find solution approaches for the indicated type of problem in the robust optimization sense and to guarantee that all solutions are feasible for the original nonlinear and non-convex formulation.

To this end, we develop three distinct methods and demonstrate their feasibility in practice on gas network problems under uncertainty. First, we study a feasibility variant of two-stage problem with an empty first stage. We show how polynomial optimization can be used for deciding robust feasibility and infeasibility. This leads to two distinct polynomial problems that are solved in practice using the Lasserre relaxation hierarchy. Numerical experiments on small cyclic gas networks show that often a low level of the relaxation hierarchy is sufficient to successfully detect robust feasibility or infeasibility.

Second, we investigate a two-stage robust problem whose constraints have a certain structural property. In this setting, we present a reformulation approach that allows a transformation of the two-stage problem into a standard single-stage optimization problem. We also show how feasible solutions for the original nonlinear program (NLP) can be obtained from a relaxed problem formulation. In our case, we propose to use a well-known piecewise-linear relaxation technique that can be formulated as a mixed-integer linear program (MILP). Finally, we demonstrate the feasibility of this approach by solving a series of real-world problems on the natural gas network of Greece.

Incorporation of joint work with other authors The results of this thesis have been developed in collaboration with other researchers. In particular, the author was supervised by Prof. Liers and Prof. Stingl within subproject B06 of the CRC154[1]. The results have been published in the following two articles. Chapter 4 on polynomial methods is joint work with Prof. Vera[2]; a preliminary version of this chapter has appeared as

[1] CRC/Transregio 154—Mathematical modelling, simulation and optimization using the example of gas networks (trr154.fau.de)

[2] Tilburg University, Tilburg, The Netherlands.

D. Aßmann, F. Liers, M. Stingl, and J. C. Vera. 2018. "Deciding robust feasibility and infeasibility using a set containment approach: an application to stationary passive gas network operations". *SIAM Journal on Optimization* 28 (3): 2489–2517. doi:10.1137/17M112470X.

The subsequent chapter 5 on the reformulation approach is mainly based on

D. Aßmann, F. Liers, and M. Stingl. 2019. "Decomposable robust two-stage optimization: An application to gas network operations under uncertainty". *Networks* 74 (1): 40–61. doi:10.1002/net.21871.

At the beginning of each chapter, we indicate in more detail which results originate from the author of this thesis.

The structure of this thesis This thesis is organized into six chapters.

Chapter 2 provides an introduction to the modeling of gas networks. We also present some of the known properties such as uniqueness and existence of solutions and extend these results to our context.

Chapter 3 is dedicated to robust optimization. We introduce the robust optimization methodology, formulate the two-stage gas network problem, and discuss the limitations of known approaches in this setting.

Chapter 4 addresses the polynomial optimization methods for deciding robustness of a two-stage robust problem without a first stage. In particular, we develop one approach for deciding feasibility and one approach for deciding infeasibility. Moreover, we show how to eliminate absolute values from the gas network problem and present some benchmarks of both methods on small instances.

Chapter 5 presents a reformulation approach that allows a transformation of a two-stage robust problem to an ordinary single-stage optimization problem. We discuss the influence of using relaxations for this problem and showcase an aggregation idea that can be used to reduce the number of subproblems. Together with well-known piecewise linearization techniques, we show how the gas network problem can be solved with a series of MILPs. Using the real-world gas network of Greece, we finally demonstrate the practical viability of our method.

Chapter 6 concludes this thesis with a discussion and comparison of the developed methods.

2 Stationary gas network operations

The practical feasibility of the methods developed in this thesis for solving challenging, two-stage robust optimization problems is demonstrated using the example of gas network problems under uncertainty. Problems of this kind are well suited for this purpose as they lead to models with a two-stage structure and non-convex constraints. As they arise from a real-world context, they also offer several possibilities for robust treatment. This chapter gives a brief introduction to the modeling of gas transport problems, highlights some important mathematical properties of these models, and finally gives a literature review of existing solution methods.

Most of the material in this chapter stems from the book Koch et al. (2015), the survey article by Ríos-Mercado and Borraz-Sánchez (2015), and from references in these two sources.

This chapter is structured as follows. Section 2.1 gives a brief introduction to the mathematical models of components found in natural gas transport networks. Based on these models, section 2.2 derives a stationary gas transport problem with linear models for compressors and control valves. Section 2.3 then shows how this optimization problem can be transformed into an alternative form with fewer variables. Section 2.4 is dedicated to the existence of unique solutions for the considered problem. The chapter concludes with section 2.5, which provides a literature review of existing solutions methods for nominal gas network problems.

2.1 Network components

A natural gas transport network consists of a series of interconnected pipes and various other network elements such as We provide a brief overview of models for pipes, compressors, (control) valves, and short pipes. The descriptions here are derived from Fügenschuh et al. (2015).

Pipes

Fluid dynamics is a branch of physics that deals with the motion of fluids, i.e., gases, liquids, and plasmas. A mathematical model for fluids in motion is given by the Navier-Stokes equations, a set of nonlinear PDEs that can be used to model phenomena ranging from very large scale weather dynamics and ocean currents to very small scale effects like the blood flow in the blood vessels. In particular, the flow of gas along a pipeline can be described by the

Euler equations, a special case of the Navier-Stokes equations for an inviscid fluid. A derivation of the mentioned PDE models and their mathematical properties is beyond the scope of this work. For a general introduction to fluid dynamics, we refer to the textbooks Kundu, Cohen, and Dowling (2015) and Landau and Lifshitz (1987). More specialized treatment of fluid flows in gas pipelines can be found in the books by Lurie (2008), Koch et al. (2015), Menon (2005), Saleh (2002), and Zucker and Biblarz (2002) as well as the article by Brouwer, Gasser, and Herty (2011).

The time-dependent Euler equations are a system of nonlinear, hyperbolic PDEs. As gas pipes have a negligible diameter when compared to their length, a common modeling choice is to average all quantities over the pipe's cross section and use a one-dimensional spatial variable. Following the presentation given in Brouwer, Gasser, and Herty (2011), the Euler equations are used in the following form to model gas dynamics in a pipe:

$$\frac{\partial}{\partial t}\rho + \frac{\partial}{\partial x}(\rho v) = 0, \tag{2.1a}$$

$$\frac{\partial}{\partial t}(\rho v) + \frac{\partial}{\partial x}(p + \rho v^2) = -\frac{\lambda}{2D}\rho v|v| - g\rho h', \tag{2.1b}$$

$$\frac{\partial}{\partial t}(\rho(\tfrac{1}{2}v^2 + e)) + \frac{\partial}{\partial x}(\rho v(\tfrac{1}{2}v^2 + e) + pv) = -\frac{k_{\mathrm{w}}}{D}(T - T_{\mathrm{w}}). \tag{2.1c}$$

The system models the conservation of mass in (2.1a), the conservation of impulse in (2.1b), and the conservation of energy in (2.1c). The unknown functions represent *gas density* $\rho(x,t) \in \mathbb{R}$ (in $\mathrm{kg\,m^{-3}}$), *gas velocity* $v(x,t) \in \mathbb{R}$ (in $\mathrm{m\,s^{-1}}$), *gas pressure* $p(x,t) \in \mathbb{R}$ (in Pa), and *gas temperature* $T(x,t) \in \mathbb{R}$ (in K). All unknown functions depend on *time* $t \in \mathbb{R}$ and *space* $x \in \mathbb{R}$. The constants in (2.1a)–(2.1c) are the *friction factor* λ (dimensionless), which models the friction between gas and pipeline wall; the *pipe diameter* D (in m); the *gravitational constant* g (in $\mathrm{m\,s^{-2}}$); the *inclination* of the pipe $h' = h'(x)$ (dimensionless) as a derivative of the pipe's absolute height $h = h(x)$ (in m); the *pipe wall surface temperature* $T_{\mathrm{w}} = T_{\mathrm{w}}(x)$ (in K); and the *heat transfer coefficient* k_{w} (in $\mathrm{W\,m^{-2}\,K^{-1}}$), which influences the heat exchange between gas and pipeline wall. Moreover, the variable $e \coloneqq c_{\mathrm{w}}T + gh$ is introduced to describe the internal energy of the gas as a sum of heat energy and potential energy, where c_{w} (in $\mathrm{J\,kg^{-1}\,K^{-1}}$) denotes the specific heat capacity of the gas.

The system above is supplemented by an equation of state for gas. An *ideal gas* follows the ideal gas law, see, e.g., Menon (2005), that relates pressure p (in $\mathrm{Pa} = \mathrm{J\,m^{-3}}$), volume V (in $\mathrm{m^3}$), and temperature T (in K) of a specified amount $\tilde{n}$ (in mol) of gas:

$$pV = \tilde{n}RT, \tag{2.2}$$

where $R = 8.314\,\mathrm{J\,K^{-1}\,mol^{-1}}$ denotes the universal gas constant. The ideal gas law (2.2) can be formulated in terms of gas density instead of gas volume. First, we express the chemical amount as $\tilde{n} = \frac{m}{M}$, where m denotes mass of the gas (in kg) and M the molar mass of the gas (in $\mathrm{kg\,mol^{-1}}$). Next, we recall that the volume of a substance (in $\mathrm{m^3}$) is the fraction of its mass and density, i.e., $V = \frac{m}{\rho}$. Plugging both equations into the ideal gas law (2.2) yields

$$p = \frac{R}{M}\rho T = R_\mathrm{s}\rho T, \tag{2.3}$$

where we denote the *specific gas constant* with $R_\mathrm{s} = \frac{R}{M}$ (in $\mathrm{J\,kg^{-1}\,K^{-1}}$).

In this form, the ideal gas law (2.2) is more appropriate for (2.1a)–(2.1c) as it links three of the four unknowns—pressure, density, and temperature—while being independent of the quantity of the considered gas. The ideal gas law is derived under the assumption of no intermolecular attraction between gas molecules as well as a point-like gas model. Many real gases—including natural gas—show considerable deviation from the ideal gas law, especially in high-pressure situations that can be present in high-throughput gas transport pipelines. To compensate for this deviation, a dimensionless *compressibility factor* $z = z(p,T) \in \mathbb{R}$ is added to (2.2). The factor depends on the chemical composition of the gas as well as its temperature and pressure. This leads to the *real gas law*:

$$p = R_\mathrm{s}\rho T z(p,T). \tag{2.4}$$

The compressibility factor of an ideal gas is $z = 1$. There are several empiric formulas for the calculation of $z(p,T)$ for real gases. Amongst others, there is the formula of the American Gas Association, see, e.g., Králik et al. (1988), which is accurate up to $70\,\mathrm{bar}$:

$$z(p,T) = 1 + 0.257\frac{p}{p_\mathrm{c}} - 0.533\frac{p}{p_\mathrm{c}}\frac{T_\mathrm{c}}{T}, \tag{2.5}$$

where we denote with T_c the *pseudocritical temperature* (in K) and with p_c the *pseudocritical pressure* (in Pa) of the gas mixture. Another formula for the compressibility factor is due to Papay (1968); see also Saleh (2002, chapter 2):

$$z(p,T) = 1 - 3.52\tfrac{p}{p_\mathrm{c}}\exp\Big(-2.26\tfrac{T}{T_\mathrm{c}}\Big) + 0.247\Big(\tfrac{p}{p_\mathrm{c}}\Big)^2\exp\Big(-1.878\tfrac{T}{T_\mathrm{c}}\Big). \tag{2.6}$$

Papay's formula can be used up to $150\,\mathrm{bar}$.

Under the assumption of one-dimensional flow in pipe direction x along a cylindrical pipe with *diameter* D (in m) and *cross-sectional area* $A = (\frac{D}{2})^2\pi$ (in $\mathrm{m^2}$), we introduce the mass flow rate q (in $\mathrm{kg\,s^{-1}}$) as

$$q = A\rho v. \tag{2.7}$$

Frictional forces between the flowing gas and the pipeline wall are described by the flow-dependent *friction factor* $\lambda(q)$. There are several empiric formulas for $\lambda(q)$ described in the literature; see e.g., Lurie (2008) and Saleh (2002). The occurring frictional forces are highly dependent on the *flow regime* which can be characterized by the dimensionless *Reynolds number*

$$Re(q) = \frac{D}{A\eta}|q|, \tag{2.8}$$

where we denote with η the dynamic viscosity of the gas (in $\mathrm{kg\,s^{-1}\,m^{-1}}$). Typically, one distinguishes between *laminar flow* at low Reynolds numbers and *turbulent flow* for Reynolds numbers exceeding a certain critical value $Re(q) \geq Re_{\mathrm{crit}} \approx 2300$; see Fügenschuh et al. (2015). Laminar flow is characterized by a smooth, constant motion in parallel layers where the dominating factor is the viscous force of the fluid. Turbulent flow, on the other hand, features chaotic flow patterns like swirling and vortices that are accompanied by rapid changes in pressure and density. In this regime, the viscous forces are not strong enough to provide sufficient damping of the medium's inertial forces.

For laminar flows, the friction factor is inverse proportional to the Reynolds number:

$$\lambda(q) = \frac{64}{Re(q)}. \tag{2.9}$$

This relation is known as the *Hagen-Poisseuille* formula; see, e.g., Franzini and Finnemore (1997).

The friction factor of turbulent flows in gas pipes can be modeled with the implicit equation of *Prandtl-Colebrook-White*; see Saleh (2002, chapter 9):

$$\frac{1}{\sqrt{\lambda(q)}} = -2\log_{10}\left(\frac{2.51}{Re(q)\sqrt{\lambda(q)}} + \frac{k}{3.71D}\right), \tag{2.10}$$

where we denote with k the *integral roughness* (in m) of the pipe. An approximation of (2.10) in explicit form is given by the *Hofer* equation; see Mischner (2012) and Hofer (1973):

$$\lambda(q) = \left(-2\log_{10}\left(\frac{4.518}{Re(q)}\log_{10}\left(\frac{Re(q)}{7}\right) + \frac{k}{3.71D}\right)\right)^{-2}. \tag{2.11}$$

A different approximation of (2.10) for very large Reynolds numbers is obtained by letting $Re \to \infty$:

$$\lambda = \left(2\log_{10}\left(\frac{D}{k}\right) + 1.138\right)^{-2}. \tag{2.12}$$

This empirical equation has been found by Nikuradse (1933). We remark that this formula provides a flow-independent approximation of the friction factor λ and hence leads to simpler models. Since the considered flowing gas typically follows a turbulent regime, we use this formula for the calculation of λ.

An approximation for the stationary, isothermal case Under certain circumstances, an explicit solution of the PDE system (2.1a)–(2.1c) can be derived. We closely follow the approach in Fügenschuh et al. (2015). First of all, we assume a *stationary* gas flow, i.e., all derivatives with respect to time t vanish. Moreover, we assume an *isothermal* model, i.e., the gas temperature T and the temperature of the pipeline T_{w} are constant and equal to some mean temperature T_{m}. This assumption is supported by the fact that—at least in Germany—most pipelines are laid underground and thus the pipeline temperature is not subject to strong fluctuations. Concerning the pipeline itself, we consider a straight, cylindrical pipe without slope that has length L (in m) and diameter D. Furthermore, a constant mean compressibility factor z_{m} is assumed for the gas. We use Papay's formula (2.6) for the computation of $z_{\mathrm{m}} = z_{\mathrm{m}}(p_{\mathrm{m}}, T_{\mathrm{m}})$. The calculation of the mean pressure p_{m} follows Geißler, Martin, et al. (2015):

$$p_{\mathrm{m}} = \tfrac{1}{2}\big(\max\{\underline{p}_{\mathrm{in}}, \underline{p}_{\mathrm{out}}\} + \min\{\overline{p}_{\mathrm{in}}, \overline{p}_{\mathrm{out}}\}\big), \tag{2.13}$$

where $\underline{p}_{\mathrm{in}}, \overline{p}_{\mathrm{in}}$ and $\underline{p}_{\mathrm{out}}, \overline{p}_{\mathrm{out}}$ are lower and upper bounds on the gas pressure at a pipe's inlet and outlet, respectively. According to Wilkinson et al. (1965), the *ram pressure term* $\frac{\partial}{\partial x}(\rho v^2)$ contributes only very little and thus can be neglected.

Taking all this into account, we simplify the PDE system (2.1a)–(2.1c). Due to constant mean temperature, we remove (2.1c). Setting all time derivatives to zero, we obtain

$$\frac{\partial}{\partial x}(\rho v) = 0, \tag{2.14a}$$

$$\frac{\partial}{\partial x} p = -\frac{\lambda(q)}{2D}\rho v|v|. \tag{2.14b}$$

The stationary continuity equation (2.14a) implies a constant product of gas density and gas velocity and therefore a constant mass flow $q = A\rho v$ along the pipe. Plugging the definition of q and the mean real gas law

$$p = R_{\mathrm{s}}\rho T_{\mathrm{m}} z_{\mathrm{m}} \tag{2.15}$$

into the stationary mass conservation equation (2.14b) yields

$$\begin{aligned}\frac{\partial}{\partial x}p = -\frac{\lambda(q)}{2D\rho}\rho v|\rho v| &= -\frac{\lambda(q)}{2D\rho}\frac{q}{A}\left|\frac{q}{A}\right| \\ &= -\frac{\lambda(q)}{2DA^2}\frac{R_{\mathrm{s}}T_{\mathrm{m}}z_{\mathrm{m}}}{p}q|q|.\end{aligned} \tag{2.16}$$

Multiplying both sides by $2p$ yields the ordinary differential equation (ODE)

$$\left(\frac{\partial}{\partial x}p\right)2p = \frac{\partial}{\partial x}p^2 = -\frac{\lambda(q)R_{\mathrm{s}}T_{\mathrm{m}}z_{\mathrm{m}}}{DA^2}q|q| = -\Lambda q|q|, \tag{2.17}$$

where we define $\Lambda := \frac{\lambda(q)R_{\mathrm{s}}T_{\mathrm{m}}z_{\mathrm{m}}}{DA^2}$. This is a first-order nonlinear ODE that can be solved easily.

Lemma 2.1.1 (Koch et al. 2015, lemma 2.2)**.** *The solution $p(x)$ to* (2.17) *with initial value $p(0) = p_{\mathrm{in}}$ is given by*

$$p^2(x) = p_{\mathrm{in}}^2 - x\Lambda|q|q. \tag{2.18}$$

Proof. The solution can be verified by derivation of $p(x)$. □

We refer once more to Fügenschuh et al. (2015) and Lurie (2008), where solutions for the respective ODE on non-horizontal pipes are derived.

By evaluating (2.18) at the end of the pipe ($x = L$) and defining a *pressure drop coeffiecient* $l := \Lambda L$, we obtain a pressure drop formula for horizontal pipes:

$$p_{\mathrm{out}}^2 = p_{\mathrm{in}}^2 - \Lambda L|q|q = p_{\mathrm{in}}^2 - l|q|q, \tag{2.19}$$

where $p_{\mathrm{out}}, p_{\mathrm{in}} \in \mathbb{R}_{\geq 0}$ denote the pressure of the gas at the pipe's inlet and outlet, respectively. This relation between ingoing pressure, outgoing pressure, and mass flow along the pipe is also known as the *Weymouth equation* (Weymouth 1912).

Compressors

Compressors are used to increase gas pressure. They are one of the most complex network components in gas networks as a change in pressure is a thermodynamic process that is accompanied by changes in other physical parameters such as density, compressibility factor, and temperature. Increasing pressure can serve multiple ends. Since the gas flow is driven by a pressure gradient, gas is transported over long distances by regularly increasing the pressure with compressors, thereby compensating for the friction-based pressure

loss. Compressors are also needed when injecting gas into a higher-pressure network. Other applications include tasks related to gas storage, e.g., when filling an underground storage facility or when the pressure in a pipeline section is selectively increased in order to store gas in the pipeline itself (so-called *line-pack*). However, as storage-related aspects of gas network operations are typically transient problems, they are out of scope for this work. In our context compressors are mainly used for gas transport or to meet some pressure level for injection into another network.

There are several compressor models used in the literature, ranging from very simple to highly complex. Dynamic programming approaches like Lall and Percell (1990) and Wong and Larson (1968a) typically use a discretized set of possible compression ratios. A compressor model that allows a linear increase in pressure is proposed by Gollmer, Schultz, and Stangl (2015). Even less structured, the article by Wolf and Smeers (2000) allows an arbitrary pressure increase. More complex models like the one in Zavala (2014) arise from the physical process of gas compression as a relative pressure increase that also depends on the flow rate. The most sophisticated models take the feasible operation range of the compressor machines into account (Rose et al. 2016), as well as the combination of multiple compressors into compressor groups as in Geißler, Martin, et al. (2015) and Wu et al. (2000).

The physical functioning of a compressor machine can be modeled as an *adiabatic thermodynamic process*, i.e., there is no heat or mass exchange between the compressor and its surroundings. By supplying mechanical energy, an input volume V_{in} of gas is compressed to a smaller output volume V_{out}. This increases the pressure p_{out} as well as temperature T_{out} of the outgoing gas stream. For a comprehensive derivation of the compressor equations from the fundamental laws of thermodynamics, we refer to Fügenschuh et al. (2015).

Here, we will briefly present a model for *turbo compressors*. In terms of thermodynamics, when gas is compressed from an initial state with pressure p_{in} and temperature T_{in} to a final state with pressure p_{out}, its *specific adiabatic enthalphy*—the sum of the systems internal energy and the product of pressure and volume—increases. This change ΔH_{ad} in adiabatic enthalpy (in $\mathrm{J\,kg^{-1}}$) can be approximated with

$$\Delta H_{\mathrm{ad}} = z_{\mathrm{in}} T_{\mathrm{in}} R_{\mathrm{s}} \frac{\kappa}{\kappa - 1} \left(\left(\frac{p_{\mathrm{out}}}{p_{\mathrm{in}}} \right)^{\frac{\kappa-1}{\kappa}} - 1 \right), \tag{2.20}$$

where we denote with κ the *isentropic exponent*, with z_{in} the compressibility factor of the inflowing gas, and with R_{s} the specific gas constant of the inflowing gas; see Fügenschuh et al. (2015). The parameter κ depends on the

gas pressure and temperature during the entire process. While there are several approximations for κ available, see e.g., Schmidt, Steinbach, and Willert (2015b) for a brief discussion, in practice a constant value of $\kappa = 1.29$ is often used.

Not every change ΔH_{ad} in adiabatic enthalpy can be realized by a compressor machine. Let the volumetric flow Q (in $\mathrm{m}^3\,\mathrm{s}^{-1}$) entering the gas compressor be given by

$$Q = \frac{q}{\rho}. \tag{2.21}$$

The achievable compression is constrained by the compressor's *operation range*. It is given as a set of feasible pairs of volumetric flow Q and change in adiabatic enthalpy ΔH_{ad}. Figure 2.1 shows an exemplary operation range of a turbo compressor. The gray area represents the set of possible compressor controls. We point out that this diagram is obtained from extrapolations of experimental measurements. A more comprehensive explanation of this diagram can be found in Schmidt, Steinbach, and Willert (2015b).

The required power P (in W) for the compression process follows

$$P = \frac{\Delta H_{\mathrm{ad}} q}{\eta_{\mathrm{ad}}}, \tag{2.22}$$

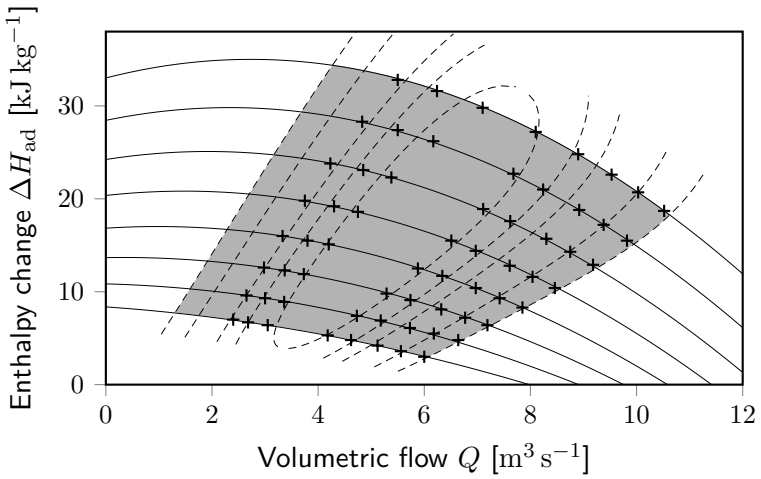

Figure 2.1: An exemplary characteristic diagram of a turbo compressor. The gray area denotes the feasible operation range, i.e., the set of viable combinations of volumetric flow and change in adiabatic energy. Reprinted/adapted by permission from RightsLink: Springer Nature Optim. and Eng. by Schmidt, Steinbach, and Willert (2015b), © 2014.

where the efficiency of the compressor machine is modeled with a dimensionless efficiency parameter $\eta_{\mathrm{ad}} \in (0, 1)$. Compressor machines are typically driven by electric drives, or by gas engines or gas turbines whose fuel is taken directly from the pipeline.

Valves and control valves

Valves are used to regulate gas flow and pressure. We distinguish several different types of valves. The most basic *valve* has two states: *closed* and *open*. When closed, gas flow is prevented and the gas pressures at the inlet and outlet are decoupled. When open, there are no restrictions and the gas flow is unhindered:

$$\text{closed valve: } q = 0 \text{ and } p_{\mathrm{in}},\, p_{\mathrm{out}} \text{ decoupled}, \tag{2.23}$$

$$\text{open valve: } q \text{ unrestricted and } p_{\mathrm{in}} = p_{\mathrm{out}}. \tag{2.24}$$

So-called *check valves* allow gas flow to pass the valve in one direction and restrict flow in the other direction. Valves and check valves are typically used to close off parts of the network like e.g., gas storage facilities, or to force the gas flow along a specific path.

Sometimes the gas pressure has to be reduced to a certain level, e.g., if gas from a high-pressure transport network is to be fed into a low-pressure regional distribution network. In this case *control valves*, also known as *pressure regulators*, are used. Control valves can be equipped with a remote control or work autonomously. Valves that cannot be remotely controlled are set up once to regulate the pressure of the outflowing gas to some fixed value $p_{\mathrm{out}}^{\mathrm{set}}$.

In this work, only remote-controlled control valves are used. Control valves with remote access are either *closed* or *active*. As with normal valves, closed control valves allow no flow, and the inlet and outlet pressures p_{in}, p_{out} are decoupled. An active valve decreases the inlet pressure p_{in} by some amount within the range $[\underline{\Delta}, \overline{\Delta}] \subseteq \mathbb{R}$. This leads to the following model:

$$\text{closed control valve: } q = 0 \text{ and } p_{\mathrm{in}},\, p_{\mathrm{out}} \text{ decoupled}; \tag{2.25}$$

$$\text{active control valve: } q \geq 0 \text{ and } 0 \leq \underline{\Delta} \leq p_{\mathrm{in}} - p_{\mathrm{out}} \leq \overline{\Delta}. \tag{2.26}$$

Similar to compressors, gas can only flow through control valves in one direction. If a bidirectional traversal is desired, an *open* mode for control valves is sometimes modeled as well.

Short pipes

Short pipes are network elements that do not exist in reality and are only introduced for modeling purposes. They follow no physical laws and their function is to set their inlet pressure p_{in} and their outlet pressures p_{out} to the same value:

$$p_{\text{in}} = p_{\text{out}}. \tag{2.27}$$

Moreover, gas flow along a short pipe is not influenced in any way. A short pipe between two points is virtually equivalent to merging those two points into one.

Short pipes are used, for example, to model pipes with negligible pressure drop, such as those inside a compressor station. Another application is the modeling of a gas storage tank, where separate injection and withdrawal points are connected to the gas storage node via short pipes.

We use short pipes mainly during the construction of test instances. Since the real-world gas network topologies from GasLib (Schmidt et al. 2017) contain network components such as resistors or valves that are outside the scope of this work, all these elements are replaced by short pipes.

2.2 Gas transport with linear active elements

The gas networks under consideration in this work consist of *pipes* and *pressure-modifying elements*. We restrict ourselves to compressors and control valves as active elements. The network topology is represented by a finite directed graph $\mathcal{G} = (\mathcal{V}, \mathcal{A})$ with nodes $\mathcal{V} = \{1, 2, \ldots, n\}$ and arcs $\mathcal{A} = \{a_1, \ldots, a_m\} \subseteq \mathcal{V} \times \mathcal{V}$. We assume that $\mathcal{G}$ is connected and contains no self-loops. Let $|\mathcal{V}| = n \in \mathbb{N}$ and $|\mathcal{A}| = m \in \mathbb{N}$ be the number of nodes and arcs in $\mathcal{G}$, respectively.

The physical state of the gas in the network is described by the nonnegative pressure $p_v \in \mathbb{R}_{\geq 0}$ at each node $v \in \mathcal{V}$ and the mass flow rate $q_a \in \mathbb{R}$ along each arc $a \in \mathcal{A}$. A positive sign of q_a for arc $a = (v, w) \in \mathcal{A}$ indicates gas flow in arc direction, i.e., from node v to node w. A negative sign of q_a implies a flow in reverse arc direction. Since the pressure variables in our models are always squared, we introduce a new nonnegative variable $\pi_v := p_v^2$ that is used in place of the squared pressures. Let $\boldsymbol{\pi} = (\pi_v)_{v \in \mathcal{V}} \in \mathbb{R}^n_{\geq 0}$ and $\boldsymbol{q} = (q_a)_{a \in \mathcal{A}} \in \mathbb{R}^m$ be the respective vectors of squared pressures and mass flow rates within the network.

Gas can be fed into or withdrawn from the network at specific points. Let $d_v \in \mathbb{R}$ be the *gas demand* at node $v \in \mathcal{V}$ (in $\mathrm{kg\,s^{-1}}$) and let $\boldsymbol{d} = (d_v)_{v\in\mathcal{V}} \in \mathbb{R}^n$ be the vector of demands for the whole network. The vector $\boldsymbol{d}$ of nodal demands is also known as the *nomination* vector. As is usual for network flow problems, the demand has to be *balanced*, i.e., $\sum_{v\in\mathcal{V}} d_v = 0$.

Due to technical, legal, or contractual obligations, the squared pressure π_v is bounded at each node $v \in \mathcal{V}$ from below by $\underline{\pi}_v \in \mathbb{R}_{\geq 0}$ and from above by $\overline{\pi}_v \in \mathbb{R}_{\geq 0}$:

$$\pi_v \in [\underline{\pi}_v, \overline{\pi}_v] \quad \text{for all } v \in \mathcal{V}. \tag{2.28}$$

We denote with $\underline{\boldsymbol{\pi}} = (\underline{\pi}_v)_{v\in\mathcal{V}} \in \mathbb{R}^n_{\geq 0}$ and $\overline{\boldsymbol{\pi}} = (\overline{\pi}_v)_{v\in\mathcal{V}} \in \mathbb{R}^n_{\geq 0}$ the vectors of lower squared pressure bounds and upper squared pressure bounds, respectively. As a short form of (2.28), we write $\boldsymbol{\pi} \in [\underline{\boldsymbol{\pi}}, \overline{\boldsymbol{\pi}}]$.

Similar to linear network flow problems, conservation of mass holds at each node:

$$\sum_{a=(v,w)\in\mathcal{A}} q_a \; - \sum_{a=(w,v)\in\mathcal{A}} q_a = d_v \quad \text{for all } v \in \mathcal{V}. \tag{2.29}$$

This set of constraints can be concisely written using the node-arc incidence matrix $\boldsymbol{A} \in \mathbb{R}^{n\times m}$. For all combinations $v \in \mathcal{V}$ and $a \in \mathcal{A}$, the entries of $\boldsymbol{A}$ are given by

$$A_{va} = \begin{cases} +1 & \text{if } a = (w, v) \in \mathcal{A} \text{ for some } w \in \mathcal{V}, \\ -1 & \text{if } a = (v, w) \in \mathcal{A} \text{ for some } w \in \mathcal{V}, \\ 0 & \text{otherwise.} \end{cases} \tag{2.30}$$

With the node-arc incidence matrix, the constraints (2.29) can be stated as

$$\boldsymbol{A}\boldsymbol{q} = \boldsymbol{d}. \tag{2.31}$$

The set of arcs $\mathcal{A}$ is partitioned into a set of pipes $\mathcal{A}_{\mathrm{pi}} \subseteq \mathcal{A}$ and a set of pressure-modifying elements $\mathcal{A}_{\mathrm{pm}} \subseteq \mathcal{A}$. Both subsets $\mathcal{A}_{\mathrm{pi}}$ and $\mathcal{A}_{\mathrm{pm}}$ are disjoint and their union is the set of arcs $\mathcal{A} = \mathcal{A}_{\mathrm{pi}} \cup \mathcal{A}_{\mathrm{pm}}$.

Pipes are so-called *passive* network elements, whereas pressure-modifying elements are *active elements*, as an operator can control their state. A gas network consisting only of pipes, i.e., $\mathcal{A} = \mathcal{A}_{\mathrm{pi}}$, is also referred to as a *passive network*. Similarly, a network is called *active* if $\mathcal{A}_{\mathrm{pm}} \neq \emptyset$, i.e., the network contains pressure-modifying elements.

Based on the descriptions in section 2.1, we now define the constraints for the individual network components.

Gas flowing along a pipe experiences a pressure drop. This aspect is modeled using the Weymouth equation (2.19). In the following, let $|x|^* := x|x|$ be the signed square function. The Weymouth equation is given by

$$\pi_w - \pi_v = -l_a q_a |q_a| = -l_a |q_a|^* \quad \text{for all } (v,w) = a \in \mathcal{A}_{\mathrm{pi}}, \tag{2.32}$$

where

$$l_a = L_a \Lambda_a = \frac{\lambda(q_a) R_{\mathrm{s}} T_{\mathrm{m}} z_{\mathrm{m}}^{(a)} L_a}{D_a A_a^2}, \tag{2.33}$$

using Nikuardse's approximation (2.12) of the friction factor

$$\lambda_a \equiv \lambda(q_a) = \Big(2\log_{10}\Big(\tfrac{D_a}{k_a}\Big) + 1.138\Big)^{-2}, \tag{2.34}$$

Papay's approximation (2.6) of the compressibility factor

$$\begin{aligned} z_{\mathrm{m}}^{(a)} &\equiv z_{\mathrm{m}}(p_{\mathrm{m}}^{(a)}, T_{\mathrm{m}}) \\ &= 1 - 3.52 \tfrac{p_{\mathrm{m}}^{(a)}}{p_{\mathrm{c}}} \exp\Big(-2.26 \tfrac{T_{\mathrm{m}}}{T_{\mathrm{c}}}\Big) + 0.247 \Big(\tfrac{p_{\mathrm{m}}^{(a)}}{p_{\mathrm{c}}}\Big)^2 \exp\Big(-1.878 \tfrac{T_{\mathrm{m}}}{T_{\mathrm{c}}}\Big), \end{aligned} \tag{2.35}$$

and a mean pressure (2.13) of

$$p_{\mathrm{m}}^{(a)} = \tfrac{1}{2}\big(\max\{\underline{p}_v, \underline{p}_w\} + \min\{\overline{p}_v, \overline{p}_w\}\big). \tag{2.36}$$

We assume that the mean pressure can be approximated a priori, e.g., by using the supplemented pressure bounds $\underline{\pi}$ and $\overline{\pi}$. The other symbols refer to the following quantities.

Parameters of the gas mixture:

R_{s}	specific gas constant,	T_{m}	mean gas temperature,
p_{c}	pseudocritical temperature,	T_{c}	pseudocritical pressure.

Parameters of each pipe $a \in \mathcal{A}_{\mathrm{pi}}$:

l_a	pressure drop coefficient,	L_a	pipe length,
D_a	pipe diameter,	A_a	pipe cross-sectional area,
k_a	integral roughness,	λ_a	friction factor,
$z_{\mathrm{m}}^{(a)}$	mean compressibility factor,	$p_{\mathrm{m}}^{(a)}$	mean gas pressure.

The magnitude of the pressure loss scales with the magnitude of the mass flow rate q_a and the *pressure drop coefficient* $l_a \in \mathbb{R}_{>0}$. Let $\boldsymbol{l} = (l_a)_{a \in \mathcal{A}_{\mathrm{pi}}} \in \mathbb{R}_{>0}^{|\mathcal{A}_{\mathrm{pi}}|}$ be the vector of all pressure drop coefficients in the network.

Pressure-modifying elements act on the squared pressure difference between two connected nodes $(v, w) \in \mathcal{A}_{\mathrm{pm}}$ and may change this difference linearly by some amount $x_a^{\mathrm{pm}} \in [\underline{x}_a^{\mathrm{pm}}, \overline{x}_a^{\mathrm{pm}}] \subseteq \mathbb{R}$:

$$\pi_w - \pi_v = x_a^{\mathrm{pm}} \quad \text{for all } (v, w) = a \in \mathcal{A}_{\mathrm{pm}}. \tag{2.37}$$

Note that we allow $\underline{x}_a^{\mathrm{pm}} \in \mathbb{R} \cup \{-\infty\}$ and $\overline{x}_a^{\mathrm{pm}} \in \mathbb{R} \cup \{\infty\}$.

We divide the group of pressure-modifying elements into three types: simplified *linear compressors* that can increase pressure, *control valves* that can decrease pressure, and *abstract pressure controllers* that can manipulate the pressure as desired. The mathematical descriptions of the three types differ only by the permitted pressure change:

$$\text{abstract pressure controller} \quad x_a^{\mathrm{pm}} \in \mathbb{R}, \tag{2.38a}$$

$$\text{compressor} \quad x_a^{\mathrm{pm}} \geq 0, \tag{2.38b}$$

$$\text{control valve} \quad x_a^{\mathrm{pm}} \leq 0. \tag{2.38c}$$

Throughout this thesis, we sometimes use "compressor" as a collective term for all pressure-modifying elements $\mathcal{A}_{\mathrm{pm}}$, since all three types of pressure modifying element follow the same mathematical model.

The abstract pressure controller is a virtual element that has no counterpart in reality. As it allows arbitrary pressure changes, it can be used to control the pressure at injection or withdrawal points. By passing the injected or withdrawn gas over this virtual element, the pressure at this point can be adjusted as an exogenous controllable variable.

Compressors are used to increase the gas pressure. We use a linear compressor model (2.37) where the increase in pressure is independent of the flow through the compressor. In general, compressors can only increase pressure if the passing gas flows through them in the correct direction. As is shown later on in section 5.2.3, tight flow bounds for our setting can be calculated easily with (5.46). The obtained bounds can be used to verify the direction constraint.

Control valves are used to decrease the gas pressure. This is important when gas from a larger transport network operating at a higher pressure is to be fed into a subnet operating at a lower pressure.

Let $\boldsymbol{x}^{\mathrm{pm}} = (x_a^{\mathrm{pm}})_{a \in \mathcal{A}_{\mathrm{pm}}} \in \mathbb{R}^{|\mathcal{A}_{\mathrm{pm}}|}$ be the vector of all pressure modifying "power levels" within the network. Moreover, let $\underline{\boldsymbol{x}}^{\mathrm{pm}} = (\underline{x}_a^{\mathrm{pm}})_{a \in \mathcal{A}_{\mathrm{pm}}} \in \mathbb{R}^{|\mathcal{A}_{\mathrm{pm}}|}$

and $\overline{\boldsymbol{x}}^{\mathrm{pm}} = (\overline{x}_a^{\mathrm{pm}})_{a\in\mathcal{A}_{\mathrm{pm}}} \in \mathbb{R}^{|\mathcal{A}_{\mathrm{pm}}|}$ be the vectors of the lower and upper limits of the squared pressure change.

Next, we describe the squared pressure change caused by pipes and pressure-modifying elements in the network by a combined set of constraints. Let $\boldsymbol{\psi} = (\psi_a)_{a\in\mathcal{A}}$ be a vector-valued function whose entries describe the change in squared pressure at all arcs $a \in \mathcal{A}$:

$$\begin{aligned} \boldsymbol{\psi}\colon \mathbb{R}^{|\mathcal{A}_{\mathrm{pi}}|} \times \mathbb{R}^{|\mathcal{A}|} \times \mathbb{R}^{|\mathcal{A}_{\mathrm{pm}}|} &\to \mathbb{R}^{|\mathcal{A}|}, \\ \psi_a(\boldsymbol{l}, \boldsymbol{q}, \boldsymbol{x}^{\mathrm{pm}}) &= \begin{cases} -l_a q_a |q_a| = -l_a |q_a|^* & \text{if } a \in \mathcal{A}_{\mathrm{pi}}, \\ x_a^{\mathrm{pm}} & \text{if } a \in \mathcal{A}_{\mathrm{pm}}. \end{cases} \end{aligned} \tag{2.39}$$

Since the pressure drop coefficients $\boldsymbol{l}$ will be treated as uncertain later on, the definition of $\boldsymbol{\psi}$ includes $\boldsymbol{l}$ as an argument. However, if $\boldsymbol{l}$ is constant, we omit this parameter from $\boldsymbol{\psi}$ to avoid complicating the notation unnecessarily.

With $\boldsymbol{\psi}$, the squared pressure change caused by a network component can be written as

$$\pi_w - \pi_v = \psi_a(\boldsymbol{q}, \boldsymbol{x}^{\mathrm{pm}}) \quad \text{for all } a \in \mathcal{A}. \tag{2.40}$$

Using the node-arc incidence matrix $\boldsymbol{A}$, constraint (2.40) for all arcs amounts to

$$\boldsymbol{A}^\top \boldsymbol{\pi} = \boldsymbol{\psi}(\boldsymbol{q}, \boldsymbol{x}^{\mathrm{pm}}). \tag{2.41}$$

Typically, we seek to minimize the cost of pressure changes that arise, e.g., due to compressor fuel consumption. As described in section 2.1, a compressor's energy consumption is directly related to the degree of compression of the gas. Given a vector $\boldsymbol{x}^{\mathrm{pm}}$ of pressure modifications, we model the total energy cost with a linear function

$$\boldsymbol{x}^{\mathrm{pm}} \mapsto \boldsymbol{c}^\top \boldsymbol{x}^{\mathrm{pm}}, \tag{2.42}$$

where $\boldsymbol{c} = (c_a)_{a\in\mathcal{A}_{\mathrm{pm}}} \in \mathbb{R}^{|\mathcal{A}_{\mathrm{pm}}|}$ is a cost vector associated with the given pressure-modifying elements. We note that for control valves and abstract energy controllers, it typically holds that $c_a = 0$.

A combination of flow conservation (2.31), squared pressure changes at each arc (2.41), bounds for nodal pressure, pressure-modifying elements,

and total energy cost objective (2.42) yields the *stationary compressor cost minimization problem*:

$$\min_{\boldsymbol{\pi},\boldsymbol{q},\boldsymbol{x}^{\mathrm{pm}}} \quad \boldsymbol{c}^{\top}\boldsymbol{x}^{\mathrm{pm}} \tag{2.43a}$$

$$\text{s.t.} \quad \boldsymbol{A}\boldsymbol{q} = \boldsymbol{d}, \tag{2.43b}$$

$$\boldsymbol{A}^{\top}\boldsymbol{\pi} = \boldsymbol{\psi}(\boldsymbol{q}, \boldsymbol{x}^{\mathrm{pm}}), \tag{2.43c}$$

$$\boldsymbol{\pi} \in [\underline{\boldsymbol{\pi}}, \overline{\boldsymbol{\pi}}], \tag{2.43d}$$

$$\boldsymbol{q} \in \mathbb{R}^{m}, \tag{2.43e}$$

$$\boldsymbol{x}^{\mathrm{pm}} \in [\underline{\boldsymbol{x}}^{\mathrm{pm}}, \overline{\boldsymbol{x}}^{\mathrm{pm}}]. \tag{2.43f}$$

Clearly, this is a nonlinear, non-convex optimization task. If the focus is on checking the satisfiability of a particular nomination, this problem is also referred to as the *stationary nomination validation problem*. In this thesis, both terms are used interchangeably.

Over the years, many approaches have been developed to solving this and other related problems in gas; we give a brief survey in section 2.5.

Remark 2.2.1. We briefly discuss the appearing units of the variables in problem (2.43). In the previous section, we carefully supplemented all appearing values and constants with their appropriate units. Hence the mass flow rate variables $\boldsymbol{q}$ are in $\mathrm{kg\,s^{-1}}$ and the squared pressure variables $\boldsymbol{\pi}$ are in Pa.

For our practical applications, however, we follow a different convention that is more common in natural gas network operations. The flow variables $\boldsymbol{q}$ are given in *thousand normal cubic meters per hour* ($1000\,\mathrm{N\,m^3\,h^{-1}}$), where one normal cubic meter of gas is the amount of gas that fills one cubic meter under normal conditions[1]. The squared pressure variables $\boldsymbol{\pi}$ as well as the compressor power variables $\boldsymbol{x}^{\mathrm{pm}}$ are given in bar^2.

Remark 2.2.2. The presented model for the gas flow in natural gas networks uses the Weymouth equation. It is an example of the more general class of *potential driven networks*; see, e.g., Gross et al. (2018) for an introduction. In such a network, the flow q_a along an arc $(v, w) = a \in \mathcal{A}$ depends on the potential difference at the incident nodes:

$$\pi_w - \pi_v = \xi_a \phi(q_a), \tag{2.44}$$

where $\phi\colon \mathbb{R} \to \mathbb{R}$ is a continuous, strictly Increasing function that satisfies $\phi(-q_a) = -\phi(q_a)$ and $\xi_a \in \mathbb{R}$ is a constant. Other examples for potential driven networks include lossless direct current electricity networks where

[1] Standard atmosphere: $15\,^{\circ}\mathrm{C}$, $1.013\,25\,\mathrm{bar}$

$\phi^{\mathrm{DC}}(q) = q$ and water networks where $\phi^{\mathrm{w}}(q) = \operatorname{sgn}(q)|q|^{1.852}$. We note that many properties of stationary gas networks still hold for a general potential driven network. This includes, e.g., the uniqueness of solutions and the decomposable structure we investigate in chapter 5.

2.3 Reduction of variables

In the recent work by Gotzes et al. (2016), the authors show how the nomination validation problem (2.43) for a passive network can be converted into an equivalent formulation by eliminating variables. Similar results have also been discovered by Osiadacz and Pienkosz (1988) and Mallinson et al. (1993). In fact, some of the ideas are already present in Kirchhoff's laws for electrical circuits; see Kirchhoff (1847).

More precisely, all squared pressure variables and all but $|\mathcal{V}| - 1$ flow variables are removed from the model. In this section, we extend the result of Gotzes et al. (2016) for gas networks consisting exclusively of pipes to networks with active elements. A similar result for networks with active elements is derived in Gollmer, Schultz, and Stangl (2015). We note that besides changing the notation to include pressure-modifying elements, no new major mathematical steps are necessary to extend their result to active networks in our setting.

The central idea of the reformulation is to express feasible flows within the network as a combination of a flow along a spanning tree of the graph and a flow along cycles of the graph. This is a well-known decomposition that is used, e.g., in the network simplex algorithm; see Ahuja, Magnanti, and Orlin (1993).

While the linear flow part is straightforward, the difficulty lies in translating the pressures correctly into this description. The squared pressure at each node $v \in \mathcal{V}$ is expressed relative to an arbitrarily chosen root node $r \in \mathcal{V}$ by defining an aggregated pressure change along the unique path from r to v in a fixed spanning tree. Moreover, similar to Kirchhoff's loop rule in electrical circuits, the total pressure change along each cycle must sum up to zero.

In the following, we introduce the reduced model of Gotzes et al. (2016) and derive a graph-theoretical interpretation. This graph-centric view allows us to use a simpler notation and will also be useful for later results.

Graph matrices We present properties of the node-arc incidence matrix and introduce the path and cycle matrices of a graph. The material in this paragraph is based on Bapat (2014, ch. 2, ch. 5). A short summary of the

conventions we use in connection with graphs can be found in the notation chapter on page xi. In particular, we would like to point out that we treat all graphs as if they were undirected; the direction of the edges is only relevant for the sign of the flow direction in the gas network context.

In the following, let $\mathcal{G} = (\mathcal{V}, \mathcal{A})$ be a connected digraph with $\mathcal{V} = \{1, \dots, n\}$ and $\mathcal{A} = \{a_1, \dots, a_m\}$. Let $\mathcal{B} \subseteq \mathcal{A}$ denote the arcs of a spanning tree $\mathcal{T} = (\mathcal{V}, \mathcal{B})$ of $\mathcal{G}$ and let $\mathcal{N} = \mathcal{A} \setminus \mathcal{B}$ denote the remaining arcs. We call $\mathcal{T}$ the *$\mathcal{B}$-induced spanning tree* or the *spanning tree induced by $\mathcal{B}$*. W.l.o.g., we select $r = 1 \in \mathcal{V}$ as root node. Furthermore, we assume that $\mathcal{B} = \{a_1, \dots, a_{n-1}\}$ and $\mathcal{N} = \{a_n, \dots, a_m\}$. This situation can always be achieved by renaming nodes and edges.

First, we consider the *node-arc incidence matrix* $\boldsymbol{A} \in \mathbb{R}^{n \times m}$ of $\mathcal{G}$. The rows of $\boldsymbol{A}$ are indexed by the nodes $\mathcal{V}$ and the columns of $\boldsymbol{A}$ are indexed by the arcs $\mathcal{A}$. We recall the previously given definition that the entries of $\boldsymbol{A}$ satisfy $A_{va} = +1$ if $a = (w, v) \in \mathcal{A}$, $A_{va} = -1$ if $a = (v, w) \in \mathcal{A}$, and $A_{va} = 0$ otherwise. Since $\mathcal{G}$ is connected, $\boldsymbol{A}$ has rank $n - 1$, and hence an arbitrary row can be removed without changing the solution space; see, e.g., Ahuja, Magnanti, and Orlin (1993). After removing the row $\boldsymbol{A}_{r\cdot}$ corresponding to a root node r from $\boldsymbol{A}$, we obtain the *reduced node-arc incidence matrix* $\tilde{\boldsymbol{A}} \in \mathbb{R}^{(n-1) \times m}$ with full rank.

Every spanning tree $\mathcal{T}$ of $\mathcal{G}$ corresponds to a basis $\mathcal{B}$ of $\tilde{\boldsymbol{A}}$ and vice versa; see Ahuja, Magnanti, and Orlin (1993, p. 442). Taking the $\mathcal{B}$-induced spanning tree into account, we partition $\tilde{\boldsymbol{A}}$ into a nonsingular basic submatrix $\tilde{\boldsymbol{A}}_{\mathcal{B}} \in \mathbb{R}^{(n-1) \times (n-1)}$ and a nonbasic submatrix $\tilde{\boldsymbol{A}}_{\mathcal{N}} \in \mathbb{R}^{(n-1) \times (m-n+1)}$:

$$\boldsymbol{A} = \left[\begin{array}{c} \boldsymbol{A}_{r\cdot} \\ \hline \tilde{\boldsymbol{A}} \end{array}\right] = \left[\begin{array}{c|c} \boldsymbol{A}_{r\mathcal{B}} & \boldsymbol{A}_{r\mathcal{N}} \\ \hline \tilde{\boldsymbol{A}}_{\mathcal{B}} & \tilde{\boldsymbol{A}}_{\mathcal{N}} \end{array}\right]. \tag{2.45}$$

While the basic part $\tilde{\boldsymbol{A}}_{\mathcal{B}}$ corresponds to the spanning tree $\mathcal{T}$, the nonbasic part $\tilde{\boldsymbol{A}}_{\mathcal{N}}$ can be seen as a representation of fundamental cycles in $\mathcal{G}$. A *fundamental cycle* is the unique cycle that emerges after adding arc a to the $\mathcal{B}$-induced spanning tree $\mathcal{T}$. We assume that the orientation of this cycle follows the orientation of $a = (v, w)$, i.e., the nodes in the cycle occur in order $v, w, \dots, v$. Altogether, each arc $a \in \mathcal{N}$ corresponds to one fundamental cycle and vice versa.

Next, we present two results from Bapat (2014) that relate submatrices of the reduced node-arc incidence matrix to paths and cycles in the graph.

The first lemma shows how the inverse of the basic submatrix of the node-arc incidence matrix encodes paths in the corresponding spanning tree. We define a *reduced path matrix* that encodes the unique paths from the root

node to all other nodes in the $\mathcal{B}$-induced spanning tree. Since all paths in a tree are uniquely determined, this matrix is well-defined once a spanning tree of $\mathcal{G}$ is selected. Let $\tilde{\boldsymbol{P}} \in \mathbb{R}^{(n-1)\times(n-1)}$ be a matrix whose rows are indexed by $v \in \mathcal{V} \setminus \{r\}$ and whose columns are indexed by $a \in \mathcal{B}$. Each row $\tilde{\boldsymbol{P}}_{v\cdot}$ of $\tilde{\boldsymbol{P}}$ contains the incidence vector of the unique path from root node r to a different node $v \in \mathcal{V} \setminus \{r\}$. We abbreviate $v \to w$ as a symbol for the (unique) path from v to w in $\mathcal{T}$. Hence, the reduced path matrix $\tilde{\boldsymbol{P}}$ is defined as

$$\tilde{P}_{v,a} = \begin{cases} +1 & \text{if } a \text{ is on } r \to v \text{ and in path direction,} \\ -1 & \text{if } a \text{ is on } r \to v \text{ and in reverse path direction,} \\ 0 & \text{otherwise,} \end{cases} \tag{2.46}$$

where $v \in \mathcal{V} \setminus \{r\}$ and $a \in \mathcal{B}$.

Similarly, we introduce a *(full) path matrix* that encodes the paths between two pairs of nodes $v, w \in \mathcal{V}$ in the spanning tree. Let $\boldsymbol{P} \in \mathbb{R}^{n^2\times m}$ be a matrix whose rows are indexed by pairs of nodes $v, w \in \mathcal{V}$ and whose columns are indexed by arcs $a \in \mathcal{B}$. A row $\boldsymbol{P}_{vw,\cdot}$ of $\boldsymbol{P}$ is the incidence vector of the unique path from v to w in the $\mathcal{B}$-induced spanning tree $\mathcal{T}$. Hence, the path matrix is defined as

$$P_{vw,a} = \begin{cases} +1 & \text{if } a \text{ is on } v \to w \text{ and in path direction,} \\ -1 & \text{if } a \text{ is on } v \to w \text{ and in reverse path direction,} \\ 0 & \text{otherwise,} \end{cases} \tag{2.47}$$

where $v, w \in \mathcal{V}$ and $a \in \mathcal{B}$. A path from v to w can be constructed by taking the path from v to r followed by taking the path from r to w. Deleting all arcs that are shared by both paths leads to the unique path from v to w. Therefore, the incidence vector $\boldsymbol{P}_{vw,\cdot}$ of the path $v \to w$ satisfies

$$\boldsymbol{P}_{vw,\cdot} = -\tilde{\boldsymbol{P}}_{v,\cdot} + \tilde{\boldsymbol{P}}_{w,\cdot}, \tag{2.48}$$

where we let $\tilde{\boldsymbol{P}}_{r,\cdot} = (0, \ldots, 0)$ for the sake of convenience.

We point out that $P_{vv,\cdot} = (0, \ldots, 0)$ for all $v \in \mathcal{V}$. While this leads to a more convenient notation, these rows are usually ignored in the upcoming practical applications.

The following lemma characterizes $\tilde{\boldsymbol{P}}$ in terms of the node-arc incidence matrix.

Lemma 2.3.1 (Bapat 2014, thm. 2.10)**.** *Let $\mathcal{G} = (\mathcal{V}, \mathcal{A})$ be a connected digraph and let $\mathcal{B} \subseteq \mathcal{A}$ induce a spanning tree $\mathcal{T}$ of $\mathcal{G}$ with root $r \in \mathcal{V}$ as defined above.*

Let $\tilde{\boldsymbol{A}}$ be the corresponding reduced node-arc incidence matrix of $\mathcal{G}$ and let $\tilde{\boldsymbol{P}}$ be the corresponding reduced path matrix as defined above.

Then the columns $(\tilde{\boldsymbol{A}}_{\mathcal{B}}^{-1})_{\cdot v}$ of $\tilde{\boldsymbol{A}}_{\mathcal{B}}^{-1}$ are the incidence vectors of the (unique) paths from root node r to all other nodes $v \in \mathcal{V} \setminus \{r\}$ in $\mathcal{T}$, i.e.,

$$\tilde{\boldsymbol{P}} = (\tilde{\boldsymbol{A}}_{\mathcal{B}}^{-1})^{\top}. \tag{2.49}$$

Remark 2.3.2. We give a short explanation of this result. Let $v \in \mathcal{V}$ with $v \neq r$ be given. A column $(\tilde{\boldsymbol{A}}_{\mathcal{B}}^{-1})_{\cdot v}$ of $\tilde{\boldsymbol{A}}_{\mathcal{B}}^{-1}$ that corresponds to $v \in \mathcal{V}$ is the solution of the linear equation system

$$\tilde{\boldsymbol{A}}_{\mathcal{B}}(\tilde{\boldsymbol{A}}_{\mathcal{B}}^{-1})_{\cdot v} = \boldsymbol{e}_v, \tag{2.50}$$

where $\boldsymbol{e}_v \in \mathbb{R}^{|\mathcal{V}|-1}$ is the v-th standard basis vector. We can interpret this system as a linear flow network problem. Hence, $(\tilde{\boldsymbol{A}}_{\mathcal{B}}^{-1})_{\cdot v}$ denotes a linear flow in the $\mathcal{B}$-spanning tree $\mathcal{T}$ that transports one unit from the root node r to the node v. Other nodes in the network have a demand of zero. All paths between pairs of nodes are uniquely determined in a tree and thus the flow along each arc is either zero or a unit flow in positive or negative arc direction. Thus the columns of $\tilde{\boldsymbol{A}}_{\mathcal{B}}^{-1}$ only contain values in $\{0, \pm 1\}$ and are the incidence vectors of paths in the spanning tree $\mathcal{T}$.

The second lemma gives a full description of the fundamental cycles in $\mathcal{G}$ after a spanning tree $\mathcal{T}$ is selected. It was already mentioned that given a $\mathcal{B}$-induced spanning tree of $\mathcal{G}$, the fundamental cycles of $\mathcal{G}$ are uniquely determined. In the following, we refer to the fundamental cycle that is defined by $a \in \mathcal{N}$ as the *a-fundamental cycle*. The direction of a fundamental cycle is determined by the direction of $a \in \mathcal{N}$. We define a *cycle matrix* $\boldsymbol{C} \in \mathbb{R}^{(m-n+1)\times m}$ whose rows encode the fundamental cycles of $\mathcal{G}$. The rows of $\boldsymbol{C}$ are indexed by the set of arcs $\mathcal{N}$ that are not in the spanning tree; the columns of $\boldsymbol{C}$ are indexed by the set of arcs $\mathcal{A}$ of $\mathcal{G}$. We define

$$C_{a,a'} = \begin{cases} +1 & \text{if } a' \text{ is on } a\text{-fund. cycle and in cycle direction,} \\ -1 & \text{if } a' \text{ is on } a\text{-fund. cycle and in reverse cycle dir.,} \\ 0 & \text{otherwise,} \end{cases} \tag{2.51}$$

where $a \in \mathcal{N}$ and $a' \in \mathcal{A}$.

The following result shows how the cycle matrix can be computed from the node-arc incidence matrix. The lemma is based on Bapat (2014, thm. 5.6) and is modified to fit our notation.

Lemma 2.3.3 (Bapat 2014, thm. 5.6)**.** *Let $\mathcal{G} = (\mathcal{V}, \mathcal{A})$ be a connected digraph. Let $\mathcal{B} \subseteq \mathcal{A}$ induce a spanning tree $\mathcal{T}$ of $\mathcal{G}$ with root $r \in \mathcal{V}$. Let $\tilde{\boldsymbol{A}}$ be the corresponding reduced node-arc incidence matrix of $\mathcal{G}$ and let $\boldsymbol{C}$ be the corresponding cycle matrix.*

Then the cycle matrix can be written as

$$\boldsymbol{C} = [\boldsymbol{C}_{\mathcal{B}} \mid \boldsymbol{C}_{\mathcal{N}}] = [-(\tilde{\boldsymbol{A}}_{\mathcal{B}}^{-1}\tilde{\boldsymbol{A}}_{\mathcal{N}})^{\top} \mid \boldsymbol{I}], \tag{2.52}$$

i.e., $\boldsymbol{C}_{\mathcal{B}} = -(\tilde{\boldsymbol{A}}_{\mathcal{B}}^{-1}\tilde{\boldsymbol{A}}_{\mathcal{N}})^{\top}$ and $\boldsymbol{C}_{\mathcal{N}} = \boldsymbol{I}$, where $\boldsymbol{C}_{\mathcal{B}}$ ($\boldsymbol{C}_{\mathcal{N}}$) denotes the basic (nonbasic) part of $\boldsymbol{C}$ and where $\boldsymbol{I}$ denotes the $(m - n + 1) \times (m - n + 1)$ identity matrix.

Remark 2.3.4. Again we give a short explanation of this result. For a fixed spanning tree $\mathcal{T}$, every nonbasic arc $a \in \mathcal{N}$ induces a single fundamental cycle and by definition every $a \in \mathcal{N}$ can only be contained in one fundamental cycle. Hence, $\boldsymbol{C}_{\mathcal{N}} = \boldsymbol{I}$.
For ease of explanation let us assume that $|\mathcal{N}| = 1$, i.e., $\mathcal{G}$ contains a single fundamental cyle. Then $\tilde{\boldsymbol{A}}_{\mathcal{N}}$ is a column vector corresponding to the single arc $a = (v, w) \in \mathcal{N}$. Let us further assume that $v, w \neq r$. From the definition of $\boldsymbol{A}$, we recall that

$$(\tilde{A}_{\mathcal{N}})_v = -1,\ (\tilde{A}_{\mathcal{N}})_w = +1, \text{ and } (\tilde{A}_{\mathcal{N}})_x = 0 \text{ for } x \in \mathcal{V} \setminus \{v, w\}. \tag{2.53}$$

Thus we can interpret the vector $-\tilde{\boldsymbol{A}}_{\mathcal{B}}^{-1}\boldsymbol{A}_{\mathcal{N}} = \tilde{\boldsymbol{A}}_{\mathcal{B}}^{-1}(-\boldsymbol{A}_{\mathcal{N}})$ as the solution of a linear network flow problem that transports one unit of flow from w to v in the $\mathcal{B}$-induced spanning tree of $\mathcal{G}$. Again, this solution contains only values from $\{\pm 1, 0\}$ and is the incidence vector of the unique path from w to v in $\mathcal{T}$. We observe that the nonbasic part $\boldsymbol{C}_{\mathcal{N}} = \boldsymbol{I}$ adds the arc (v, w) to this w, v-path in $\mathcal{B}$ and hence gives rise to a cycle in $\mathcal{G}$ that is encoded in $\boldsymbol{C} = [\boldsymbol{C}_{\mathcal{B}} \mid \boldsymbol{C}_{\mathcal{N}}]$.

Flow decomposition into spanning tree and cycles After presenting some general results on graph matrices, we return to the gas network setting and introduce the reduced model. With basis $\mathcal{B}$ and nonbasis $\mathcal{N}$, let $(\boldsymbol{\psi}_{\mathcal{B}}, \boldsymbol{\psi}_{\mathcal{N}})$ and $(\boldsymbol{q}_{\mathcal{B}}, \boldsymbol{q}_{\mathcal{N}})$ be the respective partitions of $\boldsymbol{\psi}$ and $\boldsymbol{q}$ into basic and nonbasic components. In the reduced model, all but the nonbasic flow variables $\boldsymbol{q}_{\mathcal{N}} \in \mathbb{R}^{|\mathcal{N}|}$ can be eliminated. We call the remaining variables $\boldsymbol{q}_{\mathcal{N}} \in \mathbb{R}^{|\mathcal{N}|}$ *cycle flows* or *cycle flow variables*.

In the same way as the reduced node-arc incidence matrix $\tilde{\boldsymbol{A}}$ is created by removing a row from $\boldsymbol{A}$, we create a reduced demand vector $\tilde{\boldsymbol{d}} \in \mathbb{R}^{n-1}$ by removing the entry belonging to the root node r. From basic linear algebra, we known that the solution space of the linear equation system

$$\tilde{\boldsymbol{A}}\boldsymbol{q} = \tilde{\boldsymbol{d}} \tag{2.54}$$

can be parameterized by the nonbasic variables $\boldsymbol{q}_{\mathcal{N}}$:

$$\boldsymbol{q}_{\mathcal{B}} = \tilde{\boldsymbol{A}}_{\mathcal{B}}^{-1}(\tilde{\boldsymbol{d}} - \tilde{\boldsymbol{A}}_{\mathcal{N}}\boldsymbol{q}_{\mathcal{N}}) = \underbrace{\tilde{\boldsymbol{A}}_{\mathcal{B}}^{-1}\tilde{\boldsymbol{d}}}_{\substack{\text{flow on}\\ \text{spanning tree}}} - \underbrace{\tilde{\boldsymbol{A}}_{\mathcal{B}}^{-1}\tilde{\boldsymbol{A}}_{\mathcal{N}}\boldsymbol{q}_{\mathcal{N}}}_{\substack{\text{flow along}\\ \text{cycles}}}. \tag{2.55}$$

A closer look at this equation reveals the structure of feasible flows.

The first summand of the right-hand side is the unique solution of the linear equation system $\tilde{\boldsymbol{A}}_{\mathcal{B}}\boldsymbol{q}_{\mathcal{B}} = \tilde{\boldsymbol{d}}$. Since $\tilde{\boldsymbol{A}}_{\mathcal{B}}$ represents the $\mathcal{B}$-induced spanning tree, this linear equation system describes the unique flow $\boldsymbol{q}_{\mathcal{B}}$ on the spanning tree that satisfies demand $\tilde{\boldsymbol{d}}$.

Next, we consider the second summand of the right-hand side. We apply lemma 2.3.3 to rewrite

$$-\tilde{\boldsymbol{A}}_{\mathcal{B}}^{-1}\tilde{\boldsymbol{A}}_{\mathcal{N}}\boldsymbol{q}_{\mathcal{N}} = (-\tilde{\boldsymbol{A}}_{\mathcal{B}}^{-1}\tilde{\boldsymbol{A}}_{\mathcal{N}})\boldsymbol{q}_{\mathcal{N}} = \boldsymbol{C}_{\mathcal{B}}^{\top}\boldsymbol{q}_{\mathcal{N}} \tag{2.56}$$

and observe that this expression denotes a linear combination of flows along the fundamental cycles of $\mathcal{G}$ when restricted to the $\mathcal{B}$-induced spanning tree.

In total, the parameterization (2.55) can be interpreted as the unique flow on a spanning tree in $\mathcal{G}$ that satisfies the demand, to which a linear combination of flows along cycles of $\mathcal{G}$ are added. This structural result is well-known in linear network flow theory and is used, for example, in the network simplex method to solve minimum-cost network flow problems; see, e.g., Ahuja, Magnanti, and Orlin (1993, ch. 11).

Based on (2.55), we define a vector-valued function $\boldsymbol{q}^{\mathrm{ext}}(\cdot)$ that maps a nonbasic flow vector $\boldsymbol{q}_{\mathcal{N}}$ to flows in the whole network. Each entry $q_a^{\mathrm{ext}}(\boldsymbol{q}_{\mathcal{N}})$ denotes the flow at arc $a \in \mathcal{A}$ resulting from the cycle flow vector $\boldsymbol{q}_{\mathcal{N}}$:

$$\begin{aligned} \boldsymbol{q}^{\mathrm{ext}} &\colon \mathbb{R}^{|\mathcal{V}|} \times \mathbb{R}^{|\mathcal{N}|} \to \mathbb{R}^{|\mathcal{A}|}, \\ q_a^{\mathrm{ext}}(\boldsymbol{d}, \boldsymbol{q}_{\mathcal{N}}) &= \begin{cases} \left(\tilde{\boldsymbol{A}}_{\mathcal{B}}^{-1}(\tilde{\boldsymbol{d}} - \tilde{\boldsymbol{A}}_{\mathcal{N}}\boldsymbol{q}_{\mathcal{N}})\right)_a & \text{if } a \in \mathcal{B}, \\ (\boldsymbol{q}_{\mathcal{N}})_a & \text{if } a \in \mathcal{N}. \end{cases} \end{aligned} \tag{2.57}$$

Since the demand $\boldsymbol{d}$ will be treated as an uncertain parameter later on, the definition of $\boldsymbol{q}^{\mathrm{ext}}$ includes $\boldsymbol{d}$ as an argument. However, if $\boldsymbol{d}$ is constant, we omit this parameter from $\boldsymbol{q}^{\mathrm{ext}}$ to avoid complicating the notation unnecessarily.

By construction, the flow extension map satisfies $\boldsymbol{q} = \boldsymbol{q}^{\mathrm{ext}}(\boldsymbol{q}_{\mathcal{N}})$. Inserting this equation into the gas network problem eliminates all flow variables except $\boldsymbol{q}_{\mathcal{N}}$.

Pressure change along paths An important aspect of the reduced model is the total pressure change along paths in the $\mathcal{B}$-induced spanning tree in $\mathcal{G}$. For this purpose, we define a vector-valued function $\tilde{\boldsymbol{g}}$ whose entries $(\tilde{g}_v)_{v\in\mathcal{V}\setminus\{r\}}$ denote the aggregated pressure change between root node r and all other nodes in $\mathcal{G}$. We call $\tilde{\boldsymbol{g}}$ the *reduced aggregated pressure change function*:

$$\begin{aligned}\tilde{\boldsymbol{g}}\colon \mathbb{R}^{|\mathcal{B}|}\times\mathbb{R}^{|\mathcal{A}_{\mathrm{pm}}\cap\mathcal{B}|}&\to\mathbb{R}^{|\mathcal{V}|-1},\\ \tilde{\boldsymbol{g}}(\boldsymbol{q}_{\mathcal{B}},\boldsymbol{x}_{\mathcal{B}}^{\mathrm{pm}})&=(\tilde{\boldsymbol{A}}_{\mathcal{B}}^{-1})^{\top}\boldsymbol{\psi}_{\mathcal{B}}(\boldsymbol{q}_{\mathcal{B}},\boldsymbol{x}_{\mathcal{B}}^{\mathrm{pm}})\\ &=\tilde{\boldsymbol{P}}\boldsymbol{\psi}_{\mathcal{B}}(\boldsymbol{q}_{\mathcal{B}},\boldsymbol{x}_{\mathcal{B}}^{\mathrm{pm}}),\end{aligned}\tag{2.58}$$

where $\tilde{\boldsymbol{P}}$ denotes the path matrix of the spanning tree as it appears in lemma 2.3.1. The function has a simple interpretation. Let $v\neq r$ be given. Then

$$\begin{aligned}\tilde{g}_v(\boldsymbol{q}_{\mathcal{B}},\boldsymbol{x}_{\mathcal{B}}^{\mathrm{pm}})&=\left[(\tilde{\boldsymbol{A}}_{\mathcal{B}}^{-1})^{\top}\right]_{v\cdot}\boldsymbol{\psi}_{\mathcal{B}}(\boldsymbol{q}_{\mathcal{B}},\boldsymbol{x}_{\mathcal{B}}^{\mathrm{pm}}) &(2.59)\\ &=\tilde{\boldsymbol{P}}_{v\cdot}\boldsymbol{\psi}_{\mathcal{B}}(\boldsymbol{q}_{\mathcal{B}},\boldsymbol{x}_{\mathcal{B}}^{\mathrm{pm}}) &(2.60)\\ &=\sum_{a\in\mathcal{B}}\tilde{P}_{va}\psi_a(q_a,x_a^{\mathrm{pm}}) &(2.61)\\ &=\sum_{a\in\mathcal{B}\cap\mathcal{A}_{\mathrm{pi}}}\tilde{P}_{va}\psi_a(q_a)+\sum_{a\in\mathcal{B}\cap\mathcal{A}_{\mathrm{pm}}}\tilde{P}_{va}\psi_a(x_a^{\mathrm{pm}}) &(2.62)\\ &=-\sum_{a\in\mathcal{B}\cap\mathcal{A}_{\mathrm{pi}}}\tilde{P}_{va}l_a|q_a|^{*}+\sum_{a\in\mathcal{B}\cap\mathcal{A}_{\mathrm{pm}}}\tilde{P}_{va}x_a^{\mathrm{pm}} &(2.63)\end{aligned}$$

denotes the sum of all pressure changes along the unique path in the $\mathcal{B}$-induced spanning tree from root node r to node v. When taking (2.40) into account, we observe that (2.61) is a telescopic sum of squared pressure differences. Hence, it follows that

$$\pi_v-\pi_r=\tilde{g}_v(\boldsymbol{q}_{\mathcal{B}},\boldsymbol{x}_{\mathcal{B}}^{\mathrm{pm}})\quad\text{for all } v\in\mathcal{V}\setminus\{r\},\tag{2.64}$$

since only the squared pressure variables of the first and last node of the path are preserved.

Finally, we plug $\boldsymbol{q}^{\mathrm{ext}}$ into $\tilde{\boldsymbol{g}}$ and incorporate the root node $r\in\mathcal{V}$ to obtain the general *aggregated pressure change function*:

$$\begin{aligned}&\boldsymbol{g}\colon\mathbb{R}^{|\mathcal{N}|}\times\mathbb{R}^{|\mathcal{A}_{\mathrm{pm}}\cap\mathcal{B}|}\to\mathbb{R}^{|\mathcal{V}|},\\ &g_v(\boldsymbol{q}_{\mathcal{N}},\boldsymbol{x}_{\mathcal{B}}^{\mathrm{pm}})=\begin{cases}0 & \text{if } v=r,\\ \tilde{g}_v(\boldsymbol{q}_{\mathcal{B}}^{\mathrm{ext}}(\boldsymbol{q}_{\mathcal{N}}),\boldsymbol{x}_{\mathcal{B}}^{\mathrm{pm}}) & \text{if } v\neq r,\end{cases}\quad\text{for all } v\in\mathcal{V}.\end{aligned}\tag{2.65}$$

Similar to (2.64), function g_v satisfies

$$\pi_v - \pi_r = g_v(\boldsymbol{q}_{\mathcal{N}}, \boldsymbol{x}_{\mathcal{B}}^{\mathrm{pm}}) \quad \text{for all } v \in \mathcal{V}. \tag{2.66}$$

Next, we will use $\boldsymbol{g}$ to calculate the aggregated pressure between any pair of nodes in the graph.

Pressure changes on arbitrary paths in the spanning tree The pressure change between two arbitrary nodes $v, w \in \mathcal{V}$ in the network can be obtained by combining the pressure change from r to v with the pressure change from r to w. We already established in (2.66) that

$$\pi_v - \pi_r = g_v(\boldsymbol{q}_{\mathcal{N}}, \boldsymbol{x}_{\mathcal{B}}^{\mathrm{pm}}), \tag{2.67a}$$
$$\pi_w - \pi_r = g_w(\boldsymbol{q}_{\mathcal{N}}, \boldsymbol{x}_{\mathcal{B}}^{\mathrm{pm}}). \tag{2.67b}$$

Taking the difference of the previous two equations yields

$$\pi_w - \pi_v = g_w(\boldsymbol{q}_{\mathcal{N}}, \boldsymbol{x}_{\mathcal{B}}^{\mathrm{pm}}) - g_v(\boldsymbol{q}_{\mathcal{N}}, \boldsymbol{x}_{\mathcal{B}}^{\mathrm{pm}}). \tag{2.67c}$$

Recalling the definition of $\boldsymbol{g}$ in (2.65) and property (2.48) of the full path matrix, we rewrite the previous equation and obtain

$$\pi_w - \pi_v = \tilde{\boldsymbol{P}}_{w\cdot} \boldsymbol{\psi}_{\mathcal{B}}(\boldsymbol{q}_{\mathcal{B}}^{\mathrm{ext}}(\boldsymbol{q}_{\mathcal{N}}), \boldsymbol{x}_{\mathcal{B}}^{\mathrm{pm}}) - \tilde{\boldsymbol{P}}_{v\cdot} \boldsymbol{\psi}_{\mathcal{B}}(\boldsymbol{q}_{\mathcal{B}}^{\mathrm{ext}}(\boldsymbol{q}_{\mathcal{N}}), \boldsymbol{x}_{\mathcal{B}}^{\mathrm{pm}}) \tag{2.68}$$
$$= (\tilde{\boldsymbol{P}}_{w\cdot} - \tilde{\boldsymbol{P}}_{v\cdot}) \boldsymbol{\psi}_{\mathcal{B}}(\boldsymbol{q}_{\mathcal{B}}, \boldsymbol{x}_{\mathcal{B}}^{\mathrm{pm}}) \tag{2.69}$$
$$= \boldsymbol{P}_{vw,\cdot} \boldsymbol{\psi}_{\mathcal{B}}(\boldsymbol{q}_{\mathcal{B}}, \boldsymbol{x}_{\mathcal{B}}^{\mathrm{pm}}), \tag{2.70}$$

where we let $\tilde{\boldsymbol{P}}_{r\cdot} = (0, \dots, 0)$ for the sake of convenience.

As a final piece of notation we introduce upper bounds on pressure change along a path. Let $\underline{\boldsymbol{\pi}}, \overline{\boldsymbol{\pi}} \in \mathbb{R}^n$ denote the vectors of lower and upper squared pressures at each node, respectively. Let $\Delta\boldsymbol{\pi} \in \mathbb{R}^{n^2} = (\Delta\pi_{vw})_{v,w\in\mathcal{V}}$ be a vector that is indexed by pairs of nodes. The entries of this vector are defined as

$$\Delta\pi_{vw} = \overline{\pi}_w - \underline{\pi}_v \quad \text{for all } v, w \in \mathcal{V}. \tag{2.71}$$

The elements of $\Delta\boldsymbol{\pi}$ arise from (2.68) by taking the maximum of the left-hand side when considering the pressure bounds $\pi_v \in [\underline{\pi}_v, \overline{\pi}_v]$. Therefore, we deduce from (2.68) and (2.71) that any feasible network solution has to satisfy

$$\boldsymbol{P}_{vw,\cdot} \boldsymbol{\psi}_{\mathcal{B}}(\boldsymbol{q}_{\mathcal{B}}, \boldsymbol{x}_{\mathcal{B}}^{\mathrm{pm}}) = \pi_w - \pi_v \leq \Delta\pi_{vw} \quad \text{for all } v, w \in \mathcal{V}. \tag{2.72}$$

These inequalities impose upper bounds on the pressure change along all paths in the $\mathcal{B}$-induced spanning tree.

The reduced model With this preparatory work, we can establish an equivalent formulation of the constraint system of the gas network problem (2.43). We first give this result in an algebraic notation that is more close to the original result for passive networks by Gotzes et al. (2016). Afterward, we present a more compact variant using the path and cycle matrices.

Theorem 2.3.5 (Aßmann, Liers, and Stingl 2019)**.** *Let $\mathcal{G} = (\mathcal{V}, \mathcal{A})$ be a connected digraph with nodes $\mathcal{V}$ and arcs $\mathcal{A}$, where $\mathcal{A} = \mathcal{A}_{\mathrm{pi}} \cup \mathcal{A}_{\mathrm{pm}}$ is partitioned into a set of pipes $\mathcal{A}_{\mathrm{pi}}$ and a set of pressure-modifying elements $\mathcal{A}_{\mathrm{pm}}$. Let $\boldsymbol{d} \in \mathbb{R}^{\mathcal{V}}$ be a balanced vector of demands and let $\boldsymbol{l} \in \mathbb{R}^{\mathcal{A}_{\mathrm{pi}}}_{\geq 0}$ be a the vector of pressure loss coefficients. Let $\underline{\boldsymbol{\pi}}, \overline{\boldsymbol{\pi}} \in \mathbb{R}^{|\mathcal{V}|}$ and $\underline{\boldsymbol{x}}^{\mathrm{pm}}, \overline{\boldsymbol{x}}^{\mathrm{pm}} \in \mathbb{R}^{|\mathcal{A}_{\mathrm{pm}}|}$ denote the squared pressure bounds and compressor power bounds, respectively. Let $\tilde{\boldsymbol{A}}$ be the node-arc incidence matrix of $\mathcal{G}$ after removing the row corresponding to an arbitrary root node $r \in \mathcal{V}$, with a partition $(\tilde{\boldsymbol{A}}_{\mathcal{B}}, \tilde{\boldsymbol{A}}_{\mathcal{N}})$ into basis and nonbasis as described above. Let $\boldsymbol{\psi}$ be defined as in* (2.39)*. Let $(\boldsymbol{\psi}_{\mathcal{B}}, \boldsymbol{\psi}_{\mathcal{N}})$ and $(\boldsymbol{q}_{\mathcal{B}}, \boldsymbol{q}_{\mathcal{N}})$ be the corresponding partitions of $\boldsymbol{\psi}$ and $\boldsymbol{q}$, respectively. Let $\boldsymbol{g}$ be the aggregated pressure drop function as defined in* (2.65)*.*

Then (2.43) *has a feasible point if and only if the following reduced system in variables $\boldsymbol{q}_{\mathcal{N}}$, $\boldsymbol{x}^{\mathrm{pm}}$ has a solution:*

$$\tilde{\boldsymbol{A}}_{\mathcal{N}}^{\top} \tilde{\boldsymbol{g}}(\boldsymbol{q}_{\mathcal{N}}, \boldsymbol{x}^{\mathrm{pm}}_{\mathcal{B}}) = \boldsymbol{\psi}_{\mathcal{N}}(\boldsymbol{q}_{\mathcal{N}}, \boldsymbol{x}^{\mathrm{pm}}_{\mathcal{N}}), \tag{2.73a}$$

$$g_w(\boldsymbol{q}_{\mathcal{N}}, \boldsymbol{x}^{\mathrm{pm}}_{\mathcal{B}}) - g_v(\boldsymbol{q}_{\mathcal{N}}, \boldsymbol{x}^{\mathrm{pm}}_{\mathcal{B}}) \leq \overline{\pi}_w - \underline{\pi}_v \quad \text{for all } v, w \in \mathcal{V}, \tag{2.73b}$$

$$\boldsymbol{x}^{\mathrm{pm}} \in [\underline{\boldsymbol{x}}^{\mathrm{pm}}, \overline{\boldsymbol{x}}^{\mathrm{pm}}] \subseteq \mathbb{R}^{|\mathcal{A}_{\mathrm{pm}}|}, \tag{2.73c}$$

$$\boldsymbol{q}_{\mathcal{N}} \in \mathbb{R}^{|\mathcal{N}|}. \tag{2.73d}$$

Moreover, any solution $\boldsymbol{q}^*_{\mathcal{N}}, \boldsymbol{x}^{\mathrm{pm}*}$ of (2.73) *is feasible for* (2.43) *by calculating $\boldsymbol{q}^*_{\mathcal{B}} = \tilde{\boldsymbol{A}}_{\mathcal{B}}^{-1}(\tilde{\boldsymbol{d}} - \tilde{\boldsymbol{A}}_{\mathcal{N}} \boldsymbol{q}^*_{\mathcal{N}})$ and $\pi^*_v = \pi^*_r + g_v(\boldsymbol{q}^*_{\mathcal{N}}, \boldsymbol{x}^{\mathrm{pm}*}_{\mathcal{B}})$ for $v \in \mathcal{V}$. The value of π^*_r is an arbitrary given element of*

$$\Big[\max_{v \in \mathcal{V}} \{\underline{\pi}_v - g_v(\boldsymbol{q}^*_{\mathcal{N}}, \boldsymbol{x}^{\mathrm{pm}*}_{\mathcal{B}})\},\ \min_{v \in \mathcal{V}} \{\overline{\pi}_v - g_v(\boldsymbol{q}^*_{\mathcal{N}}, \boldsymbol{x}^{\mathrm{pm}*}_{\mathcal{B}})\}\Big]. \tag{2.74}$$

Conversely, given a feasible $\boldsymbol{q}^*, \boldsymbol{\pi}^*, \boldsymbol{x}^{\mathrm{pm}*}$ for (2.43)*, the vectors $\boldsymbol{q}^*_{\mathcal{N}}$ and $\boldsymbol{x}^{\mathrm{pm}*}$ are feasible for* (2.73)*.*

Proof. The original result of Gotzes et al. (2016) is established for pipe-only networks, i.e., for $\mathcal{A}_{\mathrm{pm}} = \emptyset$. However, the form of the pressure drop law is never exploited explicitly. Therefore, it is not difficult to see that their result still holds for networks with compressors or more general constraints of the form

$$\pi_w - \pi_v = \alpha_a(q_a) \quad \text{for all } (v, w) = a \in \mathcal{A}, \tag{2.75}$$

where α_a is some scalar-valued function of the flow q_a. □

Remark 2.3.6. Next, we write system (2.73) in a compact fashion using the previously introduced path and cycle matrices. With lemma 2.3.3, equation system (2.73a) can be written in terms of the cycle matrix $\boldsymbol{C}$ as follows. The left-hand side of (2.73a) is equal to

$$\tilde{\boldsymbol{A}}_{\mathcal{N}}^{\top}\tilde{\boldsymbol{g}}(\boldsymbol{q}_{\mathcal{N}}, \boldsymbol{x}_{\mathcal{B}}^{\mathrm{pm}}) = \underbrace{\tilde{\boldsymbol{A}}_{\mathcal{N}}^{\top}(\tilde{\boldsymbol{A}}_{\mathcal{B}}^{-1})^{\top}}_{=-\boldsymbol{C}_{\mathcal{B}}} \boldsymbol{\psi}_{\mathcal{B}}(\boldsymbol{q}_{\mathcal{B}}^{\mathrm{ext}}(\boldsymbol{q}_{\mathcal{N}}), \boldsymbol{x}_{\mathcal{B}}^{\mathrm{pm}}) \tag{2.76}$$

$$= -\boldsymbol{C}_{\mathcal{B}}\boldsymbol{\psi}_{\mathcal{B}}(\boldsymbol{q}_{\mathcal{B}}^{\mathrm{ext}}(\boldsymbol{q}_{\mathcal{N}}), \boldsymbol{x}_{\mathcal{B}}^{\mathrm{pm}})). \tag{2.77}$$

Similarly, we write the right-hand side of (2.73a) as

$$\boldsymbol{\psi}_{\mathcal{N}}(\boldsymbol{q}_{\mathcal{N}}, \boldsymbol{x}_{\mathcal{N}}^{\mathrm{pm}}) = \boldsymbol{I}\boldsymbol{\psi}_{\mathcal{N}}(\boldsymbol{q}_{\mathcal{N}}, \boldsymbol{x}_{\mathcal{N}}^{\mathrm{pm}}) = \boldsymbol{C}_{\mathcal{N}}\boldsymbol{\psi}_{\mathcal{N}}(\boldsymbol{q}_{\mathcal{N}}, \boldsymbol{x}_{\mathcal{N}}^{\mathrm{pm}}), \tag{2.78}$$

where we denote with $\boldsymbol{I}$ an identity matrix of appropriate dimension. Combining (2.76) and (2.78), and again with lemma 2.3.3, we obtain

$$-\boldsymbol{C}_{\mathcal{B}}\boldsymbol{\psi}_{\mathcal{B}}(\boldsymbol{q}_{\mathcal{B}}^{\mathrm{ext}}(\boldsymbol{q}_{\mathcal{N}}), \boldsymbol{x}_{\mathcal{B}}^{\mathrm{pm}}) = \boldsymbol{C}_{\mathcal{N}}\boldsymbol{\psi}_{\mathcal{N}}(\boldsymbol{q}_{\mathcal{N}}, \boldsymbol{x}_{\mathcal{N}}^{\mathrm{pm}}) \tag{2.79}$$

$$\iff \boldsymbol{C}\boldsymbol{\psi}(\boldsymbol{q}^{\mathrm{ext}}(\boldsymbol{q}_{\mathcal{N}}), \boldsymbol{x}^{\mathrm{pm}}) = \boldsymbol{0}. \tag{2.80}$$

This system enforces that the pressure loss along the fundamental cycles of $\mathcal{G}$ is zero.

The inequalities (2.73b) can be written using the full path matrix of the $\mathcal{B}$-induced spanning tree as was shown in (2.72):

$$g_w(\boldsymbol{q}_{\mathcal{N}}, \boldsymbol{x}_{\mathcal{B}}^{\mathrm{pm}}) - g_v(\boldsymbol{q}_{\mathcal{N}}, \boldsymbol{x}_{\mathcal{B}}^{\mathrm{pm}}) \leq \overline{\pi}_w - \underline{\pi}_v \quad \text{for all } v, w \in \mathcal{V} \tag{2.81}$$

$$\iff \boldsymbol{P}\boldsymbol{\psi}_{\mathcal{B}}(\boldsymbol{q}_{\mathcal{B}}^{\mathrm{ext}}(\boldsymbol{q}_{\mathcal{N}}), \boldsymbol{x}_{\mathcal{B}}^{\mathrm{pm}}) \leq \Delta\boldsymbol{\pi}. \tag{2.82}$$

This set of inequalities limits the pressure change along each path.

Altogether, system (2.73) can be formulated equivalently as

$$\boldsymbol{C}\boldsymbol{\psi}(\boldsymbol{q}^{\mathrm{ext}}(\boldsymbol{q}_{\mathcal{N}}), \boldsymbol{x}^{\mathrm{pm}}) = \boldsymbol{0}, \tag{2.83a}$$

$$\boldsymbol{P}\boldsymbol{\psi}_{\mathcal{B}}(\boldsymbol{q}_{\mathcal{B}}^{\mathrm{ext}}(\boldsymbol{q}_{\mathcal{N}}), \boldsymbol{x}_{\mathcal{B}}^{\mathrm{pm}}) \leq \Delta\boldsymbol{\pi}, \tag{2.83b}$$

$$\boldsymbol{q}_{\mathcal{N}} \in \mathbb{R}^{|\mathcal{N}|}, \tag{2.83c}$$

$$\boldsymbol{x}^{\mathrm{pm}} \in [\underline{\boldsymbol{x}}^{\mathrm{pm}}, \overline{\boldsymbol{x}}^{\mathrm{pm}}] \tag{2.83d}$$

Example 2.3.7. *Since the reduced formulation is of central importance for our later results, we exemplify the reformulation here on the basis of a small network.*

Let $\mathcal{G} = (\mathcal{V}, \mathcal{A})$ be a graph that models a passive gas network with nodes $\mathcal{V} = \{v_1, v_2, v_3\}$ and arcs $\mathcal{A} = \mathcal{A}_{\mathrm{pi}} = \{a_{12}, a_{23}, a_{31}\} = \{(v_1, v_2), (v_2, v_3), (v_3, v_1)\}$;

see fig. 2.2 for a visualization. Let $\boldsymbol{d} \in \mathbb{R}^{|\mathcal{V}|}$ be a balanced vector of demands, let $\underline{\boldsymbol{\pi}}, \overline{\boldsymbol{\pi}} \in \mathbb{R}^{|\mathcal{V}|}$ be the respective vectors of lower and upper squared pressure bounds and let $\boldsymbol{l} \in \mathbb{R}^{|\mathcal{A}|}_{\geq 0}$ be the vector of pressure drop coefficients.

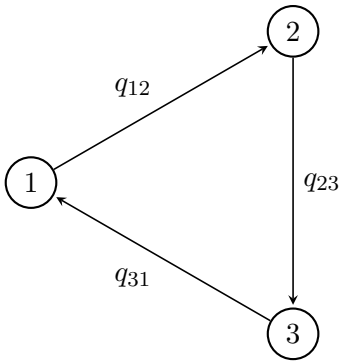

Figure 2.2: Network with three nodes and one cycle.

We select $r = v_1$ as root node and choose a basis $\mathcal{B} = \{a_{12}, a_{23}\}$ and nonbasis $\mathcal{N} = \{a_{31}\}$. As already mentioned, we observe that the arcs in $\mathcal{B}$ form a spanning tree of $\mathcal{G}$.

In this setting, the corresponding node-arc incidence matrix $\boldsymbol{A} \in \mathbb{R}^{|\mathcal{V}| \times |\mathcal{A}|}$ and its partitions are given by

$$\boldsymbol{A} = \begin{array}{c} \\ v_1 \\ v_2 \\ v_3 \end{array} \begin{array}{c} \begin{array}{ccc} a_{12} & a_{23} & a_{31} \end{array} \\ \left(\begin{array}{cc|c} -1 & 0 & 1 \\ \hline 1 & -1 & 0 \\ 0 & 1 & -1 \end{array}\right) \end{array} =: \left[\begin{array}{c|c} \boldsymbol{A}_{r\mathcal{B}} & \boldsymbol{A}_{r\mathcal{N}} \\ \hline \tilde{\boldsymbol{A}}_{\mathcal{B}} & \tilde{\boldsymbol{A}}_{\mathcal{N}} \end{array}\right] \tag{2.84}$$

and thus $\tilde{\boldsymbol{A}}_{\mathcal{B}}^{-1} = \left(\begin{smallmatrix} 1 & 1 \\ 0 & 1 \end{smallmatrix}\right)$.

The reduced path matrix is given by

$$\tilde{\boldsymbol{P}} = (\tilde{\boldsymbol{A}}_{\mathcal{B}}^{-1})^{\top} = \begin{array}{c} \\ v_1v_2 \\ v_1v_3 \end{array} \begin{array}{c} \begin{array}{cc} a_{12} & a_{23} \end{array} \\ \begin{pmatrix} 1 & 0 \\ 1 & 1 \end{pmatrix} \end{array}. \tag{2.85}$$

We notice that the first row of $\tilde{\boldsymbol{P}}$ encodes the path from v_1 to v_2 whereas the second row encodes the path from v_1 to v_3. The full path matrix is given by

$$\boldsymbol{P}^\top = \begin{array}{c} \\ a_{12} \\ a_{23} \end{array} \begin{array}{c} \begin{array}{cccccccccc} v_1v_1 & v_1v_2 & v_1v_3 & v_2v_1 & v_2v_2 & v_2v_3 & v_3v_1 & v_3v_2 & v_3v_3 \end{array} \\ \begin{pmatrix} 0 & 1 & 1 & -1 & 0 & 0 & -1 & 0 & 0 \\ 0 & 0 & 1 & 0 & 0 & 1 & -1 & -1 & 0 \end{pmatrix}. \end{array} \tag{2.86}$$

Finally, the cycle matrix is given by

$$\boldsymbol{C} = [\boldsymbol{C}_\mathcal{B} \mid \boldsymbol{C}_\mathcal{N}] = [-(\tilde{\boldsymbol{A}}_\mathcal{B}^{-1}\tilde{\boldsymbol{A}}_\mathcal{N})^\top \mid \boldsymbol{I}] = \begin{pmatrix} 1 & 1 & 1 \end{pmatrix}. \tag{2.87}$$

We observe that the single fundamental cycle in $\mathcal{G}$ denotes the only row of $\boldsymbol{C}$.

As in (2.55), we parameterize the basic flows by the nonbasic flows:

$$\boldsymbol{q}_\mathcal{B} = \tilde{\boldsymbol{A}}_\mathcal{B}^{-1}(\tilde{\boldsymbol{d}} - \tilde{\boldsymbol{A}}_\mathcal{N}\boldsymbol{q}_\mathcal{N}) = \begin{pmatrix} d_2 + d_3 \\ d_3 \end{pmatrix} + \begin{pmatrix} 1 \\ 1 \end{pmatrix} q_{31}, \tag{2.88}$$

and thus the flow extension map (2.57) is given by

$$\boldsymbol{q}^{\mathrm{ext}}(q_{31}) = \begin{pmatrix} q_{12} \\ q_{23} \\ q_{31} \end{pmatrix} = \begin{pmatrix} d_2 + d_3 \\ d_3 \\ 0 \end{pmatrix} + \begin{pmatrix} 1 \\ 1 \\ 1 \end{pmatrix} q_{31}. \tag{2.89}$$

Next, we formulate the aggregated pressure drop (2.65). For a more concise presentation, let $|x|^* := |x|x$. The basic aggregated pressure change function is given by

$$\tilde{\boldsymbol{g}}(\boldsymbol{q}) = (\tilde{\boldsymbol{A}}_\mathcal{B}^{-1})^\top \boldsymbol{\psi}_\mathcal{B}(\boldsymbol{q}) = \begin{pmatrix} \psi_{12}(q_{12}) \\ \psi_{12}(q_{12}) + \psi_{23}(q_{23}) \end{pmatrix} \tag{2.90}$$

$$= \begin{pmatrix} -l_{12}|q_{12}|^* \\ -l_{12}|q_{12}|^* - l_{23}|q_{23}|^* \end{pmatrix}. \tag{2.91}$$

After adding the flow extension map (2.89), we obtain the full aggregated pressure change function

$$\boldsymbol{g}(q_{31}) = \begin{pmatrix} g_1(q_{31}) \\ g_2(q_{31}) \\ g_3(q_{31}) \end{pmatrix} = \begin{pmatrix} 0 \\ -l_{12}|d_2 + d_3 + q_{31}|^* \\ -l_{12}|d_2 + d_3 + q_{31}|^* - l_{23}|d_3 + q_{31}|^* \end{pmatrix}. \tag{2.92}$$

With these preparations, we formulate the constraints of the reduced system (2.73)*:*

$$l_{12}|d_2 + d_3 + q_{31}|^* + l_{23}|d_3 + q_{31}|^* + l_{31}|q_{31}|^* = 0, \tag{2.93a}$$

$$\underline{\pi}_2 - \overline{\pi}_1 \leq -l_{12}|d_2 + d_3 + q_{31}|^* \leq \overline{\pi}_2 - \underline{\pi}_1, \tag{2.93b}$$

$$\underline{\pi}_3 - \overline{\pi}_2 \leq -l_{23}|d_3 + q_{31}|^* \leq \overline{\pi}_3 - \underline{\pi}_2, \tag{2.93c}$$

$$\underline{\pi}_1 - \overline{\pi}_3 \leq l_{12}|d_2 + d_3 + q_{31}|^* + l_{23}|d_3 + q_{31}|^* \leq \overline{\pi}_1 - \underline{\pi}_3. \tag{2.93d}$$

We observe that the equation (2.93a) *sets the pressure loss along the only cycle to zero. The subsequent inequalities* (2.93b)–(2.93d) *bound the pressure drop along all possible paths by the squared pressure bounds at the first and last node of the path.*

An equivalent formulation using the path and cycle matrices is given by

$$\boldsymbol{C}\boldsymbol{\psi}(\boldsymbol{q}^{\mathrm{ext}}(q_{23})) = \boldsymbol{0}, \tag{2.94a}$$

$$\boldsymbol{P}\boldsymbol{\psi}_{\mathcal{B}}(\boldsymbol{q}_{\mathcal{B}}^{\mathrm{ext}}(q_{23})) \leq \Delta\boldsymbol{\pi}, \tag{2.94b}$$

where $\Delta\boldsymbol{\pi}$ *is defined as in* (2.71)*.*

2.4 Existence and uniqueness of flows

Results concerning the existence and uniqueness of flows and pressures in connected passive gas networks with algebraic pressure drop have been established multiple times in the literature; see Collins et al. (1977), Maugis (1977), and Ríos-Mercado et al. (2002). In the recent work by Gugat, Schultz, and Wintergerst (2018), the results for the algebraic model are generalized to a network of coupled Euler equations.

First, we reproduce results from the literature concerning uniqueness by Collins et al. (1977), and existence by Ríos-Mercado et al. (2002). A closer look at the employed proof techniques is worthwhile as they reveal other interesting structural properties of the gas transport problem. Afterward, an extension to networks with active elements is presented.

Existence and uniqueness for pipe-only networks

We consider a model for passive gas transport without pressure bounds:

$$\boldsymbol{A}\boldsymbol{q} = \boldsymbol{d}, \tag{2.95a}$$

$$\boldsymbol{A}^\top\boldsymbol{\pi} = \boldsymbol{\psi}(\boldsymbol{q}), \tag{2.95b}$$

$$\boldsymbol{\pi} \in \mathbb{R}^{|\mathcal{V}|}, \tag{2.95c}$$

$$\boldsymbol{q} \in \mathbb{R}^{|\mathcal{A}|}. \tag{2.95d}$$

Note that we also allow negative squared pressure values, even though these have no real-world interpretation. We sometimes refer to this formulation as the *problem of state* or the *state equations*, as it purely represents the physical model without exogenous pressure bounds. The *(physical) state* of the network is given by the flow rate along the arcs and the pressures at the nodes.

Collins et al. (1977) and Maugis (1977) show that if a feasible flow with admissible pressures exists for the physical state problem, then the flow solution is unique. Their result is derived from properties of an auxiliary linear network flow problem with a strictly convex objective function. In their proof, they utilize that the Karush–Kuhn–Tucker (KKT) optimality conditions of this problem are equivalent to the state problem (2.95). The dual variables in this system can be identified with the squared pressure variables of the state problem (2.95).

Lemma 2.4.1 (Collins et al. 1977; Maugis 1977)**.** *Suppose $\boldsymbol{q}^* \in \mathbb{R}^{|\mathcal{A}|}$ and $\boldsymbol{\pi}^* \in \mathbb{R}^{|\mathcal{V}|}$ solve* (2.95)*. Then $\boldsymbol{q}^*$ is unique and the set $\mathcal{X} \subseteq \mathbb{R}^{|\mathcal{A}|} \times \mathbb{R}^{|\mathcal{V}|}$ of feasible flow, squared pressure solutions $(\boldsymbol{q}, \boldsymbol{\pi})$ can be written as*

$$\mathcal{X} = \{(\boldsymbol{q}, \boldsymbol{\pi}) \mid (\boldsymbol{q}, \boldsymbol{\pi}) \text{ feasible for } (2.95)\} \tag{2.96}$$

$$= \{(\boldsymbol{q}^*, \boldsymbol{\pi}) \mid \boldsymbol{\pi} = \boldsymbol{\pi}^* + \eta \mathbb{1},\ \eta \in \mathbb{R}\}, \tag{2.97}$$

where $\mathbb{1} = (1, \ldots, 1)^\top \in \mathbb{R}^{|\mathcal{V}|}$ is a vector of ones.

Proof. This proof follows the presentation in Humpola et al. (2015), which in turn is adapted from Collins et al. (1977). It uses basic results from convex optimization that is found in any textbook on the subject, e.g., Boyd and Vandenberghe (2004).

To show uniqueness of $\boldsymbol{q}^*$ we introduce an auxiliary optimization problem

$$\min_{\boldsymbol{q} \in \mathbb{R}^{|\mathcal{A}|}} \quad -\sum_{a \in \mathcal{A}} \int_0^{q_a} \psi_a(t)\, \mathrm{d}t \tag{2.98a}$$

$$\text{s.t.} \quad \boldsymbol{A}\boldsymbol{q} = \boldsymbol{d}. \tag{2.98b}$$

The pressure drop functions $\psi_a(q_a) = -l_a |q_a| q_a$ for each arc $a \in \mathcal{A}_{\mathrm{pi}}$ are strictly decreasing and continuous, and hence the integral $\int_0^{q_a} \psi_a(t)\, \mathrm{d}t$ exists and is a strictly concave function in q_a. Since the objective (2.98a) is the negative sum of these integrals, it is a strictly convex function in $\boldsymbol{q}$. With (2.98) being a strictly convex minimization problem, a standard result in convex optimization implies that there is at most one optimal solution $\boldsymbol{q}^*$.

As a first step, we establish that the state problem (2.95) is in fact the Lagrange multiplier optimality condition system of the strictly convex problem (2.98). The squared pressure variables arise naturally as the Lagrange multipliers of the auxiliary problem (2.98). Since the Lagrange multiplier optimality conditions are necessary and sufficient for convex minimization problems, we conclude that (2.98) has an optimal solution $\boldsymbol{q}^*$ if and only if there are Lagrange multipliers (sq. pressures) $\boldsymbol{\pi}^*$ such that $(\boldsymbol{q}^*, \boldsymbol{\pi}^*)$ solves (2.95). Let

$$L(\boldsymbol{q}, \boldsymbol{\pi}) = -\sum_{a \in \mathcal{A}} \int_0^{q_a} \psi_a(t)\,\mathrm{d}t + \boldsymbol{\pi}^\top (\boldsymbol{A}\boldsymbol{q} - \boldsymbol{d}) \tag{2.99}$$

be the corresponding Lagrange function, where we denote with $\boldsymbol{\pi} \in \mathbb{R}^{|\mathcal{V}|}$ the Lagrange multipliers. We know from convex optimization that the stationarity condition $\nabla_{\boldsymbol{q}} L = \boldsymbol{0}$ is necessary and sufficient for any optimal point of the convex minimization problem (2.98):

$$\nabla_{\boldsymbol{q}} L = -\boldsymbol{\psi}(\boldsymbol{q}) + \boldsymbol{\pi}^\top \boldsymbol{A} = \boldsymbol{0}. \tag{2.100}$$

We observe that is this in fact the pressure drop constraint (2.95b)

$$\boldsymbol{A}^\top \boldsymbol{\pi} = \boldsymbol{\psi}(\boldsymbol{q}). \tag{2.101}$$

Therefore any minimizer $\boldsymbol{q}^*$ of (2.98) together with admissible Lagrange multipliers $\boldsymbol{\pi}$ solves the state problem (2.95).

Next, we look at the structure of the squared pressure solutions. As the pressure variables are unbounded and only appear in the pressure drop model (2.95b), their values are determined solely by this equation system. The set of feasible squared pressure values is thus given by the solution space of the linear equation system

$$\boldsymbol{A}^\top \boldsymbol{\pi} = \boldsymbol{\psi}(\boldsymbol{q}^*). \tag{2.102}$$

A basic result from graph theory states that the rank of the $|\mathcal{V}| \times |\mathcal{A}|$ node-arc incidence matrix $\boldsymbol{A}$ of a connected graph $\mathcal{G} = (\mathcal{V}, \mathcal{A})$ is equal to $|\mathcal{V}| - 1$; see, e.g., Ahuja, Magnanti, and Orlin (1993). Therefore the null space of $\boldsymbol{A}^\top$ is one-dimensional. By construction of $\boldsymbol{A}$ its columns sum up to zero and thus the vector $\mathbb{1} = (1, \ldots, 1)^\top$ of ones satisfies $\boldsymbol{A}^\top \mathbb{1} = \boldsymbol{0}$. Summarizing our observations, we conclude that all solutions of (2.102) can be written as $\boldsymbol{\pi}^* + \eta \mathbb{1}$ for $\eta \in \mathbb{R}$. □

While the preceding lemma provides insight into the structure of the feasible set, it is unclear whether solutions exist at all. This is where Ríos-Mercado

et al. (2002) comes into play. Besides a similar result regarding uniqueness of flows and structure of the set of feasible squared pressures, they also give a proof for the existence of a feasible flow in a pipe-only network.

The result by Ríos-Mercado et al. (2002) uses the cycle equations (2.83a)

$$\boldsymbol{C}\boldsymbol{\psi}(\boldsymbol{q}^{\mathrm{ext}}(\boldsymbol{q}_{\mathcal{N}})) = \boldsymbol{0} \tag{2.103}$$

of the reduced model (2.83) as a starting point. By exploiting some monotonicity properties within this equation system, it can be shown that a solution exists and is unique. In fact, this is already evident in example 2.3.7, where the left-hand side of the cycle equation (2.93a) is a strictly increasing, continuous function that tends from $-\infty$ to $+\infty$ and thus has a unique root. Due to equivalence of the formulations, existence of a solution for the state problem follows immediately.

Theorem 2.4.2 (Ríos-Mercado et al. 2002)**.** *Let*

$$\boldsymbol{C}\boldsymbol{\psi}(\boldsymbol{q}^{\mathrm{ext}}(\boldsymbol{q}_{\mathcal{N}})) = \boldsymbol{0} \tag{2.104}$$

be the cycle equation system (2.83a) *of the reduced model corresponding to the state problem* (2.95) *of a passive network. Then there exists a unique* $\boldsymbol{q}_{\mathcal{N}}^{*} \in \mathbb{R}^{|\mathcal{N}|}$ *that solves* (2.104)*.*

Since the derivation of this result is substantive and employs concepts from operator theory, we will not reproduce it here and instead refer to Ríos-Mercado et al. (2002).

Remark 2.4.3. As a flow solution always exists for the state problem, feasibility of the passive nomination validation problem with pressure bounds only depends on whether a pressure solution exists that does not violate the given bounds. The fact that a unique flow solution always exists and that only the pressure bounds are decisive for the overall feasibility will play an important role in the robust methods presented in chapters 4 and 5.

For easier referencing, we summarize the obtained results in the following proposition.

Proposition 2.4.4. *Let* $\boldsymbol{A} \in \mathbb{R}^{|\mathcal{V}|\times|\mathcal{A}|}$ *be the node-arc incidence matrix of a connected, passive gas network represented by the digraph* $\mathcal{G} = (\mathcal{V}, \mathcal{A})$ *with balanced demand* $\boldsymbol{d} \in \mathbb{R}^{|\mathcal{V}|}$ *and without pressure bounds. Then the set*

$$\mathcal{X} = \{(\boldsymbol{q}, \boldsymbol{\pi}) \in \mathbb{R}^{|\mathcal{A}|} \times \mathbb{R}^{|\mathcal{V}|} \mid \boldsymbol{A}\boldsymbol{q} = \boldsymbol{d},\ \boldsymbol{A}^{\top}\boldsymbol{\pi} = \boldsymbol{\psi}(\boldsymbol{q})\} \tag{2.105}$$

of feasible flow, squared pressure pairs has the following properties:

1. *A flow solution always exists and is unique, i.e.,*

$$\left|\{\boldsymbol{q} \mid \exists\, \boldsymbol{\pi} \text{ with } (\boldsymbol{q}, \boldsymbol{\pi}) \in \mathcal{X}\}\right| = 1. \tag{2.106}$$

2. *Given a flow solution $\boldsymbol{q}^*$, the set $\mathcal{X}$ of feasible points has the form*

$$\mathcal{X} = \{(\boldsymbol{q}^*, \boldsymbol{\pi}) \mid \boldsymbol{\pi} = \boldsymbol{\pi}^* + \eta \mathbb{1},\ \eta \in \mathbb{R}\}, \tag{2.107}$$

where $\boldsymbol{\pi}^*$ can be computed with $\pi_v^* = \pi_r^* + g_v(\boldsymbol{q}_{\mathcal{N}}^*)$ for all $v \in \mathcal{V}$ after fixing the pressure $\boldsymbol{\pi}_r^*$ at the root node to an arbitrary value.

Existence and uniqueness for networks with linear active elements

We extend proposition 2.4.4 to networks with pressure-modifying elements. The physical state of such a network is described by the system

$$\boldsymbol{A}\boldsymbol{q} = \boldsymbol{d}, \tag{2.108a}$$
$$\boldsymbol{A}^\top \boldsymbol{\pi} = \boldsymbol{\psi}(\boldsymbol{q}, \boldsymbol{x}^{\mathrm{pm}}), \tag{2.108b}$$
$$\boldsymbol{x}^{\mathrm{pm}} \in [\underline{\boldsymbol{x}}^{\mathrm{pm}}, \overline{\boldsymbol{x}}^{\mathrm{pm}}], \tag{2.108c}$$
$$\boldsymbol{\pi} \in [\underline{\boldsymbol{\pi}}, \overline{\boldsymbol{\pi}}], \tag{2.108d}$$
$$\boldsymbol{q} \in \mathbb{R}^m. \tag{2.108e}$$

For our proof, we require the mild assumption that no active element is part of a cycle.

Assumption 1. *Let a gas network problem with compressors over a digraph $\mathcal{G}$ be given. Then no pressure-modifying element is part of a cycle in $\mathcal{G}$.*

This assumption merits further discussion. From a stationary point of view, cycles with pressure-modifying elements are not very useful. We consider a simple example network that has one cycle with one compressor; see fig. 2.3.

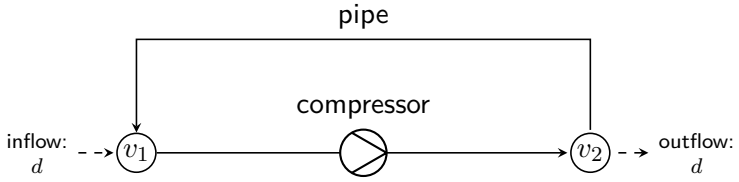

Figure 2.3: A compressor as an element of a two-node cycle.

Gas is injected at the compressor's inlet v_1 and withdrawn at the compressor's outlet v_2. After compression, the pressure at v_2 is larger than the pressure at v_1. As we know, gas flows from points of higher pressure to points of lower pressure. Thus, gas is flowing back from v_2 to v_1 over the parallel pipe. This backflow causes an inefficient situation where gas circulates on the whole cycle.

In real-world networks, e.g., the ones provided by GasLib, active elements in fact do occur in cycles. There are several reasons why this is may not be problematic. Real gas networks contain a richer set of active elements than we consider here. For example, valves can restrict flow in one or both direction of an arc. Essentially, these elements modify the graph topology since closing an arc with a valve may break a cycle and convert the network to a tree topology. Thus, by carefully placing and combining active elements, a network operator can indeed use compressors within a cycle without causing backflows. Furthermore, compressors may be beneficial in an instationary setting where gas is compressed, e.g., only for a short timespan.

Altogether, our methods cannot deal with the full range of active elements that would be necessary for using compressors in cycles. For this reason, we only allow the use of pressure-modifying elements outside cycles.

Next, we extend proposition 2.4.4 to networks with active elements.

Theorem 2.4.5 (Aßmann, Liers, and Stingl 2019)**.** *We consider a connected gas network with a fixed compressor power vector $\boldsymbol{x}^{\mathrm{pm}*}$. Suppose assumption 1 is satisfied, i.e., no pressure-modifying element is part of a cycle. Then proposition 2.4.4 still holds.*

Proof. The proof here is an alternative to the one given in Aßmann, Liers, and Stingl (2019). While using similar ideas, it is more elementary and hence a bit easier to follow.

We prove the theorem by induction over the number $k = |\mathcal{A}_{\mathrm{pm}}| \in \mathbb{N}_0$ of pressure-modifying elements.

For $k = 0$ the network consists only of pipes and the statement follows from proposition 2.4.4.

Suppose theorem 2.4.5 holds for networks with $k \in \mathbb{N}_0$ active elements. We consider a connected gas network with $|\mathcal{A}_{\mathrm{pm}}| = k + 1$ pressure-modifying elements. Let $\mathcal{G} = (\mathcal{V}, \mathcal{A})$ denote the corresponding graph and let $\boldsymbol{d} \in \mathbb{R}^{|\mathcal{V}|}$ denote the balanced vector of demands. Thus, the feasibility system is given by

$$\begin{aligned} \boldsymbol{A}\boldsymbol{q} &= \boldsymbol{d}, & \boldsymbol{A}^\top \boldsymbol{\pi} &= \boldsymbol{\psi}(\boldsymbol{q}, \boldsymbol{x}^{\mathrm{pm}*}), \\ \boldsymbol{\pi} &\in \mathbb{R}^{|\mathcal{V}|}, & \boldsymbol{q} &\in \mathbb{R}^{|\mathcal{A}|}. \end{aligned} \tag{P}$$

We select an arbitrary active element $a_{\mathrm{act}} = (\sigma, \tau) \in \mathcal{A}_{\mathrm{pm}}$ and remove it from $\mathcal{G}$. Due to assumption 1, no active element is part of a cycle and thus removing arc a_{act} leads to a partition of $\mathcal{G}$ into two separate graphs $\mathcal{G}_1 = (\mathcal{V}_1, \mathcal{A}_1)$ and $\mathcal{G}_2 = (\mathcal{V}_2, \mathcal{A}_2)$. W.l.o.g., we assume $\sigma \in \mathcal{V}_1$ and $\tau \in \mathcal{V}_2$.

Since a_{act} is not part of a cycle, it is the only arc that connects the two sets of nodes $\mathcal{V}_1$ and $\mathcal{V}_2$. As the total demand in each $\mathcal{V}_i$ may not be balanced, the surplus or missing quantity must be satisfied by the flow over a_{act} in $\mathcal{G}$:

$$q^*_{\mathrm{act}} = \sum_{v \in \mathcal{V}_2} d_v = -\sum_{v \in \mathcal{V}_1} d_v. \tag{2.109}$$

Let $\boldsymbol{d}_i = (d_v)_{v \in \mathcal{V}_i} \in \mathbb{R}^{|\mathcal{V}_i|}$, $i = 1, 2$, denote a partition of the demand vector $\boldsymbol{d}$ according to $\mathcal{V}_i$. With this and the flow along a_{act} we construct balanced demand vectors

$$\bar{\boldsymbol{d}}_1 = \boldsymbol{d}_1 + q^*_{\mathrm{act}} \boldsymbol{e}_\sigma \quad \text{and} \quad \bar{\boldsymbol{d}}_2 = \boldsymbol{d}_2 - q^*_{\mathrm{act}} \boldsymbol{e}_\tau, \tag{2.110}$$

where we denote with $\boldsymbol{e}_i$ the standard i-th basis vector of suitable dimension.

We consider the two gas problems for $i = 1, 2$ on $\mathcal{G}_i$ with demand $\bar{\boldsymbol{d}}_i$:

$$\begin{aligned} \boldsymbol{A}_i \boldsymbol{q}_i &= \bar{\boldsymbol{d}}_i, & \boldsymbol{A}_i^\top \boldsymbol{\pi}_i &= \boldsymbol{\psi}_i(\boldsymbol{q}_i, x_i^{\mathrm{pm}*}), \\ \boldsymbol{\pi}_i &\in \mathbb{R}^{|\mathcal{V}_i|}, & \boldsymbol{q}_i &\in \mathbb{R}^{|\mathcal{A}_i|}, \end{aligned} \tag{P_i}$$

where $x_i^{\mathrm{pm}*}$ and $\boldsymbol{\psi}_i$ denote their respective counterparts in $\mathcal{G}_i$. By construction, each graph $\mathcal{G}_i$ is connected, has a balanced demand vector and contains at most k active elements. Due to the induction hypothesis, theorem 2.4.5 holds and we obtain solutions $\boldsymbol{q}_i^*$ and $\boldsymbol{\pi}_i^*$ for each problem (P_i). As a feasible squared pressure vector remains feasible after adding a constant to the squared pressure at each node, we further assume that the solutions satisfy

$$(\boldsymbol{\pi}_1^*)_\sigma = 0 \quad \text{and} \quad (\boldsymbol{\pi}_2^*)_\tau = x^{\mathrm{pm}*}_{a_{\mathrm{act}}}. \tag{2.111}$$

Next, we show that a combination of the solutions of (P_i) is feasible for the original problem (P). Let

$$\boldsymbol{q}^* := \begin{pmatrix} \boldsymbol{q}_1^* \\ \boldsymbol{q}_2^* \\ q^*_{\mathrm{act}} \end{pmatrix} \quad \text{and} \quad \boldsymbol{\pi}^* := \begin{pmatrix} \boldsymbol{\pi}_1^* \\ \boldsymbol{\pi}_2^* \end{pmatrix}. \tag{2.112}$$

We recall that $\boldsymbol{A}, \boldsymbol{A}_1, \boldsymbol{A}_2$ denote the node-arc incidence matrices of $\mathcal{G}, \mathcal{G}_1, \mathcal{G}_2$, respectively. We observe that the column in $\boldsymbol{A}$ corresponding to a_{act} can be written as $\boldsymbol{A}_{\cdot a_{\mathrm{act}}} = -\boldsymbol{e}_\sigma + \boldsymbol{e}_\tau$. Then

$$\boldsymbol{A}\boldsymbol{q}^* = \left(\begin{array}{c|c|c} \boldsymbol{A}_1 & \boldsymbol{0} & \\ \hline \boldsymbol{0} & \boldsymbol{A}_2 & \boldsymbol{A}_{\cdot a_{\mathrm{act}}} \end{array}\right) \begin{pmatrix} \boldsymbol{q}_1^* \\ \boldsymbol{q}_2^* \\ q_{\mathrm{act}}^* \end{pmatrix} = \begin{pmatrix} \bar{\boldsymbol{d}}_1 \\ \bar{\boldsymbol{d}}_2 \end{pmatrix} + \boldsymbol{A}_{\cdot a_{\mathrm{act}}} q_{\mathrm{act}}^* \tag{2.113}$$

$$= \begin{pmatrix} \bar{\boldsymbol{d}}_1 \\ \bar{\boldsymbol{d}}_2 \end{pmatrix} + (-\boldsymbol{e}_\sigma + \boldsymbol{e}_\tau) q_{\mathrm{act}}^* \overset{(2.110)}{=} \begin{pmatrix} \boldsymbol{d}_1 \\ \boldsymbol{d}_2 \end{pmatrix} = \boldsymbol{d} \tag{2.114}$$

and

$$\boldsymbol{A}^\top \boldsymbol{\pi}^* = \left(\begin{array}{c|c} \boldsymbol{A}_1^\top & 0 \\ \hline 0 & \boldsymbol{A}_2^\top \\ \hline \multicolumn{2}{c}{\boldsymbol{A}_{\cdot a_{\mathrm{act}}}^\top} \end{array}\right) \begin{pmatrix} \boldsymbol{\pi}_1^* \\ \boldsymbol{\pi}_2^* \end{pmatrix} = \begin{pmatrix} \boldsymbol{A}_1^\top \boldsymbol{\pi}_1^* \\ \boldsymbol{A}_2^\top \boldsymbol{\pi}_2^* \\ \boldsymbol{A}_{\cdot a_{\mathrm{act}}}^\top \boldsymbol{\pi}^* \end{pmatrix} = \begin{pmatrix} \boldsymbol{\psi}_1(\boldsymbol{q}^*, x_1^{\mathrm{pm}*}) \\ \boldsymbol{\psi}_2(\boldsymbol{q}^*, x_2^{\mathrm{pm}*}) \\ -\pi_\sigma^* + \pi_\tau^* \end{pmatrix} \tag{2.115}$$

$$\overset{(2.111)}{=} \begin{pmatrix} \boldsymbol{\psi}_1(\boldsymbol{q}^*, x_1^{\mathrm{pm}*}) \\ \boldsymbol{\psi}_2(\boldsymbol{q}^*, x_2^{\mathrm{pm}*}) \\ x_{a_{\mathrm{act}}}^{\mathrm{pm}*} \end{pmatrix} = \boldsymbol{\psi}(\boldsymbol{q}^*, \boldsymbol{x}^{\mathrm{pm}*}). \tag{2.116}$$

Hence, the solution $(\boldsymbol{q}^*, \boldsymbol{\pi}^*)$ are feasible for the original problem (P).

Moreover, uniqueness of $\boldsymbol{q}^*$ follows from the observation that $q_{a_{\mathrm{act}}}^*$ is uniquely determined by (2.109) and that any other feasible solution $(\boldsymbol{q}^*)'$ for (P) would lead to different flow solutions for the partitioned problems (P_i), a contradiction to the induction hypothesis.

Since $\boldsymbol{A}$ is a $|\mathcal{V}| \times |\mathcal{A}|$ node-arc incidence matrix with rank $|\mathcal{V}| - 1$, the set of all feasible squared pressures is again given by $\{\boldsymbol{\pi}^* + (1, \dots, 1)^\top \eta \,|\, \eta \in \mathbb{R}\}$. □

Remark 2.4.6. We give a few observations regarding the consequences of sections 2.3 and 2.4. Firstly, we note that a flow solution on a tree-shaped network is already uniquely determined by the demand vector and the linear flow system (2.43b) alone. This is not the case for networks with cycles, where uniqueness of flow solutions only holds true by taking the cycle equations (2.73a) into account as well.

Secondly, considering the gas transport problem without pressure bounds, i.e., (2.43b)–(2.43e), we found that not only the flow solutions are unique, but also the squared pressures up to a constant shift. In essence, all squared pressures are determined uniquely relative to the squared pressure at an arbitrarily selected node. Thus, by fixing the pressure at one node in a connected network, the remaining degree of freedom given by the pressure shift is eliminated and the flow and pressure solution is unique.

2.5 Solving nominal gas transport problems

Before introducing uncertainties into the nomination validation problem, we give an overview of the solution approaches for the nominal setting. This is a crucial step on the way to a robust treatment of the problem, as robust models often arise from an extension or reformulation of the nominal models. Often the type of the chosen nominal model—e.g., linear or nonlinear, convex or nonconvex, continuous or mixed-integer, algebraic or PDE-based—determines the applicable robustness approaches.

The overview of the literature given here follows the broader setting of this thesis, i.e., the stationary nomination validation problem. In particular, we omit results used exclusively for the simulation of gas networks. While transient optimization problems in gas are interesting and relevant in a variety of real-world as well as academic problems, we see the treatment of the stationary case as a necessary first step towards more complex models. Hence, we mention work that deals with transient problems only marginally.

For a comprehensive treatment of (optimization) problems in natural gas transportation networks, we refer to the survey article by Ríos-Mercado and Borraz-Sánchez (2015) and the book by Koch et al. (2015).

One of the first approaches for the optimization of natural gas transport networks is dynamic programming (DP). A summary of the results up until 1998 is given by Carter (1998). DP approaches are used to minimize fuel consumption in networks consisting only of pipes and compressors. For these approaches, the feasible operating range of each compressor is discretized and modeled as a finite set of achievable pressure changes. Besides providing global optimal compressor controls, DP has the additional advantage that the nonlinear pressure drop aspects can be handled easily. A disadvantage of these approaches is the "curse of dimensionality", which can lead to computational costs that increase rapidly with the number of elements in the network.
The first use of DP in gas network operations is described by Wong and Larson (1968a), where linear or *gun barrel networks* are optimized. Subsequent improvements to tree-structured networks appear in Wong and Larson (1968b) and Lall and Percell (1990). An extension to networks with cycles is considered by Gilmour, Luongo, and Schroeder (1989). They derive a hybrid approach where tree-shaped subnetworks are treated with DP and the remaining network by enumeration. Another extension for series-parallel graphs is given by Borraz-Sánchez and Ríos-Mercado (2004), who use non-sequential DP to aggregate compressors and subnetworks into virtual units.

Another large group of solution approaches uses MILP models to tackle gas transport problems. Since gas physics is inherently nonlinear, an essen-

tial part of all MILP models is how the nonlinearities are modeled. Typical strategies include linear or piecewise-linear approximations and outer approximation schemes. The main strength of these methods is that combinatorial aspects arising from active elements, e.g., the binary decision of switching a compressor on or off, can be incorporated easily into an integrated model. Moreover, contemporary MILP solvers are very stable and performant, so that even large-scale networks with hundreds of nodes and pipes can be solved reliably; see Pfetsch et al. (2015). On the other hand, using an MILP in this setting has a number of drawbacks. Since all nonlinearities have to be expressed with linear or mixed-integer linear constraints, there is always some approximation error. Although many models allow arbitrary fine approximations, this may quickly lead to large MILPs that are difficult to solve. Expressing more complex aspects of gas physics, like the implicit dependence of the friction factor on the Reynolds number, variable gas temperature, or mixing of different gases, can also be challenging as this often requires multivariate nonlinear functions. Therefore MILP-based approaches typically use simplified gas physics.
In one of the first articles that use linear techniques for gas, Pratt and Wilson (1984) combine binary variables that model switching decisions for the compressors with a consecutive linearizations schema until convergence is attained. In Wolf and Smeers (2000), the Belgian natural gas network is modeled with the convex problem (2.98) that is subsequently approximated by a series of linear underestimators. Taylor expansions at the endpoints of the pressure drop equations' domains are used by Rømo et al. (2009) to construct outer approximations. Their approach also incorporates gas mixing aspects as a multi-commodity flow problem. Martin, Möller, and Moritz (2006) develop an MILP model where the non-convex Weymouth equations are approximated by piecewise-linear functions. This idea is further refined and extended in the following articles. A transient piecewise-linear model has been derived in Mahlke, Martin, and Moritz (2010). By modeling the nonlinearities with piecewise-linear over- and underestimators, Geißler et al. (2012) introduce a systematic way of constructing relaxations for nonlinear functions. This makes it easier to control the error, and infeasible instances can be detected early on by an infeasible relaxation. Mixed-integer models for a wide range of active elements, such as compressors, compressor stations, (control-) valves, and resistors, were introduced in Geißler, Martin, et al. (2015). While the piecewise-linear modeling techniques allow an arbitrarily small error by using a finer discretization, this can also lead to intractable models due to a large number of binary variables that are required. To mitigate this, Geißler, Morsi, and Schewe (2013) and Burlacu, Geißler, and Schewe (2019) develop adaptive

refinement strategies for general mixed-integer nonlinear programs (MINLPs) that are demonstrated on gas network problems. Recent works by Gugat et al. (2018b) and Sirvent (2018) investigate how nonlinear functions without an algebraic representation—e.g., arising as solutions of PDEs—can be incorporated into an MILP. This allows the use of more complex models for gas physics. Another model extension appears in Geißler, Morsi, Schewe, and Schmidt (2015), where an alternating direction method is used to include gas mixing by tracking the heat power of the different gases.

There are also many results that aim to solve a nonlinear—and typically non-convex—formulation of the gas transport problem as-is. This offers several advantages. Compared to the previous group of MILP-based methods, many of the NLP-approaches can use their respective models of gas physics without further approximations. Hence, using more complex models for gas physics is often easier compared to the MILP approaches. Disadvantages of NLP-based methods are the inherent difficulty of finding globally optimal solutions and the inclusion of binary decision variables.
Both Furey (1993) and Ehrhardt and Steinbach (2003) apply sequential quadratic programming to the gas network problem. Interior point methods are used by Steinbach (2007). In Schmidt, Steinbach, and Willert (2015a) the gas transport problem is formulated as a mathematical program with equilibrium constraints. High-detail models for stationary gas physics and active elements are derived in Schmidt, Steinbach, and Willert (2015b). In the subsequent article Schmidt, Steinbach, and Willert (2016), their accuracy is evaluated by comparison with a simulation tool. The publications by Hamam and Brameller (1971), Mallinson et al. (1993), and Ríos-Mercado et al. (2002) first describe a reduction technique and then solve the resulting problems with nonlinear programming methods. In the same spirit, Wu et al. (2000) propose different relaxations for modeling the feasible compressor operation range and compressor cost. An MINLP formulation is considered in Humpola and Fügenschuh (2015). The resulting problem is solved by spatial branching together with convex relaxations that are considered once all binary variables are fixed. Finally, Misra et al. (2015) present a geometric programming approach with a focus on compressor operations.

Comparing both the two groups of MILP and NLP-based methods, it is evident that they complement each other well. While mixed-integer linear approaches suffer from a comparatively coarse representation of the physical properties of the gas, incorporating combinatorial aspects that arise in switchable active elements is straightforward. On the other hand, nonlinear programming methods allow very detailed physical models but have diffi-

culties with discrete elements. Altogether, this has motivated a combined approach. Domschke et al. (2011) propose a combination of piecewise-linear mixed-integer models with a sequential quadratic programming approach for a transient gas transport problem. A similar approach is described in Pfetsch et al. (2015) and Koch et al. (2015) for the stationary case. In a first step, a coarse MILP approximation is used as a heuristic to find candidate solutions for the binary decision variables. In a second step, the binary decision variables are fixed to these candidate solutions, and their feasibility is validated with a high-detail nonlinear model.

Convex relaxations are used in the context of expansion planning for gas networks by Babonneau, Nesterov, and Vial (2012) and Borraz-Sánchez et al. (2016).

Optimal control questions in transient gas transportation networks are also studied in several articles. We mention Baumrucker and Biegler (2010), who use mathematical programming with equilibrium constraints. Zlotnik, Chertkov, and Backhaus (2015) optimize a dynamic gas flow setting with varying injections and withdrawals. A stochastic line-pack problem is studied by Zavala (2014). The recent work by Gugat et al. (2018a) solves a transient instantaneous optimal control problem with a series of MILPs.

Over the years many heuristic approaches have also been developed. We mention simulated annealing by Mahlke, Martin, and Moritz (2007), tabu search by Borraz-Sánchez and Ríos-Mercado (2009), ant colony optimization by Chebouba et al. (2009), and a heuristic two-stage approach that repeatedly optimize pressure and flow solutions by Ríos-Mercado, Kim, and Boyd (2006).

3 Robust treatment of gas transport

Mathematical models for real-world problems often include uncertain data. As these uncertainties can have a significant influence on the quality and feasibility of the solutions, the question arises how these effects can be treated appropriately. The aim of such a treatment can be, for example, minimizing the influence of uncertainties on the solutions, giving guarantees regarding the solution quality, or finding solutions that are entirely immune to small fluctuations of the data. Depending on the available information, e.g., from previous observations or expert knowledge, fundamentally different solution paradigms can be pursued.

One of these solution paradigms is robust optimization, which is explained in more detail here. Robust optimization in the broadest sense aims to find solutions that are in some way safeguarded against all parameter realizations from an a priori selected set of likely values. We explain this methodology and the motivation behind it in more detail using the gas network problem (2.43) under uncertainty. Afterward, the general aspects and ideas of robust optimization are formalized in an abstract setting. Taking the previous discussion of uncertainties in gas into account, we ultimately model the gas transport problem under uncertainty as a two-stage robust optimization problem with a non-convex second stage. This formulation, as well as its abstract counterpart, serve as a basis for the approaches developed in the following chapters. We give a short literature review of the general solution methods for robust optimization and highlight some of the challenges arising from the application of known methods to the gas network problem.

This chapter is structured as follows. In section 3.1, the sources and influences of uncertainties in real-world problems and their possible treatment are discussed using the gas network problem as an example. In addition, we give a brief overview of previously investigated gas transport problems under uncertainty in the literature. Section 3.2 introduces the robust optimization methodology, including a short literature review on general solution approaches In section 3.3, we apply the robust optimization methodology to the gas network transport problem with linear pressure-modifying elements, leading to a two-stage robust problem with a non-convex second stage. We close the chapter with section 3.4, outlining the challenges and limitations of using standard approaches to solve the gas transport problem.

3.1 Motivation

This section aims to motivate at a high level the reasons for choosing a two-stage robust optimization problem to model gas transport under uncertainty. A rigorous mathematical introduction to general robust optimization and the two-stage model for gas transport follow in sections 3.2 and 3.3, respectively.

Optimization problems that arise from real-world settings can often only be formulated with a loss of accuracy. This may be due to, e.g., an incomplete or empirical description of the underlying processes, model simplifications, or inaccurate knowledge of model parameters; see Ben-Tal, El Ghaoui, and Nemirovski (2009) for some concrete examples. Typically, all three of the previously mentioned factors occur in gas transport problems. For example, several model simplifications and empirical laws are used for our model of the gas transport problem; see chapter 2.

There are several strategies for dealing with these inaccuracies. Often, a main goal is to characterize the impact of the uncertainties and, if necessary, to adapt the mathematical model in such a way that their influence is minimized. Investigating the discrepancy between mathematical models with different degrees of detail can be done experimentally by comparing them with a more precise model or real-world data. In the same way, the influence of empirical laws on the overall system can be evaluated; see Schmidt, Steinbach, and Willert (2015b, 2016) for such a comparison in gas network operations. While the previous methods are more experimental in nature, it may also be possible to analytically derive error estimators between different mathematical models, e.g., between a simplified and a non-simplified ODE or PDE model. Error estimators for gas networks are studied in, e.g., Mehrmann, Schmidt, and Stolwijk (2018) and Domschke, Kolb, and Lang (2015).

In this thesis, however, we are not dealing with uncertainties due to modeling decisions, but rather with uncertainties in the given data and parameters. These inaccuracies in the data are present in many real-world applications and may arise from a variety of factors; see Ben-Tal and Nemirovski (2002) for a more in-depth discussion. For example, every physical quantity can only be measured up to a certain precision, and some parameters may only be measurable with great effort or have to be estimated. If these inaccurate parameters are used in an optimization model, mathematical solutions might arise that are infeasible in reality because of the differences between the measured or estimated data and the "real" data. Similarly, mathematical models can lead to solutions with too much precision, e.g., too many decimal digits, which in reality cannot be implemented with the necessary accuracy. The frequent occurrence of infeasible solutions caused by uncertainties was studied in Ben-

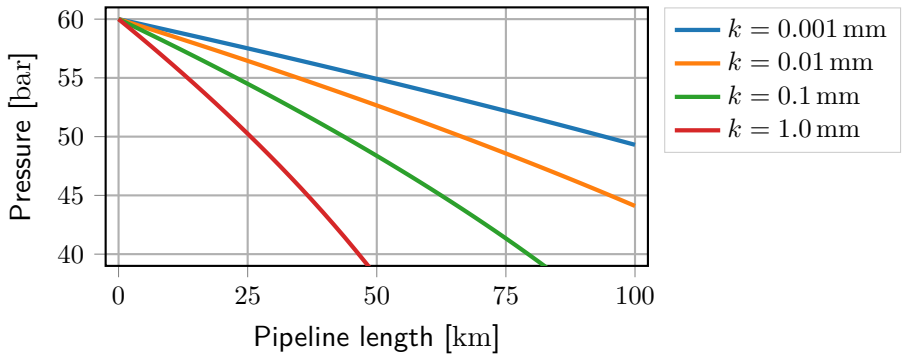

Figure 3.1: Influence of the integral roughness k on the pressure loss along a $100\,\mathrm{km}$ long pipeline. Other parameters: diameter $D = 50\,\mathrm{cm}$, volumetric flow $q = 250 \times 1000\,\mathrm{N\,m^3\,h^{-1}}$.

Tal and Nemirovski (2000) by using perturbed LPs. It is thus desirable to find solutions that are in a certain sense immunized or *robust* against fluctuations in the models' parameters.

We consider two parameters of the gas transport problem as uncertain: the pressure drop coefficient $\boldsymbol{l} \in \mathbb{R}^{|\mathcal{A}_{\mathrm{pi}}|}_{>0}$ occurring in the Weymouth equation (2.32) and the demand vector $\boldsymbol{d} \in \mathbb{R}^{|\mathcal{V}|}$.

We briefly recall that the Weymouth equation

$$\pi_w - \pi_v = -l_a q_a |q_a| \tag{3.1}$$

models the pressure drop between two connected nodes $(v, w) = a \in \mathcal{A}_{\mathrm{pi}}$. The magnitude of the pressure change depends on the flow along the pipe and the pressure drop coefficient l_a. The pressure drop coefficient is influenced by various physical properties of the pipe such as length, diameter, integral roughness, as well as the chemical properties of the gas mixture. This thesis is inspired by uncertainties in pipe roughness since this parameter increases over time as the pipe ages and deteriorates. Measuring the current value of this parameter can be difficult or even impossible. It can therefore often only be estimated on the basis of the age of the pipe or its use; see Farshad, Rieke, and Garber (2001). Since no other information such as a probability distribution is known, a robust treatment of this parameter is appropriate. As we consider the entire pressure drop coefficient to be uncertain, any uncertainty in one of the aforementioned parameters can also be treated with our methods.

The pressure loss in a pipeline depending on pipeline length and integral roughness factor is illustrated in fig. 3.1. We observe that the pressure loss is strongly influenced by the length of the pipeline and the integral roughness.

We note that the selected pipeline parameters and flow rate are similar to situations found in GasLib-134, i.e., the natural gas network of Greece. This observation is confirmed by Osiadacz and Chaczykowski (2010), who determine from a comparison with a real-world pipeline that the friction factor has a high impact on the state of the network.

The demand d_v at each node $v \in \mathcal{V}$ is another quantity that can be affected by uncertainty. For example, gas consumption in cities is highly temperature-dependent due to heating; see Heitsch et al. (2015). Although there are stochastic forecast models based on past climate data, the exact future consumption is naturally unknown and can only be estimated. Another source of uncertainty in demand is associated with the energy turnaround and the increasing presence of renewable energy sources in the power grid. The energy production from some renewable energy sources such as wind and solar is strongly dependent on the weather. To mitigate this unreliable energy production, gas-fired power plants are valued as a flexible energy source to compensate for fluctuations in renewable energy production; see Chertkov, Backhaus, and Lebedev (2015). The gas consumption of these power plants can thus be modeled as an uncertain quantity.

Depending on the available data and the desired protection against uncertainties, there are different modeling approaches for problems affected by uncertainty. If probability distributions for the uncertain parameters are known or can be estimated, stochastic programming approaches may be feasible; see, e.g., Birge and Louveaux (2011) and references therein. For example, the aim can be to optimize the expected value of an objective function given an underlying probability distribution. Another stochastic approach is *chance constraints*, where a constraint only has to be fulfilled with a certain probability. Clearly, all these approaches require a suitable model of the underlying probability distribution. For example, a probability distribution for the gas demand of a city can be determined well from historical data, as it depends mainly on the ambient temperature; see Heitsch et al. (2015). However, this typically does not apply to gas entering the network, as this quantity of gas is more price- and market-oriented. If the probability distribution is difficult or impossible to determine, robust optimization approaches may be more appropriate. The same applies if a probabilistic guarantee is not sufficient and instead protection against all possible scenarios is required. Finally, the inclusion of complex distribution information can quickly lead to very challenging stochastic problems. In comparison, robust approaches are often simpler and hence easier to solve, but also often lead to more conservative solutions compared to sophisticated stochastic models.

We now introduce the basic ideas of robust optimization. In the robust optimization paradigm, the values of uncertain parameters are assumed to be in a predefined compact set, the so-called *uncertainty set* or *uncertainty region*; see Ben-Tal, El Ghaoui, and Nemirovski (2009). Elements of this set are also called *scenarios*. For example, uncertainties in one-dimensional parameters such as the integral roughness factor can be modeled as a simple interval. This reflects the notion that all realizations of this parameter lie between some (typically estimated) lower and upper bound. While uncorrelated parameters lead to an uncertainty region in the form of a hyperrectangle, correlated parameters can be expressed with differently shaped sets such as ellipsoids.

The idea of robust optimization is to find solutions that are immune against all possible realizations of uncertain data from the uncertainty set. Feasible points with this property are said to be *robust feasible*. Optimizing over the set of robust feasible points yields solutions that provide the best possible objective function value for the worst scenario.

Problems under uncertainty often deal with making decisions under incomplete information. Many applications have a multilevel structure where phases in which information is revealed alternate with phases in which decisions are made; see, e.g., Ben-Tal et al. (2004) for a robust optimization perspective and Bard (1998) for a more general bilevel point of view. For example, betting on the outcome of a soccer match is typically a single-stage process. The bet must be placed without knowledge of the final outcome before the game begins. However, there are so-called "live bets" where the placed wager can be modified after the game has started. If, for example, this is permitted at halftime, a customer can use her knowledge about the course of the game so far and adjust her bet accordingly. Her second decision on the half-time break fundamentally depends on the information observed so far. This is an example of a two-stage problem. Depending on the stage in which a decision is taken, we further distinguish the problem variables into *first-stage variables* and *second-stage variables*. These variables are also called *here-and-now* and *wait-and-see* variables. While first-stage variables do not depend on the actual realization of the uncertainty, second-stage (or further stage variables) can depend on all information that has been revealed in previous stages.

From the point of view of the gas network operator, the nomination validation problem under uncertainty is a single-stage problem: the decision how the active elements are configured has to be taken without exact knowledge of the uncertain parameters. However, not all problem variables are decisions that can be taken by the operator. All auxiliary variables that model physical quantities like pressure or flow within the network cannot be controlled

directly by the network operator but arise as the network's state from nature. These variables of state depend on the (uncertain) physical parameters and on the decisions of the network operator. Therefore, a two-stage structure is appropriate for the nomination validation problem under uncertainty. The operator's configuration of the active elements is a first-stage variable, as it has to be decided without prior knowledge of the uncertainty. On the other hand, the physical state of the network, i.e., pressures and flows, is a result of the operator's decision as well as the laws of physics that have perfect knowledge of the uncertain parameters. As such, these quantities depend on the uncertainty and are best modeled as second-stage variables.

Gas transport under uncertainty

More specifically in the gas context, uncertainties have been considered in several publications.

We distinguish between stochastic and robust applications and begin with stochastic approaches. Gotzes et al. (2016) derive an analytic description of the set of feasible load scenarios for a given network in a stationary setting. The authors use this description together with a procedure called *spheric-radial decomposition* to estimate the probability that a load scenario arising from given probability distribution is feasible. They demonstrate that their method outperforms a standard Monte Carlo method for probability estimation. Chertkov, Backhaus, and Lebedev (2015) examine the influence of unreliable wind energy generation on pressure fluctuations in a connected natural gas pipeline system. To this end, they study the effect of varying gas injections as well as pressure levels at all points along a straight pipeline. The authors identify points of peak fluctuations within the pipeline and propose to factor this information into compressor operations.

Transient models combined with stochastic aspects have been studied in the context of line-pack problems. Hedging a transient line-pack problem against a discrete set of future scenarios is studied in Carter and Rachford (2003). A similar problem is considered by Zavala (2014). Starting from a transient PDE model together with a finite set of time-dependent demand profiles, the author develops a discretized stochastic optimal control model for a line-pack problem. The presented approach generates policies for the operator to control the compressors within the network. Moreover, the objective function is supplemented with a risk metric to help operators reduce volatility within the system.

Next, we consider robust optimization approaches. Mostly, these publications focus on uncertainties in demand. Vuffray, Misra, and Chertkov (2015) present a robust treatment of load fluctuations in a stationary gas network. The demand at a subset of nodes is allowed to fluctuate within a given hypercube. The authors develop a two-stage robust optimization problem whose objective is to find a cost-minimal injection pattern such that all possible fluctuations can be satisfied by the network. By exploiting monotonicity properties of the feasible flows, they show how this task can be tackled by replacing the robust constraints by a finite number of inequalities. Robinius et al. (2019) study a network design problem under uncertainty. It consists of selecting pipe diameters for a tree-shaped network such that all demands from a box uncertainty set intersected with a balancing hyperplane can be satisfied. By exploiting monotonicity, the authors derive a combinatorial polynomial-time algorithm that generates a finite set of critical load scenarios. It is shown that optimal pipe dimensioning for this finite scenario set is also optimal for the original robust optimization task under the box uncertainty set. Labbé, Plein, and Schmidt (2018) investigate the *booking validation problem* on tree-shaped gas networks. In essence, the problem is to decide whether a gas network can satisfy all demands from a given box uncertainty intersected with a balancing hyperplane set. Similar to Robinius et al. (2019), the authors develop a combinatorial polynomial-time method that identifies critical scenarios. Subsequently, these critical scenarios are used to answer the booking validation question.

Finally, there is research concerned with a combination of robust and stochastic aspects. In González Grandón, Heitsch, and Henrion (2017), the previously discussed work by Gotzes et al. (2016) has been extended to incorporate uncertain pressure drop coefficients. The authors analytically derive a robust counterpart for a tree-shaped network where the pressure drop coefficient of each pipe can fluctuate within a given interval. By including this counterpart in the probability estimation approach of Gotzes et al. (2016), the probability of a feasible load scenario for a robust problem can be estimated. Adelhütte et al. (2018) present a new class of robust/stochastic so-called *probust* optimization tasks using the example of gas networks. They study a gas network problem where a robust constraint regarding the demand has to be satisfied with high probability. In particular, the outflow at withdrawal nodes is subject to a stochastic model while the inflow at injection nodes is subject to the robust/stochastic constraint. The robust aspect represents an uncertainty in the inflowing gas quantity: while the total amount is known, the gas can be distributed (almost) arbitrarily among a set of input nodes. The authors

propose a procedure that uses the spheric radial decomposition combined with an MILP penalty function approach to estimate the overall probability for feasibility in this setting.

3.2 The robust optimization methodology

Before diving deeper into the mathematical model for the gas transport problem under uncertainty, we briefly review the general robust optimization setting. For a more comprehensive treatment, we refer the reader to the book by Ben-Tal, El Ghaoui, and Nemirovski (2009) or the review articles by Gorissen, Yanıkoğlu, and Hertog (2015), Bertsimas, Brown, and Caramanis (2011), and Gabrel, Murat, and Thiele (2014).

The first basic ideas of robust optimization appear in Soyster (1973). In this article, an LP whose columns are subject to parameter uncertainties is considered. Additionally, the notion of "robustness", i.e., finding solutions that are feasible for all parameter realizations, is also present. Similar ideas are also investigated in robust optimal control; see, e.g., Zhou, Doyle, and Glover (1996). In the 1990s, the foundations for modern optimization were laid in the articles by El Ghaoui and Lebret (1997), El Ghaoui, Oustry, and Lebret (1999), and Ben-Tal and Nemirovski (1998, 1999). Since then intensive research has been carried out in this area. The material in this section follows Ben-Tal, El Ghaoui, and Nemirovski (2009).

A robust optimization task is a family of optimization problems that is parameterized by an *uncertainty set* $\mathcal{U} \subseteq \mathbb{R}^{n_u}$, $n_u \in \mathbb{N}$:

$$\left\{ \min_{\boldsymbol{z} \in \mathbb{R}^{n_z}} \{ \boldsymbol{f}(\boldsymbol{z}) \mid \boldsymbol{h}(\boldsymbol{u}, \boldsymbol{z}) = \boldsymbol{0},\ \boldsymbol{g}(\boldsymbol{u}, \boldsymbol{z}) \leq \boldsymbol{0} \} \right\}_{\boldsymbol{u} \in \mathcal{U}}. \tag{$\mathrm{P}_{\mathcal{U}}$}$$

In addition to the problem variables $\boldsymbol{z} \in \mathbb{R}^{n_z}$ with $n_z \in \mathbb{N}$, the constraint functions $\boldsymbol{h} \colon \mathbb{R}^{n_u} \times \mathbb{R}^{n_z} \to \mathbb{R}^{m_h}$ and $\boldsymbol{g} \colon \mathbb{R}^{n_u} \times \mathbb{R}^{n_z} \to \mathbb{R}^{m_g}$ for $m_h, m_g \in \mathbb{N}_0$ accept an additional *data* vector $\boldsymbol{u} \in \mathcal{U}$. We assume that the uncertainty region $\mathcal{U}$ is a compact convex set that comprises all meaningful realizations of the uncertain parameters. Without loss of generality, we assume an objective function $\boldsymbol{f} \colon \mathbb{R}^{n_z} \to \mathbb{R}$ that is certain, see Ben-Tal et al. (2004) for a justification.

The goal of robust optimization is to find solutions for ($\mathrm{P}_{\mathcal{U}}$) which are immunized against all possible choices $\boldsymbol{u} \in \mathcal{U}$. In the most basic setting, all problem variables have to be fixed before the uncertainty becomes known. This leads to the *static robust counterpart* (Ben-Tal and Nemirovski 2002)

$$\min_{\boldsymbol{z}} \{ \boldsymbol{f}(\boldsymbol{z}) \mid \boldsymbol{h}(\boldsymbol{u}, \boldsymbol{z}) = \boldsymbol{0},\ \boldsymbol{g}(\boldsymbol{u}, \boldsymbol{z}) \leq \boldsymbol{0} \quad \forall \boldsymbol{u} \in \mathcal{U} \}, \tag{RC}$$

where the feasible region is the set of all $\boldsymbol{z}$ that are feasible for all possible realizations of the uncertainty $\boldsymbol{u} \in \mathcal{U}$. Since the uncertainty set parameterizes infinitely many constraints, (RC) is a *semi-infinite problem*. Solving these kinds of problems in practice requires a strategy to deal with the infinite number of constraints. We highlight two general ways to solve robust counterparts. If (RC) is an LP with a polyhedral uncertainty set, duality-based arguments allow a reformulation of (RC) as a finite LP; see Ben-Tal, El Ghaoui, and Nemirovski (2009, chapter 1). Moreover, the size of the resulting problem is polynomial in the size of the original problem under uncertainty. The book by Ben-Tal, El Ghaoui, and Nemirovski (2009) provides similar reformulation strategies for linear, conic quadratic, or semidefinite problems over different types of uncertainty sets. These results are generalized in Ben-Tal, Hertog, and Vial (2015) to convex nonlinear constraints that are concave in the uncertain parameter. Under some mild regularity conditions, the authors describe a systematic way to construct a finite robust counterpart over a convex and bounded uncertainty region.

A different solution idea for robust problems is the *adversarial approach*, where the continuous uncertainty set $\mathcal{U}$ is replaced by a finite set $\hat{\mathcal{U}} \subseteq \mathcal{U}$ of *critical scenarios*; see Bienstock and Özbay (2008) and Gorissen, Yanıkoğlu, and Hertog (2015) for more details. This set is then perpetually extended with more scenarios until robust feasibility of the whole problem can be proven. However, depending on the problem structure and the shape of the uncertainty set, this procedure may only be exact at the limit. For example, the adversarial approach terminates in a finite number of steps for linear constraints over a polyhedral uncertainty set, as the critical scenarios are the finitely many vertices of the polyhedron. In Bertsimas, Dunning, and Lubin (2016), the adversarial approach is compared with a reformulation approach by a series of numerical experiments for different combinations of problem structure and type of the uncertain region. In general, the adversarial approach is very flexible and can be applied to a broader range of problems compared to duality-based arguments. However, it may be required to solve subproblems to global optimality, which can be difficult if the problem is non-convex.

For some applications, static robustness is the wrong modeling choice, e.g., when problem variables can adjust to the revealed uncertainty. In this case, a two-stage approach has to be used. Here, the problem variables are partitioned into *first-stage* and *second-stage* variables: $\boldsymbol{z} = (\boldsymbol{x}, \boldsymbol{y}) \in \mathbb{R}^{n_z} = \mathbb{R}^{n_x + n_y}$ with $n_x, n_y \in \mathbb{N}_0$. First-stage or *here-and-now* variables $\boldsymbol{x} \in \mathbb{R}^{n_x}$ have to be fixed before the uncertainty becomes known, whereas second-stage or *wait-and-see* variables $\boldsymbol{y} \in \mathbb{R}^{n_y}$ can be decided with knowledge of the revealed uncertainty.

Since the second-stage variables thus depend on the uncertain parameter, they are also called *adjustable variables*. The notion of different actions happening at different points in time or under different information directly leads to the *adjustable robust counterpart* (Ben-Tal et al. 2004)

$$\min_{\boldsymbol{x}} \{\boldsymbol{f}(\boldsymbol{x}) \mid \exists \boldsymbol{x}\ \forall \boldsymbol{u} \in \mathcal{U}\ \exists \boldsymbol{y} \text{ with } \boldsymbol{h}(\boldsymbol{u}, \boldsymbol{x}, \boldsymbol{y}) = \boldsymbol{0},\ \boldsymbol{g}(\boldsymbol{u}, \boldsymbol{x}, \boldsymbol{y}) \leq \boldsymbol{0}\}. \quad \text{(ARC)}$$

W.l.o.g., the objective only depends on here-and-now variables.

We notice that in (ARC), the condition "$\forall \boldsymbol{u} \in \mathcal{U}\ \exists \boldsymbol{y}$" merely is the definition of a function $\boldsymbol{y} \colon \mathcal{U} \to \mathbb{R}^{n_y}$ that maps the uncertainty set to the space of the second-stage variables. Thus we rewrite the adjustable robust counterpart (ARC) by introducing a functional dependency between second-stage variables and uncertain parameters:

$$\min_{\boldsymbol{x},\, \boldsymbol{y}(\cdot)} \{\boldsymbol{f}(\boldsymbol{x}) \mid \boldsymbol{h}(\boldsymbol{u}, \boldsymbol{x}, \boldsymbol{y}(\boldsymbol{u})) = \boldsymbol{0},\ \boldsymbol{g}(\boldsymbol{u}, \boldsymbol{x}, \boldsymbol{y}(\boldsymbol{u})) \leq \boldsymbol{0} \quad \forall \boldsymbol{u} \in \mathcal{U}\}. \quad \text{(ARC-DR)}$$

The function $\boldsymbol{y}(\cdot)$ is an a priori unknown variable and is determined endogenously as part of the optimization task. It is also called a *decision rule*. By stating the (ARC) in such a way, the two-stage structure is converted into a single-stage structure similar to (RC). In principle, the previously discussed techniques for single-stage problems can then be applied. However, unlike the static robust counterpart, one of the unknowns is a function, making (ARC) an infinite-dimensional problem over an infinite number of constraints. In general, this problem is NP-hard; see Guslitser (2002).

Next, we give a brief overview of some important results and aspects concerning adjustable robust optimization. For a more in-depth survey, we refer to Yanıkoğlu, Gorissen, and Hertog (2018). A typical solution approach for solving multi-stage robust problems is to constrain the decision rules $\boldsymbol{y}(\cdot)$ to a predefined class of functions. For example, Ben-Tal et al. (2004) introduce an *affinely adjustable robust counterpart* by enforcing an affine linear decision rule structure on an uncertain LP. If no uncertain parameter appears as a coefficient of a second-stage variable, the problem is said to have *fixed recourse* and can be reformulated as an LP. On the other hand, problems with *random recourse*, i.e., where products of uncertain parameters and second-stage variables appear, are NP-hard; see Ben-Tal et al. (2004). For this case, Ben-Tal et al. (2004) propose an approximation using a semidefinite program (SDP); see also Kuhn, Wiesemann, and Georghiou (2011). Many classes of decision rules have been studied in the literature, we mention piecewise-linear decision rules (Chen and Zhang 2009) as well as polynomial decision rules (Bertsimas, Iancu, and Parrilo 2011). The predefined function class is often not rich

enough to contain the best possible, i.e., the fully adjustable decision rule $\boldsymbol{y}^*(\cdot)$. Hence, this solution approach generally produces more conservative solutions when compared to the fully-adjustable solution. Nevertheless, there are some simple problem classes where "optimal" decisions rules are known; see Bertsimas, Iancu, and Parrilo (2010).

The decision rule approach becomes more challenging once adjustable binary (or integer) variables are introduced. In Bertsimas and Georghiou (2015, 2018), binary variables for adjustable MILPs are modeled as piecewise functions with a fixed number of pieces. For purely binary problems, K-*adaptability* is a concept that allows the binary decision rule vector to take on any of K values. This idea was first studied in Bertsimas and Caramanis (2010) and later by Hanasusanto, Kuhn, and Wiesemann (2015) who provide a MILP reformulation. Another idea that has generated some research interest is to approximate arbitrary decision rules through partitioning of the uncertainty set. By allowing each partition to have its own (constant) decision rule, arbitrary piecewise (constant) functions can be expressed. The question of how good partitions can be selected during an iterative procedure was studied by Bertsimas and Dunning (2016), Postek and Hertog (2016), and Romeijnders and Postek (2018).

There are also some alternative solution approaches without the need for decision rules. For example, a Fourier-Motzkin elimination is used in Zhen, Hertog, and Sim (2018) to convert an adjustable LP with fixed recourse to a static robust optimization problems. A different approach by Takeda, Taguchi, and Tütüncü (2008) shows that under a certain quasiconvexity property, two-stage NLPs can be reduced to static robust problems. Finally, Zeng and Zhao (2013) proposes a general constraint-and-column generation algorithm for two-stage problems with linear constraints. The presented Benders-style cutting plane method relies on solving bilinear subproblems to global optimality.

This concludes the general overview of the "standard" approaches of robust optimization. A direct application of these general methods to the gas network problem is challenging; the reasons for this are discussed in greater detail in section 3.4.

3.3 A two-stage robust model for gas transport

We consider the gas transport problem with uncertainties in the pressure drop coefficients $\boldsymbol{l}$ and with uncertainties in the demand vector $\boldsymbol{d}$. Let $\mathcal{L} \subseteq \mathbb{R}_{>0}^{|\mathcal{A}_{\text{pi}}|}$ denote the uncertainty set of the pressure drop coefficients, and let $\mathcal{D} \subseteq \mathbb{R}^{|\mathcal{V}|}$ denote the uncertainty set of the demands. When not explicitly stated

otherwise, the considered problems are affected by both types of uncertainty, i.e., by a combined uncertainty set

$$\mathcal{U} = \mathcal{L} \times \mathcal{D}. \tag{3.2}$$

In the following, we introduce a canonical definition of each uncertainty set and formulate the two-stage robust problem.

Uncertain pressure drop coefficients This is an *arc-wise* uncertainty and influences the pressure drop between two incident nodes. For all pipes $a \in \mathcal{A}_{\mathrm{pi}}$, let $\underline{l}_a$, $\overline{l}_a \in \mathbb{R}_{>0}$ with $0 < \underline{l}_a \leq \overline{l}_a$ be given. This leads to the uncertainty set

$$\mathcal{L} := \{\boldsymbol{l} \in \mathbb{R}_{>0}^{|\mathcal{A}_{\mathrm{pi}}|} \mid \underline{l}_a \leq l_a \leq \overline{l}_a \quad \text{for all } a \in \mathcal{A}_{\mathrm{pi}}\}, \tag{3.3}$$

which is also known as a *box uncertainty*.

Uncertain demand This *node-wise* uncertainty has an impact on the solution space of the linear network flow problem. For all nodes $v \in \mathcal{V}$, let $\underline{d}_v$, $\overline{d}_v \in \mathbb{R}$ with $\underline{d}_v \leq \overline{d}_v$ be given. As the overall demand always has to be balanced, the uncertainty set includes a balancing constraint:

$$\mathcal{D} := \left\{ \boldsymbol{d} \in \mathbb{R}^{|\mathcal{V}|} \;\middle|\; \begin{array}{ll} \underline{d}_v \leq d_v \leq \overline{d}_v & \text{for all } v \in \mathcal{V} \\ \sum_{v \in \mathcal{V}} d_v = 0 & \end{array} \right\}. \tag{3.4}$$

A polyhedral set of the form $\mathcal{D}$ is called *hose polytope*; see Duffield et al. (1999).

Remark 3.3.1. Our methods are in general also applicable to other types of uncertainty sets. The shape of the uncertainty set typically determines the type of the resulting robust counterparts. For example, polyhedral uncertainty sets are described by linear functions and therefore lead to LPs or MILPs. Similarly, ellipsoidal uncertainty sets defined over the Lorentz cone lead to (mixed-integer) convex quadratic problems.

We already established in section 3.1 that a robust treatment of the gas network problem (2.43) requires a two-stage model. Starting from the nominal problem (2.43), we formulate the two-stage nomination validation problem with a linear compressor model under uncertainty. The compressor power variables $\boldsymbol{x}^{\mathrm{pm}}$ can be controlled by an operator and hence are first-stage vari-

ables, whereas the physical state of the network, i.e., squared pressure vector $\boldsymbol{\pi}$ and flow vector $\boldsymbol{q}$ are second-stage variables:

$$\min_{\boldsymbol{x}^{\mathrm{pm}}} \ \boldsymbol{c}^\top \boldsymbol{x}^{\mathrm{pm}} \tag{3.5a}$$

$$\text{s.t. } \boldsymbol{x}^{\mathrm{pm}} \in [\underline{\boldsymbol{x}}^{\mathrm{pm}}, \overline{\boldsymbol{x}}^{\mathrm{pm}}], \tag{3.5b}$$

$$\text{s.t. for all } (\boldsymbol{l}, \boldsymbol{d}) \in \mathcal{U} \text{ there is } \boldsymbol{q}, \boldsymbol{\pi} \text{ with}$$

$$\boldsymbol{A}\boldsymbol{q} = \boldsymbol{d}, \tag{3.5c}$$

$$\boldsymbol{A}^\top \boldsymbol{\pi} = \boldsymbol{\psi}(\boldsymbol{l}, \boldsymbol{q}, \boldsymbol{x}^{\mathrm{pm}}), \tag{3.5d}$$

$$\boldsymbol{\pi} \in [\underline{\boldsymbol{\pi}}, \overline{\boldsymbol{\pi}}], \tag{3.5e}$$

$$\boldsymbol{q} \in \mathbb{R}^{|\mathcal{A}|}. \tag{3.5f}$$

We apply theorem 2.3.5 to obtain a *reduced* version of (3.5):

$$\min_{\boldsymbol{x}^{\mathrm{pm}}} \ \boldsymbol{c}^\top \boldsymbol{x}^{\mathrm{pm}} \tag{3.6a}$$

$$\text{s.t. } \boldsymbol{x}^{\mathrm{pm}} \in [\underline{\boldsymbol{x}}^{\mathrm{pm}}, \overline{\boldsymbol{x}}^{\mathrm{pm}}], \tag{3.6b}$$

$$\text{s.t. for all } (\boldsymbol{l}, \boldsymbol{d}) \in \mathcal{U} \text{ there is } \boldsymbol{q}_{\mathcal{N}} \in \mathbb{R}^{|\mathcal{N}|} \text{ with}$$

$$\boldsymbol{C}\boldsymbol{\psi}(\boldsymbol{l}, \boldsymbol{q}^{\mathrm{ext}}(\boldsymbol{d}, \boldsymbol{q}_{\mathcal{N}}), \boldsymbol{x}^{\mathrm{pm}}) = \boldsymbol{0}, \tag{3.6c}$$

$$\boldsymbol{P}\boldsymbol{\psi}_{\mathcal{B}}(\boldsymbol{l}_{\mathcal{B}}, \boldsymbol{q}^{\mathrm{ext}}_{\mathcal{B}}(\boldsymbol{d}, \boldsymbol{q}_{\mathcal{N}}), \boldsymbol{x}^{\mathrm{pm}}_{\mathcal{B}}) \leq \Delta\boldsymbol{\pi}. \tag{3.6d}$$

Both problem formulations will later be useful in different contexts.

Remark 3.3.2. As is outlined in theorem 2.3.5, any choice of root node pressure from the interval (2.74) leads to a feasible solution. The question now is how to select a suitable element and how to treat this additional degree of freedom in the light of a two-stage robust formulation. The point of view here is that the network operator is satisfied with the guarantee that a feasible state within the pressure bounds of the network exists and thus a further selection a root node pressure is not necessary. It is important to understand that by formulating the state equation in the form (3.6c) and (3.6d), the remaining degree of freedom present in the parameter η of proposition 2.4.4 is eliminated and hence does not appear as a second-stage variable.

On the other hand, if for some reason a unique pressure solution is required, an arbitrary value of the interval (2.74) has to be chosen for the root node pressure π_r. This is equivalent to fixing the parameter η.

Setting the root node pressure can be accomplished either a priori by means of a boundary condition, or by an extra controllable variable modeled as an abstract pressure controller, or by a decision that has to be taken after the uncertainties are revealed. We note that the latter case is beyond the scope of this thesis.

Remark 3.3.3. The *booking validation problem* in gas network operations is a two-stage robust optimization problem that is very similar to the two-stage problem developed here; see Labbé, Plein, and Schmidt (2018) and Hiller et al. (2015). It is an important task for gas network operators and consists in deciding whether a certain set of demands (a *booking*) can always be transported by the network or not. However, there is a crucial difference compared to problem (3.5). While we consider all active elements as first-stage variables, the booking validation treats all active elements as second-stage variables. This reflects the fact that a gas network operator exhausts all available means in order to satisfy a given supply and demand situation. As the active elements are modeled as second-stage variables, the booking validation is therefore a more general version of problem (3.5).

3.4 Limits of known robust optimization approaches

As we have seen, the nomination validation problem under uncertainty naturally leads to a two-stage nonlinear robust problem (3.5). More precisely, the problem is continuous with an infinite number of non-convex constraints and an infinite number of variables.

Often, robust optimization approaches rely on strong duality or global optimality to solve the robust counterpart. Due to the non-convex nature of gas physics, these concepts cannot be directly applied here.

At this point, two basic ideas can be pursued. Both approaches differ in the order of robustification and problem transformation. On the one hand, we can seek to construct a piecewise-linear approximation of the nonlinear model (3.5) so that the standard techniques of linear robust optimization can be applied. On the other hand, we can essentially keep the nonlinear structure, formulate a robust counterpart, and then look for tractable methods for this type of problem. Both approaches were thoroughly explored for this thesis. While the second idea leads to two fruitful solution approaches detailed in chapters 4 and 5, the first idea quickly leads to several challenging problems and drawbacks. The rest of this section is dedicated to a discussion of these challenging factors arising from the first idea.

We start with the method of Geißler et al. (2012) to construct a piecewise-linear relaxation with an a priori chosen error bound $\varepsilon > 0$. An approximation of (3.5) is constructed by replacing the nonlinear constraint functions with relaxations based on piecewise-linear functions. For each nonlinear constraint, two piecewise-linear functions are constructed that respectively underestimate and overestimate the nonlinear function on its domain. Taking these

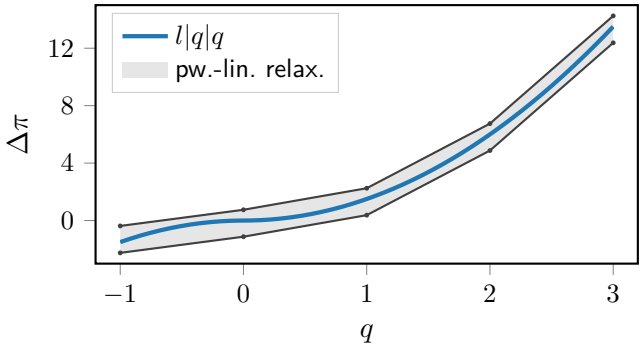

Figure 3.2: A piecewise-linear relaxation (gray area) of the Weymouth equation (blue line). The nonlinear function is bounded by piecewise-linear functions (dark gray lines) from above and below.

two functions as the boundary of a new feasible region, a relaxation for the original nonlinear constraint is obtained; see fig. 3.2 for a visualization of this idea. Moreover, by an appropriate selection of sampling points as presented in Geißler et al. (2012), a relaxation with an approximation quality is constructed in the sense that the distance between any relaxation point and the nearest value of the nonlinear function is bounded by the a priori given error ε.

By construction, the piecewise-linear model has two properties: the original nonlinear constraints are never violated by more than ε, and an infeasible relaxation indicates an infeasible NLP. This approach has already been successfully applied to the gas transport problem and allows solving the nominal problem for comparatively large networks; see Pfetsch et al. (2015) and Geißler, Martin, et al. (2015). Its successful use in the nominal setting and the fact that the relaxed model can be formulated as a linear MILP makes it very attractive as a starting point for robust treatment. We note that one advantage of this approach is that any active elements can be handled if it can be modeled by mixed-integer constraints. This includes, e.g., more complex models for valves and compressors as described in section 2.1.

In Aßmann (2014), a single-stage MILP variant of (3.5) with complex active elements under uncertain roughness was investigated. A single-stage model forces a feasible pressure and flow solution for all elements of the uncertainty set. As was argued earlier, this is not a feasible modeling choice for the gas network problem as the physical state adjusts to the uncertain parameters. Consequently, the resulting robust counterparts are very conservative and allow only very small uncertainty sets.

Next, the two-stage MILP variant of (3.5) was investigated. A typical strategy in this setting is to model the second-stage variables using decision rules; see, e.g., Ben-Tal et al. (2004). We observe that the mixed-integer linear approximation introduces auxiliary binary variables to model the piecewise-linear functions. Hence, in order to introduce decision rules for all second-stage variables, decision rules for binary variables are required. However, designing binary decision rules is still very challenging and can drastically increase model complexity. As a simplification, one can treat the binary variables as first-stage variables. The auxiliary binary variables are required to choose the segments of the piecewise-linear functions, thus treating these helper variables as non-adjustable leads to an artificial restriction on the adjustable second-stage variables. We were able to observe this effect in a prototypical implementation where the feasibility of the robust counterpart was very sensitive to the position of the sampling points.

In order to deal with the remaining continuous second-stage variables, affine linear decision rules were introduced into the problem. As the uncertain roughness parameters appear as coefficients of the second-stage variables, the problem has random recourse. In general this is an NP-hard problem to solve exactly, however, there is an SDP-approximation that can be used instead; see Ben-Tal et al. (2004). With the auxiliary binary variables in mind, this leads to a mixed-integer semidefinite program (MISDP), which can be challenging to solve in practice. Using the software by Gally, Pfetsch, and Ulbrich (2018), we were able to solve small toy instances with no more than ten nodes and without active elements. However, the conservative nature due to first-stage binary variables and possible due to the SDP relaxation were often evident.

Another conceptual difficulty arises due to the fact that already for passive networks, proposition 2.4.4 implies that the constraints of (3.5) uniquely determine the flow within the network. Thus, there is precisely one optimal decision rule $\boldsymbol{q}^*(\cdot)$. As a solution function of a polynomial system this decision rule is in general not contained in any of the treatable classes of decision rules, e.g., affine linear, piecewise linear, or polynomial functions. If $\boldsymbol{q}^*(\cdot)$ is not contained in the employed family of decision rules, no connection can be made between infeasibility of the robust counterpart and infeasibility of the nonlinear robust model. Let us assume for a moment that affine decision rules are used and that the resulting problem turns out to be infeasible. Unlike in the nominal case, where infeasibility of the piecewise-linear relaxation implies infeasibility of the original problem, this is not the case for the affinely adjustable robust counterpart. Such a conclusion is only valid if the optimal decision rule is an affine linear function, which is not true in this case.

To conclude, an attempt to solve (3.5) with affine linear decision rules raises several obstacles that are each very challenging on their own: necessity for binary decision rules, using an MISDP approximation instead of an exact reformulation, uniquely determined second-stage variables in the nonlinear case, no connection between an infeasible robust counterpart of the piecewise-linear model and infeasibility of the NLP.

Consequently, the idea of solving a robust counterpart of the piecewise-linear problem has not been pursued further and instead we have concentrated on a direct treatment of the nonlinear robust counterpart. We exploit certain structures present in the gas problem, e.g., the unique dependence between uncertain parameters and the physical state of the network. This allows us to derive two alternative approaches for solving an active and a passive version of (3.5) that are detailed in the following chapters.

4 A general approach for two-stage robust optimization with an empty first stage

We investigate feasibility and infeasibility of nonlinear two-stage robust feasibility problems with an empty first stage. It is further assumed that the considered sets, i.e., the uncertainty set and the feasible region, are described by polynomials. Without first stage variables, the feasibility question is equivalent to deciding whether the uncertainty set is contained within the projection of the feasible region onto the uncertainty-space. Compared to set containment problems where the constraintwise description of each set is known, the description of the projection is typically not available or too expensive to compute. A main contribution of this work is how to address the projected set in our methods without an explicit construction thereof.

We develop two general approaches for answering the set containment question, one for showing feasibility and one for showing infeasibility. While the infeasibility approach has no additional requirements, the feasibility approach requires a uniqueness assumption for the second-stage variables. Given these abstract ideas, we show how they can be approximated in practice by using techniques from polynomial optimization. Afterward, an application of the well-known Lasserre relaxation hierarchy (Lasserre 2000; Parrilo 2003) leads to SDP relaxations of the resulting problems that can be solved in practice.

Two separate approaches for feasibility and infeasibility are necessary as the developed methods are based on relaxations of exact problem formulations. For example, due to the relaxation, a problem might give a negative answer although the problem is, in fact, feasible.

The effectivity of our methods is tested on a variety of cyclic gas network instances. We observe that for instances where robust feasibility or infeasibility can be decided successfully, level 2 or level 3 of the Lasserre relaxation hierarchy typically is sufficient.

The idea of using polynomial optimization to show robust feasibility via set containment was conceived in discussions between Prof. Vera, Prof. Liers, and the author during a research stay at the University of Tilburg (NL). In particular, the ideas for the infeasibility method and the number of flow directions in a graph both arose similarly. The further development and implementation of these ideas was primarily carried out by the author of this work under the supervision of Prof. Liers and Prof. Stingl. The main results of this chapter have been published in

> D. Aßmann, F. Liers, M. Stingl, and J. C. Vera. 2018. "Deciding robust feasibility and infeasibility using a set containment approach: an application to stationary

passive gas network operations". *SIAM Journal on Optimization* 28 (3): 2489–2517. doi:10.1137/17M112470X.

In the following, we repeat and extend these results as well as their presentation.

This chapter is structured as follows. Section 4.1 introduces the studied two-step robust problem and the set containment idea. A short introduction to polynomial optimization in section 4.2 establishes the necessary background knowledge for this chapter. In section 4.3, the polynomial methods for deciding between robust feasibility and robust infeasibility are developed. An application to a passive gas transport problem follows in section 4.4. We show that a tree-shaped network can be decided by linear programming and we develop techniques to remove the absolute value functions arising from the gas context. Finally, the practical applicability of the methods is demonstrated in section 4.5 with a series of numerical experiments.

4.1 Problem setting and the projection idea

In this chapter, we focus on a satisfiability variant of the general two-stage robust optimization problem (ARC) as introduced in section 3.2. The goal is to answer positively or negatively, whether

$$\forall \boldsymbol{u} \in \mathcal{U}\ \exists \boldsymbol{y} \in \mathbb{R}^{n_y} \text{ such that } \boldsymbol{h}(\boldsymbol{u}, \boldsymbol{y}) = \boldsymbol{0},\ \boldsymbol{g}(\boldsymbol{u}, \boldsymbol{y}) \geq \boldsymbol{0}, \tag{4.1}$$

that is, the question whether for all $\boldsymbol{u} \in \mathcal{U}$ there is always a feasible second-stage variable $\boldsymbol{y}(\boldsymbol{u})$ that satisfies the constraints. If this question can be answered positively, we call the problem "robust feasible" and we call it "robust infeasible" otherwise.

We briefly recall the relevant definitions. Let $\mathcal{U} \subseteq \mathbb{R}^{n_u}$ with $n_u \in \mathbb{N}$ be the uncertainty set; let $\boldsymbol{y} \in \mathbb{R}^{n_y}$ with $n_y \in \mathbb{N}$ be the second-stage variables; and let $\boldsymbol{h} \colon \mathbb{R}^{n_u} \times \mathbb{R}^{n_y} \to \mathbb{R}^{m_h}$ with $m_h \in \mathbb{N}$ as well as $\boldsymbol{g} \colon \mathbb{R}^{n_u} \times \mathbb{R}^{n_y} \to \mathbb{R}^{m_g}$ with $m_g \in \mathbb{N}$ be the vector-valued constraint functions. Moreover, we assume that the uncertainty region $\mathcal{U}$ is defined by polynomials and that all entries of the constraint functions are polynomials, i.e., $h_1, \ldots, h_{m_h}, g_1, \ldots, g_{m_g} \in \mathbb{R}[\boldsymbol{u}, \boldsymbol{y}]$.

Let $\mathcal{Y} \in \mathbb{R}^{n_u} \times \mathbb{R}^{n_y}$ be the set of all feasible pairs of uncertain data $\boldsymbol{u}$ and second-stage variables $\boldsymbol{y}$:

$$\mathcal{Y} \coloneqq \left\{(\boldsymbol{u}, \boldsymbol{y}) \in \mathbb{R}^{n_u} \times \mathbb{R}^{n_y} \mid \boldsymbol{h}(\boldsymbol{u}, \boldsymbol{y}) = \boldsymbol{0},\ \boldsymbol{g}(\boldsymbol{u}, \boldsymbol{y}) \geq \boldsymbol{0}\right\}. \tag{4.2}$$

With this definition, we observe that robust feasibility (4.1) is equivalent to the set containment question

$$\mathcal{U} \subseteq \mathrm{Proj}_{\boldsymbol{u}}(\mathcal{Y}), \tag{4.3}$$

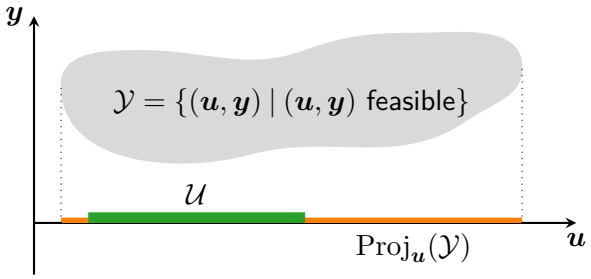

Figure 4.1: Robust feasibility is equivalent to the set containment question $\mathcal{U} \subseteq \mathrm{Proj}_{\boldsymbol{u}}(\mathcal{Y})$.

where we denote with $\mathrm{Proj}_{\boldsymbol{u}}\colon (\boldsymbol{u}, \boldsymbol{y}) \mapsto \boldsymbol{u}$ the projection map. Since set containment implies that each value of $\boldsymbol{u} \in \mathcal{U}$ is associated with at least one feasible solution $\boldsymbol{y}(\boldsymbol{u})$, the expression in (4.1) is satisfied. A visualization of the set containment idea is displayed in fig. 4.1. The gray area denotes the set $\mathcal{Y}$ of feasible $(\boldsymbol{u}, \boldsymbol{y})$ pairs, the green line represents the uncertainty set, and the orange line represents the projection of $\mathcal{Y}$ onto the uncertainty-space.

In the next subsection, the set containment idea is further explored using the example of a simple linear network flow problem over a tree.

Introductory example: linear flow problem over a tree We want to illustrate the problem and its possible solution approaches by means of a simple example. Let a linear flow problem over a tree with lower and upper edge capacities be given. We denote the vector of flows over the tree by $\boldsymbol{y}$ and the vector of demands by $\boldsymbol{u}$. We assume that the demand $\boldsymbol{u}$ of all nodes except some fixed root node fluctuates within a hyperrectangle $\mathcal{U}$ intersected with a balancing hyperplane. The data appears as an uncertain right-hand side of the flow balance equations. Then, the model can be stated as

$$\forall \boldsymbol{u} \in \mathcal{U}\ \exists \boldsymbol{y}\colon \begin{cases} \tilde{\boldsymbol{A}}\boldsymbol{y} = \boldsymbol{u}, \\ \underline{\boldsymbol{y}} \leq \boldsymbol{y} \leq \overline{\boldsymbol{y}} \end{cases} \tag{4.4}$$

for some nonsingular matrix $\tilde{\boldsymbol{A}}$; see section 2.3 for details. Our goal is to decide whether the network can satisfy all possible realizations of demand from $\mathcal{U}$.

After substituting $\boldsymbol{y} = \tilde{\boldsymbol{A}}^{-1}\boldsymbol{u}$, the problem is to check whether

$$\forall \boldsymbol{u} \in \mathcal{U}\colon \underline{\boldsymbol{y}} \leq \tilde{\boldsymbol{A}}^{-1}\boldsymbol{u} \leq \overline{\boldsymbol{y}}, \tag{4.5}$$

or equivalently

$$\mathcal{U} \subseteq \mathrm{Proj}_{\boldsymbol{u}}(\{(\boldsymbol{u}, \boldsymbol{y}) \mid \tilde{\boldsymbol{A}}\boldsymbol{y} = \boldsymbol{u},\ \underline{\boldsymbol{y}} \leq \boldsymbol{y} \leq \overline{\boldsymbol{y}}\}) = \{\boldsymbol{u} \mid \underline{\boldsymbol{y}} \leq \tilde{\boldsymbol{A}}^{-1}\boldsymbol{u} \leq \overline{\boldsymbol{y}}\}, \tag{4.6}$$

when stated as a set containment problem. This question can be decided by optimizing over the constraint functions: if

$$\max_{\boldsymbol{u}\in\mathcal{U}}\{(\tilde{\boldsymbol{A}}^{-1}\boldsymbol{u})_i\} \leq \overline{y}_i \quad \text{and} \quad \min_{\boldsymbol{u}\in\mathcal{U}}\{(\tilde{\boldsymbol{A}}^{-1}\boldsymbol{u})_i\} \geq \underline{y}_i \tag{4.7}$$

hold for all $i = 1, \ldots, n_y$, so does the set containment condition. By using linear duality, these inequalities can be checked with one linear optimization problem, see lemma 4.4.1.

In the linear flow example, we were able to exploit the simple structure to directly construct the projected set in (4.6). For more complicated linear or nonlinear constraints, this may not always be possible or may be computationally too expensive. For treating the arising problems, we will use ideas from polynomial optimization.

Set containment problems

Concerning the problem of set containment between sets defined by polynomials (basic semialgebraic sets), the general purpose doubly exponential cylindrical algebraic decomposition algorithm by Collins (1975) can be used. The algorithm allows an elimination of quantifiers from polynomial systems. Hence, it could be used for the combination of projection and set containment.

Regarding the general computational complexity of set containment problems with convex sets, we refer to Gritzmann and Klee (1994). A more practical treatment for polyhedra and special convex sets is given by Mangasarian (2002). Furthermore, an investigation of set containment regarding polytopes and spectrahedra can be found in Kellner, Theobald, and Trabandt (2013). This work is further extended in Kellner (2015) to encompass projections of polytopes and spectrahedra.

The framework of Magron, Henrion, and Lasserre (2015) for approximating image sets of compact semialgebraic sets under a polynomial map can also be used to find outer approximations of projected sets. Nevertheless, the robust question cannot be decided with their method as an outer approximation of the projected set in (4.3) could lead to a false positive conclusion regarding robust feasibility. On the other hand, outer approximations can be used for deciding robust infeasibility. However, then for each approximation a certificate against set containment still has to be derived. This would result in an algorithm with two nested optimization tasks, where each task is solved via a sum of squares based hierarchy. In this respect, our approach seems to be more direct; in particular, one of our key contributions is to avoid using an explicit description of the projection.

Optimal control is another field where the problem of set containment of basic semialgebraic sets occurs. It can be treated through relaxations of the real Positivstellensatz; see Jarvis-Wloszek et al. (2003). This approach is in a certain sense similar to the techniques presented here but cannot be applied to the projected problem.

4.2 Introduction to polynomial optimization

In this section we will briefly describe the required background knowledge from polynomial optimization. A very accessible introduction with a focus on sum of squares (SOS) polynomials is given by Parrilo (2003). For a more comprehensive treatment of the subject, we refer to Laurent (2009).

Terms and definitions We denote with $\mathbb{R}[\boldsymbol{x}] \coloneqq \mathbb{R}[x_1, \ldots, x_n]$ the ring of multivariate polynomials with real coefficients in $n \in \mathbb{N}$ variables $x_1, \ldots, x_n$. For a tuple $\boldsymbol{\alpha} = (\alpha_1, \ldots, \alpha_n) \in \mathbb{N}_0^n$ of nonnegative integers, the corresponding *monomial* is the product $\boldsymbol{x}^{\boldsymbol{\alpha}} \coloneqq \prod_{i=1}^n x_i^{\alpha_i}$.

A *polynomial* $p \in \mathbb{R}[\boldsymbol{x}]$ is a linear combination

$$p(\boldsymbol{x}) = \sum_{\boldsymbol{\alpha} \in \mathbb{N}_0^n} p_{\boldsymbol{\alpha}} \boldsymbol{x}^{\boldsymbol{\alpha}} \tag{4.8}$$

of monomials and real coefficients $p_{\boldsymbol{\alpha}} \in \mathbb{R}$ with only finitely many non-zero coefficients. With $|\boldsymbol{\alpha}| \coloneqq \sum_{i=1}^n \alpha_i$, we define the degree of p as $\deg(p) \coloneqq \max\{|\boldsymbol{\alpha}| \,|\, p_{\boldsymbol{\alpha}} \neq 0\}$. Sometimes, we identify a polynomial p of degree $\deg(p) = d$ with the vector $(p_{\boldsymbol{\alpha}})_{|\boldsymbol{\alpha}| \leq d}$ of its coefficients. Let $\mathbb{R}[\boldsymbol{x}]_d = \{p \in \mathbb{R}[\boldsymbol{x}] \mid \deg(p) \leq d\}$ denote the set of polynomials with degrees up to d.

A set $\mathcal{K} \subseteq \mathbb{R}^n$ that can be defined by finitely many polynomial equalities and inequalities is called *basic semialgebraic*. W.l.o.g., we assume that all basic semialgebraic sets can be written as

$$\mathcal{K} = \{\boldsymbol{x} \in \mathbb{R}^n \mid g_1(\boldsymbol{x}) \geq 0, \ldots, g_m(\boldsymbol{x}) \geq 0\}, \tag{4.9}$$

where $g_1, \ldots, g_m \in \mathbb{R}[\boldsymbol{x}]$ are polynomials.

Nonnegative polynomials Certificates and characterizations regarding nonnegativity of polynomials are closely connected to polynomial optimization. Let

$$\mathcal{P}[\mathcal{K}] \coloneqq \{p \in \mathbb{R}[\boldsymbol{x}] \mid p(\boldsymbol{x}) \geq 0 \quad \text{for all } \boldsymbol{x} \in \mathcal{K}\} \tag{4.10}$$

denote the set of polynomials in n variables that are nonnegative on some basic semialgebraic subset $\mathcal{K} \subseteq \mathbb{R}^n$. We denote with $\mathcal{P}[\mathcal{K}]_d \coloneqq \mathcal{P}[\mathcal{K}] \cap \mathbb{R}[\boldsymbol{x}]_d$ the subset of nonnegative polynomials with degree up to d. We abbreviate $\mathcal{P}_n \coloneqq \mathcal{P}[\mathbb{R}^n]$ and $\mathcal{P}_{n,d} \coloneqq \mathcal{P}[\mathbb{R}^n]_d$.

In general, checking nonnegativity of a polynomial is NP-hard; see Murty and Kabadi (1987). However, there is a class of polynomials where nonnegativity can be efficiently determined by semidefinite programming.

Definition 4.2.1. A polynomial $p \in \mathbb{R}[\boldsymbol{x}]$ is called *sum of squares* (SOS) if there exist $\sigma_1, \ldots, \sigma_k \in \mathbb{R}[\boldsymbol{x}]$ such that $p(\boldsymbol{x}) = \sigma_1^2(\boldsymbol{x}) + \cdots + \sigma_k^2(\boldsymbol{x})$.

In the following, the set of all SOS polynomials in n variables is denoted by

$$\Sigma_n \coloneqq \{p \in \mathbb{R}[\boldsymbol{x}] \mid p \text{ is SOS}\}. \tag{4.11}$$

Furthermore, let $\Sigma_{n,d} \coloneqq \Sigma_n \cap \mathbb{R}[\boldsymbol{x}]_d$ be the set of SOS polynomials in n variables with degree up to d.

Clearly, every SOS polynomial is nonnegative by definition and thus

$$\Sigma_n \subseteq \mathcal{P}_n \text{ as well as } \Sigma_{n,d} \subseteq \mathcal{P}_{n,d}. \tag{4.12}$$

However, not all nonnegative polynomials are SOS. In 1888, Hilbert gave the following characterization:

Theorem 4.2.1 (Hilbert 1888)**.** *The set relation $\Sigma_{n,d} \subseteq \mathcal{P}_{n,d}$ holds with equality if and only if $n = 1$, or $d = 2$, or $n = 2$ and $d = 4$.*

This result implies that nonnegative polynomials are generally not necessarily SOS polynomials. In cases where strict set inclusion holds, i.e., $\Sigma_{n,d} \subset \mathcal{P}_{n,d}$, the question arises as to what the extent of the difference between the two sets is.

On the one hand, SOS polynomials are dense within the set of nonnegative polynomials; see Lasserre and Netzer (2007). Therefore, any nonnegative polynomial can be approximated with arbitrary precision by a SOS polynomial as long as the degree of the SOS polynomial is unrestricted. On the other hand, there are significantly more nonnegative polynomials than SOS polynomials when the degree is fixed. Indeed, Blekherman (2006) shows that as the number of variables tends to infinity, the ratio of the cross sectional volumes of $\Sigma_{n,d}$ and $\mathcal{P}_{n,d}$ tends to 0.

An important quality of SOS polynomials compared to general nonnegative polynomials is that deciding whether $p \in \Sigma_n$ holds can be done efficiently in practice using SDPs.

Let $\mathcal{S}_n$ denote the vector space of real symmetric $n \times n$ matrices. For a symmetric matrix $\boldsymbol{Q} \in \mathcal{S}_n$, the notation $\boldsymbol{Q} \succeq \mathbf{0}$ indicates that $\boldsymbol{Q}$ is *positive semidefinite*, i.e., $\boldsymbol{x}^\top \boldsymbol{Q} \boldsymbol{x} \geq 0$ for all $\boldsymbol{x} \in \mathbb{R}^n$.

The next result was published independently by Shor (1987) and Choi, Lam, and Reznick (1995).

Lemma 4.2.2. *Let $p(\boldsymbol{x}) = \sum_{|\boldsymbol{\alpha}| \leq 2d} p_{\boldsymbol{\alpha}} \boldsymbol{x}^{\boldsymbol{\alpha}} \in \mathbb{R}[\boldsymbol{x}]_{2d}$ be polynomial of degree up to $2d$. Then the following are equivalent:*

1. *p is SOS.*
2. *There exists a symmetric matrix $\boldsymbol{Q}$ such that*

$$p(\boldsymbol{x}) = \boldsymbol{z}^\top \boldsymbol{Q} \boldsymbol{z} \quad \text{and} \quad \boldsymbol{Q} \succeq \mathbf{0}, \tag{4.13}$$

where $\boldsymbol{z} = (1, x_1, x_2, \ldots, x_n, x_1 x_2, \ldots, x_n^d)^\top =: (\boldsymbol{x}^{\boldsymbol{\alpha}})_{|\boldsymbol{\alpha}| \leq d}$ is a vector containing all monomials with degree up to d.

Proof. We give a proof that is based on Laurent (2009, lemma 3.8, p. 18of).

Suppose $p(\boldsymbol{x}) = \sum_{i=1}^k \sigma_i^2(\boldsymbol{x})$. Since $\deg(p) = 2d$, $\deg(\sigma_i) \leq d$ and hence we can write $\sigma_i(\boldsymbol{x}) = \sum_{|\boldsymbol{\alpha}| \leq d} (\sigma_i)_{\boldsymbol{\alpha}} \boldsymbol{x}^{\boldsymbol{\alpha}} = \operatorname{vec}(\sigma_i)^\top \boldsymbol{z}$, where we denote the vector of coefficients of σ_i with $\operatorname{vec}(\sigma_i)$. It follows that

$$p(\boldsymbol{x}) = \sum_{i=1}^k \sigma_i^2(\boldsymbol{x}) = \sum_{i=1}^k \left(\operatorname{vec}(\sigma_i)^\top \boldsymbol{z} \right)^2 = \boldsymbol{z}^\top \underbrace{\left(\sum_{i=1}^k \operatorname{vec}(\sigma_i)^\top \operatorname{vec}(\sigma_i) \right)}_{=: \boldsymbol{Q}} \boldsymbol{z}. \tag{4.14}$$

As a sum of positive semidefinite matrices, $\boldsymbol{Q}$ is positive semidefinite as well.

The reverse direction follows the same argument. Since $\boldsymbol{Q}$ is positive semidefinite and symmetric, there exists a matrix $\boldsymbol{L}$ such that $\boldsymbol{Q} = \boldsymbol{L}^\top \boldsymbol{L}$. Hence,

$$p(\boldsymbol{x}) = \boldsymbol{z}^\top \boldsymbol{Q} \boldsymbol{z} = (\boldsymbol{L}\boldsymbol{z})^\top \boldsymbol{L}\boldsymbol{z} = \sum_i (\boldsymbol{L}_{i\cdot} \boldsymbol{z})^2 \quad \text{is SOS,} \tag{4.15}$$

where $\boldsymbol{L}_{i\cdot}$ denotes the i-th row of $\boldsymbol{L}$. We note that $\boldsymbol{L}$ can be obtained from a Cholesky decomposition of $\boldsymbol{Q}$. □

The proof of lemma 4.2.2 shows how to find a SOS decomposition of a polynomial given a corresponding positive semidefinite matrix. Problem (4.13)is a standard positive SDP, i.e., a (convex) problem over the cone of positive semidefinite matrices subject to affine linear constraints; see Vandenberghe and Boyd (1996) and Wolkowicz, Saigal, and Vandenberghe (2000) for an

introduction. We index the matrix $\boldsymbol{Q}$ with the tuples β and γ, i.e., $\boldsymbol{Q} = (Q_{\beta,\gamma})_{|\beta|\leq d,|\gamma|\leq d}$. The semidefinite satisfiability problem

$$\begin{cases} p_{\boldsymbol{\alpha}} = \sum\limits_{\substack{|\beta|\leq d,|\gamma|\leq d \\ \boldsymbol{\alpha}=\beta+\gamma}} Q_{\beta,\gamma} & \text{for all } |\boldsymbol{\alpha}| \leq 2d, \\ \boldsymbol{Q} \succeq \mathbf{0} \end{cases} \tag{4.16}$$

follows from comparison of coefficients of $p(\boldsymbol{x}) = \boldsymbol{z}^\top \boldsymbol{Q} \boldsymbol{z}$. There are $\binom{n+d}{d}$ linear constraints and $\boldsymbol{Q}$ has dimension $\binom{n+d}{d} \times \binom{n+d}{d}$. Hence, the size of the SDP is polynomial if either n or d remains constant.

Example 4.2.3. *We consider $p(x, y) = 1 + 2x + 2y - 2xy + 5x^2 + 3y^2$, i.e., a bivariate polynomial of degree two. The vector of monomials with degree one is given by $\boldsymbol{z} = (1, x, y)$. We compare the coefficients of*

$$p(x, y) = 1 + x + 2y - xy + x^2 + 3y^2 \tag{4.17}$$

with the coefficients of

$$p(x,y) = \begin{pmatrix} 1 \\ x \\ y \end{pmatrix}^\top \begin{pmatrix} Q_{11} & Q_{12} & Q_{13} \\ Q_{12} & Q_{22} & Q_{23} \\ Q_{13} & Q_{23} & Q_{33} \end{pmatrix} \begin{pmatrix} 1 \\ x \\ y \end{pmatrix} \tag{4.18}$$

$$= Q_{11} + 2Q_{12}x + 2Q_{13}y + 2Q_{23}xy + Q_{22}x^2 + Q_{33}y^2 \tag{4.19}$$

and obtain

$$Q_{11} = 1, \qquad Q_{12} = 1, \qquad Q_{13} = 1, \tag{4.20}$$

$$Q_{23} = -1, \qquad Q_{22} = 5, \qquad Q_{33} = 3. \tag{4.21}$$

For ease of presentation, $p(x, y)$ has a small number of variables and small degree. As a coincidence, there is no need to solve a semidefinite feasibility problem as the resulting constraints are sufficient to uniquely define matrix $\boldsymbol{Q}$. In general, this is not the case. Application of a Cholesky decomposition to the positive symmetric matrix $\boldsymbol{Q}$ leads to

$$\boldsymbol{Q} = \begin{pmatrix} 1 & 1 & 1 \\ 1 & 5 & -1 \\ 1 & -1 & 3 \end{pmatrix} = \begin{pmatrix} 1 & 1 & 1 \\ 0 & 2 & -1 \\ 0 & 0 & 1 \end{pmatrix}^\top \begin{pmatrix} 1 & 1 & 1 \\ 0 & 2 & -1 \\ 0 & 0 & 1 \end{pmatrix} = \boldsymbol{L}^\top \boldsymbol{L}. \tag{4.22}$$

Hence the SOS decomposition of p is

$$p(x, y) = (1 + x + y)^2 + (2x - y)^2 + y^2. \tag{4.23}$$

A SOS decomposition is an easily obtainable certificate that a polynomial is nonnegative on $\mathbb{R}^n$. Next, we consider the related question of when a polynomial is nonnegative on a basic semialgebraic subset of the domain. Problems of this kind are major topics in (real) algebraic geometry; see e.g., Cox, Little, and O'Shea (2015) for an introduction. Of interest for polynomial optimization are first of all the so-called *Stellensätze*, which are structural statements about the set of polynomials that satisfy certain properties over subsets of $\mathbb{R}^n$ or $\mathbb{C}^n$ (where $\mathbb{C}$ denotes the complex numbers). One of the most famous *Stellensätze* is Hilbert's Nullstellensatz that establishes a connection between a system of (complex) polynomials and the set of their common roots. In particular, Hilbert's result can be used to derive a certificate that a system of complex polynomials has no solution, i.e., there is no point in $\mathbb{C}^n$ where all polynomials are zero.

An analogous result concerning a system of real polynomial equations and inequalities and their solutions in $\mathbb{R}^n$ is known as Stengle's *Positivstellensatz*; see Stengle (1974) and Krivine (1964). Similar to Hilbert's result, it states that either the system of real polynomials has a solution in $\mathbb{R}^n$ or there is a certificate that no solution exists. There are several variants and refinements of this result, in particular the theorems by Schmüdgen (1991) and Putinar (1993).

The variant of Putinar is particularly interesting for polynomial optimization, as it gives a characterization under mild additional assumptions that has a comparatively simple structure. Before presenting Putinar's Positivstellensatz, we introduce a special set of polynomials that are nonnegative on a given basic semialgebraic set.

Definition 4.2.2. Let $\boldsymbol{g} = (g_1, \ldots, g_m)$ with $g_i \in \mathbb{R}[\boldsymbol{x}]$ for $i = 1, \ldots, m$ be given. Then

$$\mathcal{M}[\boldsymbol{g}] = \mathcal{M}[g_1, \ldots, g_m] \tag{4.24}$$

$$\coloneqq \left\{ \sigma_0(\boldsymbol{x}) + \sum_{i=1}^{m} \sigma_i(\boldsymbol{x}) g_i(\boldsymbol{x}) \;\middle|\; \sigma_0, \ldots, \sigma_m \in \Sigma_n \right\} \tag{4.25}$$

is called *quadratic module* of $\boldsymbol{g}$.

Similarly, the *truncated quadratic module* of level $t \in \mathbb{N}$ of $\boldsymbol{g}$ is given by

$$\mathcal{M}_t[\boldsymbol{g}] \coloneqq \left\{ \sigma_0(\boldsymbol{x}) + \sum_{i=1}^{m} \sigma_i(\boldsymbol{x}) g_i(\boldsymbol{x}) \;\middle|\; \begin{array}{c} \sigma_0, \ldots, \sigma_m \in \Sigma_{n,2t} \\ \deg(\sigma_0) \leq 2t,\ \deg(\sigma_i g_i) \leq 2t \end{array} \right\}. \tag{4.26}$$

For ease of notation, we write $\mathcal{M}[\mathcal{K}]$ (resp. $\mathcal{M}_t[\mathcal{K}]$) for the quadratic module (resp. truncated quadratic module) associated with the basic semialgebraic set defined by $g_1, \ldots, g_m$ as in (4.9).

We observe that by definition, any element $p \in \mathcal{M}[\mathcal{K}]$ (resp. $p \in \mathcal{M}_t[\mathcal{K}]$) is nonnegative on the set $\mathcal{K}$, i.e., $\mathcal{M}_t[\mathcal{K}] \subseteq \mathcal{P}[\mathcal{K}]$. In addition, the chain of subset conditions

$$\mathcal{M}_1[\mathcal{K}] \subseteq \mathcal{M}_2[\mathcal{K}] \subseteq \cdots \subseteq \mathcal{M}_t[\mathcal{K}] \subseteq \cdots \subseteq \mathcal{P}[\mathcal{K}] \tag{4.27}$$

holds. The condition $p \in \mathcal{M}_t[\mathcal{K}]$ can be formulated as an SDP with $m+1$ semidefinite constraints similarly as in lemma 4.2.2; see Shor (1987) for details.

With this we formulate Putinar's Positivstellensatz.

Theorem 4.2.4 (Putinar 1993). *Let $g_1, \ldots, g_m \in \mathbb{R}[\boldsymbol{x}]$ be a given series of polynomials and let $\mathcal{K} = \{\boldsymbol{x} \in \mathbb{R}^n \mid g_1(\boldsymbol{x}) \geq 0, \ldots, g_m(\boldsymbol{x}) \geq 0\}$. Suppose there exists a constant $R \in \mathbb{N}$ such that*

$$R - (x_1^2 + \cdots + x_m^2) \in \mathcal{M}[\mathcal{K}]. \tag{4.28}$$

If $p \in \mathbb{R}[\boldsymbol{x}]$ with $p(\boldsymbol{x}) > 0$ on $\mathcal{K}$, then $p \in \mathcal{M}[\mathcal{K}]$.

In essence, this theorem states that if $\mathcal{M}[\mathcal{K}]$ satisfies (4.28), all polynomials that are positive on a basic semialgebraic subset $\mathcal{K}$ are elements of $\mathcal{M}[\mathcal{K}]$. Hence, by definition of $\mathcal{M}[\mathcal{K}]$, all positive polynomials p on $\mathcal{K}$ admit a decomposition

$$p(\boldsymbol{x}) = \sigma_0(\boldsymbol{x}) + \sigma_1(\boldsymbol{x}) g_1(\boldsymbol{x}) + \cdots + \sigma_m(\boldsymbol{x}) g_m(\boldsymbol{x}), \tag{4.29}$$

where $\sigma_0, \sigma_1, \ldots, \sigma_m$ are SOS.

The requirement (4.28) is also known as the *archimedean condition*. In particular, this condition implies compactness of $\mathcal{K}$. This property can be ensured for any $\mathcal{K}$ by adding (4.28) to the polynomial inequality functions g_i. For real-world optimization tasks, the archimedean condition is usually non-restrictive since it is equivalent to the feasible region $\mathcal{K}$ being contained in an n-dimensional ball.

Putinar's Positivstellensatz allows us to search algorithmically for a decomposition of the form (4.29). After restricting the degrees of the SOS polynomials appearing in $\mathcal{M}[\mathcal{K}]$, the condition

$$p \in \mathcal{M}_t[\mathcal{K}] \tag{4.30}$$

can be checked with a semidefinite feasibility problem. This observation is one of the key points for constructing a SOS relaxation hierarchy, which we will introduce next.

A relaxation hierarchy for polynomial optimization problems A polynomial optimization problem is an optimization problem where objective function and constraints are polynomials:

$$\begin{aligned} \inf_{\boldsymbol{x}\in\mathbb{R}^n} \; & p(\boldsymbol{x}) \\ \text{s.t.} \; & g_i(\boldsymbol{x}) \geq 0 \quad \text{for all } i = 1, \dots, m, \end{aligned} \tag{Poly}$$

with $p, g_1, \dots, g_m \in \mathbb{R}[\boldsymbol{x}]$. Problem (Poly) can be written equivalently as

$$\inf_{\boldsymbol{x}\in\mathcal{K}} p(\boldsymbol{x}), \tag{4.31}$$

where we let $\mathcal{K} \coloneqq \{\boldsymbol{x} \in \mathbb{R}^n \mid g_1(\boldsymbol{x}) \geq 0, \dots, g_m(\boldsymbol{x}) \geq 0\}$.

The class of polynomial optimization problems contains many common convex and non-convex optimization problems. For example, if objective and constraint functions $p, g_1, \dots, g_m$ are linear, (Poly) is an LP. By extending this LP with additional polynomial constraints of the form $x_i = x_i^2$, the variables are restricted to 0/1, thus modeling an integer linear program (ILP). It is well-known that ILPs are NP-hard, making polynomial programs NP-hard as well.

We observe the following property of (Poly):

$$\begin{aligned} p^* \coloneqq \inf_{\boldsymbol{x}\in\mathbb{R}^n} \; & p(\boldsymbol{x}) \quad = \quad \sup_{\lambda\in\mathbb{R}} \; \lambda \\ \text{s.t.} \; & \boldsymbol{x} \in \mathcal{K} \qquad\quad \text{s.t.} \; p(\boldsymbol{x}) - \lambda \in \mathcal{P}[\mathcal{K}], \end{aligned} \tag{4.32}$$

i.e., the infimum p^* of $p(\boldsymbol{x})$ over $\mathcal{K}$ has the same value as the largest $\lambda \in \mathbb{R}$ such that the polynomial $p(\boldsymbol{x}) - \lambda$ is nonnegative on $\mathcal{K}$. Lasserre (2000) and similarly Parrilo (2003) introduced a hierarchy of relaxations for (Poly) by replacing the set of nonnegative polynomials $\mathcal{P}[\mathcal{K}]$ by a truncated quadratic module $\mathcal{M}_t[\mathcal{K}]$. Let

$$\begin{aligned} p_t^* \coloneqq \sup_{\lambda\in\mathbb{R}} \; & \lambda \\ \text{s.t.} \; & p(\boldsymbol{x}) - \lambda \in \mathcal{M}_t[\mathcal{K}] \end{aligned} \tag{SOS$_t$}$$

denote the optimal value associated with the quadratic module of level $t \in \mathbb{N}$. This problem is commonly referred to as the SOS-relaxation of level t for (Poly). As was already mentioned, (SOS$_t$) can be formulated as an SDP (Shor 1987) and thus is a convex relaxation of the polynomial optimization problem (Poly).

Given the chain of subset relations

$$\mathcal{M}_t[\mathcal{K}] \subseteq \mathcal{M}_{t+1}[\mathcal{K}] \subseteq \cdots \subseteq \mathcal{P}[\mathcal{K}], \tag{4.33}$$

we observe that

$$p_t^* \leq p_{t+1}^* \leq \cdots \leq p^*. \tag{4.34}$$

Lasserre (2000) shows that under mild conditions, this series of optimal values converges to the optimal value p^* over $\mathcal{P}[\mathcal{K}]$. We state the convergence result in a slightly more general form. To this end, for any pair of polynomials $p(\boldsymbol{x}) = \sum_{\boldsymbol{\alpha}} p_{\boldsymbol{\alpha}} \boldsymbol{x}^{\boldsymbol{\alpha}}$ and $q(\boldsymbol{x}) = \sum_{\boldsymbol{\alpha}} q_{\boldsymbol{\alpha}} \boldsymbol{x}^{\boldsymbol{\alpha}}$, we let $p \circ q := \sum_{\boldsymbol{\alpha}} p_{\boldsymbol{\alpha}} q_{\boldsymbol{\alpha}}$. The following proposition is due to Prof. Vera.

Proposition 4.2.5. *Let $g_0, g_1, \ldots, g_m \in \mathbb{R}[\boldsymbol{x}]$ be polynomials in n variables. Let $\mathcal{K} = \{\boldsymbol{x} \in \mathbb{R}^n \mid g_1(\boldsymbol{x}) \geq 0, \ldots, g_m(\boldsymbol{x}) \geq 0\}$ be a basic semialgebraic subset that satisfies the archimedean condition* (4.28).

We consider the optimization problem $p^* = \sup\{g_0 \circ p \mid p \in \mathcal{P}[\mathcal{K}]\}$ and the sequence of relaxations $p_t^* = \sup\{g_0 \circ p \mid p \in \mathcal{M}_t[\mathcal{K}]\}$.

Then with Putinar (1993)

$$\mathcal{M}_1[\mathcal{K}] \subseteq \mathcal{M}_2[\mathcal{K}] \subseteq \cdots \subseteq \mathcal{M}_t[\mathcal{K}] \subseteq \cdots \subseteq \mathcal{P}[\mathcal{K}] \tag{4.35}$$

$$\text{and } \{p \in \mathbb{R}[\boldsymbol{x}] \mid p(\boldsymbol{x}) > 0 \quad \text{for all } \boldsymbol{x} \in \mathcal{K}\} \subseteq \bigcup_{t \in \mathbb{N}} \mathcal{M}_t[\mathcal{K}] \tag{4.36}$$

and using the same ideas as Lasserre (2000)

$$p_1^* \leq p_2^* \leq \cdots \leq p_t^* \leq \cdots \leq p^* \text{ and } p_t^* \to p^* \text{ as } t \to \infty. \tag{4.37}$$

The proposition shows how the Lasserre hierarchy can be used to find arbitrarily close approximations of the global optimal value of a general polynomial optimization problem. The hierarchy consists of a series of SDPs with increasing size of the semidefinite matrices and increasing number of constraints.

Remark 4.2.6. Our brief introduction focused solely on SOS relaxations for polynomial problems that are formed using tools form (real) algebraic geometry. However, there is another way to construct relaxations by formulating the polynomial problem as a moment problem; see Lasserre (2000). Essentially, the problem of moments is the question of whether a sequence of values $(m_{\boldsymbol{\alpha}})_{\boldsymbol{\alpha} \in \mathbb{N}^n}$ denotes the moments of a Borel measure μ, i.e., whether $m_{\boldsymbol{\alpha}} = \int \boldsymbol{x}^{\boldsymbol{\alpha}} \, \mathrm{d}\mu$.

By carefully reformulating (Poly) in terms of a moment problem and after a subsequent truncation, another hierarchy of SDPs arises. Lasserre (2000) shows that the SDPs of matching levels in the SOS, respectively moment hierarchy are dual to each and that strong duality holds if, e.g., $\mathcal{K}$ has nonempty interior.

4.3 Deciding robust feasibility and infeasibility for the general case

In this section, two approaches for deciding robustness are developed. We present a method for certifying infeasibility in section 4.3.1 as well as a method for proving feasibility in section 4.3.2.

4.3.1 A set containment approach for certifying infeasibility

A robust optimization problem is said to be infeasible if a scenario $\hat{u} \in \mathcal{U}$ exists whose corresponding problem is infeasible. We first introduce an abstract model involving arbitrary functions for solving the infeasibility problem. The model is then adapted to the considered case of polynomial functions. With this approach, negative certificates for set containment of two basic semialgebraic sets can be found.

For a subset $\mathcal{S} \subseteq \mathbb{R}^n$, let

$$\mathcal{F}[\mathcal{S}] \coloneqq \{f \colon \mathbb{R}^n \to \mathbb{R} \mid f(\boldsymbol{x}) \geq 0 \quad \text{for all } \boldsymbol{x} \in \mathcal{S}\} \tag{4.38}$$

be the set of all functions that are nonnegative on $\mathcal{K}$. The set $\mathcal{F}[\mathcal{S}]$ is nonempty since it always contains $f(\boldsymbol{x}) \equiv 0$, regardless of the particular choice of $\mathcal{S}$.

Let $\mathcal{S},\ \mathcal{T}$ be subsets of $\mathbb{R}^n$. It is clear that

$$\mathcal{S} \not\subseteq \mathcal{T} \iff \exists \boldsymbol{x} \in \mathcal{S} \text{ with } \boldsymbol{x} \notin \mathcal{T} \iff \mathcal{S} \setminus \mathcal{T} \neq \emptyset, \tag{4.39}$$

where we denote with $\mathcal{S} \setminus \mathcal{T} = \{\boldsymbol{x} \in \mathcal{S} \mid \boldsymbol{x} \notin \mathcal{T}\}$ the set difference of $\mathcal{S}$ and $\mathcal{T}$. With this definition, (4.39) can be extended to

$$\mathcal{S} \setminus \mathcal{T} \neq \emptyset \iff \exists\, f \in \mathcal{F}[\mathcal{T}] \text{ and } \boldsymbol{x} \in \mathcal{S} \text{ such that } f(\boldsymbol{x}) < 0. \tag{4.40}$$

A visualization of this idea is displayed in fig. 4.2, where a certificate for $\mathcal{S} \not\subseteq \mathcal{T}$ is shown. The function f (blue line) is nonnegative on the superset $\mathcal{T}$ (orange line). Moreover, the subset $\mathcal{S}$ (green line) contains a point $\hat{\boldsymbol{x}} \in \mathcal{S}$ with $f(\hat{\boldsymbol{x}}) < 0$. Taking both together, f and $\hat{\boldsymbol{x}}$ form a certificate against set containment. Later on we will use the uncertainty set $\mathcal{U}$ as the subset $\mathcal{S}$ and the projected set of feasible pairs $\mathrm{Proj}_{\boldsymbol{u}}(\mathcal{Y})$ as superset $\mathcal{T}$ to obtain certificates for robust infeasibility.

The previous expression (4.40) can be rewritten using an optimization problem. Let the abstract separation problem (ASep) be defined as

$$\begin{aligned} f^* \coloneqq \inf_{\boldsymbol{x}, f}\ & f(\boldsymbol{x}) \\ \text{s.t. }\ & \boldsymbol{x} \in \mathcal{S}, \\ & f \in \mathcal{F}[\mathcal{T}]. \end{aligned} \tag{ASep}$$

We use the common convention that $\inf_{\boldsymbol{x}\in\mathcal{S}} f(\boldsymbol{x}) = +\infty$ if $\mathcal{S} = \emptyset$. For the optimal value of (ASep), it holds that

$$f^* = \begin{cases} +\infty & \text{if } \mathcal{S} = \emptyset, \\ 0 & \text{if } \mathcal{S} \neq \emptyset \text{ and } \mathcal{S} \subseteq \mathcal{T}, \\ -\infty & \text{if } \mathcal{S} \neq \emptyset \text{ and } \mathcal{S} \not\subseteq \mathcal{T}. \end{cases} \tag{4.41}$$

Combining the first two cases yields

$$\mathcal{S} \not\subseteq \mathcal{T} \iff f^* = -\infty. \tag{4.42}$$

In order to tackle this optimization task in practice, the abstract problem is approximated by a polynomial optimization problem. From this point onwards, we assume that $\mathcal{S}$ and $\mathcal{T}$ are basic semialgebraic. We first replace the set of functions $\mathcal{F}[\mathcal{T}]$ by the set

$$\mathcal{P}[\mathcal{T}] = \{p \in \mathbb{R}[\boldsymbol{x}] \mid p(\boldsymbol{x}) \geq 0 \quad \text{for all } \boldsymbol{x} \in \mathcal{T}\} \tag{4.43}$$

of polynomials that are nonnegative on $\mathcal{T}$. Since both p and $\boldsymbol{x}$ are variables, $p(\boldsymbol{x})$ cannot be cast directly as part of a polynomial optimization problem. Therefore, instead of minimizing $p(\boldsymbol{x})$, we minimize the Lebesgue integral of p over $\mathcal{S}$:

$$\inf_{p} \int_{\mathcal{S}} p \, \mathrm{d}\mu \tag{4.44a}$$

$$\text{s.t. } p \in \mathcal{P}[\mathcal{T}]. \tag{4.44b}$$

A negative integral value implies the existence of some $\hat{\boldsymbol{x}} \in \mathcal{S}$ with $p(\hat{\boldsymbol{x}}) < 0$.

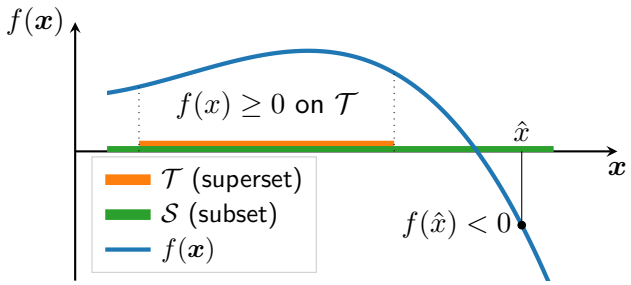

Figure 4.2: A certificate for $\mathcal{S} \not\subseteq \mathcal{T}$ consists of a function f and a point $\hat{\boldsymbol{x}} \in \mathcal{S}$ such that $f(\boldsymbol{x}) \geq 0$ on $\mathcal{T}$ and $f(\hat{\boldsymbol{x}}) < 0$.

Using the definition $p(\boldsymbol{x}) = \sum_{\boldsymbol{\alpha}} p_{\boldsymbol{\alpha}} \boldsymbol{x}^{\boldsymbol{\alpha}}$, we write the objective in terms of the moments of μ:

$$\begin{aligned} &\inf_{p} \ \sum_{\boldsymbol{\alpha}} p_{\boldsymbol{\alpha}} \int_{\mathcal{S}} \boldsymbol{x}^{\boldsymbol{\alpha}} \,\mathrm{d}\mu \\ &\text{s.t. } \ p \in \mathcal{P}[\mathcal{T}]. \end{aligned} \tag{PolySep}$$

The moments $m_{\boldsymbol{\alpha}} = \int_{\mathcal{S}} \boldsymbol{x}^{\boldsymbol{\alpha}} \,\mathrm{d}\mu$ can be calculated in advance and hence the objective of (PolySep) is a linear function in the coefficients of p. We call this problem the *polynomial separation problem*. If there exists p, such that the integral over $\mathcal{S}$ is negative, there must be some point $\boldsymbol{x} \in \mathcal{S}$ with $p(\boldsymbol{x}) < 0$. Then, by definition of p, it holds that $\boldsymbol{x} \notin \mathcal{T}$.

The integration is a weaker test for the existence of an $\boldsymbol{x} \in \mathcal{S}$ with $p(\boldsymbol{x}) < 0$ than just evaluating $p(\boldsymbol{x})$ (see lemma 4.3.1). For practical applications, the moments $\int_{\mathcal{S}} \boldsymbol{x}^{\boldsymbol{\alpha}} \,\mathrm{d}\mu$ need to be available. With respect to our application to the robust gas network problem, this is no limitation since we assume that $\mathcal{S} = \mathcal{U}$ is a hyperrectangle. In a similar context, precomputed moments of a simple superset, such as a sphere or a box, are used to approximate the volume of a basic compact semialgebraic set in Henrion, Lasserre, and Savorgnan (2009).

The next lemma identifies conditions for $\mathcal{S}, \mathcal{T}$ such that a polynomial $p \in \mathcal{P}[\mathcal{T}]$ exists with $\int_{\mathcal{S}} p(\boldsymbol{x}) \,\mathrm{d}\mu < 0$. Under these conditions, problems (ASep) and (PolySep) are equivalent in the sense that a negative objective value of (ASep) implies a negative objective value of (PolySep) and hence (PolySep) can be used to certify infeasibility as well.

Lemma 4.3.1. *Let $\mathcal{S}, \mathcal{T} \subseteq \mathbb{R}^n$ be two bounded sets with $\mathcal{S} \setminus \mathcal{T} \neq \emptyset$. Suppose that $\mathcal{S} \setminus \mathcal{T}$ contains an open subset.*
Then there exists a polynomial $p \in \mathcal{P}[\mathcal{T}]$ with $\int_{\mathcal{S}} p(\boldsymbol{x}) \,\mathrm{d}\mu < 0$.

Proof. Since $\mathcal{S} \setminus \mathcal{T}$ contains an open subset, there exist $\boldsymbol{x}_0 \in \mathbb{R}^n$ and $r > 0$ such that $\mathcal{S} \setminus \mathcal{T} \supseteq \mathcal{B}_r(\boldsymbol{x}_0) \coloneqq \{\boldsymbol{x} \in \mathbb{R}^n \mid \|\boldsymbol{x} - \boldsymbol{x}_0\|_2 < r\}$. Without loss of generality, we assume that $\boldsymbol{x}_0 = \mathbf{0}$. This can always be guaranteed by applying a simple translation to $\mathcal{S}$ and $\mathcal{T}$. Due to both sets being bounded, there exists an $R > r$ such that $\mathcal{T}, \mathcal{S} \subseteq \mathcal{B}_R(\mathbf{0})$.

We prove this lemma by constructing a polynomial $p\colon \mathbb{R}^n \to \mathbb{R}$ that is nonnegative on $\mathcal{B}_R(\mathbf{0}) \setminus \mathcal{B}_r(\mathbf{0}) \supseteq \mathcal{T}$ and satisfies $\int_{\mathcal{B}_R(\mathbf{0})} p \,\mathrm{d}\mu < 0$. If such a p exists, it holds that

$$\int_{\mathcal{S}} p \,\mathrm{d}\mu = \int_{\mathcal{S} \setminus \mathcal{B}_r(\mathbf{0})} p \,\mathrm{d}\mu + \int_{\mathcal{B}_r(\mathbf{0})} p \,\mathrm{d}\mu \tag{4.45}$$

$$\leq \int_{\mathcal{B}_R(\mathbf{0}) \setminus \mathcal{B}_r(\mathbf{0})} p \,\mathrm{d}\mu + \int_{\mathcal{B}_r(\mathbf{0})} p \,\mathrm{d}\mu = \int_{\mathcal{B}_R(\mathbf{0})} p \,\mathrm{d}\mu < 0. \tag{4.46}$$

In order to construct p, let

$$q(t) \coloneqq [c_1(t - c_2)]^2 \tag{4.47}$$

be a univariate polynomial with constants $c_1 \coloneqq \frac{2}{R^2 - r^2}$, $c_2 \coloneqq \frac{R^2 + r^2}{2}$. By construction, the following hold:

$$q(c_2) = 0, \tag{4.48a}$$
$$q(t^2) = 1 \text{ iff } t \in \{r, R\}, \tag{4.48b}$$
$$q(t^2) \geq 1 \text{ for } t \in [0, r], \tag{4.48c}$$
$$0 \leq q(t^2) \leq 1 \text{ for } t \in [r, R]. \tag{4.48d}$$

Taking the l-th ($l \in \mathbb{N}$) power of q preserves properties (4.48a)–(4.48d). Furthermore, the polynomial

$$p_l(t) \coloneqq 1 - q^l(t) \tag{4.49}$$

satisfies

$$p_l(c_2) = 1, \tag{4.50a}$$
$$p_l(t^2) = 0 \text{ iff } t \in \{r, R\}, \tag{4.50b}$$
$$p_l(t^2) \leq 0 \text{ for } t \in [0, r], \tag{4.50c}$$
$$0 \leq p_l(t^2) \leq 1 \text{ for } t \in [r, R]. \tag{4.50d}$$

Next, we show that there is some $l \in \mathbb{N}$ such that the radial symmetric polynomial $p_l(\|\boldsymbol{x}\|_2^2)$ is nonnegative on $\mathcal{B}_R(\mathbf{0}) \setminus \mathcal{B}_r(\mathbf{0}) \supseteq \mathcal{T}$ and satisfies $\int_{\mathcal{B}_R(\mathbf{0})} p_l(\|\boldsymbol{x}\|_2^2) \,\mathrm{d}\mu < 0$:

$$\int_{\mathcal{B}_R(\mathbf{0})} p_l(\|\boldsymbol{x}\|_2^2) \,\mathrm{d}\mu = \int_{\mathcal{B}_R(\mathbf{0}) \setminus \mathcal{B}_r(\mathbf{0})} p_l(\|\boldsymbol{x}\|_2^2) \,\mathrm{d}\mu + \int_{\mathcal{B}_r(\mathbf{0})} p_l(\|\boldsymbol{x}\|_2^2) \,\mathrm{d}\mu \tag{4.51}$$
$$\leq \int_{\mathcal{B}_R(\mathbf{0}) \setminus \mathcal{B}_r(\mathbf{0})} 1 \,\mathrm{d}\mu + \int_{\mathcal{B}_r(\mathbf{0})} 1 - q^l(\|\boldsymbol{x}\|_2^2) \,\mathrm{d}\mu \tag{4.52}$$
$$= \int_{\mathcal{B}_R(\mathbf{0})} 1 \,\mathrm{d}\mu - \int_{\mathcal{B}_r(\mathbf{0})} q^l(\|\boldsymbol{x}\|_2^2) \,\mathrm{d}\mu. \tag{4.53}$$

In order to complete the proof, we show that $\lim_{l \to \infty} \int_{\mathcal{B}_r(\mathbf{0})} q^l(\|\boldsymbol{x}\|_2^2) \,\mathrm{d}\mu = \infty$. Using a substitution of variables and exploiting the radial symmetry, the integral over the n-dimensional ball can be transformed into a univariate integral:

$$\int_{\mathcal{B}_r(\mathbf{0})} q^l(\|\boldsymbol{x}\|_2^2) \,\mathrm{d}\mu = \overbrace{n \int_{\mathcal{B}_1(\mathbf{0})} 1 \,\mathrm{d}\mu}^{=:\Gamma > 0} \int_0^r q^l(t^2) t^{n-1} \,\mathrm{d}t. \tag{4.54}$$

Now we calculate the difference between two integrals in the sequence while omitting the positive coefficient Γ:

$$\int_0^r q^{l+1}(t^2)t^{n-1}\,\mathrm{d}t - \int_0^r q^l(t^2)t^{n-1}\,\mathrm{d}t \tag{4.55}$$

$$= \int_0^r \overbrace{q^l(t^2)}^{\geq 1}\overbrace{t^{n-1}}^{\geq 0}\overbrace{\Big(q(t^2)-1\Big)}^{\geq 0}\,\mathrm{d}t \tag{4.56}$$

$$\geq \int_0^r t^{n-1}\Big(q(t^2)-1\Big)\,\mathrm{d}t = c > 0. \tag{4.57}$$

Since the difference between two consecutive elements of the series is bounded from below by a strictly positive constant c, the series diverges to $+\infty$. This implies the existence of some $l \in \mathbb{N}$ such that $\int_{\mathcal{B}_R(\mathbf{0})} p_l(\|\boldsymbol{x}\|_2^2)\,\mathrm{d}\mu < 0$. □

Next, we apply (PolySep) to the set containment question (4.3), i.e.,

$$\mathcal{U} \subseteq \mathrm{Proj}_{\boldsymbol{u}}(\mathcal{Y}). \tag{4.58}$$

Using $p(\boldsymbol{u}) = \sum_{\boldsymbol{\alpha}} p_{\boldsymbol{\alpha}}\boldsymbol{u}^{\boldsymbol{\alpha}}$, the corresponding optimization problem to certify infeasibility of the robust problem is

$$\begin{aligned} &\inf_{p} \ \sum_{\boldsymbol{\alpha}} p_{\boldsymbol{\alpha}} \int_{\mathcal{U}} \boldsymbol{u}^{\boldsymbol{\alpha}}\,\mathrm{d}\mu \\ &\text{s.t. } \ p \in \mathcal{P}\big[\mathrm{Proj}_{\boldsymbol{u}}(\mathcal{Y})\big]. \end{aligned} \tag{PolySepProj}$$

Without explicit knowledge of the projection $\mathrm{Proj}_{\boldsymbol{u}}(\mathcal{Y})$, it is unclear how the set $\mathcal{P}\big[\mathrm{Proj}_{\boldsymbol{u}}(\mathcal{Y})\big]$ can be expressed as part of a polynomial optimization problem. We present an equivalent model which expresses this constraint by introduction of additional linear constraints over the coefficients of the unknown polynomial.

Lemma 4.3.2. *We consider the two optimization problems*

$$\text{(PP)} \quad \begin{aligned} &\inf_{p} \ \sum_{\boldsymbol{\alpha}} p_{\boldsymbol{\alpha}} \int_{\mathcal{U}} \boldsymbol{u}^{\boldsymbol{\alpha}}\,\mathrm{d}\mu \\ &\text{s.t. } \ p \in \mathcal{P}\big[\mathrm{Proj}_{\boldsymbol{u}}(\mathcal{Y})\big] \end{aligned} \quad \textit{and} \quad \text{(PP')} \quad \begin{aligned} &\inf_{\tilde{p}} \ \sum_{\boldsymbol{\alpha},\boldsymbol{\beta}} \tilde{p}_{\boldsymbol{\alpha},\boldsymbol{\beta}} \int_{\mathcal{U}} \boldsymbol{u}^{\boldsymbol{\alpha}}\,\mathrm{d}\mu \\ &\text{s.t. } \ \tilde{p}_{\boldsymbol{\alpha},\boldsymbol{\beta}} = 0 \quad \textit{for all } \boldsymbol{\beta} \neq \mathbf{0}, \\ &\qquad \tilde{p} \in \mathcal{P}[\mathcal{Y}], \end{aligned}$$

where $p(\boldsymbol{u}) = \sum_{\boldsymbol{\alpha}} p_{\boldsymbol{\alpha}}\boldsymbol{u}^{\boldsymbol{\alpha}}$ is a polynomial in $\boldsymbol{u}$ and $\tilde{p}(\boldsymbol{u},\boldsymbol{y}) = \sum_{\boldsymbol{\alpha},\boldsymbol{\beta}} \tilde{p}_{\boldsymbol{\alpha},\boldsymbol{\beta}}\boldsymbol{u}^{\boldsymbol{\alpha}}\boldsymbol{y}^{\boldsymbol{\beta}}$ is a polynomial in both $\boldsymbol{u}$ and $\boldsymbol{y}$.

Then, any feasible point p^* of (PP) *can be extended to a feasible point $\tilde{p}^*$ of* (PP') *and vice versa. Furthermore, the feasible points p^* and $\tilde{p}^*$ have the same objective values.*

Proof. Let p^* be any feasible point of (PP) that has objective value $z^* = \sum_{\boldsymbol{\alpha}} p^*_{\boldsymbol{\alpha}} \int_{\mathcal{U}} \boldsymbol{u}^{\boldsymbol{\alpha}} \,\mathrm{d}\mu$. Consider the inclusion map from $\mathbb{R}[\boldsymbol{u}]$ to $\mathbb{R}[\boldsymbol{u}, \boldsymbol{y}]$, which maps p^* to $\tilde{p}^*$ where $\tilde{p}^*(\boldsymbol{u}, \boldsymbol{y}) = \sum_{\boldsymbol{\alpha},\boldsymbol{\beta}} \tilde{p}^*_{\boldsymbol{\alpha},\boldsymbol{\beta}} \boldsymbol{u}^{\boldsymbol{\alpha}} \boldsymbol{y}^{\boldsymbol{\beta}}$ and

$$\tilde{p}^*_{\boldsymbol{\alpha},\boldsymbol{\beta}} \coloneqq \begin{cases} p^*_{\boldsymbol{\alpha}} & \text{if } \boldsymbol{\beta} = \mathbf{0}, \\ 0 & \text{if } \boldsymbol{\beta} \neq \mathbf{0}. \end{cases} \tag{4.59}$$

By construction, for any $\boldsymbol{u} \in \mathrm{Proj}_{\boldsymbol{u}}(\mathcal{Y})$ and $\boldsymbol{y} \in \mathbb{R}^{n_y}$, we have $\tilde{p}^*(\boldsymbol{u}, \boldsymbol{y}) = p^*(\boldsymbol{u}) \geq 0$. Therefore, $\tilde{p}^* \in \mathcal{P}\big[\mathrm{Proj}_{\boldsymbol{u}}(\mathcal{Y}) \times \mathbb{R}^{n_y}\big] \subseteq \mathcal{P}[\mathcal{Y}]$. That is, $\tilde{p}^*$ is feasible for (PP').

Let $\tilde{p}^*$ be any feasible point of (PP'). Since all coefficients $\tilde{p}^*_{\boldsymbol{\alpha},\boldsymbol{\beta}}$ with $\boldsymbol{\beta} \neq \mathbf{0}$ are zero, $\tilde{p}^*$ is independent of $\boldsymbol{y}$ and it holds that $\tilde{p}^* \in \mathcal{P}\big[\mathrm{Proj}_{\boldsymbol{u}}(\mathcal{Y}) \times \mathbb{R}^{n_y}\big]$. Let $p^*(\boldsymbol{u}) = \sum_{\boldsymbol{\alpha}} p^*_{\boldsymbol{\alpha}} \boldsymbol{u}^{\boldsymbol{\alpha}}$ be the remaining polynomial in $\boldsymbol{u}$. Together with $\tilde{p}^* \in \mathcal{P}\big[\mathrm{Proj}_{\boldsymbol{u}}(\mathcal{Y}) \times \mathbb{R}^{n_y}\big]$, this implies $p^* \in \mathcal{P}\big[\mathrm{Proj}_{\boldsymbol{u}}(\mathcal{Y})\big]$. □

For the remainder of this section, we assume that the problem is robust infeasible, i.e., $\tilde{\mathcal{U}} \coloneqq \mathcal{U} \setminus \mathrm{Proj}_{\boldsymbol{u}}(\mathcal{Y})$ is non-empty. In order to apply lemma 4.3.1, $\tilde{\mathcal{U}}$ has to contain an open subset. The next proposition shows that for the given sets, this is no restriction since such a subset always exists. Given a set $\mathcal{S} \subseteq \mathbb{R}^n$, we denote with $\mathrm{cl}(\mathcal{S})$, $\mathrm{int}(\mathcal{S})$, $\partial\mathcal{S}$, and $\mathcal{S}^{\mathrm{C}}$ the closure, interior, boundary, and complement of $\mathcal{S}$, respectively. In this work, the uncertainty set $\mathcal{U}$ is assumed to be a full-dimensional hyperrectangle or full-dimensional polyhedron. Therefore, $\mathcal{U} = \mathrm{cl}\big(\mathrm{int}(\mathcal{U})\big)$ always holds for our choices of $\mathcal{U}$.

Proposition 4.3.3. *Let $\mathcal{U} \subseteq \mathbb{R}^{n_u}$ be a set with $\mathcal{U} = \mathrm{cl}\big(\mathrm{int}(\mathcal{U})\big)$. Let $\mathcal{Y} \subseteq \mathbb{R}^{n_u} \times \mathbb{R}^{n_y}$ be a compact set and let $\tilde{\mathcal{U}} = \mathcal{U} \setminus \mathrm{Proj}_{\boldsymbol{u}}(\mathcal{Y}) \neq \emptyset$. Then $\tilde{\mathcal{U}}$ contains an open subset.*

Proof. We need to show that $\mathrm{int}(\tilde{\mathcal{U}}) = \mathrm{int}(\mathcal{U}) \cap \big(\mathrm{Proj}_{\boldsymbol{u}}(\mathcal{Y})\big)^{\mathrm{C}} \neq \emptyset$. Since $\mathcal{Y}$ is compact, $\mathrm{Proj}_{\boldsymbol{u}}(\mathcal{Y})$ is closed and thus $\big(\mathrm{Proj}_{\boldsymbol{u}}(\mathcal{Y})\big)^{\mathrm{C}}$ is an open set.

Pick any $\boldsymbol{u} \in \tilde{\mathcal{U}} = \mathcal{U} \cap \big(\mathrm{Proj}_{\boldsymbol{u}}(\mathcal{Y})\big)^{\mathrm{C}}$. If $\boldsymbol{u} \in \mathrm{int}(\mathcal{U})$, then $\boldsymbol{u} \in \mathrm{int}(\tilde{\mathcal{U}})$ holds as well since $\big(\mathrm{Proj}_{\boldsymbol{u}}(\mathcal{Y})\big)^{\mathrm{C}}$ is an open set.
Otherwise, assume that $\boldsymbol{u} \in \partial\mathcal{U}$. With $\boldsymbol{u} \in \big(\mathrm{Proj}_{\boldsymbol{u}}(\mathcal{Y})\big)^{\mathrm{C}}$, there exists $\varepsilon > 0$ such that $\mathcal{B}_\varepsilon(\boldsymbol{u}) \subseteq \big(\mathrm{Proj}_{\boldsymbol{u}}(\mathcal{Y})\big)^{\mathrm{C}}$. Since $\mathcal{U} = \mathrm{cl}\big(\mathrm{int}(\mathcal{U})\big)$, there exists $\boldsymbol{u}' \in \mathrm{int}(\mathcal{U}) \cap \mathcal{B}_\varepsilon(\boldsymbol{u}) \subseteq \big(\mathrm{Proj}_{\boldsymbol{u}}(\mathcal{Y})\big)^{\mathrm{C}}$. Therefore, $\boldsymbol{u}' \in \mathrm{int}(\tilde{\mathcal{U}})$.

This concludes that for the given sets, $\tilde{\mathcal{U}}$ always contains an open subset if $\tilde{\mathcal{U}}$ is non-empty. □

With proposition 4.3.3 and lemma 4.3.1, the separation problem (PolySep) can certify infeasibility if the assumptions of proposition 4.3.3 are satisfied. In practice, this optimization problem is then approximated by some finite relaxation of the Lasserre hierarchy using proposition 4.2.5. The question remains whether for sufficiently large levels of the hierarchy, the separation polynomial as given by lemma 4.3.1 can always be found. After all, not all positive polynomials can be expressed by SOS polynomials. This is no restriction as the following proposition shows.

Proposition 4.3.4. *There is some finite level of the Lasserre hierarchy for which the corresponding SDP approximation of* (PolySep) *yields a negative objective if* $\tilde{\mathcal{U}} \neq \emptyset$.

Proof. By proposition 4.3.3, $\tilde{\mathcal{U}} \neq \emptyset$ implies the existence of some open subset in $\tilde{\mathcal{U}}$. Then lemma 4.3.1 guarantees the existence of a polynomial p with strictly negative objective value for the abstract polynomial optimization problem. Consider then the SDP approximation of (PolySep). Since SOS polynomials are dense (Lasserre and Netzer 2007) in the set of nonnegative polynomials and by the continuity of the integral, there is always a SOS polynomial close to the p with a negative objective value. □

4.3.2 A set containment approach for certifying feasibility

In the setting of this chapter, deciding robust feasibility is equivalent to answering the set containment question

$$\mathcal{U} \subseteq \mathrm{Proj}_{\boldsymbol{u}}(\mathcal{Y}). \tag{4.60}$$

Since an explicit description of $\mathrm{Proj}_{\boldsymbol{u}}(\mathcal{Y})$ is typically not available, we show how the question above can be decided equivalently using nonprojected sets under an additional assumption. The set $\mathcal{Y}$ of all feasible pairs of uncertain data and second-stage variables can be written naturally as an intersection in the following way. Let

$$\mathcal{Y} = \mathcal{H} \cap \mathcal{G} \tag{4.61a}$$

with

$$\mathcal{H} \coloneqq \{(\boldsymbol{u}, \boldsymbol{y}) \in \mathbb{R}^{n_u} \times \mathbb{R}^{n_y} \mid \boldsymbol{h}(\boldsymbol{u}, \boldsymbol{y}) = \boldsymbol{0}\}, \tag{4.61b}$$

$$\mathcal{G} \coloneqq \{(\boldsymbol{u}, \boldsymbol{y}) \in \mathbb{R}^{n_u} \times \mathbb{R}^{n_y} \mid \boldsymbol{g}(\boldsymbol{u}, \boldsymbol{y}) \geq \boldsymbol{0}\}. \tag{4.61c}$$

In our approach, we require that the equation system $\boldsymbol{h}(\hat{\boldsymbol{u}}, \boldsymbol{y}) = \boldsymbol{0}$ has a unique solution in $\boldsymbol{y}$ given an arbitrary $\hat{\boldsymbol{u}} \in \mathcal{U}$. Let

$$\mathcal{H}_{\mathcal{U}} \coloneqq \{(\boldsymbol{u}, \boldsymbol{y}) \in \mathcal{U} \times \mathbb{R}^{n_y} \mid \boldsymbol{h}(\boldsymbol{u}, \boldsymbol{y}) = \boldsymbol{0}\} \tag{4.62}$$

be the restriction of $\mathcal{H}$ to the pairs containing elements of the uncertainty set. Now we can write the above requirement formally:

Assumption 2. *For all $\hat{\boldsymbol{u}} \in \mathcal{U}$, the system $\boldsymbol{h}(\hat{\boldsymbol{u}}, \boldsymbol{y}) = \boldsymbol{0}$ has exactly one solution $\hat{\boldsymbol{y}} \in \mathbb{R}^{n_y}$.*

If the previous assumption is satisfied, let $\boldsymbol{y}^* \colon \mathcal{U} \to \mathbb{R}^{n_y}$ be the (unique) function that maps elements of the uncertainty set to solutions. That is, for all $\hat{\boldsymbol{u}} \in \mathcal{U}$, let $\boldsymbol{y}^*(\hat{\boldsymbol{u}}) \in \mathbb{R}^{n_y}$ be the unique solution $\boldsymbol{y}^*$ of $\boldsymbol{h}(\hat{\boldsymbol{u}}, \boldsymbol{y}) = \boldsymbol{0}$ with a fixed $\hat{\boldsymbol{u}}$. Using the uncertainty-to-solution function $\boldsymbol{y}^*$, the set $\mathcal{H}_{\mathcal{U}}$ can be rephrased as $\mathcal{H}_{\mathcal{U}} = \{(\boldsymbol{u}, \boldsymbol{y}^*(\boldsymbol{u})) \mid \boldsymbol{u} \in \mathcal{U}\}$.

Remark 4.3.5. Uniqueness of solutions as in assumption 2 is a feature of many physical systems that are modeled as a system of PDEs. For instance, for a wide class of boundary value problems the uniqueness of the solution follows from the famous lemma of Lax and Milgram (1954) for arbitrary right-hand sides using a coercivity assumption. This directly implies that uniqueness and assumption 2 also hold for PDEs with uncertain coefficients, as long as the coercivity is maintained on the whole uncertainty set.

The set $\mathcal{H}_{\mathcal{U}}$ comprises all uncertainty-dependent solutions of the state equation $\boldsymbol{h}(\boldsymbol{u}, \boldsymbol{y}) = \boldsymbol{0}$, whereas the set $\mathcal{G}$ is described by the given state constraints. Moreover, we remark that an explicit construction of the function $\boldsymbol{y}^*(\cdot)$ is never required; we merely introduce $\boldsymbol{y}^*$ to simplify the presentation.

The next lemma shows how the unique dependency between $\boldsymbol{u}$ and $\boldsymbol{y}$ leads to an equivalent projectionless formulation of the set containment question $\mathcal{U} \subseteq \mathrm{Proj}_{\boldsymbol{u}}(\mathcal{Y})$.

Lemma 4.3.6. *Let $\mathcal{U} \subseteq \mathbb{R}^{n_u}$ with $n_u \in \mathbb{N}$, and let $\boldsymbol{y}^* \colon \mathcal{U} \to \mathbb{R}^{n_y}$ with $n_y \in \mathbb{N}$. Let $\mathcal{H}_{\mathcal{U}} \coloneqq \{(\boldsymbol{u}, \boldsymbol{y}^*(\boldsymbol{u})) \in \mathbb{R}^{n_u} \times \mathbb{R}^{n_y} \mid \boldsymbol{u} \in \mathcal{U}\}$, and let $\mathcal{G} \subseteq \mathbb{R}^{n_u} \times \mathbb{R}^{n_y}$.*
Then

$$\mathcal{U} \subseteq \mathrm{Proj}_{\boldsymbol{u}}(\mathcal{H}_{\mathcal{U}} \cap \mathcal{G}) \iff \mathcal{H}_{\mathcal{U}} \subseteq \mathcal{G}. \tag{4.63}$$

Proof. Suppose $\mathcal{U} \subseteq \mathrm{Proj}_{\boldsymbol{u}}(\mathcal{H}_{\mathcal{U}} \cap \mathcal{G})$. Pick any $(\boldsymbol{u}, \boldsymbol{y}) \in \mathcal{H}_{\mathcal{U}}$. Due to the projection, there exists $\boldsymbol{y}'$ with $(\boldsymbol{u}, \boldsymbol{y}') \in \mathcal{H}_{\mathcal{U}} \cap \mathcal{G}$. The variable $\boldsymbol{y}$ is uniquely determined for any $\boldsymbol{u} \in \mathcal{U}$. Therefore, $\boldsymbol{y} = \boldsymbol{y}' = \boldsymbol{y}^*(\boldsymbol{u})$ holds and thus $(\boldsymbol{u}, \boldsymbol{y}) \in \mathcal{G}$.

Suppose $\mathcal{H}_{\mathcal{U}} \subseteq \mathcal{G}$. Pick any $\boldsymbol{u} \in \mathcal{U}$, and let $\boldsymbol{y} = \boldsymbol{y}^*(\boldsymbol{u})$. Then $(\boldsymbol{u}, \boldsymbol{y}) \in \mathcal{H}_{\mathcal{U}} \subseteq \mathcal{G}$ and thus $(\boldsymbol{u}, \boldsymbol{y}) \in \mathcal{H}_{\mathcal{U}} \cap \mathcal{G}$. This implies $\boldsymbol{u} \in \mathrm{Proj}_{\boldsymbol{u}}(\mathcal{H}_{\mathcal{U}} \cap \mathcal{G})$. □

This lemma can be applied to all problems where a subset of the constraints defines a unique solution for each possible realization of the data. Even if $\boldsymbol{y}^*(\cdot)$ is only given implicitly by the solution of some (in)equality system, the lemma is still applicable.

If assumption 2 holds, lemma 4.3.6 allows us to answer the original set containment problem (4.3) by deciding the equivalent set containment problem

$$\mathcal{H}_{\mathcal{U}} \subseteq \mathcal{G}. \tag{4.64}$$

This set containment problem can be decided with the $i = 1, \ldots, m_g$ optimization problems

$$\begin{aligned} &\inf_{\boldsymbol{u},\boldsymbol{y}} \; g_i(\boldsymbol{u}, \boldsymbol{y}) \\ &\text{s.t.} \;\; (\boldsymbol{u}, \boldsymbol{y}) \in \mathcal{H}_{\mathcal{U}}. \end{aligned} \tag{MinCons$_i$}$$

The objective values of all m_g problems are nonnegative, if and only if $\mathcal{H}_{\mathcal{U}} \subseteq \mathcal{G}$. In cases where global optimality cannot be obtained easily, the criterion can be weakened by replacing the optimization problems (MinCons$_i$) with relaxations since nonnegative objective values of the relaxations imply nonnegative objective values of the original problems. However, this a sufficient but not necessary criterion since $\mathcal{H}_{\mathcal{U}} \subseteq \mathcal{G}$ might hold but at the same time some optimization problems can have negative objective values due to the relaxation.

The next lemma shows how the set containment question can still be decided if the considered sets are partitioned into subsets. This will be important when eliminating the absolute values of the gas transport problem later.

Lemma 4.3.7. *Let $\mathcal{U} \subseteq \mathbb{R}^{n_u}$ with $n_u \in \mathbb{N}$, and let $\boldsymbol{y}^* \colon \mathcal{U} \to \mathbb{R}^{n_y}$ with $n_y \in \mathbb{N}$. Let $\mathcal{H}_{\mathcal{U}} := \{(\boldsymbol{u}, \boldsymbol{y}^*(\boldsymbol{u})) \in \mathbb{R}^{n_u} \times \mathbb{R}^{n_y} \mid \boldsymbol{u} \in \mathcal{U}\}$, and let $\mathcal{G} \subseteq \mathbb{R}^{n_u} \times \mathbb{R}^{n_y}$. Let $\mathcal{S}_i$, $i \in \mathcal{I}$, be a collection of sets with $\mathcal{S}_i \subseteq \mathbb{R}^{n_u} \times \mathbb{R}^{n_y}$ such that $\bigcup_{i\in\mathcal{I}} \mathcal{S}_i = \mathbb{R}^{n_u} \times \mathbb{R}^{n_y}$.*

Then

$$\mathcal{U} = \operatorname{Proj}_{\boldsymbol{u}}(\mathcal{H}_{\mathcal{U}}) \subseteq \operatorname{Proj}_{\boldsymbol{u}}(\mathcal{H}_{\mathcal{U}} \cap \mathcal{G}) \tag{4.65}$$

$$\iff$$

$$\operatorname{Proj}_{\boldsymbol{u}}(\mathcal{H}_{\mathcal{U}} \cap \mathcal{S}_i) \subseteq \operatorname{Proj}_{\boldsymbol{u}}(\mathcal{H}_{\mathcal{U}} \cap \mathcal{G} \cap \mathcal{S}_i) \quad \textit{for all } i \in \mathcal{I}. \tag{4.66}$$

Proof.

$$\mathcal{U} = \operatorname{Proj}_{\boldsymbol{u}}(\mathcal{H}_{\mathcal{U}}) \subseteq \operatorname{Proj}_{\boldsymbol{u}}(\mathcal{H}_{\mathcal{U}} \cap \mathcal{G}) \tag{4.67}$$

$$\overset{\text{lemma 4.3.6}}{\iff} \quad \mathcal{H}_{\mathcal{U}} \subseteq \mathcal{G} \iff \mathcal{H}_{\mathcal{U}} \cap \mathcal{S}_i \subseteq \mathcal{G} \cap \mathcal{S}_i \quad \text{for all } i \in \mathcal{I}. \tag{4.68}$$

Let $\mathcal{U}_i' \coloneqq \operatorname{Proj}_{\boldsymbol{u}}(\mathcal{H}_{\mathcal{U}} \cap \mathcal{S}_i)$. Rewriting $\mathcal{H}_{\mathcal{U}} \cap \mathcal{S}_i$ yields

$$\begin{aligned}
\mathcal{H}_{\mathcal{U}} \cap \mathcal{S}_i &= \{(\boldsymbol{u}, \boldsymbol{y}) \mid \boldsymbol{y} = \boldsymbol{y}^*(\boldsymbol{u}),\ \boldsymbol{u} \in \mathcal{U},\ (\boldsymbol{u}, \boldsymbol{y}) \in \mathcal{S}_i\} && (4.69)\\
&= \{(\boldsymbol{u}, \boldsymbol{y}) \mid \boldsymbol{y} = \boldsymbol{y}^*(\boldsymbol{u}),\ \boldsymbol{u} \in \mathcal{U},\ (\boldsymbol{u}, \boldsymbol{y}^*(\boldsymbol{u})) \in \mathcal{S}_i\} && (4.70)\\
&= \{(\boldsymbol{u}, \boldsymbol{y}) \mid \boldsymbol{y} = \boldsymbol{y}^*(\boldsymbol{u}),\ \boldsymbol{u} \in \{\boldsymbol{u} \mid \boldsymbol{u} \in \mathcal{U},\ (\boldsymbol{u}, \boldsymbol{y}^*(\boldsymbol{u})) \in \mathcal{S}_i\}\} && (4.71)\\
&= \{(\boldsymbol{u}, \boldsymbol{y}) \mid \boldsymbol{y} = \boldsymbol{y}^*(\boldsymbol{u}),\ \boldsymbol{u} \in \operatorname{Proj}_{\boldsymbol{u}}(\mathcal{H}_{\mathcal{U}} \cap \mathcal{S}_i)\} && (4.72)\\
&= \mathcal{H}_{\operatorname{Proj}_{\boldsymbol{u}}(\mathcal{H}_{\mathcal{U}} \cap \mathcal{S}_i)} = \mathcal{H}_{\mathcal{U}_i'}. && (4.73)
\end{aligned}$$

Then

$$\begin{aligned}
&\mathcal{H}_{\mathcal{U}} \cap \mathcal{S}_i = \mathcal{H}_{\mathcal{U}_i'} \subseteq \mathcal{G} \cap \mathcal{S}_i \quad \text{for all } i \in \mathcal{I} && (4.74)\\
&\qquad \overset{\text{lemma 4.3.6}}{\iff} && (4.75)\\
&\mathcal{U}_i' = \operatorname{Proj}_{\boldsymbol{u}}(\mathcal{H}_{\mathcal{U}_i'}) \subseteq \operatorname{Proj}_{\boldsymbol{u}}(\mathcal{H}_{\mathcal{U}_i'} \cap \mathcal{G}) \\
&\qquad\qquad = \operatorname{Proj}_{\boldsymbol{u}}(\mathcal{H}_{\mathcal{U}} \cap \mathcal{G} \cap \mathcal{S}_i) \quad \text{for all } i \in \mathcal{I}. && (4.76)
\end{aligned}$$

□

For practical applications the optimization problems (MinCons_i) need to be solved to global optimality. As mentioned earlier, if global optimality cannot be ensured, a relaxation of the given problem can also suffice. The structure of the optimization problems depends on the defining functions of $\mathcal{H}_{\mathcal{U}}, \mathcal{G}$. For the gas network problem, these typically are polynomials or piecewise polynomials. Using the ideas of section 4.4.3, the piecewise polynomial functions can be reformulated in terms of pure polynomials. Instead of solving the resulting polynomial optimization problems (MinCons_i), SOS or moment relaxation of these problems can be applied. These relaxations form a hierarchy of SDPs; see Parrilo (2003) and Lasserre (2000), respectively.

4.4 Deciding robustness for the passive gas network problem

In this section, we apply our methods to a variant of the gas network problem under uncertainty. While using the same general structure as (3.5), we consider a version without first-stage variables, i.e., a passive network without compressors. Moreover, we only deal with uncertainties in the pipes' roughness values, i.e., in the pressure drop coefficients. Since the gas network problem is modeled by piecewise polynomial functions due to the occuring absolute value functions, we discuss how a purely polynomial formulation can obtained through case distinctions. The resulting polynomial feasibility system will be tackled using methods from section 4.3.

4.4.1 The passive gas network problem under uncertainty

We consider a stationary passive gas network without compressors under uncertainty. It is assumed that the pressure drop coefficient of each pipe is uncertain and lies within some a priori known interval

$$l_a \in [\underline{l}_a, \bar{l}_a] \quad \text{for all } a \in \mathcal{A}, \tag{4.77}$$

where $\underline{l}_a, \bar{l}_a \in \mathbb{R}$ and $0 < \underline{l}_a \leq \bar{l}_a$. Hence, the uncertainty set $\mathcal{U} \subseteq \mathbb{R}^{|\mathcal{A}_{\mathrm{pi}}|}_{>0}$ is a hyperrectangle of the form (3.3):

$$\mathcal{U} := \mathcal{L} = \{\boldsymbol{l} \in \mathbb{R}^{|\mathcal{A}_{\mathrm{pi}}|} \mid \underline{l}_a \leq l_a \leq \bar{l}_a \quad \text{for all } a \in \mathcal{A}_{\mathrm{pi}}\}, \tag{4.78}$$

with $\underline{\boldsymbol{l}}, \bar{\boldsymbol{l}} \in \mathbb{R}^{|\mathcal{A}_{\mathrm{pi}}|}$ and $\mathbf{0} < \underline{\boldsymbol{l}} \leq \bar{\boldsymbol{l}}$.

The gas network problem under consideration is a variant of problem (3.5) as defined in section 3.3 without active elements and no objective function. For reference, we restate this feasibility problem in its reduced form:

Decide whether for all $\boldsymbol{l} \in \mathcal{U}$ there is $\boldsymbol{q}_{\mathcal{N}} \in \mathbb{R}^{|\mathcal{N}|}$ with

$$\boldsymbol{C}\boldsymbol{\psi}(\boldsymbol{l}, \boldsymbol{q}^{\mathrm{ext}}(\boldsymbol{q}_{\mathcal{N}})) = \mathbf{0}, \tag{4.79a}$$

$$\boldsymbol{P}\boldsymbol{\psi}_{\mathcal{B}}(\boldsymbol{l}_{\mathcal{B}}, \boldsymbol{q}^{\mathrm{ext}}_{\mathcal{B}}(\boldsymbol{q}_{\mathcal{N}})) \leq \Delta\boldsymbol{\pi}. \tag{4.79b}$$

Mirroring (4.61a) and (4.62), we introduce the sets defined by the equality and inequality constraints:

$$\mathcal{H} := \{(\boldsymbol{l}, \boldsymbol{q}_{\mathcal{N}}) \in \mathbb{R}^{|\mathcal{A}_{\mathrm{pi}}|} \times \mathbb{R}^{|\mathcal{N}|} \mid \boldsymbol{C}\boldsymbol{\psi}(\boldsymbol{l}, \boldsymbol{q}^{\mathrm{ext}}(\boldsymbol{q}_{\mathcal{N}})) = \mathbf{0}\}, \tag{4.80}$$

$$\mathcal{H}_{\mathcal{U}} := \{(\boldsymbol{l}, \boldsymbol{q}_{\mathcal{N}}) \in \mathcal{H} \mid \boldsymbol{l} \in \mathcal{U}\}, \tag{4.81}$$

$$\mathcal{G} := \{(\boldsymbol{l}, \boldsymbol{q}_{\mathcal{N}}) \in \mathbb{R}^{|\mathcal{A}_{\mathrm{pi}}|} \times \mathbb{R}^{|\mathcal{N}|} \mid \boldsymbol{P}\boldsymbol{\psi}_{\mathcal{B}}(\boldsymbol{l}_{\mathcal{B}}, \boldsymbol{q}^{\mathrm{ext}}_{\mathcal{B}}(\boldsymbol{q}_{\mathcal{N}})) \leq \Delta\boldsymbol{\pi}\}, \tag{4.82}$$

and with that $\mathcal{Y} := \mathcal{H} \cap \mathcal{G}$.

The set $\mathcal{H}$ (resp., $\mathcal{H}_{\mathcal{U}}$) contains all feasible combinations $\boldsymbol{l}, \boldsymbol{q}_{\mathcal{N}}$ (resp., with $\boldsymbol{l} \in \mathcal{U}$) arising from the cycle flow equations. The set $\mathcal{G}$ can be seen as all combinations $\boldsymbol{l}, \boldsymbol{q}_{\mathcal{N}}$ that are feasible for the given pressure bounds. Taking the intersection of $\mathcal{H}$ and $\mathcal{G}$ yields $\mathcal{Y}$, the set of all feasible uncertainty/solution pairs of the given gas transport problem.

Moreover, we observe that equality system (4.79a) satisfies assumption 2, since a unique flow solution $\boldsymbol{q}^*_{\mathcal{N}}(\boldsymbol{l})$ always exists for any $\boldsymbol{l} \in \mathcal{U}$ due to proposition 2.4.4

The task is now to decide whether the network has a feasible flow for all $\boldsymbol{l} \in \mathcal{U}$. Let $\mathrm{Proj}_{\boldsymbol{l}}(\mathcal{Y})$ be the projection of the feasible pairs of pressure drop coefficients and flows onto the space of the uncertainty set. This set contains all pressure

drop coefficients which admit a feasible flow in the corresponding problem. In this context, deciding robustness with respect to $\mathcal{U}$ is equivalent to checking whether the uncertainty set $\mathcal{U}$ is contained in the projection $\mathrm{Proj}_{\boldsymbol{l}}(\mathcal{Y})$:

$$\mathcal{U} \subseteq \mathrm{Proj}_{\boldsymbol{l}}(\mathcal{Y}) = \{\boldsymbol{l} \mid \exists\, \boldsymbol{q}_{\mathcal{N}} \colon (\boldsymbol{l}, \boldsymbol{q}_{\mathcal{N}}) \in \mathcal{Y}\}. \tag{4.83}$$

4.4.2 Deciding robust feasibility on tree networks

First, we consider the special case of a network whose underlying topology is a tree. Since there are no cycles, we have $\mathcal{B} = \mathcal{A}$ and $\mathcal{N} = \emptyset$. Consequently, the description of $\mathcal{Y}$ does not contain any cycle flow variables $\boldsymbol{q}_{\mathcal{N}}$ and no equality constraints. Moreover, with nonbasic variables, we have $\boldsymbol{q} = \boldsymbol{q}_{\mathcal{B}}$, $\boldsymbol{\psi} = \boldsymbol{\psi}_{\mathcal{B}}$, and $\boldsymbol{l} = \boldsymbol{l}_{\mathcal{B}}$. We note that the flow solution $\boldsymbol{q}^* = \tilde{\boldsymbol{A}}_{\mathcal{B}}^{-1}\tilde{\boldsymbol{d}}$ is constant and can be precomputed. Recalling the definition of $\psi_a(q_a^*, l_a) = -l_a|q_a^*|q_a^*$, we infer that ψ_a is a linear function of l_a for all $a \in \mathcal{A}_{\mathrm{pi}}$.

With this in mind, we observe that the set

$$\mathcal{Y} = \{\boldsymbol{l} \in \mathbb{R}^{|\mathcal{A}_{\mathrm{pi}}|} \mid \boldsymbol{P}\boldsymbol{\psi}(\boldsymbol{l}, \boldsymbol{q}^*) \leq \Delta\boldsymbol{\pi}\} \tag{4.84}$$

is defined by linear inequalities in $\boldsymbol{l}$ and hence is a polyhedron.

In this case, checking robust feasibility with respect to a given polyhedral uncertainty set $\mathcal{U}$ is equivalent to deciding the set containment problem

$$\mathcal{U} \subseteq \mathrm{Proj}_{\boldsymbol{l}}(\mathcal{Y}) = \mathcal{Y} \tag{4.85}$$

for two polyhedral sets $\mathcal{U}$ and $\mathcal{Y}$. As the following lemma by Mangasarian (2002) shows, this can be done efficiently with LP duality.

Lemma 4.4.1 (Mangasarian 2002). *Let $\mathcal{S} \coloneqq \{\boldsymbol{x} \in \mathbb{R}^n \mid \boldsymbol{S}\boldsymbol{x} \geq \boldsymbol{s}\}$ and let $\mathcal{T} \coloneqq \{\boldsymbol{x} \in \mathbb{R}^n \mid \boldsymbol{T}\boldsymbol{x} \leq \boldsymbol{t}\} \neq \emptyset$ be two polyhedral sets, where $\boldsymbol{S} \in \mathbb{R}^{m\times n}$, $\boldsymbol{s} \in \mathbb{R}^n$ and $\boldsymbol{T} \in \mathbb{R}^{k\times n}$, $\boldsymbol{t} \in \mathbb{R}^n$ with $k, m, n \in \mathbb{N}$.*

Then the following statements are equivalent:

1. *$\mathcal{T} \subseteq \mathcal{S}$; that is:*
$$\boldsymbol{T}\boldsymbol{x} \leq \boldsymbol{t} \implies \boldsymbol{S}\boldsymbol{x} \geq \boldsymbol{s}. \tag{4.86}$$
2. *For $i = 1, \ldots, m$, the m LPs are solvable and satisfy:*
$$\min_x\{(\boldsymbol{S}\boldsymbol{x})_i \mid \boldsymbol{T}\boldsymbol{x} \leq \boldsymbol{t}\} \geq s_i. \tag{4.87}$$
3. *There exists a matrix $\boldsymbol{W} \in \mathbb{R}^{m\times k}$ such that*
$$\boldsymbol{S} + \boldsymbol{W}\boldsymbol{T} = \boldsymbol{0},\ \boldsymbol{s} + \boldsymbol{W}\boldsymbol{t} \leq \boldsymbol{0},\ \boldsymbol{W} \geq \boldsymbol{0}, \tag{4.88}$$
where $\boldsymbol{W} \geq \boldsymbol{0}$ means that all entries of $\boldsymbol{W}$ are nonnegative.

Corollary 4.4.2. *Let $\mathcal{U} = \{\boldsymbol{l} \in \mathbb{R}^{|\mathcal{A}_{\mathrm{pi}}|} \mid \boldsymbol{T}\boldsymbol{l} \leq \boldsymbol{t}\}$ be a polyhedral uncertainty set. Let $\mathcal{Y} = \{\boldsymbol{l} \in \mathbb{R}^{|\mathcal{A}_{\mathrm{pi}}|} \mid \boldsymbol{S}\boldsymbol{l} \geq \boldsymbol{s}\}$ be the polyhedral set of feasible pressure drop coefficients $\boldsymbol{l}$ for a gas transport problem over a tree-shaped network.*

Then robustness with respect to $\mathcal{U}$ can be decided by solving an LP.

Robust feasibility of tree networks as a function of a node's pressure

Corollary 4.4.2 allows us to characterize robustness of a tree network in terms of the pressure at an arbitrary chosen node. W.l.o.g., we select the tree's root node $r \in \mathcal{V}$ as the basis of our considerations. Suppose the squared pressure at this node is fixed, i.e., $\pi_r := \underline{\pi}_r = \overline{\pi}_r$. Our aim is to specify all π_r such that the gas network problem is robust feasible.

As can be inferred from (4.84), the pressure bounds only appear as constants in the linear inequality constraints. With the conventions of the previous corollary, the set of feasible pressure drop coefficients can thus be expressed in terms of the root node's pressure π_r:

$$\mathcal{Y}(\pi_r) := \{\boldsymbol{l} \mid \boldsymbol{S}\boldsymbol{l} \geq \boldsymbol{s}(\pi_r)\}. \tag{4.89}$$

Considering π_r as a variable, the right-hand side $\boldsymbol{s}$ of the linear inequality system is a linear function $\boldsymbol{s}\colon \mathbb{R} \to \mathbb{R}^{|\mathcal{A}_{\mathrm{pi}}|}$ of π_r. Applying lemma 4.4.1 to the set containment question $\mathcal{U} \subseteq \mathcal{Y}(\pi_r)$ yields

$$\mathcal{U} = \{\boldsymbol{l} \mid \boldsymbol{T}\boldsymbol{l} \leq \boldsymbol{t}\} \subseteq \{\boldsymbol{l} \mid \boldsymbol{S}\boldsymbol{l} \geq \boldsymbol{s}(\pi_r)\} = \mathcal{Y}(\pi_r) \tag{4.90}$$

$$\iff \mathcal{W}(\pi_r) := \left\{ \boldsymbol{W} \in \mathbb{R}^{m \times k}_{\geq 0} \;\middle|\; \begin{matrix} \boldsymbol{S} + \boldsymbol{W}\boldsymbol{T} = \boldsymbol{0} \\ \boldsymbol{s}(\pi_r) + \boldsymbol{W}\boldsymbol{t} \leq \boldsymbol{0} \end{matrix} \right\} \neq \emptyset. \tag{4.91}$$

Lemma 4.4.3. *Given a tree network $\mathcal{G} = (\mathcal{V}, \mathcal{A})$ with root node r and a polyhedral uncertainty set $\mathcal{U}$. Then the network is robust feasible if and only if the root node's squared pressure satisfies*

$$\pi_r \in [\underline{\pi}^*_r, \overline{\pi}^*_r] \tag{4.92}$$

with $\underline{\pi}^*_r$, $\overline{\pi}^*_r$ being optimal values of the LPs

$$\begin{aligned} \underline{\pi}^*_r &:= \min_{\pi_r, \boldsymbol{W}} \pi_r \;\text{ s.t. }\; \boldsymbol{W} \in \mathcal{W}(\pi_r), \\ \overline{\pi}^*_r &:= \max_{\pi_r, \boldsymbol{W}} \pi_r \;\text{ s.t. }\; \boldsymbol{W} \in \mathcal{W}(\pi_r), \end{aligned} \tag{4.93}$$

where $\mathcal{W}(\pi_r)$ is defined as in (4.91).

Proof. The set $\{(\pi_r, \boldsymbol{W}) \mid \boldsymbol{W} \in \mathcal{W}(\pi_r)\}$ is polyhedral and thus convex. Therefore, the set of all feasible π_r can be described by the interval

$$[\underline{\pi}_r^*, \overline{\pi}_r^*], \tag{4.94}$$

whose endpoints are the optimal values of the LPs (4.93). □

4.4.3 Eliminating the absolute value functions

In order to apply tools from polynomial optimization to a general gas network problem with cycles, the constraining functions of $\mathcal{Y}$ have to be converted to a polynomial representation. Currently, the pressure drop equations

$$\pi_w - \pi_v = -l_a|q_a|q_a = \psi_a(q_a) \quad \text{for all } (v,w) \in \mathcal{A}_{\mathrm{pi}} \tag{4.95}$$

introduce absolute values into the problem. After elimination of the absolute values, $\mathcal{Y}$ is transformed from a piecewise polynomial representation to an equivalent but purely polynomial description. Depending on the topology of a given instance, it may be possible to eliminate a lot of absolute values in advance since all arcs which are not part of a cycle have fixed flow direction. For example, in the case of tree networks, all directions are known in advance. Apart from that, the flow direction can be fixed by other preprocessing algorithms, e.g., flow/pressure propagation or bound tightening methods. Further discussion on that topic can be found in Geißler (2011) and in section 5.2.3.

This chapter presents three different methods for the elimination of absolute values. First, a technique from mixed-integer linear optimization is employed to model absolute values using binary variables. With this method, both the feasibility and the infeasibility method can be used. Next, the implications of straightforward case distinction are discussed. In general, this technique can only be used for the feasibility method, as will be explained later. Finally, the case distinction idea is further investigated for networks which contain a single cycle. In this setting, the absolute values can be eliminated by restricting the uncertainty set to polyhedral subsets. It is shown how the overall problem can be decomposed into linearly many subproblems which can be decided with both methods.

Elimination by auxiliary binary variables

By introducing additional binary variables, the absolute value functions can be eliminated. This technique is very similar to what is typically done in mixed-integer linear optimization. We demonstrate the idea using the example of

$x|x|$, where $x \in \mathbb{R}$ is a scalar variable. First, assume that $|x|$ is bounded by some $M \in \mathbb{R}$: $|x| \leq M$. This is a natural assumption since the flows within the network cannot become arbitrarily large. By adding the constraint $b = b^2$ for $b \in \mathbb{R}$, we model a binary variable $b \in \{0, 1\}$. Then, the signed-square expression $y = x|x|$ can be stated equivalently using polynomials via

$$y = (2b - 1)x^2, \tag{4.96a}$$
$$(-1 + b)M \leq x \leq bM, \tag{4.96b}$$
$$b = b^2. \tag{4.96c}$$

Applying this construction to each absolute value function on each arc $a \in \mathcal{A}_{\mathrm{pi}}$ yields a purely polynomial description of $\mathcal{Y}$ that can be used in the feasibility and infeasibility methods.

Elimination by case distinction: the general case

Considering the original, non-reduced problem definition (3.5), each pipe $a \in \mathcal{A}_{\mathrm{pi}}$ introduces an absolute value from its pressure drop equation. In general, one might expect that by eliminating each absolute value function, the problem would be split into $2^{|\mathcal{A}_{\mathrm{pi}}|}$ cases. This paragraph shows how the number of cases mainly depends on the number of fundamental cycles in the graph and thus can be much smaller than $2^{|\mathcal{A}_{\mathrm{pi}}|}$. We remark that the following results identify the feasible flow directions in a linear network flow model instead of the gas transport problem. However, this is no restriction since adding constraints concerning the gas physics reduces the number of possible cases even further.

Due to lemma 4.3.7, the overall set containment problem can be decided by splitting the problem into a series of subproblems. Each subproblem arises by restricting the original problem to certain subsets, e.g., to orthants of $\mathbb{R}^{|\mathcal{A}_{\mathrm{pi}}|}$ for the absolute value case distinction. Let $\{\mathcal{O}_1, \ldots, \mathcal{O}_{2^{|\mathcal{A}_{\mathrm{pi}}|}}\} = \{\mathbb{R}_{\geq 0}, \mathbb{R}_{\leq 0}\}^{|\mathcal{A}_{\mathrm{pi}}|}$ be the set of orthants in $\mathbb{R}^{|\mathcal{A}_{\mathrm{pi}}|}$. In the non-reduced model (3.5), the additional constraint $\boldsymbol{q} \in \mathcal{O}_i$ restricts the flow to a specific orthant and allows the elimination of all absolute value functions. In the reduced model, the variables $\boldsymbol{q}_{\mathcal{B}}$ are replaced by $\boldsymbol{q}_{\mathcal{B}} = \tilde{\boldsymbol{A}}_{\mathcal{B}}^{-1}(\tilde{\boldsymbol{d}} - \tilde{\boldsymbol{A}}_{\mathcal{N}}\boldsymbol{q}_{\mathcal{N}})$. The transformed case distinction is

$$\begin{pmatrix} \boldsymbol{q}_{\mathcal{B}} \\ \boldsymbol{q}_{\mathcal{N}} \end{pmatrix} = \begin{pmatrix} \tilde{\boldsymbol{A}}_{\mathcal{B}}^{-1}(\tilde{\boldsymbol{d}} - \tilde{\boldsymbol{A}}_{\mathcal{N}}\boldsymbol{q}_{\mathcal{N}}) \\ \boldsymbol{q}_{\mathcal{N}} \end{pmatrix} \in \mathcal{O}_i. \tag{4.97}$$

By considering the reduced model, the next proposition shows that the number of case distinctions mainly depends on the number of fundamental cycles in the graph.

Proposition 4.4.4. *Let $\mathcal{G} = (\mathcal{V}, \mathcal{A}_{\mathrm{pi}})$ be a connected digraph with $|\mathcal{A}_{\mathrm{pi}}|$ arcs and $|\mathcal{N}|$ fundamental cycles. Then there can be at most*

$$\sum_{i=0}^{|\mathcal{N}|} \binom{|\mathcal{A}_{\mathrm{pi}}|}{i} \in \mathcal{O}(|\mathcal{A}_{\mathrm{pi}}|^{|\mathcal{N}|}) \tag{4.98}$$

many feasible flow directions in the network. The corresponding subproblems can be constructed in running time $\mathcal{O}(|\mathcal{A}_{\mathrm{pi}}|^{|\mathcal{N}|})$.

Proof. The problem of finding all feasible flow directions can be reduced to a problem concerning the arrangement of hyperplanes. For ease of exposition, consider the nonnegative orthant $\mathcal{O}^+ = \mathbb{R}_{\geq 0}^{|\mathcal{A}_{\mathrm{pi}}|}$. Using the flow function $\boldsymbol{q}^{\mathrm{ext}}$ as defined in (2.57), fixing the flow direction to this orthant amounts to the constraint $\boldsymbol{q}^{\mathrm{ext}}(\boldsymbol{q}_{\mathcal{N}}) \in \mathcal{O}^+$, i.e., $\boldsymbol{q}^{\mathrm{ext}}(\boldsymbol{q}_{\mathcal{N}}) \geq \mathbf{0}$. Each entry $(q_a^{\mathrm{ext}})_{a \in \mathcal{A}_{\mathrm{pi}}}$ of $\boldsymbol{q}^{\mathrm{ext}}$ defines a hyperplane in $\mathbb{R}^{|\mathcal{N}|}$. Consider the regions that can arise by segmenting $\mathbb{R}^{|\mathcal{N}|}$ using the hyperplanes in $\boldsymbol{q}^{\mathrm{ext}}$. For all $a \in \mathcal{A}_{\mathrm{pi}}$, each region is a subset of either $q_a^{\mathrm{ext}}(\boldsymbol{q}_{\mathcal{N}}) < 0$ or $q_a^{\mathrm{ext}}(\boldsymbol{q}_{\mathcal{N}}) > 0$. Therefore, the flow direction on all arcs in the graph is constant on each region. The total number of regions that can be constructed in $\mathbb{R}^{|\mathcal{N}|}$ using $|\mathcal{A}_{\mathrm{pi}}|$ hyperplanes is bounded by $\sum_{i=0}^{|\mathcal{N}|} \binom{|\mathcal{A}_{\mathrm{pi}}|}{i} \in \mathcal{O}(|\mathcal{A}_{\mathrm{pi}}|^{|\mathcal{N}|})$; see Zaslavsky (1975). Furthermore, constructing all regions can be achieved in running time $\mathcal{O}(|\mathcal{A}_{\mathrm{pi}}|^{|\mathcal{N}|})$ using the algorithm of Edelsbrunner, O'Rourke, and Seidel (1986). □

However, there is an issue arising when using lemma 4.3.7 as the subproblems are of the type

$$\mathrm{Proj}_{\boldsymbol{l}}(\mathcal{H}_{\mathcal{U}} \cap \mathcal{O}_i) \subseteq \mathrm{Proj}_{\boldsymbol{l}}(\mathcal{H}_{\mathcal{U}} \cap \mathcal{G} \cap \mathcal{O}_i). \tag{4.99}$$

The feasibility method can be employed as is, since optimizing over a projected set poses no restriction. On the other hand, the infeasibility method cannot be applied as easily since it requires the moments over the uncertainty set. In case of the given subproblems, this is the set $\mathrm{Proj}_{\boldsymbol{l}}(\mathcal{H}_{\mathcal{U}} \cap \mathcal{O}_i)$. In general, it is unclear how the moments can be obtained without explicitly constructing the projection. Nevertheless, this is possible for networks with one cycle. The next section gives the description of $\mathrm{Proj}_{\boldsymbol{l}}(\mathcal{H}_{\mathcal{U}} \cap \mathcal{O}_i)$ for this case. In this setting, the infeasibility method can be applied since the projected set is polyhedral.

Elimination by case distinction: a shortcut for networks with one cycle

On networks with only one cycle, a considerable simplification can be applied. The absolute values can be eliminated by restricting the problem to certain

subsets of the uncertainty set. In contrast, the previous case distinction method relied on restricting the flow variables. The advantage of using subsets of the uncertainty set for this purpose is that the infeasibility method can be applied as well since it requires explicit knowledge of the uncertainty set.

For the purpose of this chapter, we assume a directed cyclic graph where each arc points to a different node:

Assumption 3. *Let $\mathcal{G} = (\mathcal{V}, \mathcal{A}_{\text{pi}})$ be a directed cyclic graph with $\mathcal{V} = \{1, \dots, n\}$, $\mathcal{A}_{\text{pi}} = \{(1,2), (2,3), \dots, (n-1, n), (n, 1)\}$, and non-zero demand $\boldsymbol{d} \in \mathbb{R}^{|\mathcal{V}|}$.*

Due to the cyclic structure, the arcs can be uniquely identified by their first node. We assume the last edge to be part of the nonbasis; thus there is only one problem variable $q_n \in \mathbb{R}$ with $\boldsymbol{q}_{\mathcal{N}} \equiv q_n$. Employing a similar construction as that in Gotzes et al. (2016, ch. 6.1), we obtain the set $\mathcal{H}$ of feasible $(\boldsymbol{l}, q_n)$-combinations and the associated cycle flow equation.

Proposition 4.4.5. *Let assumption 3 be satisfied.*
Then $\mathcal{H} = \{(\boldsymbol{l}, q_n) \in \mathbb{R}_{>0}^{|\mathcal{A}_{\text{pi}}|} \times \mathbb{R} \mid h(\boldsymbol{l}, q_n) = 0\}$ with

$$h(\boldsymbol{l}, q_n) \coloneqq \sum\nolimits_{a \in \mathcal{A}_{\text{pi}}} \psi_a(l_a, q_a) = \sum\nolimits_{a \in \mathcal{A}_{\text{pi}}} \psi_a(l_a, q_n - \beta_a) \tag{4.100}$$

$$= \sum\nolimits_{a \in \mathcal{A}_{\text{pi}}} -l_a |q_a|^* = \sum\nolimits_{a \in \mathcal{A}_{\text{pi}}} -l_a |q_n - \beta_a|^* \tag{4.101}$$

for some $\beta_a \in \mathbb{R}$ for $a \in \mathcal{A}_{\text{pi}}$. The constraint $h(\boldsymbol{l}, q_n) = 0$ is the cycle flow equation.

Using h, a characterization of the set of all pressure drop coefficients $\boldsymbol{l}$, which lead to the flow q_n being bounded in some interval can be found:

Lemma 4.4.6. *Let assumption 3 be satisfied. Let $\underline{q}_n, \overline{q}_n \in \mathbb{R}$, $\boldsymbol{l} \in \mathbb{R}_{>0}^{|\mathcal{A}_{\text{pi}}|}$ and let h be as in proposition 4.4.5. Then*

$$\{\boldsymbol{l} \in \mathbb{R}_{>0}^{|\mathcal{A}_{\text{pi}}|} \mid h(\boldsymbol{l}, q_n) = 0 \text{ and } \underline{q}_n \le q_n \le \overline{q}_n\}$$
$$= \{\boldsymbol{l} \in \mathbb{R}_{>0}^{|\mathcal{A}_{\text{pi}}|} \mid h(\boldsymbol{l}, \overline{q}_n) \le 0,\ h(\boldsymbol{l}, \underline{q}_n) \ge 0\}. \tag{4.102}$$

Proof. For constant $\boldsymbol{l} \in \mathbb{R}_{>0}^{|\mathcal{A}_{\text{pi}}|}$, the function $h(\boldsymbol{l}, q_n)$ is monotonically decreasing in q_n since

$$\frac{\mathrm{d}}{\mathrm{d}q_n} h(\boldsymbol{l}, q_n) = \sum_{i=0}^{n} \frac{\mathrm{d}}{\mathrm{d}q_n} \psi_a(q_n - \beta_i) = -\sum_{i=0}^{n} l_i 2 |q_n - \beta_i| \le 0. \tag{4.103}$$

Furthermore, $\lim_{q_n \to \pm\infty} h(\boldsymbol{l}, q_n) = \mp\infty$.

Let

$$\mathcal{S}_1 \coloneqq \{\boldsymbol{l} \in \mathbb{R}_{>0}^{|\mathcal{A}_{\mathrm{pi}}|} \mid h(\boldsymbol{l}, q_n) = 0,\ \underline{q}_n \leq q_n\} \tag{4.104}$$

$$\mathcal{S}_2 \coloneqq \{\boldsymbol{l} \in \mathbb{R}_{>0}^{|\mathcal{A}_{\mathrm{pi}}|} \mid h(\boldsymbol{l}, \underline{q}_n) \geq 0\}. \tag{4.105}$$

We show $\mathcal{S}_1 = \mathcal{S}_2$ first.

Pick $\boldsymbol{l} \in \mathcal{S}_1$. By definition of $\mathcal{S}_1$, there is $\underline{q}_n \leq q_n$ with $h(\boldsymbol{l}, q_n) = 0$. Since $h(\boldsymbol{l}, \cdot)$ is monotonically decreasing, $h(\boldsymbol{l}, \underline{q}_n) \geq h(\boldsymbol{l}, q_n) = 0$. Therefore, $\boldsymbol{l} \in \mathcal{S}_2$.

Pick $\boldsymbol{l} \in \mathcal{S}_2$. Since h is continuous in q_n, and $\lim_{q_n \to \infty} h(\boldsymbol{l}, q_n) = -\infty$ together with $h(\boldsymbol{l}, \underline{q}_n) \geq 0$, the intermediate value theorem implies that there exists q_n with $h(\boldsymbol{l}, q_n) = 0$. Therefore, $\boldsymbol{l} \in \mathcal{S}_1$.

This shows $\mathcal{S}_1 = \mathcal{S}_2$. There is a similar result where the inequalities in the definitions of $\mathcal{S}_1$, $\mathcal{S}_2$ are flipped. Together, both results prove that

$$\begin{aligned}\{\boldsymbol{l} \in \mathbb{R}_{>0}^{|\mathcal{A}_{\mathrm{pi}}|} \mid h(\boldsymbol{l}, q_n) = 0 \text{ and } \underline{q}_n \leq q_n \leq \overline{q}_n\} \\ = \{\boldsymbol{l} \in \mathbb{R}_{>0}^{|\mathcal{A}_{\mathrm{pi}}|} \mid h(\boldsymbol{l}, \overline{q}_n) \leq 0,\ h(\boldsymbol{l}, \underline{q}_n) \geq 0\}.\end{aligned} \tag{4.106}$$

□

With this lemma, restricting q_n to a given interval can be expressed equivalently by restricting the considered pressure drop coefficients $\boldsymbol{l}$. Furthermore, the constraints for $\boldsymbol{l}$ are hyperplanes in $\mathbb{R}^{|\mathcal{A}_{\mathrm{pi}}|}$ as $h(\boldsymbol{l}, q_n)$ is linear in $\boldsymbol{l}$.

An exemplary application of this lemma is depicted in fig. 4.3. We consider a three-node cyclic network with nodes $\mathcal{V} = \{v_1, v_2, v_3\}$ as shown on the right side of the figure. Furthermore, let two arcs be affected by uncertain

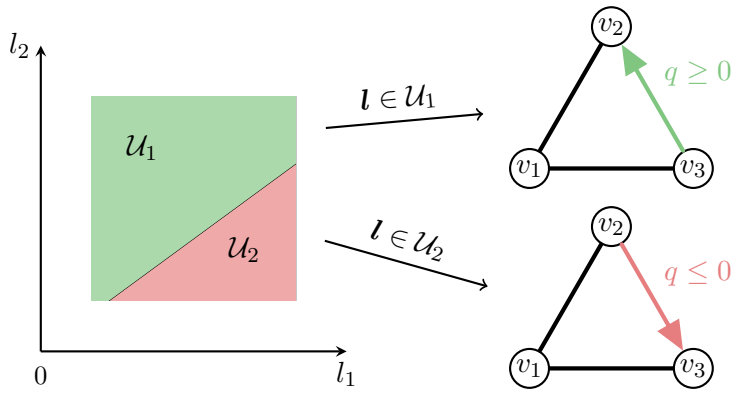

Figure 4.3: Lemma 4.4.6 characterizes flow directions on a cycle by subsets of the uncertainty region $\mathcal{U} = \mathcal{U}_1 \cup \mathcal{U}_2$.

pressure drop coefficients l_1 and l_2. These uncertain parameters arise from a rectangular uncertainty set $\mathcal{U}$ as shown on the left. Let q denote the flow along the arc from v_2 to v_3. We apply lemma 4.4.6 to the bound $q \geq 0$ and obtain a hyperplane in $\boldsymbol{l}$-space. This hyperplane partitions $\mathcal{U}$ into two polyhedra $\mathcal{U}_1$ (green) and $\mathcal{U}_2$ (red). Again by lemma 4.4.6, we know that restricting $\boldsymbol{l} \in \mathcal{U}_1$ implies that $q \geq 0$ and hence the absolute function can be eliminated from the pressure drop equation on that arc.

We adapt a procedure from Gotzes et al. (2016, prop. 5) to our setting in order to identify intervals for the flow q_n that guarantee constant flow direction on all arcs of the network. Once the possible subsets are identified, we apply lemma 4.4.6 to relate the obtained flow intervals to subsets in the space of the uncertainty.

The absolute value functions only occur in the form $l_a|q_a|^* = l_a|q_a|q_a$. From proposition 4.4.5, the flow q_a is given by

$$q_a^{\mathrm{ext}}(q_n) = q_n - \beta_a \quad \text{for all } a \in \mathcal{A}_{\mathrm{pi}}. \tag{4.107}$$

Therefore, the absolute value $|q_a^{\mathrm{ext}}(q_n)| = |q_n - \beta_a|$ can be eliminated by restricting the flow q_n to either $q_n \geq \beta_a$ or $q_n \leq \beta_a$.

Next, we reorder $\beta_1, \beta_1, \ldots, \beta_n$ such that $\beta_{i_1} \leq \beta_{i_2} \leq \cdots \leq \beta_{i_n}$. With this in mind, taking any consecutive pair $\beta_{i_j}, \beta_{i_{j+1}}$ yields an interval for q_n such that the flow over the whole network has constant direction. Due to Gotzes et al. (2016) and the non-zero demand from assumption 3, the solutions of $h(\boldsymbol{l}, q_n) = 0$ can only be within $[\beta_{i_1}, \beta_{i_n}]$ for any fixed $\boldsymbol{l}$. Therefore, the absolute values can be eliminated by restricting q_n to the intervals

$$[\beta_{i_0}, \beta_{i_1}], \qquad [\beta_{i_1}, \beta_{i_2}], \qquad \ldots \qquad [\beta_{i_{n-1}}, \beta_{i_n}]. \tag{4.108}$$

Applying lemma 4.4.6 to these intervals yields an equivalent condition for constant flow directions in the space of the uncertainty.

Proposition 4.4.7. *Let assumption 3 be satisfied, and let*

$$\mathcal{U}_j \coloneqq \mathcal{U} \cap \{\boldsymbol{l} \in \mathbb{R}_{>0}^{|\mathcal{A}_{\mathrm{pi}}|} \mid h(\boldsymbol{l}, \beta_{i_{j+1}}) \leq 0,\ h(\boldsymbol{l}, \beta_{i_j}) \geq 0\} \tag{4.109}$$

for all $j = 1, \ldots n-1$.

Then the set containment question $\mathcal{U} \subseteq \mathrm{Proj}_{\boldsymbol{l}}(\mathcal{Y}) = \mathrm{Proj}_{\boldsymbol{l}}(\mathcal{H}_{\mathcal{U}} \cap \mathcal{G})$ *can be decided by solving the subproblems*

$$\mathcal{U}_j \subseteq \mathrm{Proj}_{\boldsymbol{l}}(\mathcal{H}_{\mathcal{U}_j} \cap \mathcal{G}) \quad \textit{for all } j = 1, \ldots n-1. \tag{4.110}$$

Finally, we remark that if $\mathcal{U}$ is polyhedral then $\mathcal{U}_j$ is polyhedral as well.

4.5 Numerical experiments

In this section, some practical results of the feasibility and infeasibility approaches on a set of small gas networks under uncertainty are presented. Instead of considering arbitrary gas networks, we focus on highlighting our methods' performance on the core problem: deciding a single cycle under uncertainty. Using lemma 4.4.3, the feasibility of any subtree in a given network can be reduced if the pressure at the root node is contained in a precomputed interval. This allows us to remove any subtree by updating the pressure bounds at the intersecting node with the remaining network. Assuming there is only one remaining cycle, lemma 4.4.6 is then used to split the problem into subproblems on subsets of the uncertainty set while eliminating all absolute values. Since this just increases the number of problems to consider but does not fundamentally change their nature, we start with a single cycle and uncertainty sets that guarantee constant flow direction on all arcs.

The example networks are cyclic over graph $\mathcal{G} = (\mathcal{V}, \mathcal{A}_{\text{pi}})$ with nodes $\mathcal{V} = \{1, 2, \dots, n\}$ for $n \in \{2, 3, \dots, 7\}$ and arcs $\mathcal{A}_{\text{pi}} = \{(1,2), (2,3), \dots, (n-1, n), (n, 1)\}$. A family of uncertainty sets is considered:

$$\mathcal{U}(c) = \bigtimes_{a \in \mathcal{A}_{\text{pi}}} [1, c], \text{ where we let } c \in [2, 4]. \tag{4.111}$$

Furthermore, we define two special uncertainty sets,

$$\mathcal{U}_{\text{feas}} \coloneqq \mathcal{U}(2) \quad \text{and} \quad \mathcal{U}_{\text{infeas}} \coloneqq \mathcal{U}(4), \tag{4.112}$$

which we want to investigate regarding easibility and infeasibility, respectively.

Table 4.1 shows the parameters of the considered instances. The columns denote the nodes within the network. Each row denotes the specific instance with n nodes. Within each row, the demand and bounds of the squared pressure π_v at each node are displayed in the first and second lines, respectively. Every network's $\mathcal{G}$-set (see (4.80)) is made up of $n(n-1)$ non-trivial inequalities g_i, where $i \in \mathcal{I}$. Each inequality is checked for *feasibility* using (MinCons$_i$); all inequalities are checked at once for *infeasibility* using (PolySepProj). Both optimization tasks are solved using SDP relaxations of the problems. We remark that (PolySepProj) could be applied to all constraints individually. However, experiments show that solving the problem for a single constraint individually is only marginally faster than solving the problem for all constraints at once. Therefore, we solve the infeasibility problem once with all constraints combined rather than up to $|\mathcal{I}|$ subproblems by considering each constraint on its own.

Table 4.1: Demand and squared pressure bounds per node v for each test network.

		node $v \in V$						
		1	2	3	4	5	6	7
n=2	demand d_v	-10	10					
	bounds π_v	[0, 200]	[140, 200]					
n=3	demand d_v	-10	2	8				
	bounds π_v	[0, 200]	[0, 200]	[130, 200]				
n=4	demand d_v	-10	2	6	2			
	bounds π_v	[0, 200]	[0, 200]	[115, 200]	[0, 200]			
n=5	demand d_v	-10	1	1	6	2		
	bounds π_v	[0, 200]	[0, 200]	[0, 200]	[100, 200]	[0, 200]		
n=6	demand d_v	-10	1	1	6	1	1	
	bounds π_v	[0, 200]	[0, 200]	[0, 200]	[70, 200]	[0, 200]	[0, 200]	
n=7	demand d_v	-10	1	1	1	4	2	1
	bounds π_v	[0, 200]	[0, 200]	[0, 200]	[0, 200]	[50, 200]	[0, 200]	[0, 200]

All experiments were carried out on a machine with a quad core Intel Xeon E3-1240 v5 CPU running at $3.5\,\mathrm{GHz}$ each and $16\,\mathrm{GB}$ of RAM.The methods were implemented using MATLAB R2016b. GloptiPoly 3.8 (Henrion, Lasserre, and Löfberg 2009) was used for the feasibility models since it provides a straightforward interface for solving polynomial optimization problems. Since the infeasibility method exceeds the capabilities of GloptiPoly, this approach was implemented using the SOS-module of YALMIP R20160930 (Löfberg 2009). The resulting SDP problems were solved with MOSEK 8 (MOSEK 2011) using 4 threads.

Some problems were not solvable with the desired precision. This happened although we evaluated the problems on a variety of solvers including SeDuMi (Sturm 1999) and SDPT3 (Toh, Todd, and Tütüncü 1999) as well as on a third modeling tool, SOSTOOLS (Papachristodoulou et al. 2013). The ultimately selected combination of MOSEK with GloptiPoly and YALMIP offered the most robust behavior amongst all considered possibilities.

4.5.1 Effectiveness of the methods

The effectiveness of both methods can be measured in the typical running times of the semidefinite subproblems as well as in hierarchy level at which set containment can be decided.

First, the results of both methods on a fixed network are presented. Table 4.2 shows the outcome of both methods for the $n = 3$ instance over $\mathcal{U}_{\text{infeas}}$. The columns are separated into groups concerning the feasibility

Table 4.2: Objectives of the feasibility method solving (MinCons$_i$) and infeasibility method solving (PolySepProj) for the three node instance over $\mathcal{U}_{\text{infeas}}$. Each row in the feasibility group denotes the subproblem with objective function g_i.

	feasibility		infeasibility	
i	level 2	level 3	level 2	level 3
1	**216.89**	217.39		
2	**53.09**	-		
3	**228.63**	228.63	0.00	**unbnd**
4	−116.79	-		
5	**201.67**	-		
6	−35.99	**20.34**		

method (MinCons$_i$) and the infeasibility method (PolySepProj) with a further distinction into the employed hierarchy level. The rows in the feasibility part denote the constraint g_i which is minimized. Since the infeasibility method is applied to all constraints at once, there is only one row of results in the infeasibility part of the table. Cells marked by "-" indicate numerical difficulties, i.e., we were unable to solve the specific problem to the desired precision.
The feasibility approach has a positive objective for five out of six subproblems, thus confirming set containment for those constraints. Out of these five problems, four were decided on the second hierarchy level while one required a level 3 solution. When applying the infeasibility approach, the level 3 model is unbounded, thereby refuting set containment. Overall, the instance therefore is not robust feasible.

Next, the required levels of the relaxation hierarchy are evaluated. For this purpose, each constraint of each instance is considered for set containment while gradually increasing the hierarchy level from two to four. Once a subproblem is solved successfully, the corresponding number of solved problems on this specific level is incremented in the table.

Table 4.3 contains the feasibility methods' results for all instances on the smaller uncertainty set $\mathcal{U}_{\text{feas}}$. Each row denotes the considered instance with n nodes and a total of $|\mathcal{I}|$ subproblems. The columns indicate how many of the feasibility problems were solved successfully on the respective level. For any subproblem, only the first success is counted; thus the sum of each row can be at most $|\mathcal{I}|$. If the rowwise sum is less than $|\mathcal{I}|$, this implies that some problems were not solvable with the desired precision.

It can be observed that the feasibility approach almost exclusively confirms set containment at the second level. At most one subproblem per instance

Table 4.3: For a given instance with n nodes, count how many subproblems out of $\mathcal{I}$ were solved successfully using the feasibility method. Positive outcomes of each subproblem are counted only once on the smallest level. All instances were solved over the $\mathcal{U}_{\text{feas}}$ uncertainty set.

n	$\lvert\mathcal{I}\rvert$	level 2	level 3	level 4
2	2	1	1	0
3	6	5	1	0
4	12	11	1	0
5	20	19	1	0
6	30	29	1	0
7	42	42	0	0

required solving of a level 3 problem. As suspected, all instances are robust feasibly with this uncertainty region.

Using the larger uncertainty set $\mathcal{U}_{\text{infeas}}$, both the feasibility and the infeasibility method were applied to all instances. Table 4.4 summarizes all results. Each row denotes the considered instance with n nodes. The columns are separated into groups according to the employed method with further distinction for the used hierarchy level. Each column in the feasibility group indicates how many of the feasibility problems were solved successfully. For any subproblem, only the first success is counted; therefore the sum of each row in the feasibility group can be at most $|\mathcal{I}|$. The columns in the infeasibility group denote the status of the corresponding problem. Cells marked with "zero obj." indicate global optimality of the considered problem but an objective value of

Table 4.4: For a given instance with n nodes, the left group of column counts how many subproblems of $\mathcal{I}$ were solved successfully using the feasibility method. For each subproblem, a positive outcome is counted only once on the smallest level. The results of the infeasibility method are displayed in the right column group. All instances were solved over the $\mathcal{U}_{\text{infeas}}$ uncertainty set.

		feasibility			infeasibility		
n	$\lvert I\rvert$	level 2	level 3	level 4	level 2	level 3	level 4
2	2	1	0	0	zero obj.	✓	✓
3	6	4	1	0	zero obj.	✓	✓
4	12	9	1	0	zero obj.	✓	✓
5	20	16	1	0	zero obj.	✓	✓
6	30	25	1	0	zero obj.	✓	✓
7	42	36	2	0	zero obj.	-	-

zero, which is insufficient to show certify infeasibility. Cells marked with a checkmark (✓) represent an unbounded objective and thus a negative answer to the set containment question. As usual, "-" marks numerical difficulties.

Many feasibility problems were solved successfully at the second hierarchy level. Set containment of some constraints could not be confirmed with the feasibility method using the given levels. This is due either to numerical problems or to negative objective values. However, for almost all instances, the infeasibility method was able to provide a certificate against set containment using the third hierarchy level relaxation. This shows that $\mathcal{U}_{\text{infeas}}$ is robust infeasible for the $n = 2, \ldots, 6$ instances.

To conclude this set of test runs, tables 4.5 and 4.6 show the characteristic running times where each row denotes the n-node instance. For the feasibility approach, the columns show mean running time and standard deviation using the specific relaxation hierarchy level. All values are aggregated over all subproblems of the given instance and hierarchy level. Since the infeasibility approach is a single problem when instance and hierarchy level are fixed, no aggregation is possible and we show the running time as-is. It can be observed that the running times are quite small for the level 2 problems but increase quickly for higher levels and larger instances.

Table 4.5: Mean value and standard deviation of the feasibility method's running time on $\mathcal{U}_{\text{feas}}$. Each row shows the aggregated values for all subproblems of the n-node instance per hierarchy level.

	level 2		level 3		level 4	
n	mean	std	mean	std	mean	std
2	0.054 s	0.043 s	0.030 s	0.000 s	0.079 s	0.009 s
3	0.027 s	0.006 s	0.075 s	0.008 s	0.460 s	0.057 s
4	0.034 s	0.008 s	0.238 s	0.014 s	2.969 s	0.115 s
5	0.055 s	0.015 s	0.893 s	0.143 s	18.600 s	2.064 s
6	0.099 s	0.024 s	3.159 s	0.399 s	97.197 s	5.473 s
7	0.178 s	0.044 s	10.750 s	1.257 s	480.710 s	40.487 s

4.5.2 Evaluation of the gap between methods

The proposed methods are based on semidefinite relaxations of polynomial problems; see section 4.2. Since the objective values of relaxed problems are smaller than or equal to the non-relaxed optimal values (for minimization problems), it is expected that the feasibility and infeasibility approaches can

Table 4.6: Running time of the infeasibility method on $\mathcal{U}_{\text{infeas}}$ where each row denotes the n-node instance and each column the respective level.

n	level 2	level 3	level 4
2	0.031 s	0.028 s	0.057 s
3	0.013 s	0.073 s	0.373 s
4	0.019 s	0.264 s	2.723 s
5	0.035 s	1.102 s	14.602 s
6	0.067 s	3.634 s	97.197 s
7	0.117 s	7.769 s	576.219 s

decide a smaller number of problems than their non-relaxed counterparts. The aim of this section is to investigate how large the "gap" between the feasibility and infeasibility approaches is. After fixing a hierarchy level, all problems which cannot be decided by either the feasibility or the infeasibility approach are said to fall into this relaxation gap. In order to compare both methods, we need to apply the infeasibility approach to the same constraint as the feasibility method. This is different from all previous tests where the infeasibility method was solved for all constraints at once.

Consider the parameterized uncertainty set $\mathcal{U}(c)$ for increasing $c \in [2, 4]$. From table 4.3, it can be derived that all subproblems are feasible for $\mathcal{U}_{\text{feas}} = \mathcal{U}(2)$. On the other hand, as table 4.4 shows, all instances are infeasible for the larger $\mathcal{U}_{\text{infeas}} = \mathcal{U}(4)$. This implies that there is always at least one violated constraint g_i when using $\mathcal{U}(4)$.

For this test set, we select one subproblem per instance that is infeasible for the larger uncertainty set. Then, the feasibility and infeasibility approaches are solved for the selected subproblems over all twenty uncertainty sets $\mathcal{U}(c)$ for $c = 2 + i\frac{1}{10}$, $i = 0, \ldots, 20$. Section 4.5.2 shows the results in more detail for the four-node instance. We consider the subproblem that is marked as infeasible in table 4.4. The objective values of the feasibility problem (MinCons_i) are marked with blue (level 2) and orange (level 3) triangles in the figure. Additionally, the values of solving (PolySepProj) are marked using green (level 3) and red (level 4) circles. We remark that the outcome of the infeasibility method for level 2 is omitted since as all subproblems were feasible but had objective value of zero. Unbounded subproblems of the infeasibility method are marked with an objective value of fifteen times their level. Missing data points can be attributed to numerical difficulties of the SDP solver.

As can be observed, no instance can be decided on the second hierarchy level since all solutions of the feasibility method have negative objective values

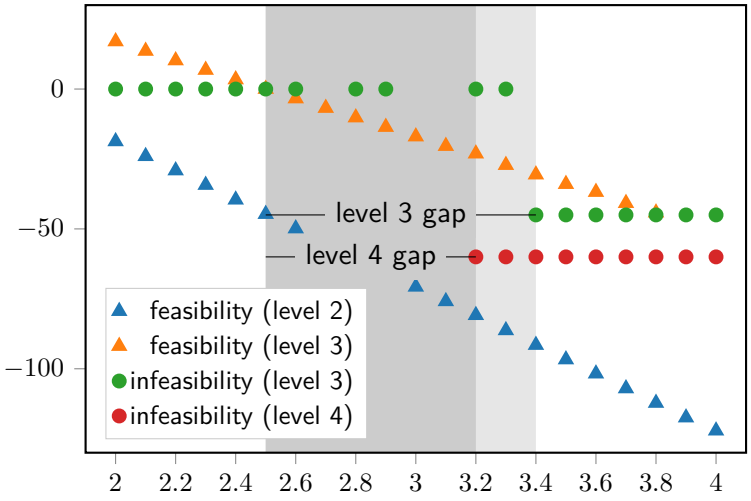

Figure 4.4: Objective values of the feasibility and infeasibility method for uncertainty sets $\mathcal{U}(c)$ with $c \in \{2.0, 2.1, \ldots, 4\}$ on the four-node instance.

and all solutions of the infeasibility method have objective value zero (not shown in the figure). On the third hierarchy level, the feasibility approach confirms set containment for $c \in \{2.0, 2.1, \ldots, 2.5\}$ as these problems have positive objective value. With the same level, the infeasibility approach finds certificates against set containment for $c \in \{3.4, \ldots, 4.0\}$. For the problems with $c \in \{2.6, \ldots, 3.3\}$, neither of the methods was able to decide set containment successfully (disregarding numerical difficulties). In this range, the feasibility method only returns negative objective values and all objective values of the infeasibility method were zero.

Increasing the hierarchy level to four leads to numerical problems for all feasibility models, but also increases the number of successfully solved infeasibility models by two ($c = 3.2$ and $c = 3.3$). This confirms the expectation that increasing the hierarchy level can lead to more certificates for non–set containment.

The results over all instances is summarized in table 4.7. For each hierarchy level, it shows both the largest value for c (indicated by c_{feas}) such that the feasibility approach confirms set containment and the smallest value for c (indicated by c_{infeas}) where a certificate for infeasibility could be obtained. Note that these bounds on c take all smaller hierarchy levels into account as well. The gap column is the difference $c_{\text{infeas}} - c_{\text{feas}}$ and indicates the range of problems which could not be solved successfully with either the feasibility or the infeasibility approach. Again it can be observed that the gap is reduced

Table 4.7: Extreme values for c where the feasibility (c_{feas}) and infeasibility (c_{infeas}) methods can solve the problem. "Gap" represents the length of the experimentally determined interval where neither feasibility nor infeasibility could be decided.

	level 3			level 4		
n	c_{feas}	c_{infeas}	gap	c_{feas}	c_{infeas}	gap
2	2.4	3.3	0.9	2.4	2.9	0.5
3	2.4	3.2	0.8	2.4	3.1	0.7
4	2.5	3.4	0.9	2.5	3.2	0.7
5	2.4	3.4	1.0	2.4	3.3	0.9
6	2.6	3.7	1.1	3.1	3.6	0.5
7	3.0			3.3		

after increasing the hierarchy level as this leads to a tighter relaxation for the feasibility approach and admits a richer set of polynomials for the infeasibility certificate.

5 A reformulation approach for two-stage robust optimization with a non-empty first stage

We show how a general two-stage robust optimization problem can be transformed into a regular single-stage problem under certain assumptions. The necessary structural properties consist of uniquely determined second-stage variables and a weak connection between first-stage and second-stage variables. By exploiting these properties, the original problem is transformed into a normal, non-robust optimization problem whose right-hand side can be precalculated by solving a series of optimization problems to global optimality. Based on this formulation it is shown how multiple elements of the right-hand side can be combined into a single optimization task. We also show that solving the subproblems to global optimality is not necessary. Using relaxations of the original description allows us to apply the presented methods to problems where obtaining globally optimal solutions can be a significant challenge. This is the case, e.g., for many non-convex problems.

The developed method is then applied to a gas transport problem under uncertainty with linear pressure-modifying elements. Since the subproblems to be solved are non-convex, we use a well-known technique to construct piecewise linear relaxations of the problems. These can then be formulated as MILPs and solved to global optimality. Since our approach requires the solution of a potentially large number of subproblems, it is crucial for the overall running time that the problem size is reduced as much as possible. To this end, we describe a variety of preprocessing techniques taken from literature and adapt them to problems with uncertain parameters. The practical feasibility and effectivity of our approach is demonstrated by benchmarks on several gas network instances, including a realistic model of the Greek natural gas network. Overall, aggregation and preprocessing allow us to solve large gas network instances under uncertainty quickly and effectively at the price of more conservative solutions.

The author of this thesis conceived all ideas within this chapter. The further development and implementation of these ideas was primarily carried out by the author of this work under the supervision of Prof. Liers and Prof. Stingl. The main results of this chapter have been published in

> D. Aßmann, F. Liers, and M. Stingl. 2019. "Decomposable robust two-stage optimization: An application to gas network operations under uncertainty". *Networks* 74 (1): 40–61. doi:10.1002/net.21871.

In the following, we repeat and extend these results as well as their presentation.

This chapter is structured as follows. The problem is studied in an abstract setting in section 5.1. In this section, the transformation to single-stage problem and the aggregation idea are developed. An application to gas network operations follows in section 5.2. Besides discussing the piecewise-linear relaxation idea, we also present preprocessing methods that can be used to obtain smaller model formulations. Section 5.3 concludes this chapter with a series of benchmarks. We show how preprocessing can reduce computation time by an order of magnitude and discuss the effects of the relaxation. Finally, using the example of the Greek natural gas network, we demonstrate how a combination of all the presented ideas leads to a very effective solution approach.

5.1 A decomposable two-stage robust optimization problem

We study a general adjustable robust problem (ARC) as introduced in section 3.2:

$$\min_{\boldsymbol{x}} \left\{ \boldsymbol{f}(\boldsymbol{x}) \mid \exists \boldsymbol{x} \;\; \forall \boldsymbol{u} \in \mathcal{U} \;\; \exists \boldsymbol{y} \text{ with } \boldsymbol{h}(\boldsymbol{u}, \boldsymbol{x}, \boldsymbol{y}) = \boldsymbol{0},\ \boldsymbol{g}(\boldsymbol{u}, \boldsymbol{x}, \boldsymbol{y}) \leq \boldsymbol{0} \right\}. \quad \text{(ARC)}$$

We briefly recall the definitions.. Let $\mathcal{U} \subseteq \mathbb{R}^{n_u}$ with $n_u \in \mathbb{N}$ be the convex and compact uncertainty set; let $\boldsymbol{x} \in \mathbb{R}^{n_x}$ and $\boldsymbol{y} \in \mathbb{R}^{n_y}$ with $n_x, n_y \in \mathbb{N}$ be the first- and second-stage variables; and let $\boldsymbol{h} \colon \mathbb{R}^{n_u} \times \mathbb{R}^{n_y} \to \mathbb{R}^{m_h}$ and $\boldsymbol{g} \colon \mathbb{R}^{n_u} \times \mathbb{R}^{n_y} \to \mathbb{R}^{m_g}$ with $m_h, m_g \in \mathbb{N}$ be the vector-valued constraint functions.

The necessary conditions for our approach are summarized as:

Assumption 4. *(a) The equation system*

$$\boldsymbol{h}(\boldsymbol{u}, \boldsymbol{x}, \boldsymbol{y}) = \boldsymbol{0} \tag{5.1}$$

does not depend on $\boldsymbol{x}$ and admits a unique solution $\boldsymbol{y}^*(\boldsymbol{u})$ for all $\boldsymbol{u} \in \mathcal{U}$.

(b) The function $\boldsymbol{g}$ is separable, i.e., there exist functions $\boldsymbol{\sigma} \colon \mathbb{R}^{n_x} \to \mathbb{R}^{m_g}$ and $\boldsymbol{\tau} \colon \mathbb{R}^{n_u} \times \mathbb{R}^{n_y} \to \mathbb{R}^{m_g}$ such that

$$\boldsymbol{g}(\boldsymbol{u}, \boldsymbol{x}, \boldsymbol{y}) = \boldsymbol{\sigma}(\boldsymbol{x}) + \boldsymbol{\tau}(\boldsymbol{u}, \boldsymbol{y}) \tag{5.2}$$

for all $(\boldsymbol{u}, \boldsymbol{x}, \boldsymbol{y}) \in \mathbb{R}^{n_u} \times \mathbb{R}^{n_x} \times \mathbb{R}^{n_y}$.

5.1.1 Transformation to single-stage problem

The next lemma shows how the abstract two-stage problem (ARC) can be transformed into to a single-stage problem given assumption 4.

Lemma 5.1.1. *Under assumption 4, the set of feasible first-stage decisions $\boldsymbol{x}$ of the adjustable robust counterpart* (ARC) *is given by*

$$\mathcal{X} = \{\boldsymbol{x} \in \mathbb{R}^{n_x} \mid \boldsymbol{\sigma}(\boldsymbol{x}) \leq \boldsymbol{\beta}\}, \tag{5.3}$$

where $\boldsymbol{\beta} = (\beta_i)_{i=1,\dots,m_g} \in \mathbb{R}^{m_g}$ with

$$\begin{aligned} \beta_i \;\coloneqq\; & -\max_{\boldsymbol{u},\boldsymbol{y}} \; \tau_i(\boldsymbol{u},\boldsymbol{y}) && \text{(5.4a)}\\ & \text{s.t. } \boldsymbol{h}(\boldsymbol{u},\boldsymbol{y}) = \boldsymbol{0}, && \text{(5.4b)}\\ & \quad \boldsymbol{u} \in \mathcal{U}, && \text{(5.4c)}\\ & \quad \boldsymbol{y} \in \mathbb{R}^{n_y}. && \text{(5.4d)} \end{aligned}$$

Proof. Due to assumption 4, the equality constraints of (ARC) only depend on $\boldsymbol{u}$ and $\boldsymbol{y}$, i.e., $\boldsymbol{h}(\boldsymbol{u},\boldsymbol{x},\boldsymbol{y}) \equiv \boldsymbol{h}(\boldsymbol{u},\boldsymbol{y})$. Furthermore the inequality constraints are separable: $\boldsymbol{g}(\boldsymbol{u},\boldsymbol{x},\boldsymbol{y}) = \boldsymbol{\sigma}(\boldsymbol{x}) + \boldsymbol{\tau}(\boldsymbol{u},\boldsymbol{y})$. Therefore, the set of feasible first-stage decisions $\boldsymbol{x}$ of (ARC) can be written as

$$\{\boldsymbol{x} \in \mathbb{R}^{n_x} \mid \forall \boldsymbol{u} \in \mathcal{U} \;\; \exists \boldsymbol{y} \text{ with } \boldsymbol{h}(\boldsymbol{u},\boldsymbol{y}) = \boldsymbol{0},\, \boldsymbol{\sigma}(\boldsymbol{x}) + \boldsymbol{\tau}(\boldsymbol{u},\boldsymbol{y}) \leq \boldsymbol{0}\}. \tag{5.5}$$

From assumption 4 it follows that there is a function $\boldsymbol{y}^*(\boldsymbol{u})$ that maps values $\boldsymbol{u}$ of the uncertainty set $\mathcal{U}$ to solutions of $\boldsymbol{h}(\boldsymbol{u},\boldsymbol{y}) = 0$. This function exists and is well-defined since solutions of the equality system exist for all $\boldsymbol{u} \in \mathcal{U}$ and are unique. Consequently, the condition $\forall \boldsymbol{u} \in \mathcal{U}\; \exists \boldsymbol{y} \in \mathbb{R}^{n_y}$ with $\boldsymbol{h}(\boldsymbol{u},\boldsymbol{y}) = \boldsymbol{0}$ in (5.5) is encoded by the function $\boldsymbol{y}^*(\boldsymbol{u})$ on $\mathcal{U}$. By plugging $\boldsymbol{y}^*(\boldsymbol{u})$ into the remaining inequality system, we obtain the feasible region of a single-stage robust optimization problem of form (RC) as introduced in section 3.2:

$$\{\boldsymbol{x} \in \mathbb{R}^{n_x} \mid \boldsymbol{\sigma}(\boldsymbol{x}) + \boldsymbol{\tau}(\boldsymbol{u},\boldsymbol{y}^*(\boldsymbol{u})) \leq \boldsymbol{0} \quad \forall \boldsymbol{u} \in \mathcal{U}\}. \tag{5.6}$$

This semi-infinite problem can be reformulated by maximizing the left-hand side of the inequality:

$$\begin{aligned} & \boldsymbol{\sigma}(\boldsymbol{x}) + \boldsymbol{\tau}(\boldsymbol{u},\boldsymbol{y}^*(\boldsymbol{u})) \leq \boldsymbol{0} && \text{for all } \boldsymbol{u} \in \mathcal{U}, && \text{(5.7)}\\ \iff \quad & \max_{\boldsymbol{u}\in\mathcal{U}} \Big\{\sigma_i(\boldsymbol{x}) + \tau_i(\boldsymbol{u},\boldsymbol{y}^*(\boldsymbol{u}))\Big\} \leq 0 && \text{for all } i = 1,\dots,m_g, && \text{(5.8)}\\ \iff \quad & \sigma_i(\boldsymbol{x}) + \max_{\boldsymbol{u}\in\mathcal{U}} \Big\{\tau_i(\boldsymbol{u},\boldsymbol{y}^*(\boldsymbol{u}))\Big\} \leq 0 && \text{for all } i = 1,\dots,m_g. && \text{(5.9)} \end{aligned}$$

After rewriting the solution function $\boldsymbol{y}^*$ in terms of $\boldsymbol{h}$ and letting

$$\beta_i \coloneqq -\max_{\boldsymbol{u}\in\mathcal{U}} \left\{\tau_i(\boldsymbol{u},\boldsymbol{y}) \middle| \boldsymbol{h}(\boldsymbol{u},\boldsymbol{y}) = \boldsymbol{0},\ \boldsymbol{y}\in\mathbb{R}^{n_y}\right\} \quad \text{for all } i = 1,\dots,m_g, \tag{5.10}$$

we obtain

$$\sigma_i(\boldsymbol{x}) + \max_{\boldsymbol{u}\in\mathcal{U}} \Big\{\tau_i(\boldsymbol{u},\boldsymbol{y}^*(\boldsymbol{u}))\Big\} = \sigma_i(\boldsymbol{x}) - \beta_i \le 0 \tag{5.11}$$

and thus set of feasible first-stage decisions $\boldsymbol{x}$ of (ARC) is equivalent to

$$\{\boldsymbol{x}\in\mathbb{R}^{n_x} \mid \boldsymbol{\sigma}(\boldsymbol{x}) \le \boldsymbol{\beta}\}. \tag{5.12}$$

□

5.1.2 Improvements by relaxation and aggregation

We want to highlight two properties of (5.3) which may be beneficial for solving such problems in practice.

Calculating β_i involves solving an optimization task to global optimality. In situations where this is not possible or where it can only be done with great effort, e.g., due to non-convex constraints, relaxations of the problem can be used instead. We propose to use convex or MILP relaxations as they lead to optimization tasks which can be solved to global optimality using available software. We consider the definition of β_i:

$$\beta_i = \underbrace{-\max_{\boldsymbol{u}\in\mathcal{U}} \left\{\tau_i(\boldsymbol{u},\boldsymbol{y}) \mid \boldsymbol{h}(\boldsymbol{u},\boldsymbol{y}) = \boldsymbol{0},\ \boldsymbol{y}\in\mathbb{R}^{n_y}\right\}}_{(\star)}. \tag{5.13}$$

Replacing $(\star)$ by a relaxed optimization problem leads to an optimal value $\beta_i' \le \beta_i$. Plugging $\boldsymbol{\beta}'$ into (5.12) yields a smaller feasible region for the first-stage decision variables $\boldsymbol{x}$:

$$\{\boldsymbol{x}\in\mathbb{R}^{n_x} \mid \boldsymbol{\sigma}(\boldsymbol{x}) \le \boldsymbol{\beta}'\} \subseteq \{\boldsymbol{x}\in\mathbb{R}^{n_x} \mid \boldsymbol{\sigma}(\boldsymbol{x}) \le \boldsymbol{\beta}\}. \tag{5.14}$$

Since the feasible region of the relaxed problem's first-stage variables is a subset of the original feasible region, solutions obtained in this fashion are still robust feasible. Depending on the quality of used relaxations, solutions obtained in this way can be more conservative, i.e., have a worse objective function value. On the other hand, using relaxations of non-convex problems typically allows us to solve much larger instances compared to using the original problem formulation.

The second observation shows how multiple optimization problems (5.10) for the calculation of the right-hand side β_i can be aggregated into one optimization task. Suppose there are two inequality constraints $g_i(\boldsymbol{u}, \boldsymbol{x}, \boldsymbol{y}) = \sigma_i(\boldsymbol{x}) + \tau_i(\boldsymbol{u}, \boldsymbol{y}) \leq 0$ for $i = 1, 2$ which are reformulated as $\sigma_1(\boldsymbol{x}) \leq \beta_1$ and $\sigma_2(\boldsymbol{x}) \leq \beta_2$ due to lemma 5.1.1. If the functions σ_1 and σ_2 are identical, both constraints can be aggregated into one constraint by setting

$$\sigma_1(\boldsymbol{x}) = \sigma_2(\boldsymbol{x}) \leq \min\{\beta_1, \beta_2\}. \tag{5.15}$$

In order to implement reduction (5.15), one can solve a single optimization problem rather than two separate ones:

$$\begin{aligned}
\min\{\beta_1, \beta_2\} &\overset{(5.10)}{=} \min_{i=1,2}\Big\{-\max_{\boldsymbol{u}\in\mathcal{U}}\{\tau_i(\boldsymbol{u}, \boldsymbol{y}) \mid \boldsymbol{h}(\boldsymbol{u}, \boldsymbol{y}) = \boldsymbol{0},\ \boldsymbol{y} \in \mathbb{R}^{n_y}\}\Big\} && (5.16)\\
&= \min_{i=1,2}\Big\{\min_{\boldsymbol{u}\in\mathcal{U}}\{-\tau_i(\boldsymbol{u}, \boldsymbol{y}) \mid \boldsymbol{h}(\boldsymbol{u}, \boldsymbol{y}) = \boldsymbol{0},\ \boldsymbol{y} \in \mathbb{R}^{n_y}\}\Big\} && (5.17)\\
&= \min_{\boldsymbol{u}\in\mathcal{U}}\Big\{\min_{i=1,2}\{-\tau_i(\boldsymbol{u}, \boldsymbol{y}) \mid \boldsymbol{h}(\boldsymbol{u}, \boldsymbol{y}) = \boldsymbol{0},\ \boldsymbol{y} \in \mathbb{R}^{n_y}\}\Big\}. && (5.18)
\end{aligned}$$

Compared to (5.10), the aggregated optimization problem (5.18) has the same feasible set but a different objective function. For MILPs, this minimum-of-functions objective structure can be modeled with binary variables.

This can be generalized to any finite number of constraints $g_1, \ldots, g_{m_g}$. We want to emphasize that this situation may not be that uncommon in practice. For example, all bounds of second-stage variables $\sigma_i(\boldsymbol{x}) + \tau_i(\boldsymbol{u}, \boldsymbol{y}) \overset{!}{=} y_i \leq \overline{y_i}$ are independent of $\boldsymbol{x}$ and can therefore be reduced to one constraint of the form $\sigma_k(\boldsymbol{x}) = 0 \leq c$ for some $c \in \mathbb{R}$.

5.2 An application to gas network operations

By exploiting structural properties of the gas network problem, we show how the two-stage problem (3.5) can be transformed to a single-stage problem. In particular, we exploit separability of the constraints (see (5.2)) and the weak connection between first-stage and second-stage variables.

Problems with a similar structure include, e.g., direct current electricity networks, water networks, and other potential driven networks. We refer to, e.g., Gross et al. (2018) and the references therein for further details.

5.2.1 The two-stage robust gas transport setting

We consider the two-stage gas transport problem (3.5) for a network with active elements under uncertainty as defined in section 3.3. The problem is

affected both by uncertain demand as in (3.3) and by uncertain pressure drop coefficients as in (3.4). Thus, the uncertainty set is given by

$$\mathcal{U} = \mathcal{L} \times \mathcal{D} \subseteq \mathbb{R}^{|\mathcal{V}|} \times \mathbb{R}^{|\mathcal{A}|}. \tag{5.19}$$

Furthermore, let assumption 1 be satisfied, i.e., no compressor is part of a cycle.

For a clearer exposition, we briefly restate the reduced problem formulation (3.6) of the adjustable robust gas transport problem with active elements:

$$\begin{aligned}
\min_{\boldsymbol{x}^{\mathrm{pm}}} \quad & \boldsymbol{c}^{\top}\boldsymbol{x}^{\mathrm{pm}} && \text{(5.20a)}\\
\text{s.t.} \quad & \boldsymbol{x}^{\mathrm{pm}} \in [\underline{\boldsymbol{x}}^{\mathrm{pm}}, \overline{\boldsymbol{x}}^{\mathrm{pm}}], && \text{(5.20b)}\\
& \quad \text{s.t. for all } (\boldsymbol{l}, \boldsymbol{d}) \in \mathcal{U} \text{ there is } \boldsymbol{q}_{\mathcal{N}} \in \mathbb{R}^{|\mathcal{N}|} \text{ with} \\
& \qquad \boldsymbol{C}\boldsymbol{\psi}(\boldsymbol{l}, \boldsymbol{q}^{\mathrm{ext}}(\boldsymbol{d}, \boldsymbol{q}_{\mathcal{N}}), \boldsymbol{x}^{\mathrm{pm}}) = \boldsymbol{0}, && \text{(5.20c)}\\
& \qquad \boldsymbol{P}\boldsymbol{\psi}_{\mathcal{B}}(\boldsymbol{l}_{\mathcal{B}}, \boldsymbol{q}^{\mathrm{ext}}_{\mathcal{B}}(\boldsymbol{d}, \boldsymbol{q}_{\mathcal{N}}), \boldsymbol{x}^{\mathrm{pm}}_{\mathcal{B}}) \leq \Delta\boldsymbol{\pi}. && \text{(5.20d)}
\end{aligned}$$

Decomposing the uncertain gas transport problem

In order to apply lemma 5.1.1 to problem (5.20) and reformulate it as a single-stage problem, we first have to show that assumption 4 is satisfied.

Theorem 5.2.1. *Suppose that assumption 1 holds. Then the constraints of the two-stage gas network problem* (5.20) *satisfy assumption 4.*

Proof. We consider equation system (5.20c):

$$\boldsymbol{C}\boldsymbol{\psi}(\boldsymbol{l}, \boldsymbol{q}^{\mathrm{ext}}(\boldsymbol{d}, \boldsymbol{q}_{\mathcal{N}}), \boldsymbol{x}^{\mathrm{pm}}) = \boldsymbol{0}. \tag{5.21}$$

From the definition of the cycle matrix (2.51), we know that each row of $\boldsymbol{C}$ is the incidence vector of a fundamental cycle in $\mathcal{G}$. Due to assumption 1, no compressor is part of a cycle and thus the system is independent of the first-stage variables $\boldsymbol{x}^{\mathrm{pm}}$.

Moreover, uniqueness and existence of a solution $\boldsymbol{q}^{*}_{\mathcal{N}}$ holds due to theorem 2.4.5. In total, the equality constraint system (5.20c) satisfies the first part of assumption 4.

With the assumption's second part in mind, we take a closer look at inequality system (5.20d):

$$\boldsymbol{P}\boldsymbol{\psi}_{\mathcal{B}}(\boldsymbol{l}_{\mathcal{B}}, \boldsymbol{q}^{\mathrm{ext}}_{\mathcal{B}}(\boldsymbol{d}, \boldsymbol{q}_{\mathcal{N}}), \boldsymbol{x}^{\mathrm{pm}}_{\mathcal{B}}) \leq \Delta\boldsymbol{\pi}. \tag{5.22}$$

We recall that each row of the path matrix $\boldsymbol{P}$ is the incidence vector of a path in the $\mathcal{B}$-induced spanning tree and each column corresponds to an arc $a \in \mathcal{A}$. Let $\mathcal{B}_{\mathrm{pi}} \coloneqq \mathcal{B} \cap \mathcal{A}_{\mathrm{pi}}$ and $\mathcal{B}_{\mathrm{pm}} \coloneqq \mathcal{B} \cap \mathcal{A}_{\mathrm{pm}}$, i.e., the set of pipes in $\mathcal{B}$ and the set pressure-modifying elements in $\mathcal{B}$. With this we split the path matrix

$$\boldsymbol{P} = \left[\boldsymbol{P}_{\mathcal{B}_{\mathrm{pi}}} \mid \boldsymbol{P}_{\mathcal{B}_{\mathrm{pm}}}\right] \tag{5.23}$$

into one part $\boldsymbol{P}_{\mathcal{B}_{\mathrm{pi}}}$ that corresponds to pipes and one part $\boldsymbol{P}_{\mathcal{B}_{\mathrm{pm}}}$ that corresponds to compressors. We observe that every entry of $\boldsymbol{\psi}_{\mathcal{B}}$ corresponds to either a pipe and depends on $\boldsymbol{q}_{\mathcal{N}}$ or a compressor and depends on $\boldsymbol{x}^{\mathrm{pm}}$. Partitioning $\boldsymbol{\psi}$ similarly as $\boldsymbol{P}$, we write (5.22) as

$$\begin{aligned} &\boldsymbol{P}\boldsymbol{\psi}_{\mathcal{B}}(\boldsymbol{l}_{\mathcal{B}}, \boldsymbol{q}^{\mathrm{ext}}_{\mathcal{B}}(\boldsymbol{d}_{\mathcal{B}}, \boldsymbol{q}_{\mathcal{N}}), \boldsymbol{x}^{\mathrm{pm}}_{\mathcal{B}}) && (5.24)\\ &\quad = \boldsymbol{P}_{\mathcal{B}_{\mathrm{pi}}}\boldsymbol{\psi}_{\mathcal{B}_{\mathrm{pi}}}(\boldsymbol{l}_{\mathcal{B}_{\mathrm{pi}}}, \boldsymbol{q}^{\mathrm{ext}}_{\mathcal{B}_{\mathrm{pi}}}(\boldsymbol{d}, \boldsymbol{q}_{\mathcal{N}})) + \boldsymbol{P}_{\mathcal{B}_{\mathrm{pm}}}\boldsymbol{\psi}_{\mathcal{B}_{\mathrm{pm}}}(\boldsymbol{x}^{\mathrm{pm}}_{\mathcal{B}_{\mathrm{pm}}}) \leq \Delta\boldsymbol{\pi}. && (5.25)\end{aligned}$$

From this, we let

$$\boldsymbol{s}(\boldsymbol{x}^{\mathrm{pm}}) \coloneqq \boldsymbol{P}_{\mathcal{B}_{\mathrm{pm}}}\boldsymbol{\psi}_{\mathcal{B}_{\mathrm{pm}}}(\boldsymbol{x}^{\mathrm{pm}}_{\mathcal{B}_{\mathrm{pm}}}) \tag{5.26}$$

and

$$\boldsymbol{t}(\boldsymbol{l}_{\mathcal{B}_{\mathrm{pi}}}, \boldsymbol{d}, \boldsymbol{q}_{\mathcal{N}}) \coloneqq \boldsymbol{P}_{\mathcal{B}_{\mathrm{pi}}}\boldsymbol{\psi}_{\mathcal{B}_{\mathrm{pi}}}(\boldsymbol{l}_{\mathcal{B}_{\mathrm{pi}}}, \boldsymbol{q}^{\mathrm{ext}}_{\mathcal{B}_{\mathrm{pi}}}(\boldsymbol{d}, \boldsymbol{q}_{\mathcal{N}})) - \Delta\boldsymbol{\pi}. \tag{5.27}$$

Altogether, this allows us to write the inequality system (5.22) as

$$\boldsymbol{s}(\boldsymbol{x}^{\mathrm{pm}}) + \boldsymbol{t}(\boldsymbol{l}_{\mathcal{B}_{\mathrm{pi}}}, \boldsymbol{d}, \boldsymbol{q}_{\mathcal{N}}) \leq \boldsymbol{0} \tag{5.28}$$

and therefore the second part of the assumption is also satisfied. □

We note that the vector-valued functions $\boldsymbol{s} = (s_{vw})_{v,w\in\mathcal{V}}$ and $\boldsymbol{t} = (t_{vw})_{v,w\in\mathcal{V}}$ are indexed like the rows of the path matrix $\boldsymbol{P}$, i.e., by pairs of nodes.

After applying lemma 5.1.1 to the two-stage robust gas transport problem (5.20), we obtain the single-stage problem

$$\begin{aligned} \min_{\boldsymbol{x}^{\mathrm{pm}}} \quad & \boldsymbol{c}^{\top}\boldsymbol{x}^{\mathrm{pm}} && (5.29a)\\ \text{s.t.} \quad & \boldsymbol{s}(\boldsymbol{x}^{\mathrm{pm}}) \leq \boldsymbol{b}, && (5.29b)\\ & \boldsymbol{x}^{\mathrm{pm}} \in [\underline{\boldsymbol{x}}^{\mathrm{pm}}, \overline{\boldsymbol{x}}^{\mathrm{pm}}], && (5.29c)\end{aligned}$$

where the entries of $\boldsymbol{b} = (b_{vw})_{vw}$ are precomputed by

$$\begin{aligned} b_{vw} \coloneqq \; - \max_{\boldsymbol{l},\boldsymbol{d},\boldsymbol{q}_{\mathcal{N}}} \quad & t_{vw}(\boldsymbol{l}_{\mathcal{B}_{\mathrm{pi}}}, \boldsymbol{d}, \boldsymbol{q}_{\mathcal{N}}) && (5.30a)\\ \text{s.t.} \quad & \boldsymbol{C}\boldsymbol{\psi}(\boldsymbol{l}, \boldsymbol{q}^{\mathrm{ext}}(\boldsymbol{d}, \boldsymbol{q}_{\mathcal{N}})) = \boldsymbol{0}, && (5.30b)\\ & (\boldsymbol{l}, \boldsymbol{d}) \in \mathcal{U}, && (5.30c)\\ & \boldsymbol{q}_{\mathcal{N}} \in \mathbb{R}^{|\mathcal{N}|}, && (5.30d)\end{aligned}$$

for $v, w \in \mathcal{V}$. Assuming (5.30) is precomputed, (5.29) reduces to an LP. As (5.30) is a non-convex optimization task, we next explain how relaxations can be computed effectively in this context.

5.2.2 Using piecewise-linear relaxations for computing b_{vw}

In order to solve the robust gas network problem via the LP (5.29), one first needs to compute b_{vw} by solving a series of nonlinear and non-convex optimization problems to global optimality. Since this is a difficult task in general, we first replace all nonlinear terms by piecewise-linear relaxations and use this surrogate model to compute the right-hand side $\boldsymbol{b}$. As is discussed in section 5.1.2, using relaxations for computing $\boldsymbol{b}$ (resp. β in the abstract notation) can lead to a smaller feasible region but preserves robust feasibility of the obtained solution.

For ease of explanation, we show how $\boldsymbol{b}$ can be computed using the original problem formulation (3.5). We express the pressure drop in each pipe equivalently by defining sets of feasible pressure drops $\mathcal{Z}_{l_a}$ for each pipe $a \in \mathcal{A}$:

$$(q_a, \lambda_a) \in \mathcal{Z}_{l_a} = \{(q, \lambda) \mid \lambda = -l_a|q|^*,\ q \in \mathbb{R}\}, \tag{5.31}$$

which is equivalent to

$$\pi_w - \pi_v = \lambda_a = -l_a|q_a|^*. \tag{5.32}$$

Lemma 5.2.2. *Let $v, w \in \mathcal{V}$ be two given nodes and let $\boldsymbol{P}_{vw,\cdot} \in \mathbb{R}^{|\mathcal{V}|-1}$ denote the row of the path matrix $\boldsymbol{P}$ that corresponds to the path from v to w. Furthermore, let $\mathcal{Z}_{l_a}$ be defined for all $a \in \mathcal{A}_{\mathrm{pi}}$ as in* (5.31).

Then, b_{vw} of (5.30) *is the optimal value of the following optimization problem:*

$$\begin{aligned}
b_{vw} \coloneqq\ & -\max_{\boldsymbol{l},\boldsymbol{d},\boldsymbol{q},\boldsymbol{\pi},\boldsymbol{\lambda}} && \boldsymbol{P}_{vw,\cdot}\boldsymbol{\lambda}_{\mathcal{B}} - \Delta\pi_{vw} && \text{(5.33a)}\\
& \text{s.t.} && \boldsymbol{A}\boldsymbol{q} = \boldsymbol{d}, && \text{(5.33b)}\\
& && \boldsymbol{A}^\top\boldsymbol{\pi} = \boldsymbol{\lambda}, && \text{(5.33c)}\\
& && (q_a, \lambda_a) \in \mathcal{Z}_{l_a} \quad \textit{for all } a \in \mathcal{A}_{\mathrm{pi}}, && \text{(5.33d)}\\
& && \boldsymbol{\lambda}_{\mathcal{A}_{\mathrm{pm}}} = \boldsymbol{0}, && \text{(5.33e)}\\
& && \boldsymbol{q} \in \mathbb{R}^{|\mathcal{A}|}, \boldsymbol{\pi} \in \mathbb{R}^{|\mathcal{V}|}, \boldsymbol{\lambda} \in \mathbb{R}^{|\mathcal{A}|}, && \text{(5.33f)}\\
& && (\boldsymbol{l}, \boldsymbol{d}) \in \mathcal{U}. && \text{(5.33g)}
\end{aligned}$$

Proof. The reduced and non-reduced model of the gas network problem are equivalent due to theorem 2.3.5. Therefore, we replace the constraints of the

reduced model (5.30) by their non-reduced counterparts (5.33b)–(5.33g). As the compressor power $\boldsymbol{x}^{\mathrm{pm}}$ has no influence on (5.30) due to assumption 1, the compressor power in the non-reduced model (5.33) is set to zero in (5.33e).

Starting from the objective function (5.33a), we transform:

$$\boldsymbol{P}_{vw,\cdot}\boldsymbol{\lambda}_{\mathcal{B}} - \Delta\pi_{vw} = \boldsymbol{P}_{vw,\mathcal{B}_{\mathrm{pi}}}\boldsymbol{\lambda}_{\mathcal{B}_{\mathrm{pi}}} + \boldsymbol{P}_{vw,\mathcal{B}_{\mathrm{pm}}}\boldsymbol{\lambda}_{\mathcal{B}_{\mathrm{pm}}} - \Delta\pi_{vw}. \tag{5.34}$$

Due to (5.33e) all compressors are set to zero, $\boldsymbol{\lambda}_{\mathcal{B}_{\mathrm{pm}}} = \mathbf{0}$, and thus

$$\boldsymbol{P}_{vw,\cdot}\boldsymbol{\lambda}_{\mathcal{B}} - \Delta\pi_{vw} = \boldsymbol{P}_{vw,\mathcal{B}_{\mathrm{pi}}}\boldsymbol{\lambda}_{\mathcal{B}_{\mathrm{pi}}} - \Delta\pi_{vw}. \tag{5.35}$$

Next, we note that (5.33d) implies $\boldsymbol{\lambda}_{\mathcal{B}_{\mathrm{pi}}} = \boldsymbol{\psi}_{\mathcal{B}_{\mathrm{pi}}}(\boldsymbol{l}_{\mathcal{B}_{\mathrm{pi}}}, \boldsymbol{q}^{\mathrm{ext}}_{\mathcal{B}_{\mathrm{pi}}}(\boldsymbol{d}, \boldsymbol{q}_{\mathcal{N}}))$ and hence

$$\boldsymbol{P}_{vw,\cdot}\boldsymbol{\lambda}_{\mathcal{B}} = \boldsymbol{P}_{vw,\mathcal{B}_{\mathrm{pi}}}\boldsymbol{\psi}_{\mathcal{B}_{\mathrm{pi}}}(\boldsymbol{l}_{\mathcal{B}_{\mathrm{pi}}}, \boldsymbol{q}^{\mathrm{ext}}_{\mathcal{B}_{\mathrm{pi}}}(\boldsymbol{d}, \boldsymbol{q}_{\mathcal{N}})) - \Delta\pi_{vw} = t_{vw}(\boldsymbol{l}_{\mathcal{B}_{\mathrm{pi}}}, \boldsymbol{d}, \boldsymbol{q}_{\mathcal{N}}) \tag{5.36}$$

holds in problem (5.33). □

Remark 5.2.3. The reformulation of lemma 5.2.2 is optional. It is just as well possible to calculate b_{vw} directly from problem (5.30) or a relaxation thereof. However, problem (5.33) of lemma 5.2.2 has two advantages over problem (5.30). Firstly, its implementation is more straightforward since it is very similar to the nominal non-reduced model. And secondly, optimization tasks for two b_{vw}, $b_{v'w'}$ differ only in the linear objectives and therefore solving multiple subproblems only amounts to changing some coefficients of the objective function. Hence, we used formulation (5.33) in our implementation.

Our aim is to solve a relaxation of problem (5.33) to global optimality. To this end, we present several relaxations of the nonlinear and non-convex set $\mathcal{Z}_{l_a}$ that can be used for that purpose. Since global optimal solutions are required to ensure robust feasibility of the obtained results, we develop piecewise-linear relaxations of $\mathcal{Z}_{l_a}$ which can be used to formulate the problem as an MILP. Of course other relaxations like linear (see section 5.2.3) or semidefinite arising from polynomial programming (see chapter 4) are also conceivable, however, we restrict ourselves to piecewise-linear relaxations as a priori error bounds can be computed. When not needed, we drop the arc-specific indices of $\mathcal{Z}_{l_a}$. Furthermore, we assume the flow variables to be in a finite interval, i.e., $q_a \in [\underline{q}_a, \overline{q}_a]$ for all $a \in \mathcal{A}$. This is no restriction as the pressure and flow variables of problem (5.33) are always bounded; see section 5.2.3 for more details regarding their computation.

Relaxations with a priori error bounds are of particular interest as they allow us to compute solutions with arbitrary precision by reducing the error ε; see Geißler et al. (2012).

Definition 5.2.1 (ε-exact relaxation)**.** Let $\mathcal{Z} = \{(x, y) \in [\underline{x}, \overline{x}] \times \mathbb{R} \mid y = f(x)\} \subseteq \mathbb{R}^2$ be the function graph of a function $f : \mathbb{R} \to \mathbb{R}$ over a finite interval $[\underline{x}, \overline{x}]$ and let $\varepsilon > 0$ be a given error. We call $\tilde{\mathcal{Z}} \subseteq [\underline{x}, \overline{x}] \times \mathbb{R}$ an *ε-exact relaxation* of $\mathcal{Z}$, if

1. $\mathcal{Z} \subseteq \tilde{\mathcal{Z}}$,
2. $|y - \tilde{y}| \leq \varepsilon$ for all $x \in [\underline{x}, \overline{x}]$ with $(x, y) \in \mathcal{Z}$ and $(x, \tilde{y}) \in \tilde{\mathcal{Z}}$.

As all presented relaxations are constructed using piecewise-linear functions, we briefly restate how to express piecewise-linear functions in MILPs using the *incremental* or *delta method*, first described by Markowitz and Manne (1957). Let $(x_i, y_i)_{i=1,\dots,k}$ be a series of points in $\mathbb{R}^2$ with $x_1 < x_2 < \cdots < x_k$. Then the graph of the piecewise-linear function with sampling points (x_i, y_i) is given by the following MILP constraints:

$$x = x_1 + \sum_{i=1,\dots,k-1} (x_{i+1} - x_i)\delta_i, \tag{5.37a}$$

$$y = y_1 + \sum_{i=1,\dots,k-1} (y_{i+1} - y_i)\delta_i, \tag{5.37b}$$

$$\delta_1 \geq z_1 \geq \delta_2 \geq z_2 \geq \cdots \geq z_{k-2} \geq \delta_{k-1}, \tag{5.37c}$$

$$\delta_i \in [0, 1] \quad \text{for all } i = 1, \dots, k-1, \tag{5.37d}$$

$$z_i \in \{0, 1\} \quad \text{for all } i = 1, \dots, k-2. \tag{5.37e}$$

In our implementation, the delta method was used exclusively since it is known for its good performance for gas network problems in practice; see Geißler (2011).

Finding approximations for $\mathcal{Z}_c$, i.e., the function graph of $cx|x|$ for a fixed $c > 0$, is straightforward as follows. After eliminating the absolute value by splitting the function graph into negative and positive parts, only square functions cx^2 need to be treated. We show next that the error of approximating cx^2 by a (piecewise) linear function only depends on the parameter c and on the distance between two adjacent sampling points but not on the position of the chosen sampling points. Indeed pick any two points (x_1, y_1), (x_2, y_2) on the graph of $f^{\text{sq}}(x) = cx^2$ with $x_1 < x_2$ and let $f^{\text{lin}}(x) = \frac{y_2 - y_1}{x_2 - x_1}(x - x_1) + y_1$ be the line connecting both points. To calculate the maximum deviation $\varepsilon = \max_x f^{\text{lin}}(x) - f^{\text{sq}}(x)$, we observe that $f^{\text{lin}}(x) - f^{\text{sq}}(x)$ is a degree-two polynomial and thus attains its extreme value between its two roots x_1 and x_2 at $x^* = \frac{1}{2}(x_1 + x_2)$. A short calculation shows that the maximum error is given by $\varepsilon = f^{\text{lin}}(x^*) - f^{\text{sq}}(x^*) = \frac{c}{2}(x_2 - x_1)^2$. Since the approximation error only depends on c and on the distance $x_2 - x_1$ between two sampling points,

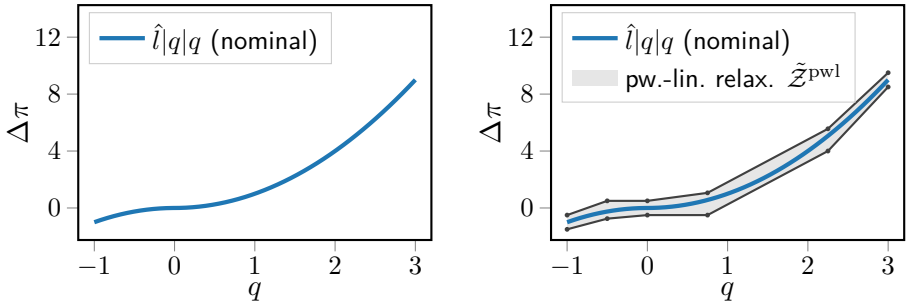

(a) Nominal pressure drop

(b) Nominal piecewise-linear relaxation

Figure 5.1: Nominal pressure drop and piecewise-linear relaxation for constant pressure drop coefficient $l = 1$ and approximation quality $\varepsilon = 1.0$.

we conclude that cx^2 can be approximated by a piecewise-linear function with a given error ε by equidistant sampling points. See fig. 5.1 for an example. The nominal pressure loss function (blue) is bounded from above and below by piecewise-linear functions (dark gray). The gray area that defined by these two functions is a relaxation of the original function graph.

Two different cases need to be distinguished when building relaxations for $\mathcal{Z}_{l_a}$, depending on whether l_a is constant or affected by uncertainty. If the coefficient l_a is constant, the standard relaxation from the literature with equidistant sampling points can be applied to obtain an ε-exact relaxation $\tilde{\mathcal{Z}}_{l_a}^{\text{pwl}} \subseteq \mathbb{R}^2$; see Geißler, Martin, et al. (2015). For the second case, we assume the pressure drop coefficient l_a to be uncertain. In general, this requires a relaxation that is parameterized by l_a so that it can adjust to the different realizations of l_a to preserve the ε-approximation quality. However, due to uncorrelated pressure drop coefficients (3.3), a simplification can be applied. Since the realization of pressure drop coefficient l_a at arc a is independent of all other uncertainties, it is sufficient to construct an ε-exact relaxation $\tilde{\mathcal{Z}}_{(a)} \subseteq \mathbb{R}^2$ of the union

$$\bigcup_{l_a \in [\underline{l}_a, \bar{l}_a]} \mathcal{Z}_{l_a}. \tag{5.38}$$

Due to continuity and monotonicity of the function value $l_a|q_a|^*$ in l_a, the union $\bigcup_{l_a \in [\underline{l}_a, \bar{l}_a]} \mathcal{Z}_{l_a}$ has no holes and its boundary can be described by piecewise functions of the form $l_a|q_a|^*$:

$$\bigcup_{l_a \in [\underline{l}_a, \bar{l}_a]} \mathcal{Z}_{l_a} = \left\{ (q, \lambda) \;\middle|\; \begin{array}{ll} -\bar{l}_a|q|^* \le \lambda \le -\underline{l}_a|q|^*, & \text{if } q \ge 0 \\ -\underline{l}_a|q|^* \le \lambda \le -\bar{l}_a|q|^*, & \text{if } q \le 0 \end{array} \right\}. \tag{5.39}$$

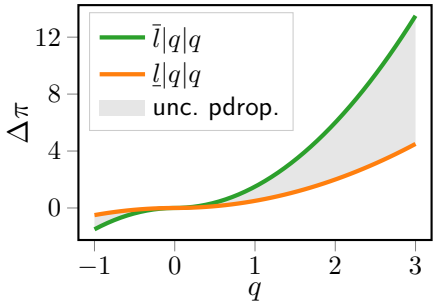

(a) Uncertain pressure drop

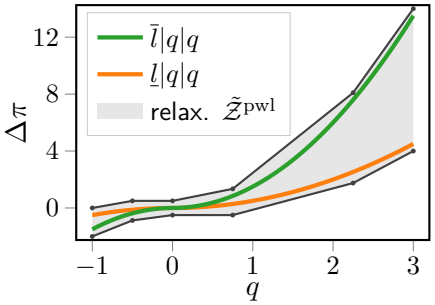

(b) Piecewise-linear relaxation under uncertainty

Figure 5.2: Pressure drop and piecewise-linear relaxation for uncertain pressure drop coefficient $l \in [0.5, 1.5]$ and approximation quality $\varepsilon = 1.0$.

Finally, the piecewise-linear relaxations for functions with constant l_a can be applied to the boundary functions of (5.39) in order to obtain a ε-exact relaxation $\tilde{\mathcal{Z}}^{\text{pwl}}_{(a)} \subseteq \mathbb{R}^2$ of the union of all possible pressure drops for the given uncertain parameters; see fig. 5.2 for an example. The figure on the left shows with green and orange solid lines the two functions corresponding to the extreme values of the uncertain parameter. The gray area between them can be interpreted as the range of the "uncertain" pressure drop, i.e., the set of flow, pressure change-pairs that can arise from the given uncertainty set. The figure on the right depicts in gray a piecewise-linear relaxation of the uncertain pressure drop on the left.

We want to emphasize that the shown relaxation ideas for nonlinear constraints under uncertainty can be applied to other NLPs as well. Although the presented model for piecewise-linear functions (5.37) can be generalized to higher dimensions (Geißler et al. 2012), the relaxation approach is most effective for univariate functions. This is often the case for problems on networks where some quantities of interest solely depend on, e.g., the flow along an arc or the potential at a specific node. As was mentioned earlier, first-stage solutions obtained through relaxations of (5.13) are always robust feasible but can be more conservative compared to exact solutions.

5.2.3 Preprocessing approaches

Before solving any of the MILPs (5.33), we apply a preprocessing step to the bounds of the flow variables to reduce the model size.

Binary variables are used for the construction of the presented piecewise-linear relaxations in section 5.2.2. The overall complexity of solving an MILP typically depends heavily on the number of discrete variables. Our settings requires solving not a single but a series of MILPs to determine the right-hand sides b_{vw}. It is therefore very desirable to speed up the solution process as much as possible.

The number of binary variables required for our application depends on the flow bounds $[\underline{q}_a, \overline{q}_a]$ and on the approximation error ε. Since the approximation error is given, we can decrease the number of required binary variables by providing strong bounds for q_a. To this end, our methods comprise two trivial bounds and an optimization method using linear relaxations. Preprocessing ideas for gas network problems can be found in Geißler (2011), including more complex procedures like pressure and flow propagation heuristics. For a broader overview of different preprocessing ideas for MILPs, we refer to the review article Puranik and Sahinidis (2017). However, we cannot use most of the mentioned ideas as is since they are tailored towards nominal problems without uncertainty. Due to the nature of our problem setting where we optimize over the uncertainty set, our preprocessing methods must preserve the full range of states in the network depending on the uncertainty. All methods are presented with the full range of uncertainty in mind, i.e., uncertain demand and uncertain pressure drop coefficients. For problems where only one or no uncertainty is given, the presented methods can often be simplified considerably.

Trivial bounds We present two trivial flow bounds, one resulting from the maximum overall total demand and one resulting from the decomposition of the linear flow solution space into tree and cycle flows. The problem is assumed to be affected by uncertain demands and uncertain pressure drop coefficients.

A trivial flow bound can be derived by calculating the maximum possible positive demand

$$d^{\text{total}} := \tfrac{1}{2} \max \{ \|\boldsymbol{d}\|_1 \mid \boldsymbol{d} \in \mathcal{D} \}. \tag{5.40}$$

However, this optimization task consists of maximizing a convex function and as such is generally not easy to solve. Since preprocessing has to be very be fast (compared to solving the actual problem MILPs), we calculate a simple upper bound on d^{total} instead. We consider uncertainty set (3.4). After omitting the balancing hyperplane, every demand parameter d_v is only affected by upper and lower bounds:

$$\underline{d}_v \leq d_v \leq \overline{d}_v \quad \text{for all } v \in \mathcal{V}. \tag{5.41}$$

With this in mind, we first bound the maximum total gas injection and withdrawal. A simple bound can be obtained from these quantities by taking the minimum of their absolute values:

$$d^+ = \sum_{v \in \mathcal{V}} \max\{0, \overline{d}_v\}, \quad d^- = \sum_{v \in \mathcal{V}} \min\{0, \underline{d}_v\}, \tag{5.42}$$

$$d^{\text{relax}} := \min\{d^+, -d^-\}. \tag{5.43}$$

The gas flow over each arc can never exceed the total injection, thus

$$q_a \in [-d^{\text{relax}}, d^{\text{relax}}] \tag{5.44}$$

is a feasible bound for all arcs $a \in \mathcal{A}$.

The previous bound can be improved considerably for certain arcs if the structure of the linear network flow solution space is exploited. Recall from (2.57) that any feasible flow $\boldsymbol{q}$ can be written as

$$\boldsymbol{q} = \tilde{\boldsymbol{A}}_{\mathcal{B}}^{-1}(\tilde{\boldsymbol{d}} - \tilde{\boldsymbol{A}}_{\mathcal{N}}\boldsymbol{q}_{\mathcal{N}}), \tag{5.45}$$

where $\boldsymbol{q}_{\mathcal{N}} \in \mathbb{R}^{|\mathcal{N}|}$ is a vector of free variables. It is known from linear flow theory that due to (5.45), the flow over all arcs which are not part of a cycle is independent of $\boldsymbol{q}_{\mathcal{N}}$, i.e., can be written as $q_a = (\tilde{\boldsymbol{A}}_{\mathcal{B}}^{-1}\tilde{\boldsymbol{d}})_a$. This allows us to find tight bounds for q_a over non-cycle arcs a by optimizing over the demand uncertainty set:

$$q_a \in \left[\min_{\boldsymbol{d} \in \mathcal{D}}\{(\tilde{\boldsymbol{A}}_{\mathcal{B}}^{-1}\tilde{\boldsymbol{d}})_a\}, \max_{\boldsymbol{d} \in \mathcal{D}}\{(\tilde{\boldsymbol{A}}_{\mathcal{B}}^{-1}\tilde{\boldsymbol{d}})_a\}\right]. \tag{5.46}$$

If it is not desirable to solve an optimization task, lower and upper bounds for (5.46) can be found with a similar approach as (5.42). We remark that for problems without demand uncertainty the exact, constant flow q_a can be evaluated by calculating $(\tilde{\boldsymbol{A}}_{\mathcal{B}}^{-1}\tilde{\boldsymbol{d}})_a$. In this case, the nonlinear pressure drop equation can be removed by evaluating the signed square function at q_a.

Bounds due to linear relaxations Every fundamental cycle introduces a free variable into the description of the flow (5.45). The flow on every arc that is part of a cycle depends on the unbounded variable $\boldsymbol{q}_{\mathcal{N}}$. Consequently, equation (5.45) cannot be used to derive finite bounds for the flow on arcs that are part of cycle. In order to derive bounds in this setting, we supplement (5.45) with a very rough approximation of the pressure drop constraints. This was done previously for the nominal case in Geißler (2011) by defining a convex hull of the pressure drop constraint's graph through linear inequalities. When

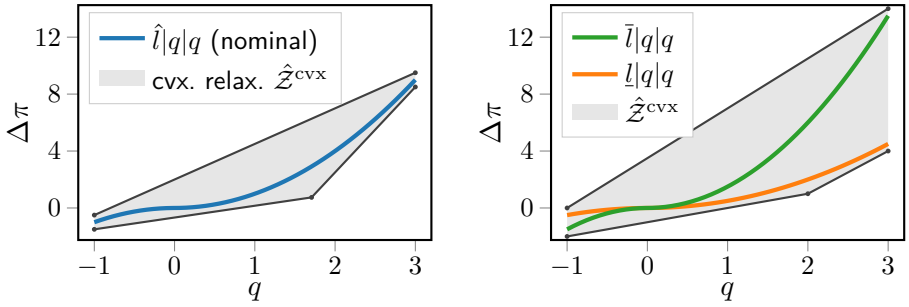

(a) Nominal linear relaxation

(b) Linear relaxation under uncertainty

Figure 5.3: Linear convex hull of nominal ($l = 1.0$) and uncertain pressure drop coefficient ($l \in [0.5, 1.5]$).

compared to the piecewise-linear relaxation approach in section 5.2.2, the defined set is still a relaxation of the original constraint but does not guarantee an ε-approximation.

Next, we generalize the linear model to incorporate uncertain pressure drop coefficients $\boldsymbol{l} \in \mathcal{U}$. To this end, we construct a convex hull $\tilde{\mathcal{Z}}^{\text{cvx}}_{(a)} \subset \mathbb{R}^2$ of the set of all possible pressure drops when given an uncertain coefficient $l_a \in [\underline{l}_a, \bar{l}_a]$

$$\tilde{\mathcal{Z}}^{\text{cvx}}_{(a)} \supset \bigcup_{l_a \in [\underline{l}_a, \bar{l}_a]} \mathcal{Z}_{l_a}. \tag{5.47}$$

See fig. 5.3 for a linear convex hull for nominal pressure drop as well as for pressure drop under uncertainty. We would like to point out that the gray area is again a relaxation of the nominal pressure drop (left figure) and of the uncertain pressure drop (right figure).

Given relaxations $\tilde{\mathcal{Z}}^{\text{cvx}}_{(a)}$ for each pipe $a \in \mathcal{A}_{\text{pi}}$, a very similar problem as (5.33) is defined by replacing the nonlinear sets (5.33d) with their corresponding relaxations. Let $\hat{\mathcal{X}}$ be the feasible region of the resulting problem. Then bounds $q_a \in [q^*_{a,\text{lb}}, q^*_{a,\text{ub}}]$ for the flow along each arc $a \in \mathcal{A}$ can be derived by minimizing and maximizing q_a over $\hat{\mathcal{X}}$:

$$q^*_{a,\text{lb}} := \min_{\boldsymbol{q},\boldsymbol{\pi} \in \hat{\mathcal{X}}} q_a, \qquad q^*_{a,\text{ub}} := \max_{\boldsymbol{q},\boldsymbol{\pi} \in \hat{\mathcal{X}}} q_a. \tag{5.48}$$

Since the problems in (5.48) are LPs, we call this the LP-based relaxation preprocessing approach. In the literature, this type of preprocessing strategy is known as *feasibility-based bounds tightening*; see Puranik and Sahinidis (2017).

We remark that in case of demand uncertainty, the problems (5.48) contain description of the uncertainty set. For pressure drop uncertainty, the uncertainty set is incorporated into the relaxations of the pressure drop equations and therefore is not present in the LPs.

Implementation details In our implementation, all three flow bounds—trivial total demand, linear flows on non-cycle arcs and LP relaxation based bounds—are combined into an iterative bound tightening procedure. Initially, trivial flow bounds (5.44) are derived for each arc to obtain finite bounds. Next, the flow bounds of all non-cycle arcs are tightened with (5.46). The procedure then enters a loop where the LPs (5.48) are solved repeatedly for all remaining arcs. In one iteration step, model (5.48) is built only once and then reused with different objectives for each flow variable. At the end of each iteration step, all flow bounds are updated with the newly calculated bound information. The algorithm terminates if either a maximum number of iterations is reached or if the Euclidean norm of the difference between the bounds of two subsequent iterations is smaller than a specified cutoff value. We use a maximum number of fifteen iterations and a cutoff value of 1.0 in our computations.

5.3 Numerical experiments on realistic instances

In this section, the performance of the developed methods is evaluated on a family of gas network instances. First, we show the advantages of the aggregation idea (5.18) over solving all subproblems individually. Using this as a basis for further study, problem running times are compared in more detail under different aspects such as relaxation quality and magnitude of uncertainty. We close this section with a benchmark using the data from the real-world Greek natural gas network in section 5.3.3.

Table 5.1: Instances for numerical experiments.

	scaling	nodes	pipes	cmprs.	ctrl. valves	short pipes
GasLib-11	1.00	11	8	2	0	1
GasLib-24	2.05	24	19	3	1	2
GasLib-40	0.67	40	39	5	0	1
GasLib-134	1.00	134	86	1	1	45

Instances and setup The studied problems are taken from GasLib Schmidt et al. (2017), a freely available collection of realistic gas network instances incorporating topology and nomination data. We used networks GasLib-11, GasLib-24, GasLib-40, and GasLib-134 with their supplemented demand and pressure nominations. GasLib-134 is a realistic model of the Greek natural gas network, which will be subject to an in-depth discussion in section 5.3.3. Some of the employed instances were slightly modified to fit the context of this thesis. All elements that are neither compressors nor control valves nor pipes are replaced by short pipes; see section 2.1. In order to satisfy assumption 1, the compressor of GasLib-40 that is part of a cycle was replaced by a short pipe as well. Furthermore, the demands of GasLib-24 and GasLib-40 were scaled to obtain nominations whose corresponding robust problems are feasible for all studied uncertainty sets and have non-zero optimal solutions, i.e., compressors have to be used to reach feasibility. Table 5.1 gives an overview of the features of the used instances. We abbreviate compressors with "cmprs." and control valves with "ctrl. valves".

Each instance can be affected by uncertainty. We use relative perturbations around the nominal demand values or pressure drop coefficients as uncertainty sets. A unified naming scheme of the defined uncertainty sets is utilized for both demand and pressure drop uncertainty. The network's demand or pressure drop coefficients may be affected independently by four levels of uncertainty: *nominal* (no uncertainty), *small*, *medium*, and *large*; see table 5.2. Any combination of the provided levels defines an uncertainty set for the numerical experiments, ranging from no uncertainty ("nominal demand and nominal pressure drop") to the combination of large demand uncertainty with large pressure drop uncertainty. The chosen uncertainty level is then applied to all affected elements, i.e., demands or pressure drop coefficients. Thus, there are 16 uncertainty sets in total. The concrete definitions can be found in table 5.2.

All experiments were carried out on a machine with a quad core Intel Xeon E3-1240 v5 CPU running at 3.5 GHz each and 16 GB of RAM. The LPs and MILPs were solved using Gurobi 7.5 (Gurobi Optimization, Inc. 2017) using 4 threads.

5.3.1 Running time improvements due to preprocessing and aggregation

In the following, the influence of the preprocessing strategy and the aggregation step on the runtime is examined in more detail.

Table 5.2: Every combination of demand and pressure drop uncertainty level defines an uncertainty set used in the numerical study.

	demand	press. drop coeff.
nominal	$\{\boldsymbol{d}\}$	$\{\boldsymbol{l}\}$
small	$[0.95 \cdot \boldsymbol{d},\ 1.05 \cdot \boldsymbol{d}]$	$[\boldsymbol{l},\ 1.10 \cdot \boldsymbol{l}]$
medium	$[0.90 \cdot \boldsymbol{d},\ 1.10 \cdot \boldsymbol{d}]$	$[\boldsymbol{l},\ 1.50 \cdot \boldsymbol{l}]$
large	$[0.80 \cdot \boldsymbol{d},\ 1.20 \cdot \boldsymbol{d}]$	$[\boldsymbol{l},\ 2.00 \cdot \boldsymbol{l}]$

Running time improvements due to preprocessing We compare preprocessing strategies on GasLib-11 and GasLib-24 since GasLib-40 is already too large to be solved in an acceptable timespan without preprocessing. In order to cover a wide range of problems, we derive average running times of instance groups where each group contains all combinations of aggregated/individual, approximation quality $\varepsilon \in 0.01, 0.1, 1.0$ and uncertainty set. Hence, each group consists of 96 instances.

We take a look at the average running times depending on the employed preprocessing method; see table 5.3. The columns denote the different preprocessing choices: *trivial* from equation (5.44), *treeflows* (5.46), and LP-based bound tightening (5.48) ("*opt*"). The number in brackets represents the relative speedup compared to the trivial preprocessing bounds. The speedups from treeflows preprocessing is negligible, possibly due to the fact that the studied GasLib instances contain only few arcs that are not part of a cycle. We observe a dramatic speedup of a factor of about 30 to 50 when the LP-based bound tightening is used.

Table 5.3: Mean running times when using different preprocessing strategies. The number in brackets denotes the speedup compared to "trivial" preprocessing.

	trivial	treeflows	opt
GasLib-11	$14.67\,\mathrm{s}$ $(1.0\times)$	$11.47\,\mathrm{s}$ $(1.3\times)$	$0.46\,\mathrm{s}$ $(31.6\times)$
GasLib-24	$327.09\,\mathrm{s}$ $(1.0\times)$	$327.14\,\mathrm{s}$ $(1.0\times)$	$6.24\,\mathrm{s}$ $(52.4\times)$

Running time improvements due to aggregation First, we compare the individual model with the aggregated model. Recall that in order to calculate the right-hand side of (5.29) with problem (5.33), we can either solve $\mathcal{O}(|\mathcal{V}|^2)$ individual problems to obtain each b_{vw} or we can solve a smaller number of problems after applying the aggregation idea (5.15).

Table 5.4: Mean running times of individual and aggregated models after LP-based preprocessing. The numbers in brackets denote the speedup compared to the individual model.

	individual	aggregated
GasLib-11	0.67 s (1.0×)	0.26 s (2.6×)
GasLib-24	11.07 s (1.0×)	1.41 s (7.8×)
GasLib-40	193.84 s (1.0×)	21.37 s (9.1×)

Table 5.4 shows the mean running times on instances GasLib-11, GasLib-24, and GasLib-40 when choosing to solve all problems *individually* or in an *aggregated* fashion. The running times are averages of instance groups where each group contains all 48 possible combinations of approximation quality $\varepsilon \in \{0.01, 0.1, 1.0\}$ and uncertainty set. All problems were preprocessed with LP-based bound tightening. The numbers in brackets denote the relative speedup compared to the slowest method. We observe a mean speedup factor of about 8 to 9 for the larger instances and a smaller speedup of about 2.6 for the smallest instance when using the aggregated model.

In total, a combination of LP-based bound tightening and an aggregation of subproblems yields a mean speedup factor of up to 400 for GasLib-24 when omitting preprocessing and solving all problems individually; see tables 5.3 and 5.4.

Next, we investigate the individual and aggregated methods in more detail. The overall running time for solving the robust gas network problem mainly consists of running times of the preprocessing LPs, running times of the MILP subproblems, and running time of the last LP for deciding a configuration of the active elements. In our setting, solving all occurring LPs is trivial and can be done within fractions of a second. Therefore, we focus on the performance of the MILP subproblems when LP-based preprocessing has been applied.

Table 5.5: Number of MILP subproblems for individual and aggregated models, together with their mean and total running times.

	individual			aggregated		
	#probs	rt. mean	rt. total	#probs	rt. mean	rt. total
GasLib-11	110	0.01 s	0.66 s	7	0.03 s	0.24 s
GasLib-24	552	0.02 s	11.01 s	21	0.06 s	1.35 s
GasLib-40	1560	0.12 s	193.30 s	31	0.67 s	20.83 s

Table 5.5 gives a more detailed summary of the mean running times for the individual and aggregation method. As before, every cell is the average over all possible combinations of approximation quality $\varepsilon \in \{0.01, 0.1, 1.0\}$ and uncertainty sets for a total number of 48 combinations. We use LP-based preprocessing for all instances. The columns are partitioned into one group related to solving all problems individually and one group where the aggregation method is applied. In each column group, we list the number of required subproblems together with their mean and total running times. We observe that applying the aggregation method drastically reduces the required number of subproblems. For the studied instances, the running times of the aggregated models increases at a smaller rate compared to the reduction of problems. Thus, the increase in complexity of the aggregated models is easily compensated by the smaller number of instances that need to be solved.

5.3.2 Influence of the piecewise-linear relaxation

Next, we investigate the influence of the relaxation parameter on the optimal value of the problem. Larger values of ε lead to coarser relaxations of the nonlinear constraints and therefore lead to more conservative solutions. Using the GasLib-11, GasLib-24, and GasLib-40 instances, we solve the robust problem for the "large $\times$ large" combination of uncertainty sets (see table 5.2) and for varying relaxation parameters $\varepsilon \in \{0.001, 0.01, 0.1, 1.0, 10.0\}$. All comparisons in this paragraph are relative to the solution obtained with the smallest relaxation parameter $\varepsilon = 0.001$, which we assume to be "close enough" to the exact solution of the original nonlinear two-stage robust problem. We use LP-based preprocessing and the aggregation method for all problems. The results are summarized in table 5.6. Each column corresponds to a different choice of ε. We assumesociate three rows with each gas network instance, where the first row denotes the absolute objective function value, the second row denotes the relative increase when compared to the finest relaxation $\varepsilon = 0.001$, and the third row denotes the running time.

As a general trend, the objective value increases with the relaxation parameter ε as well as with the instance size. Furthermore, we observe an increase in running times for decreasing relaxation parameters. This is to be expected since a smaller ε leads to better approximations and thus to larger MILP models with more binary variables and constraints.

Concerning the optimal value, we observe a very small relative increase for GasLib-11 and GasLib-24 of at most $3\,\%$ for all choices of ε. Even for the largest instance GasLib-40, the additional cost due the chosen relaxation only

Table 5.6: Absolute and relative comparison of optimal total compressor cost for different relaxation parameters ε together with their respective running times.

	relaxation parameter ε				
	0.001	0.01	0.1	1.0	10.0
GasLib-11	763.78	763.79	763.90	764.76	768.15
		+0.002 %	+0.016 %	+0.128 %	+0.572 %
	30.74 s	3.21 s	0.44 s	0.14 s	0.08 s
GasLib-24	647.83	647.86	648.08	649.93	665.37
		+0.004 %	+0.039 %	+0.325 %	+2.708 %
	130.27 s	16.25 s	2.59 s	0.66 s	0.32 s
GasLib-40	45.12	45.16	45.69	49.50	79.21
		+0.102 %	+1.281 %	+9.711 %	+75.575 %
	2948.58 s	374.17 s	42.30 s	10.05 s	3.67 s

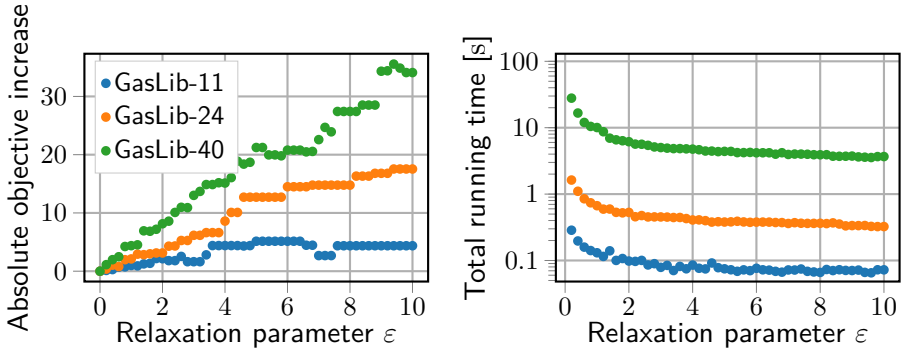

Figure 5.4: Influence of the relaxation parameter ε on objective and running time. The absolute increase of objective in the left picture is shown relative to $\varepsilon = 0.001$.

amounts to about 10 % for a comparatively small $\varepsilon = 1.0$. Only for the largest choice of $\varepsilon = 10.0$ does the objective increase significantly by 76 %.

Next, we want to highlight the quality of solutions that can be found within the fixed timespan of 1 minute. As shown in table 5.6, we can solve GasLib-11 for $\varepsilon = 0.001$, GasLib-24 for $\varepsilon = 0.01$, and GasLib-40 for $\varepsilon = 0.1$ within this timespan. Moreover, the additional cost due to relaxation is very small: +0.004 % for GasLib-24 and +1.281 % for GasLib-40. This demonstrates that our method can be used to find high quality robust solutions within a short timespan.

Finally, we want to investigate the influence of ε on the absolute magnitude of the optimal value and the total running times of the resulting problems.

To this end, the left part of fig. 5.4 shows the absolute increase of objective relative to the smallest choice of $\varepsilon = 0.001$ for all three networks. The right part displays the corresponding total running times on a logarithmic scale. We observe a seemingly linear dependence of the optimal value on the choice of ε and note that the displayed curves are almost, but not completely, monotonically increasing. The lack of monotonicity is due to the fact that the feasible region of a piecewise-linear relaxation with parameter ε_1 is not necessarily a subset of the feasible region of another relaxation with $\varepsilon_2 > \varepsilon_1$. In fact, two piecewise-linear relaxations that are constructed with different ε can have very different sampling points.

When comparing both figures, we observe the objectives to scale almost linearly with ε. In contrast, the corresponding running times scale exponentially for $\varepsilon \leq 1$, but are influenced only very little by the relaxation parameter for $\varepsilon \geq 2$. Since the running times for $\varepsilon \in [2, 10]$ are about the same, there is no reason not to solve the problem with smaller values of ε and thus profit from higher quality solutions. On the other hand, the improvement of objective for small relaxation parameters, e.g., $\varepsilon \in (0, 1]$ is so small that taking values from that range seems to be unjustified when taking the potentially large increase of running times into account. In short, there seems to be a sweet spot at $1 \leq \varepsilon \leq 2$ where high quality solutions can be obtained at comparatively small computational cost.

5.3.3 The natural gas network of Greece

We conclude this section on numerical results with a case study on a real-world network. GasLib-134 models the Greek natural gas network, which extends over a total length of $7000\,\mathrm{km}$ between the Greek border with Turkey in the north and Athens in the south. It features a tree structured topology with a small number of active elements. Figure 5.5 is a map of mainland Greece, where the natural gas pipeline network is marked with a solid line. The numbers in circles represent cross-border interconnection points with other countries and are therefore some of the most important injection and withdrawal points in the network. Please note that the dotted lines can be ignored as they represent planned pipeline projects.

The network description is supplemented by 1234 real load situations, which are available in the form of daily data between November 1, 2011 and February 17, 2016. After excluding 28 days due to conflicting data, the 1006 remaining nominations are used for our computations. All $57\,888$ combinations of $\varepsilon \in \{0.01, 0.1, 1.0\}$, nominations, and uncertainty sets are solved with the aggregation method using LP-based preprocessing. We remark that the

Figure 5.5: The natural gas network of Greece. Solid lines represent pipelines, and the thickness of the line reflects the pipe diameter. Dashed lines are planned projects. The numbers in circles mark cross-border interconnection points with other countries. With permission from ENTSOG (2016).

Table 5.7: Mean running times of all 1006 instances for different choices of ε and uncertainty set.

		$\varepsilon = 0.01$	$\varepsilon = 0.1$	$\varepsilon = 1.0$
demand	pdrop coeff.			
nominal	nominal	0.04 s	0.04 s	0.04 s
small	small	1.27 s	0.94 s	0.86 s
medium	medium	8.86 s	4.83 s	3.55 s
large	large	95.05 s	39.63 s	27.05 s

aggregation step reduces the number of subproblems from the initial 17 822 to 7.

Possibly due to the employed preprocessing strategy on a tree network, we found the solution value to be independent of the tested values for ε. As was to be expected, since this is real-world data, all "nominal×nominal" problems are feasible. In addition, an increase in the number of infeasible instances becomes evident as the sizes of the uncertainty sets increase.

In order to shorten the presentation, we limit ourselves to a portion of the uncertainty sets where demand and pressure drop coefficient are affected by the same level of uncertainty and examine the average running time as a function of the approximation parameter. The results are displayed in table 5.7. Small to medium uncertainty sets have mean running times in the order of seconds whereas large uncertainty sets are in the order of minutes.

As our approach is relying on the solution of MILPs, outliers with long running times are to be expected. We investigate this behavior in fig. 5.6, where the x-axis denotes a fixed period of time and the y-axis denotes the percentage of all instances with the largest uncertainty set that can be successfully solved within this timespan. We observe that all instances can be solved in a few minutes. Even for the best approximation quality of $\varepsilon = 0.01$, over 90 % of the instances are solved in less than 5 min.

A distinct feature of our approach is that the feasible set of the robust two-stage problem is explicitly calculated in the form of a polytope; see (5.29). This allows us to compare the regions of robust feasibility for different uncertainty sets; see fig. 5.7. We choose an approximation quality of $\varepsilon = 0.1$ and the nomination of December 30, 2014 as this load situation is robust feasible for all uncertainty sets. To improve readability, we choose the same level of uncertainty for both demand and pressure drop coefficients ranging from "nominal" to "large". As expected, we observe an inverse relation between size of the robust feasible region and size of the uncertainty set.

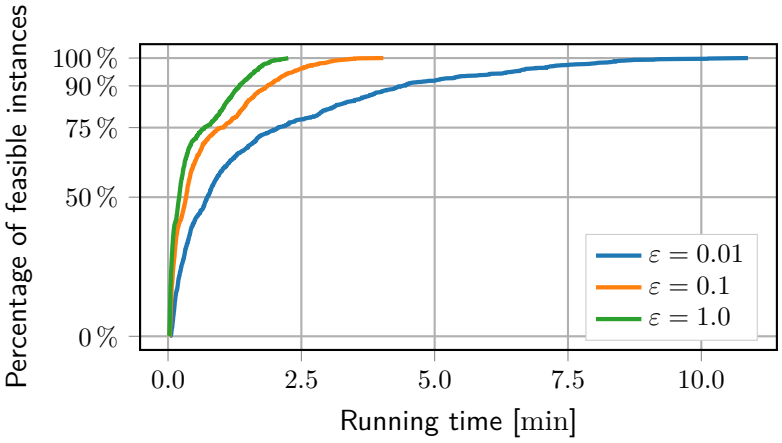

Figure 5.6: Percentage of instances with the largest uncertainty set that can be successfully solved in a fixed period of time.

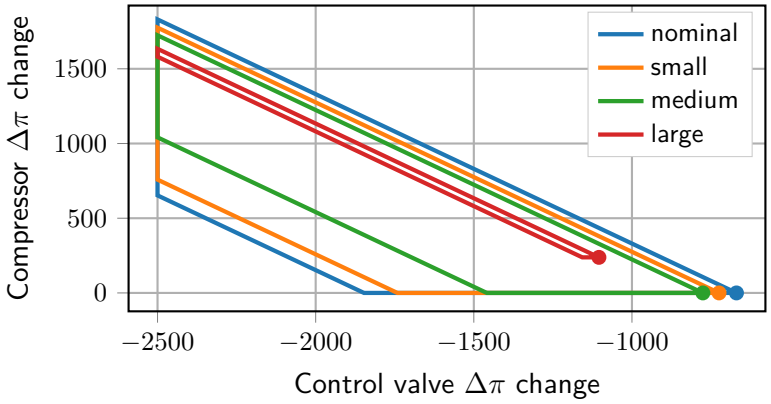

Figure 5.7: Different regions of robust feasible compressor/control valve configurations for $\varepsilon = 0.1$ on December 30, 2014. The filled dots indicate points of minimal compressor operations.

6 Discussion and comparison of the presented methods

Natural gas as an energy source and the corresponding operation of natural gas pipelines are playing an increasingly important role. Gas network operations are often influenced by random factors, such as fluctuations in energy demand or market developments. In this thesis, we studied problems arising from natural gas transport under uncertainty in the form of general two-stage robust optimization problems with a non-convex second stage and a uniqueness property for the second-stage variables. Solving problems of this kind is very challenging for several reasons such as the two-stage structure and the non-convex constraints. We argued in section 3.4 that the non-convex structure together with the uniquely determined second-stage variables makes it difficult to apply standard robust optimization techniques like decision rules and reformulations. Moreover, solutions obtained in this way from an approximated model give no guarantees regarding robustness of the original nonlinear problem formulation.

In order to meet these challenges, we developed novel methods to address this general class of two-stage robust optimization problems. Our approaches use relaxations of the non-convex constraints and exploit the uniqueness of the second-stage variables. Altogether, this allows us to find solutions that are guaranteed to be robust feasible for the original nonlinear formulation.

Next, we will briefly review the presented methods. First, a decision variant of the two-stage problem with empty first stage has been considered in chapter 4. We propose to solve this problem by deciding an equivalent set containment question concerning the feasible region and the uncertainty set. Using methods from polynomial optimization, we developed two approaches for solving this problem—one for deciding feasibility and one for deciding infeasibility. As we solve relaxations of the proposed methods in practice, two distinct methods are necessary since a single method cannot be expected to solve both parts of the question. Both approaches were tested on a variety of small cyclic gas network instances. For problems where deciding robustness is possible, we observed that typically level 2 or level 3 of the Lasserre hierarchy were sufficient.

The second approach, introduced in chapter 5, is a reformulation idea for the two-stage problem with a first stage. Under some additional assumptions for the constraints, the two-stage problem can be transformed into an ordinary single-stage optimization problem whose right-hand is computed by a series

of subproblems. Additionally, we presented an aggregation idea that makes it possible to reduce the number of subproblems that have to be solved. We also showed how relaxations of the subproblems can be used to find solutions that are robust for the original problem formulation. For a practical application to gas network operations, we adapted preprocessing techniques to the uncertain case and used a known piecewise linearization technique to treat the non-convex aspects. The practical feasibility and effectiveness of this approach was demonstrated with benchmarks on the realistic natural gas network of Greece. A combination of all these techniques permitted us to quickly find robust feasible solutions for the original nonlinear problem formulation. These solutions are slightly more conservative due to the relaxations used.

Comparing both presented approaches for robust feasibility, i.e., the polynomial feasibility method and the mixed-integer reformulation idea, we notice that both follow similar ideas. We point out that this comparison does not include the polynomial infeasibility method as it uses a different approach that only works in conjunction with polynomial optimization techniques. Relaxations of the non-convex second stage are used to find bounds for the second-stage variables that can ultimately be used to prove robustness of the original problem formulation. In particular, we use SDP and MILP relaxations that can be solved to global optimality for ensuring robustness. Since only global optimality is important, the employed relaxations could be replaced; that is, polynomial relaxations could be used in the MILP reformulation method and vice versa. However, this would not be very useful in a practical application, as both methods have different strengths and weaknesses which are closely linked to the employed relaxation. In the following, we will briefly compare the advantages and disadvantages of our methods.

First of all, we take a closer look at the polynomial methods, starting with its advantages. Using the Lasserre relaxation hierarchy allows us to systematically construct SDP relaxations for arbitrary complex polynomials that can be solved easily in practice with off-the-shelf software. Moreover, the two developed methods directly work with the nonlinear formulation without the need for additional approximations. Possibly, the Lasserre hierarchy can find an exact solution at a small relaxation level.

As a downside, the gap between relaxations and the (unknown) exact solution can only be controlled by the hierarchy level. This can be very costly while the resulting solutions are still far from the exact solution. In addition, increasing the hierarchy level or the number of problem variables quickly leads to SDPs that are too large and cannot be solved in practice.

Next, we evaluate the MILP reformulation approach, starting with the positive aspects. Current commercial MILP solvers are very performant and even very large problems can often be solved in a short time span. Thus, the presented method can be used to solve comparatively large two-stage robust problems. Another upside of using MILPs is that discrete first or second-stage variables could be included easily. The presented aggregation idea is a potent way of reducing the number of subproblems that have to be solved. Together with the preprocessing ideas, we demonstrated a dramatic performance increase. By using mixed-integer relaxations, it is possible to precisely control the approximation quality, i.e., the maximum error between relaxations and the original nonlinear function.

The reformulation approach also has some shortcomings. There is no systematic way of constructing piecewise-linear relaxations of arbitrary nonlinear functions without additional assumptions such as Lipschitz continuity. Often problem specific knowledge has to be invested in order to find good sampling points for the piecewise-linear functions. Moreover, approximating high-dimensional functions is possible, but can quickly lead to difficult mixed-integer formulations with a large number of variables. This is naturally also the case when we seek to increase the approximation quality by introducing additional sampling points.

This discussion makes it clear that the strengths of the two general approaches lie in different areas. The polynomial method is suitable for polynomial problems with complex nonlinear aspects and a small number of variables. While this approach has the potential to find an exact solution at a finite level of the relaxation hierarchy, all other feasible solutions also guarantee robustness for the original problem formulation. On the other hand, the MILP reformulation method is well suited for large problems where the nonlinear aspects can be handled well with the piecewise-linear relaxation technique. Similar to the polynomial method, the solutions obtained with this method are guaranteed to be robust feasible for the original nonlinear problem. These solutions, however, are always slightly more conservative because of the relaxations used. Altogether, appropriate solution approach depends on the structure of the problem at hand.

Taking the results of this thesis into account, there are different directions for future research. One possibility is further studies of two-stage robust optimization problems with uniquely determined second-stage variables. The unique dependence of a system's state on its boundary conditions is a property that is shared by many mathematical models arising from real-world problems. Consequently, this class of robust optimization tasks is found in a variety of

applications under uncertainty. As far as the application to gas networks is concerned, it would surely be of interest to extend our methods to a richer set of active elements with more complex behaviors. In that case, however, some of the additional assumptions for the second stage structure may no longer be fulfilled, and hence the developed methods would have to be adapted accordingly. Finally, many of the gas network properties such as uniqueness and existence of solutions also hold for other potential driven networks like DC power flow or water networks. Due to their close similarity with gas networks, our methods could also be applied to problems from these domains.

Bibliography

D. Adelhütte, D. Aßmann, T. Gonzàlez Grandòn, M. Gugat, H. Heitsch, F. Liers, R. Henrion, et al. 2018. "Joint model of probabilistic/robust (probust) constraints with application to gas network optimization". Preprint available at https://opus4.kobv.de/opus4-trr154/frontdoor/index/index/docId/215.

AG Energiebilanzen e.V. 2019a. *Bruttostromerzeugung in Deutschland ab 1990 nach Energieträgern*. Visited on 1. Februar. https://ag-energiebilanzen.de/index.php?article_id=29&fileName=20181214_brd_stromerzeugung1990-2018.pdf.

———. 2019b. *Energieverbrauch in Deutschland im Jahr 2017*. Visited on 26. Januar. https://ag-energiebilanzen.de/index.php?article_id=29&fileName=ageb_jahresbericht2017_20180315-02_dt.pdf.

Agency for the Cooperation of Energy Regulators. 2015. *European Gas Target Model review and update*. Visited on February 16, 2019. https://www.acer.europa.eu/Events/Presentation-of-ACER-Gas-Target-Model-/Documents/European%20Gas%20Target%20Model%20Review%20and%20Update.pdf.

R. K. Ahuja, T. L. Magnanti, and J. B. Orlin. 1993. *Network flows*. Theory, algorithms, and applications. Englewood Cliffs, NJ: Prentice Hall.

D. Aßmann. 2014. „Nominierungsvalidierung bei Gasnetzen: Einfluss und mögliche Behandlung von Unsicherheiten". Masterarbeit, Friedrich-Alexander-Universität Erlangen-Nürnberg.

D. Aßmann, F. Liers, and M. Stingl. 2019. "Decomposable robust two-stage optimization: An application to gas network operations under uncertainty". *Networks* 74 (1): 40–61. doi:10.1002/net.21871.

D. Aßmann, F. Liers, M. Stingl, and J. C. Vera. 2018. "Deciding robust feasibility and infeasibility using a set containment approach: an application to stationary passive gas network operations". *SIAM Journal on Optimization* 28 (3): 2489–2517. doi:10.1137/17M112470X.

F. Babonneau, Y. Nesterov, and J.-P. Vial. 2012. "Design and operations of gas transmission networks". *Operations Research* 60 (1): 34–47. doi:10.1287/opre.1110.1001.

R. B. Bapat. 2014. *Graphs and matrices.* 2nd edition. Universitext. London: Springer. doi:10.1007/978-1-4471-6569-9.

J. F. Bard. 1998. *Practical bilevel optimization.* Volume 30. Nonconvex Optimization and its Applications. Algorithms and applications. Kluwer Academic Publishers, Dordrecht. doi:10.1007/978-1-4757-2836-1.

B. T. Baumrucker and L. T. Biegler. 2010. "MPEC strategies for cost optimization of pipeline operations". *Computers & Chemical Engineering* 34 (6): 900–913. doi:10.1016/j.compchemeng.2009.07.012.

A. Ben-Tal, A. Goryashko, E. Guslitzer, and A. Nemirovski. 2004. "Adjustable robust solutions of uncertain linear programs". *Mathematical Programming* 99 (2, Ser. A): 351–376. doi:10.1007/s10107-003-0454-y.

A. Ben-Tal and A. Nemirovski. 1998. "Robust convex optimization". *Mathematics of Operations Research* 23 (4): 769–805. doi:10.1287/moor.23.4.769.

———. 1999. "Robust solutions of uncertain linear programs". *Operations Research Letters* 25 (1): 1–13. doi:10.1016/S0167-6377(99)00016-4.

A. Ben-Tal, L. El Ghaoui, and A. Nemirovski. 2009. *Robust optimization.* Princeton Series in Applied Mathematics. Princeton, NJ: Princeton University Press. doi:10.1515/9781400831050.

A. Ben-Tal, D. den Hertog, and J.-P. Vial. 2015. "Deriving robust counterparts of nonlinear uncertain inequalities". *Mathematical Programming* 149 (1-2, Ser. A): 265–299. doi:10.1007/s10107-014-0750-8.

A. Ben-Tal and A. Nemirovski. 2000. "Robust solutions of linear programming problems contaminated with uncertain data". *Mathematical Programming* 88 (3, Ser. A): 411–424. doi:10.1007/PL00011380.

———. 2002. "Robust optimization—methodology and applications". *Mathematical Programming* 92 (3, Ser. B): 453–480. doi:10.1007/s101070100286.

D. Bertsimas, D. B. Brown, and C. Caramanis. 2011. "Theory and applications of robust optimization". *SIAM Review* 53 (3): 464–501. doi:10.1137/080734510.

D. Bertsimas and C. Caramanis. 2010. "Finite adaptability in multistage linear optimization". *IEEE Transactions on Automatic Control* 55 (12): 2751–2766. doi:10.1109/TAC.2010.2049764.

D. Bertsimas and I. Dunning. 2016. "Multistage robust mixed-integer optimization with adaptive partitions". *Operations Research* 64 (4): 980–998. doi:10.1287/opre.2016.1515.

D. Bertsimas, I. Dunning, and M. Lubin. 2016. "Reformulation versus cutting-planes for robust optimization: a computational study". *Computational Management Science* 13 (2): 195–217. doi:10.1007/s10287-015-0236-z.

D. Bertsimas and A. Georghiou. 2015. "Design of near optimal decision rules in multistage adaptive mixed-integer optimization". *Operations Research* 63 (3): 610–627. doi:10.1287/opre.2015.1365.

———. 2018. "Binary decision rules for multistage adaptive mixed-integer optimization". *Mathematical Programming* 167 (2, Ser. A): 395–433. doi:10.1007/s10107-017-1135-6.

D. Bertsimas, D. A. Iancu, and P. A. Parrilo. 2010. "Optimality of affine policies in multistage robust optimization". *Mathematics of Operations Research* 35 (2): 363–394. doi:10.1287/moor.1100.0444.

D. Bertsimas, D. A. Iancu, and P. A. Parrilo. 2011. "A hierarchy of near-optimal policies for multistage adaptive optimization". *IEEE Transactions on Automatic Control* 56 (12): 2809–2824. doi:10.1109/TAC.2011.2162878.

D. Bienstock and N. Özbay. 2008. "Computing robust basestock levels". *Discrete Optimization* 5 (2): 389–414. doi:10.1016/j.disopt.2006.12.002.

J. R. Birge and F. Louveaux. 2011. *Introduction to stochastic programming*. 2nd edition. Springer Series in Operations Research and Financial Engineering. New York: Springer. doi:10.1007/978-1-4614-0237-4.

G. Blekherman. 2006. "There are significantly more nonnegative polynomials than sums of squares". *Israel Journal of Mathematics* 153:355–380. doi:10.1007/BF02771790.

C. Borraz-Sánchez, R. Bent, S. Backhaus, H. Hijazi, and P. Van Hentenryck. 2016. "Convex relaxations for gas expansion planning". *INFORMS Journal on Computing* 28 (4): 645–656. doi:10.1287/ijoc.2016.0697.

C. Borraz-Sánchez and R. Z. Ríos-Mercado. 2004. "A non-sequential dynamic programming approach for natural gas network optimization". *WSEAS Transactions on Systems* 3 (4): 1384–1389.

C. Borraz-Sánchez and R. Z. Ríos-Mercado. 2009. "Improving the operation of pipeline systems on cyclic structures by tabu search". *Computers & Chemical Engineering* 33 (1): 58–64. doi:10.1016/j.compchemeng.2008.07.009.

S. Boyd and L. Vandenberghe. 2004. *Convex optimization.* Cambridge: Cambridge University Press. doi:10.1017/CBO9780511804441.

J. Brouwer, I. Gasser, and M. Herty. 2011. "Gas pipeline models revisited: model hierarchies, nonisothermal models, and simulations of networks". *Multiscale Modeling & Simulation* 9 (2): 601–623. doi:10.1137/100813580.

Bundesamt für Wirtschaft und Ausfuhrkontrolle. 2019. Visited on 26. Januar. http://www.bafa.de/SharedDocs/Downloads/DE/Energie/egas_entwicklung_1991.xls?__blob=publicationFile&v=10.

Bundesgesetzblatt. 2011. „Dreizehntes Gesetz zur Änderung des Atomgesetzes". *Bundesgesetzblatt* 43:1704–1705. Visited on 26. Januar 2019. http://www.bgbl.de/xaver/bgbl/start.xav?startbk=Bundesanzeiger_BGBl&jumpTo=bgbl111s1704.pdf.

R. Burlacu, B. Geißler, and L. Schewe. 2019. "Solving mixed-integer nonlinear programmes using adaptively refined mixed-integer linear programmes". *Optimization Methods and Software.* doi:10.1080/10556788.2018.1556661.

R. G. Carter. 1998. "Pipeline optimization: dynamic programming after 30 years". In *Proceedings of the 30th PSIG Annual Meeting.*

R. G. Carter and H. H. Rachford. 2003. "Optimizing line-pack management to hedge against future load uncertainty". In *PSIG Annual Meeting.* Pipeline Simulation Interest Group.

A. Chebouba, F. Yalaoui, A. Smati, L. Amodeo, K. Younsi, and A. Tairi. 2009. "Optimization of natural gas pipeline transportation using ant colony optimization". *Computers & Operations Research* 36 (6): 1916–1923. doi:10.1016/j.cor.2008.06.005.

X. Chen and Y. Zhang. 2009. "Uncertain linear programs: extended affinely adjustable robust counterparts". *Operations Research* 57 (6): 1469–1482. doi:10.1287/opre.1080.0605.

M. Chertkov, S. Backhaus, and V. Lebedev. 2015. "Cascading of fluctuations in interdependent energy infrastructures: Gas-grid coupling". *Applied Energy* 160:541–551. doi:10.1016/j.apenergy.2015.09.085.

M. D. Choi, T. Y. Lam, and B. Reznick. 1995. "Sums of squares of real polynomials". In *K-theory and algebraic geometry: connections with quadratic forms and division algebras (Santa Barbara, CA, 1992),* 58:103–126. Proc. Sympos. Pure Math. Providence, RI: Amer. Math. Soc.

G. E. Collins. 1975. "Quantifier elimination for real closed fields by cylindrical algebraic decomposition". In *Automata theory and formal languages (Second GI Conf., Kaiserslautern, 1975),* 134–183. Lecture Notes in Comput. Sci., Vol. 33. Berlin: Springer. doi:10.1007/3-540-07407-4_17.

M. Collins, L. Cooper, R. Helgason, J. Kennington, and L. LeBlanc. 1977. "Solving the pipe network analysis problem using optimization techniques". *Management Science* 24 (7): 747–760. doi:10.1287/mnsc.24.7.747.

D. A. Cox, J. Little, and D. O'Shea. 2015. *Ideals, varieties, and algorithms.* 4th edition. Undergraduate Texts in Mathematics. An introduction to computational algebraic geometry and commutative algebra. Cham: Springer. doi:10.1007/978-3-319-16721-3.

P. Domschke, B. Geißler, O. Kolb, J. Lang, A. Martin, and A. Morsi. 2011. "Combination of nonlinear and linear optimization of transient gas networks". *INFORMS Journal on Computing* 23 (4): 605–617. doi:10.1287/ijoc.1100.0429.

P. Domschke, O. Kolb, and J. Lang. 2015. "Adjoint-based error control for the simulation and optimization of gas and water supply networks". *Applied Mathematics and Computation* 259:1003–1018. doi:10.1016/j.amc.2015.03.029.

N. G. Duffield, P. Goyal, A. Greenberg, P. Mishra, K. K. Ramakrishnan, and J. E. van der Merive. 1999. "A Flexible Model for Resource Management in Virtual Private Networks". In *Proceedings of the Conference on Applications, Technologies, Architectures, and Protocols for Computer Communication,* 95–108. SIGCOMM '99. Cambridge, MA: ACM. doi:10.1145/316188.316209.

H. Edelsbrunner, J. O'Rourke, and R. Seidel. 1986. "Constructing arrangements of lines and hyperplanes with applications". *SIAM Journal on Computing* 15 (2): 341–363. doi:10.1137/0215024.

K. Ehrhardt and M. C. Steinbach. 2003. "Nonlinear Optimization in Gas Networks". In *Modeling, Simulation and Optimization of Complex Processes, Proceedings of the International Conference on High Performance Scientific Computing, Hanoi, Vietnam,* 139–148. doi:10.1007/3-540-27170-8_11.

L. El Ghaoui and H. Lebret. 1997. "Robust solutions to least-squares problems with uncertain data". *SIAM Journal on Matrix Analysis and Applications* 18 (4): 1035–1064. doi:10.1137/S0895479896298130.

L. El Ghaoui, F. Oustry, and H. Lebret. 1999. "Robust solutions to uncertain semidefinite programs". *SIAM Journal on Optimization* 9 (1): 33–52. doi:10.1137/S1052623496305717.

ENTSOG. 2016. "Transmission Capacity Map 2016: The European Natural Gas Network (Capacities at cross-border points on the primary market)". Visited on February 6, 2019. https://www.entsog.eu/sites/default/files/2018-10/ENTSOG_CAP_MAY2016_A0FORMAT.pdf.

F. Farshad, H. Rieke, and J. Garber. 2001. "New developments in surface roughness measurements, characterization, and modeling fluid flow in pipe". *Journal of Petroleum Science and Engineering* 29 (2): 139–150. doi:10.1016/S0920-4105(01)00096-1.

J. B. Franzini and E. J. Finnemore. 1997. *Fluid Mechanics with Engineering Applications.* New York: McGraw-Hill.

A. Fügenschuh, B. Geißler, R. Gollmer, A. Morsi, M. E. Pfetsch, J. Rövekamp, M. Schmidt, K. Spreckelsen, and M. C. Steinbach. 2015. "Physical and technical fundamentals of gas networks". In Koch, Hiller, Pfetsch, and Schewe 2015, chapter 2.

B. P. Furey. 1993. "A sequential quadratic programming-based algorithm for optimization of gas networks". *Automatica* 29 (6): 1439–1450. doi:10.1016/0005-1098(93)90008-H.

V. Gabrel, C. Murat, and A. Thiele. 2014. "Recent advances in robust optimization: an overview". *European Journal of Operational Research* 235 (3): 471–483. doi:10.1016/j.ejor.2013.09.036.

T. Gally, M. E. Pfetsch, and S. Ulbrich. 2018. "A framework for solving mixed-integer semidefinite programs". *Optimization Methods & Software* 33 (3): 594–632. doi:10.1080/10556788.2017.1322081.

B. Geißler. 2011. "Towards Globally Optimal Solutions for MINLPs by Discretization Techniques with Applications in Gas Network Optimization". PhD thesis, Friedrich-Alexander-Universität Erlangen-Nürnberg.

B. Geißler, A. Martin, A. Morsi, and L. Schewe. 2012. "Using piecewise linear functions for solving MINLPs". In *Mixed integer nonlinear programming,* 154:287–314. IMA Vol. Math. Appl. New York: Springer. doi:10.1007/978-1-4614-1927-3_10.

———. 2015. "The MILP-relaxation approach". In Koch, Hiller, Pfetsch, and Schewe 2015, chapter 6.

B. Geißler, A. Morsi, and L. Schewe. 2013. "A new algorithm for MINLP applied to gas transport energy cost minimization". In *Facets of combinatorial optimization,* 321–353. Heidelberg: Springer. doi:10.1007/978-3-642-38189-8_14.

B. Geißler, A. Morsi, L. Schewe, and M. Schmidt. 2015. "Solving power-constrained gas transportation problems using an MIP-based alternating direction method". *Computers & Chemical Engineering* 82:303–317. doi:10.1016/j.compchemeng.2015.07.005.

B. Gilmour, C. Luongo, and D. Schroeder. 1989. *Optimization in natural gas transmission networks: a tool to improve operational efficiency.* Technical report. Stoner Associates Inc.

R. Gollmer, R. Schultz, and C. Stangl. 2015. "The reduced NLP heuristic". In Koch, Hiller, Pfetsch, and Schewe 2015, chapter 8.

T. González Grandón, H. Heitsch, and R. Henrion. 2017. "A joint model of probabilistic/robust constraints for gas transport management in stationary networks". *Computational Management Science* 14 (3): 443–460. doi:10.1007/s10287-017-0284-7.

B. L. Gorissen, İ. Yanıkoğlu, and D. den Hertog. 2015. "A practical guide to robust optimization". *Omega* 53:124–137. doi:10.1016/j.omega.2014.12.006.

C. Gotzes, H. Heitsch, R. Henrion, and R. Schultz. 2016. "On the quantification of nomination feasibility in stationary gas networks with random load". *Mathematical Methods of Operations Research* 84 (2): 427–457. doi:10.1007/s00186-016-0564-y.

U. Gotzes, N. Heinecke, B. Hiller, J. Rövekamp, and T. Koch. 2015. "Regulatory rules for gas markets in germany and other european countries". In Koch, Hiller, Pfetsch, and Schewe 2015, chapter 3.

P. Gritzmann and V. Klee. 1994. "On the complexity of some basic problems in computational convexity. I. Containment problems". Trends in discrete mathematics, *Discrete Mathematics* 136 (1-3): 129–174. doi:10.1016/0012-365X(94)00111-U.

M. Gross, M. E. Pfetsch, L. Schewe, M. Schmidt, and M. Skutella. 2018. "Algorithmic results for potential-based flows: Easy and hard cases". *Networks*. doi:10.1002/net.21865.

M. Gugat, G. Leugering, A. Martin, M. Schmidt, M. Sirvent, and D. Wintergerst. 2018a. "MIP-based instantaneous control of mixed-integer PDE-constrained gas transport problems". *Computational Optimization and Applications* 70 (1): 267–294. doi:10.1007/s10589-017-9970-1.

———. 2018b. "Towards simulation based mixed-integer optimization with differential equations". *Networks* 72 (1): 60–83. doi:10.1002/net.21812.

M. Gugat, R. Schultz, and D. Wintergerst. 2018. "Networks of pipelines for gas with nonconstant compressibility factor: stationary states". *Computational & Applied Mathematics* 37 (2): 1066–1097. doi:10.1007/s40314-016-0383-z.

Gurobi Optimization, Inc. 2017. *Gurobi optimizer reference manual*. http://www.gurobi.com.

E. Guslitser. 2002. "Uncertainty-immunized solutions in linear programming". Master's thesis, Technion, Israeli Institute of Technology. http://citeseerx.ist.psu.edu/viewdoc/download?doi=10.1.1.623.2382&rep=rep1&type=pdf.

Y. M. Hamam and A. Brameller. 1971. "Hybrid method for the solution of piping networks". *Proceedings of the Institution of Electrical Engineers* 118 (11): 1607–1612. doi:10.1049/piee.1971.0292.

G. A. Hanasusanto, D. Kuhn, and W. Wiesemann. 2015. "K-adaptability in two-stage robust binary programming". *Operations Research* 63 (4): 877–892. doi:10.1287/opre.2015.1392.

H. Heitsch, R. Henrion, H. Leövey, R. Mirkov, A. Möller, W. Römisch, and I. Wegner-Specht. 2015. "Empirical observations and statistical analysis of gas demand data". In Koch, Hiller, Pfetsch, and Schewe 2015, chapter 13.

D. Henrion, J.-B. Lasserre, and C. Savorgnan. 2009. "Approximate volume and integration for basic semialgebraic sets". *SIAM Review* 51 (4): 722–743. doi:10.1137/080730287.

D. Henrion, J.-B. Lasserre, and J. Löfberg. 2009. "GloptiPoly 3: moments, optimization and semidefinite programming". *Optimization Methods & Software* 24 (4-5): 761–779. doi:10.1080/10556780802699201.

C. Hewicker and S. Kesting. 2009. "The New Entry-exit Model in the EU and Its Consequences for Gas Supply Companies". In *Handbook Utility Management,* edited by A. Bausch and B. Schwenker, 477–491. Berlin, Heidelberg: Springer. doi:10.1007/978-3-540-79349-6_28.

D. Hilbert. 1888. "Über die Darstellung definiter Formen als Summe von Formenquadraten". *Mathematische Annalen* 32 (3): 342–350. doi:10.1007/BF01443605.

B. Hiller, C. Hayn, H. Heitsch, R. Henrion, H. Leövey, A. Möller, and W. Römisch. 2015. "Methods for verifying booked capacities". In Koch, Hiller, Pfetsch, and Schewe 2015, 291–315.

P. Hofer. 1973. „Beurteilung von Fehlern in Rohrnetzberechnungen". *GWF—Gas/Erdgas* 11:113–119.

J. Humpola and A. Fügenschuh. 2015. "Convex reformulations for solving a nonlinear network design problem". *Computational Optimization and Applications* 62 (3): 717–759. doi:10.1007/s10589-015-9756-2.

J. Humpola, A. Fügenschuh, B. Hiller, T. Koch, T. Lehmann, R. Lenz, R. Schwarz, and J. Schweiger. 2015. "The specialized MINLP approach". In Koch, Hiller, Pfetsch, and Schewe 2015, chapter 7.

Z. Jarvis-Wloszek, R. Feeley, W. Tan, K. Sun, and A. Packard. 2003. "Some controls applications of sum of squares programming". In *Proceedings of the 42nd IEEE International Conference on Decision and Control,* 5:4676–4681. Washington, DC: IEEE. doi:10.1109/CDC.2003.1272309.

K. Kellner. 2015. "Positivstellensatz Certificates for Containment of Polyhedra and Spectrahedra". PhD thesis, Johann Wolfgang Goethe-Universität Frankfurt am Main.

K. Kellner, T. Theobald, and C. Trabandt. 2013. "Containment problems for polytopes and spectrahedra". *SIAM Journal on Optimization* 23 (2): 1000–1020. doi:10.1137/120874898.

G. Kirchhoff. 1847. "Über die Auflösung der Gleichungen, auf welche man bei der Untersuchung der linearen Vertheilung galvanischer Ströme geführt wird". *Annalen der Physik und Chemie* 148 (12): 497–508. doi:10.1002/andp.18471481202.

T. Koch, B. Hiller, M. E. Pfetsch, and L. Schewe, editors. 2015. *Evaluating gas network capacities.* Volume 21. MOS-SIAM Series on Optimization. Philadelphia, PA: Society for Industrial / Applied Mathematics (SIAM). doi:10.1137/1.9781611973693.

Kommission "Wachstum, Strukturwandel und Beschäftigung". 2019. *Abschlussbericht*. 26. Januar. Visited on 29. Januar 2019. http://www.spiegel.de/media/media-44069.pdf.

J. Králik, P. Stiegler, Z. Vostrý, and J. Záworka. 1988. *Dynamic Modeling of Large-scale Networks with Application to Gas Distribution.* Volume 6. Studies in Automation and Control. Amsterdam: Elsevier.

J.-L. Krivine. 1964. "Anneaux préordonnés". *Journal d'Analyse Mathématique* 12:307–326. doi:10.1007/BF02807438.

D. Kuhn, W. Wiesemann, and A. Georghiou. 2011. "Primal and dual linear decision rules in stochastic and robust optimization". *Mathematical Programming* 130 (1, Ser. A): 177–209. doi:10.1007/s10107-009-0331-4.

P. Kundu, I. Cohen, and D. Dowling. 2015. *Fluid Mechanics.* 6th edition. Boston, MA: Academic Press. doi:10.1016/C2012-0-00611-4.

M. Labbé, F. Plein, and M. Schmidt. 2018. "Bookings in the European Gas Market: Characterisation of Feasibility and Computational Complexity Results". Preprint available at http://www.optimization-online.org/DB%5fHTML/2018/12/6977.html.

H. Lall and P. Percell. 1990. "A dynamic programming based gas pipeline optimizer". In *Analysis and Optimization of Systems,* edited by A. Bensoussan and J. Lions, 144:123–132. Lecture Notes in Control and Information Sciences. Berlin/Heidelberg: Springer. doi:10.1007/bfb0120035.

L. D. Landau and E. M. Lifshitz. 1987. *Fluid Mechanics.* 2nd edition. Volume 6. Course of Theoretical Physics. Oxford: Pergamon Press. doi:10.1016/C2013-0-03799-1.

J.-B. Lasserre. 2000. "Global optimization with polynomials and the problem of moments". *SIAM Journal on Optimization* 11 (3): 796–817. doi:10.1137/S1052623400366802.

J.-B. Lasserre and T. Netzer. 2007. "SOS approximations of nonnegative polynomials via simple high degree perturbations". *Mathematische Zeitschrift* 256 (1): 99–112. doi:10.1007/s00209-006-0061-8.

M. Laurent. 2009. "Sums of squares, moment matrices and optimization over polynomials". In *Emerging applications of algebraic geometry,* 149:157–270. IMA Vol. Math. Appl. New York: Springer. doi:10.1007/978-0-387-09686-5_7.

P. D. Lax and A. N. Milgram. 1954. "Parabolic equations". In *Contributions to the theory of partial differential equations,* 167–190. Annals of Mathematics Studies, no. 33. Princeton, NJ: Princeton University Press.

J. Löfberg. 2009. "Pre- and post-processing sum-of-squares programs in practice". *IEEE Transactions on Automatic Control* 54 (5): 1007–1011. doi:10.1109/TAC.2009.2017144.

M. V. Lurie. 2008. *Modeling of Oil Product and Gas Pipeline Transportation.* Weinheim: Wiley-VCH.

V. Magron, D. Henrion, and J.-B. Lasserre. 2015. "Semidefinite approximations of projections and polynomial images of semialgebraic sets". *SIAM Journal on Optimization* 25 (4): 2143–2164. doi:10.1137/140992047.

D. Mahlke, A. Martin, and S. Moritz. 2010. "A mixed integer approach for time-dependent gas network optimization". *Optimization Methods & Software* 25 (4-6): 625–644. doi:10.1080/10556780903270886.

D. Mahlke, A. Martin, and S. Moritz. 2007. "A simulated annealing algorithm for transient optimization in gas networks". *Mathematical Methods of Operations Research* 66 (1): 99–115. doi:10.1007/s00186-006-0142-9.

J. Mallinson, A. E. Fincham, S. P. Bull, J. S. Rollett, and M. L. Wong. 1993. "Methods for optimizing gas transmission networks". *Annals of Operations Research* 43 (8): 443–454. doi:10.1007/BF02024841.

O. L. Mangasarian. 2002. "Set containment characterization". *Journal of Global Optimization* 24 (4): 473–480. doi:10.1023/A:1021207718605.

H. M. Markowitz and A. S. Manne. 1957. "On the solution of discrete programming problems". *Econometrica. Journal of the Econometric Society* 25:84–110. doi:10.2307/1907744.

A. Martin, M. Möller, and S. Moritz. 2006. "Mixed integer models for the stationary case of gas network optimization". *Mathematical Programming* 105 (2-3, Ser. B): 563–582. doi:10.1007/s10107-005-0665-5.

J. J. Maugis. 1977. "Étude de réseaux de transport et de distribution de fluide". *RAIRO Operations Research* 11 (2): 243–248. doi:10.1051/ro/1977110202431.

V. Mehrmann, M. Schmidt, and J. J. Stolwijk. 2018. "Model and ddiscretization error adaptivity within stationary gas transport optimization". *Vietnam Journal of Mathematics* 46 (4): 779–801. doi:10.1007/s10013-018-0303-1.

E. Menon. 2005. *Gas Pipeline Hydraulics.* Boca Raton, FL: CRC Press.

J. Mischner. 2012. "Notices about hydraulic calculations of gas pipelines". *GWF—Gas/Erdgas* 4:158–273.

S. Misra, M. W. Fisher, S. Backhaus, R. Bent, M. Chertkov, and F. Pan. 2015. "Optimal compression in natural gas networks: a geometric programming approach". *IEEE Transactions on Control of Network Systems* 2 (1): 47–56. doi:10.1109/TCNS.2014.2367360.

MOSEK. 2011. *The MOSEK Optimization Toolbox for MATLAB Manual.* Revision 128. Copenhagen, Denmark: MOSEK.

K. G. Murty and S. N. Kabadi. 1987. "Some NP-complete problems in quadratic and nonlinear programming". *Mathematical Programming* 39 (2): 117–129. doi:10.1007/BF02592948.

J. Nikuradse. 1933. *Strömungsgesetze in Rauhen Rohren.* Forschungsheft auf dem Gebiete des Ingenieurwesens. Düsseldorf: VDI-Verlag.

A. J. Osiadacz and M. Chaczykowski. 2010. "Verification of Transient Gas Flow Simulation Model". In *PSIG Annual Meeting.* Pipeline Simulation Interest Group.

A. Osiadacz and K. Pienkosz. 1988. "Methods of steady-state simulation for gas networks". *International Journal of Systems Science* 19 (7): 1311–1321. doi:10.1080/00207728808559576.

A. Papachristodoulou, J. Anderson, G. Valmorbida, S. Prajna, P. Seiler, and P. A. Parrilo. 2013. *SOSTOLS: sum of squares optimization toolbox for MATLAB.* Available from eng.ox.ac.uk/control/sostools.

I. Papay. 1968. *OGIL musz. tud. kozl.* Budapest.

P. A. Parrilo. 2003. "Semidefinite programming relaxations for semialgebraic problems". Algebraic and geometric methods in discrete optimization, *Mathematical Programming* 96 (2, Ser. B): 293–320. doi:10.1007/s10107-003-0387-5.

M. E. Pfetsch, A. Fügenschuh, B. Geißler, N. Geißler, R. Gollmer, B. Hiller, J. Humpola, et al. 2015. "Validation of nominations in gas network optimization: models, methods, and solutions". *Optimization Methods & Software* 30 (1): 15–53. doi:10.1080/10556788.2014.888426.

K. Postek and D. den Hertog. 2016. "Multistage adjustable robust mixed-integer optimization via iterative splitting of the uncertainty set". *INFORMS Journal on Computing* 28 (3): 553–574. doi:10.1287/ijoc.2016.0696.

K. F. Pratt and J. G. Wilson. 1984. "Optimisation of the operation of gas transmission systems". *Transactions of the Institute of Measurement and Control* 6 (4): 261–269. doi:10.1177/014233128400600411.

Y. Puranik and N. V. Sahinidis. 2017. "Domain reduction techniques for global NLP and MINLP optimization". *Constraints. An International Journal* 22 (3): 338–376. doi:10.1007/s10601-016-9267-5.

M. Putinar. 1993. "Positive polynomials on compact semi-algebraic sets". *Indiana University Mathematics Journal* 42 (3): 969–984. doi:10.1512/iumj.1993.42.42045.

R. Z. Ríos-Mercado and C. Borraz-Sánchez. 2015. "Optimization problems in natural gas transportation systems: A state-of-the-art review". *Applied Energy* 147:536–555. doi:10.1016/j.apenergy.2015.03.017.

R. Z. Ríos-Mercado, S. Kim, and E. A. Boyd. 2006. "Efficient operation of natural gas transmission systems: A network-based heuristic for cyclic structures". *Computers & Operations Research* 33:2323–2351. doi:10.1016/j.cor.2005.02.003.

R. Z. Ríos-Mercado, S. Wu, L. R. Scott, and E. A. Boyd. 2002. "A Reduction Technique for Natural Gas Transmission Network Optimization Problems". *Annals of Operations Research* 117 (1-4): 217–234. doi:10.1023/A:1021529709006.

M. Robinius, L. Schewe, M. Schmidt, D. Stolten, J. Thürauf, and L. Welder. 2019. "Robust optimal discrete arc sizing for tree-shaped potential networks". *Computational Optimization and Applications* 73 (3): 791–819. doi:10.1007/s10589-019-00085-x.

W. Romeijnders and K. Postek. 2018. "Piecewise constant decision rules via branch-and-bound based scenario detection for integer adjustable robust optimization". arXiv: 1805.10079.

F. Rømo, A. Tomasgard, L. Hellemo, M. Fodstad, B. H. Eidesen, and B. Pedersen. 2009. "Optimizing the Norwegian Natural Gas Production and Transport". *Interfaces* 39 (1): 46–56. doi:10.1287/inte.1080.0414.

D. Rose, M. Schmidt, M. C. Steinbach, and B. M. Willert. 2016. "Computational optimization of gas compressor stations: MINLP models versus continuous reformulations". *Mathematical Methods of Operations Research* 83 (3): 409–444. doi:10.1007/s00186-016-0533-5.

J. Saleh. 2002. *Fluid Flow Handbook.* New York, NY: McGraw-Hill.

M. Schmidt, D. Aßmann, R. Burlacu, J. Humpola, I. Joormann, N. Kanelakis, T. Koch, et al. 2017. "GasLib – A Library of Gas Network Instances". *Data* 2 (4): article 40. doi:10.3390/data2040040.

M. Schmidt, M. C. Steinbach, and B. M. Willert. 2015a. "An MPEC based heuristic". In Koch, Hiller, Pfetsch, and Schewe 2015, chapter 9.

———. 2015b. "High detail stationary optimization models for gas networks". *Optimization and Engineering* 16 (1): 131–164. doi:10.1007/s11081-014-9246-x.

———. 2016. "High detail stationary optimization models for gas networks: validation and results". *Optimization and Engineering* 17 (2): 437–472. doi:10.1007/s11081-015-9300-3.

K. Schmüdgen. 1991. "The K-moment problem for compact semi-algebraic sets". *Mathematische Annalen* 289 (2): 203–206. doi:10.1007/BF01446568.

N. Z. Shor. 1987. "A class of estimates for the global minimum of polynomial functions". *Kibernetika,* number 6: 9–11, 133.

M. Sirvent. 2018. *Incorporating Differential Equations into Mixed-Integer Programming for Gas Transport Optimization.* FAU Studies Mathematics & Physics Band 13. Erlangen: FAU University Press. doi:10.25593/978-3-96147-114-0.

A. L. Soyster. 1973. "Convex Programming with Set-Inclusive Constraints and Applications to Inexact Linear Programming". *Operations Research* 21 (5): 1154–1157.

M. C. Steinbach. 2007. "On PDE solution in transient optimization of gas networks". *Journal of Computational and Applied Mathematics* 203 (2): 345–361. doi:10.1016/j.cam.2006.04.018.

G. Stengle. 1974. "A nullstellensatz and a positivstellensatz in semialgebraic geometry". *Mathematische Annalen* 207:87–97. doi:10.1007/BF01362149.

J. F. Sturm. 1999. "Using SeDuMi 1.02, a MATLAB toolbox for optimization over symmetric cones". Interior point methods, *Optimization Methods and Software* 11/12 (1-4): 625–653. doi:10.1080/10556789908805766.

A. Takeda, S. Taguchi, and R. H. Tütüncü. 2008. "Adjustable robust optimization models for a nonlinear two-period system". *Journal of Optimization Theory and Applications* 136 (2): 275–295. doi:10.1007/s10957-007-9288-8.

K. C. Toh, M. J. Todd, and R. H. Tütüncü. 1999. "SDPT3—a MATLAB software package for semidefinite programming, version 1.3". Interior point methods, *Optimization Methods and Software* 11/12 (1-4): 545–581. doi:10.1080/10556789908805762.

L. Vandenberghe and S. Boyd. 1996. "Semidefinite programming". *SIAM Review* 38 (1): 49–95. doi:10.1137/1038003.

A. Varone and M. Ferrari. 2015. "Power to liquid and power to gas: An option for the German Energiewende". 45:207–218. doi:10.1016/j.rser.2015.01.049.

M. Vuffray, S. Misra, and M. Chertkov. 2015. "Monotonicity of dissipative flow networks renders robust maximum profit problem tractable: general analysis and application to natural gas flows". In *2015 54th IEEE Conference on Decision and Control (CDC),* 4571–4578. Washington, DC: IEEE. doi:10.1109/CDC.2015.7402933.

Wagner, Elbling & Company. 2016. *Gutachten zu Potentialen weiterer nationaler oder grenzüberschreitender Gasmarktgebietsintegrationen sowie den damit verbundenen Auswirkungen auf den deutschen Gasmarkt.* Gutachten im Auftrag der Bundesnetzagentur. Visited on 16. Februar 2019. https://www.bundesnetzagentur.de/SharedDocs/Downloads/DE/Sachgebiete/Energie/Unternehmen_Institutionen/NetzzugangUndMesswesen/Gas/GutachtenBNetzAMarktintegrationWECOM.pdf.

T. R. Weymouth. 1912. "Problems in natural gas engineering". *Transactions of the American Society of Mechanical Engineers* 34 (1349): 185–231.

J. F. Wilkinson, D. V. Holliday, E. H. Batey, and K. W. Hannah. 1965. *Transient Flow in Natural Gas Transmission Systems.* New York, NY: American Gas Association.

D. de Wolf and Y. Smeers. 2000. "The gas transmission problem solved by an extension of the simplex algorithm". *Management Science* 46 (11): 1454–1465. doi:10.1287/mnsc.46.11.1454.12087.

H. Wolkowicz, R. Saigal, and L. Vandenberghe, editors. 2000. *Handbook of semidefinite programming.* Volume 27. International Series in Operations Research & Management Science. Theory, algorithms, and applications. Boston, MA: Kluwer Academic Publishers. doi:10.1007/978-1-4615-4381-7.

P. J. Wong and R. E. Larson. 1968a. "Optimization of natural-gas pipeline systems via dynamic programming". *IEEE Transactions on Automatic Control* 13 (5): 475–481. doi:10.1109/TAC.1968.1098990.

P. J. Wong and R. E. Larson. 1968b. "Optimization of tree-structured natural-gas transmission networks". *Journal of Mathematical Analysis and Applications* 24:613–626. doi:10.1016/0022-247X(68)90014-0.

S. Wu, R. Z. Ríos-Mercado, E. A. Boyd, and L. R. Scott. 2000. "Model relaxations for the fuel cost minimization of steady-state gas pipeline networks". *Mathematical and Computer Modelling* 31 (2): 197–220. doi:10.1016/S0895-7177(99)00232-0.

İ. Yanıkoğlu, B. L. Gorissen, and D. den Hertog. 2018. "A survey of adjustable robust optimization". *European Journal of Operational Research.* doi:https://doi.org/10.1016/j.ejor.2018.08.031.

T. Zaslavsky. 1975. "Facing up to arrangements: face-count formulas for partitions of space by hyperplanes". *Memoirs of the American Mathematical Society* 1 (154): vii+102.

V. M. Zavala. 2014. "Stochastic optimal control model for natural gas networks". *Computers & Chemical Engineering* 64:103–113. doi:10.1016/j.compchemeng.2014.02.002.

B. Zeng and L. Zhao. 2013. "Solving two-stage robust optimization problems using a column-and-constraint generation method". *Operations Research Letters* 41 (5): 457–461. doi:10.1016/j.orl.2013.05.003.

J. Zhen, D. den Hertog, and M. Sim. 2018. "Adjustable robust optimization via Fourier-Motzkin elimination". *Operations Research* 66 (4): 1086–1100. doi:10.1287/opre.2017.1714.

K. Zhou, J. C. Doyle, and K. Glover. 1996. *Robust and Optimal Control.* Upper Saddle River, NJ: Prentice-Hall, Inc.

A. Zlotnik, M. Chertkov, and S. Backhaus. 2015. "Optimal control of transient flow in natural gas networks". In *2015 54th IEEE Conference on Decision and Control (CDC),* 4563–4570. Washington, DC: IEEE. doi:10.1109/CDC.2015.7402932.

R. D. Zucker and O. Biblarz. 2002. *Fundamentals of Gas Dynamics.* Hoboken, NJ: John Wiley & Sons.

Natural gas is an important source of energy that is regarded as essential for achieving the politically set climate goals. In particular, gas-fired power plants are valued as flexible buffers to compensate for fluctuations in renewable electricity generation. Moreover, gas network operators face new challenges due to the liberalization of the European gas market. Under the newly introduced entry-exit market regime, gas network operators have to ensure that all possible market outcomes can be transported over the network.

Hence, the operators of gas networks require new aids for decision-making under uncertain conditions such as load fluctuations or inaccuracies in physical parameters.

To this end, this thesis investigates a general class of two-stage robust optimization problems using the example of gas network operations under uncertainty. Three general solution methods are developed for this problem class. The first two approaches use ideas from polynomial optimization to decide robust feasibility or infeasibility. Both procedures consider polynomial formulations that are approximated by semidefinite programs via the Lasserre relaxation hierarchy. The third approach is based on a transformation of the two-stage robust problem into a number of single-stage optimization problems. The resulting subproblems are approximated by mixed-integer linear programs. By combining this method with additional preprocessing and aggregation steps, it is demonstrated that real-world problems can be solved efficiently within a short time.

ISBN 978-3-96147-233-8

FAU UNIVERSITY PRESS 2019